EXPRESSION OF ACC OXIDASE GENES IN WHITE CLOVER (*Trifolium repens* L.) ROOTS IN RESPONSE TO PHOSPHATE SUPPLY

A thesis presented
in partial fulfillment of the requirements for the degree of

Doctor of Philosophy
in Plant Molecular Biology

at

Massey University
Palmerston North, New Zealand

MARISSA B. ROLDAN

2008

ABSTRACT

The differential expression of members of the *Trifolium repens* ACC oxidase (*TR-ACO*) gene family and accumulation of TR-ACO proteins in white clover roots, and the temporal *TR-ACO* gene expression and TR-ACO protein accumulation in response to phosphate (Pi) stress has been investigated. Four-node stolon cuttings of wild type and transgenic white clover (designated *TR-ACOp::GUS* and *TR-ACO1p::mGFP5-ER*) plants were rooted and acclimatised in Hoagland's solution, and then subjected to either a Pi sufficiency (1 mM Pi) treatment or a Pi depletion (10 μM Pi) treatment over a designated time course.

Using semi quantitative Reverse Transcriptase-Polymerase Chain Reaction (sqRT-PCR) and gene-specific primers it has been determined that the *TR-ACO* genes are differentially expressed in the roots of white clover. The *TR-ACO1* transcript abundance was greater in the lateral roots when compared to the main roots. By immunodetection analysis using antibodies raised against TR-ACO1, recognition of a protein of expected size (*ca.* 36 kDa) was also greater in the lateral roots. The tissue-specific localisation of *TR-ACO1* promoter activity was investigated first by light microscopy using a single genetic line of white clover transformed with a *TR-ACO1p::GUS* gene construct, and results then confirmed by confocal microscopy using several genetically independent lines of transgenic plants transformed with a *TR-ACO1p::mGFP5 ER* gene construct. In these lines, the *TR-ACO1* promoter activity was primarily located in the meristem of the main and lateral roots, lateral root primordia as well as in the pericycle of the root with nodes of expression in the emerging lateral roots, suggesting a role for ethylene in the development of young tissues where cells are actively dividing.

In terms of *TR-ACO2*, greater transcript abundance and protein accumulation of TR-ACO2 were also observed in the lateral roots when compared to the main roots. Histochemical GUS staining of roots of a single genetically-independent line transformed with a *TR-ACO2p::GUS* construct showed predominant promoter activity in the mature tissues of both the main and lateral roots but not in the meristematic tissues. In contrast, *TR-ACO3* showed greater transcript abundance in the main roots relative to the lateral roots, and the promoter activity, as determined using a single genetically- independent line of *TR-ACO3p::GUS* transformed plants was predominantly in the mature tissues of the main roots

In response to Pi depletion, the members of *TR-ACO* gene family were temporally expressed in the white clover roots. Using sqRT-PCR, the *TR-ACO1* transcript abundance was greater in Pi depleted roots at 12 h and 24 h after Pi depletion in both wild type plants and in the one genetically-independent line of white clover transformed with the *TR-ACO1p::mGFP5-ER* construct examined. Similarly, by western analysis using both α-TR-ACO1 and commercially available α-GFP antibodies (for the transformed line), a greater accumulation of proteins was consistently observed in Pi depleted roots from the first up to the seventh day after Pi depletion. By confocal microscopy, it was determined for several genetically-independent line of white clover transformed with *TR-ACO1p::mGFP5-ER* that under Pi depletion more intense GFP fluorescence over a time course of 1 d, 4 d, and 7 d was observed, when compared to plants grown under Pi sufficiency.

For *TR-ACO2*, there was no significant difference in transcript accumulation and protein accumulation in response to short term Pi depletion of up to seven days. However, at 15 d and 21 d after Pi depletion there was a greater protein accumulation in

the roots of Pi depleted plants relative to the Pi sufficient roots. Further, when main and lateral roots were compared, a greater protein accumulation occurred in the lateral roots. For *TR-ACO3*, there was no consistent trend of transcript accumulation in response to Pi depletion over a 24 h period. While a marked reduction in transcript accumulation was noted in Pi depleted roots at 1h, 12 h, 24 h, there was an increase in transcript accumulation at 6 h and 18 h after Pi depletion, indicating that factors other than Pi supply may be affecting gene regulation.

Root morphological studies revealed an increase in the main root length and lateral root production in white clover in response to Pi depletion with a greatest growth rate noted between the sixth and ninth day after Pi depletion, and this period overlapped with accumulation of TR-ACO1 protein suggesting a role for ethylene in the Pi stress induced lateral root production in white clover. The differential regulation of the three *TR-ACO* genes in white clover roots in response to Pi depletion further suggests the divergence in terms of regulation of the ethylene biosynthetic pathway, which may play an important role in fine tuning the responses of plants to particular environmental cues.

ACKNOWLEDGEMENTS

In the completion of my thesis I am truly indebted to several individuals who in one way or another have contributed valuable inputs in making this project a worthwhile achievement.

My deepest expression of gratitude goes to my supervisors, Professors Michael T. McManus and Paula E. Jameson for all the support extended. Michael, you are indeed an excellent supervisor. Thank you for your kindness and untiring effort in mentoring, for guiding me in beating the challenges along the way, and for your patience in editing my writings. The deep concern and support you have accorded in the course of my studies have given me lots of inspiration to pursue this degree. Paula, you have shared a lot of inputs in a variety of ways. The constant moral support and concern you have shown have motivated me to carry on. Your patience in editing my thesis is highly appreciated. For all sorts of assistance you have extended, I am earnestly grateful.

Special thanks to Dr. Balance Chen for generously providing the *TR-ACOp::GUS* white clover plants used in my initial experiments, and for allowing me to use his *TR-ACO1* promoter. I also thank you Balance for sharing your valuable expertise in DNA manipulation and techniques in white clover transformation. I am equally grateful to Miss Susanna Leung for the technical assistance extended, and for providing the *TR-ACO1p::mGFP5-ER* construct used in this thesis. I would never forget when I was incapable of doing my lab work for couple of weeks due to mishap, and you had been so kind to look after my plants both in the growth chamber and in the glasshouse. Susanna, your kindness and friendliness are sincerely appreciated.

I also extend my thanks to the following: Dr Peter Farley for his kind assistance in the use of the Fluorostar plate reader for my phosphate assay; Associate Professor Al

Rowland, Chad Johnson and Suzanne Lambie for their valuable help in the confocal microscopy; Dr. Don Hunter for his kind assistance in the MUG assay; Dr Sarah Dorling for sharing her expertise in protein works, and for some constructive comments towards the improvement of my oral presentation skills; and Trish McLenahan for sharing some valuable techniques in molecular biology.

I am also thankful to all members of the MTM lab, namely, Sarah, Susanna, Matt, Fiona, Rachael, Jan, Elizabeth, Aluh, Ludivine, Phuong, Jaruwan, and,Sam, for the friendship, and for maintaining a lab atmosphere conducive for scientific pursuit for the time being.

My gratefulness also goes to some kindhearted people of the IMBS, namely: Dr. Kathryn Stowell, Pat Munro, Cynthia Cresswell and Ann Truter, for efficiently sharing bits of relevant information from time to time, and for the ready help with smiles each time their assistance is sought for.

This acknowledgement wouldn't be complete without mentioning the funding bodies particularly the Massey Doctoral Scholarship, and the Foundation for Research Science and Technology, which provided the research/study grant. Special thanks also to the New Zealand Society of Plant Biologists (NZSPB), New Zealand Society of Biochemistry and Molecular Biology NZSBMB), and IMBS, Massey University for providing the travel grants for attending conferences either local or international.

Finally, I am sincerely thankful to Lando, my husband, and my three lovely sons RJ, Joshua and Johnuel for their love and encouragements that serve as my life inspiration to strive further.

Table of Contents

List of Figures

List of Tables

List of Abbreviations

1^{o}Ab	Primary antibody
2^{o}Ab	Secondary antibody
A_{260}	Absorbance at 260 nm
A_{595}	Absorbance at 595 nm
ACC	1- aminocyclopropane-1-carboxylic acid
ACO	ACC oxidase
ACS	ACC synthase
Adomet	*S*-adenosyl-$_{L}$-methionine
AHK	*Arabidopsis* histidine kinase
AM	Apical meristem
Amp^{100}	Ampicillin (100 $mg.ml^{-1}$)
APS	Ammonium persulfate
APase	Acid phosphatase
ARR	Amplex red reagent
Au	Arbitrary unit
AVG	Aminoethoxyvinylglycine
6-BAP	6-Benzylamino purine
BCIP	5 bromo-4-chloro-3-indolyl phosphate
bp	Base pair
BME	2-β-Mercaptoethanol
BSA	Bovine serum albumin
^{O}C	Degrees Celsius
ca	Approximately
CaMV	Cauliflower mosaic virus
Cef^{300}	Cefotaxime ($300mg.ml^{-1}$)
cm	Centimetre
CTR	Constitutive triple response
dATP	2′ deoxyadenosine 5′-triphosphate
dCTP	2′deoxycytidine 5′-triphosphate
dGTP	2′deoxyguanosine 5′-triphosphate
DEPC	Diethyl pyrocarbonate
DMF	Dimethylformamide

DMSO	Dimethyl sulfoxide
DNase	Deoxyribonuclease
dNTP	Deoxynucleotide triphosphate
DPX	Dibutyl phthalate xylene
DTT	Dithiothreitol
DW	Dry weight
E. coli	*Echerichia coli*
EDTA	Ethylenediaminetetraacetic acid
EFE	Ethylene forming enzyme
EIN	Ethylene insensitive
ELISA	Enzyme-linked immunosorbent assay
ETOH	Ethanol
ETR	Ethylene triple response
EtBr	Ethidium bromide
FAA	Formalin acetic acid
FU	Fluorescence unit
FW	Fresh weight
g	g force
GFP	Green fluorescent protein
GMO	Genetically modified organism
GUS	*E. coli* β-Glucuronidase
h	Hour
HCl	Hydrochloric acid
HRP	Horse radish peroxidase
IAA	Indole-3-acetic acid
IPTG	Isopropyl-β-$_D$ – thiogalactopyranoside
Kan^{200}	Kanamycin (200 $mg.ml^{-1}$)
Kb	Kilo basepair
kDa	Kilo daltons
K_M	Substrate concentration at half maximum reaction rate
kPa	kilo Pascal
L	Litre
LB	Luria-Bertani (media or broth)
LR	Lateral root

LRP	Lateral root primordium
M	Molar, moles per litre
MACC	1-(malonylamino) cyclopropane-1-carboxylate
MADS	The conserved domain of MCMI, AGAMOUS, DEFICIENS and SRF
MAPK	Mitogen activated protein kinase
1-MCP	1-methylcyclopropene
MDH	malate dehydrogenase
mg	milligram
Milli-Q water	water purified by a Milli-purification system
min	Minute
mL	Millilitre
Mr	Relative molecular mass (g/mol)
MR	Main root
MS	Murashige and Skoog base media
MUG	4-methyl umbelliferyl glucuronide
n	Number of replicates
NAA	1-naphthaleneacetic acid
NAD	Nicotinamide adenine dinucleotide
NaOAc	Sodium acetate
NBT	Nitrotetrazolium blue chloride
NCBI	National Center for Biotechnology Information
nL	Nanolitre
ng	Nanogram
nmol	Nanomole
NOS	Nopaline synthase
npt II	Neomycin phosphotransferase II
OD_{600}	Optical density 600 nm
ORF	Open reading frame
PAGE	Polyacrylamide gel electrophoresis
PBS	Phosphate buffered saline
PBST	Phosphate buffered saline-Tween 20
PCR	Polymerase chain reaction
PEPC	Phosphoenolpyruvate carboxylase

PGU	Plant Growth Unit
pH	-Log [H^+]
Pi	Inorganic phosphate, orthophosphate
PI	Propidium iodide
ppm	Parts per million
PVDF	Polyvinylidine difluoride
RACE	3'- rapid amplification of cDNA ends
RH	Relative humidity
Rnase	Ribonuclease
RO	Reverse osmosis
rpm	Revolutions per minute
RT-PCR	Reverse transcriptase- polymerase chain reaction
SAM	Shoot apical meristem
SAP	Shrimp alkaline phosphatase
SDS	Sodium dodecyl sulphate
s.e.	Standard error of the mean
SSC	Saline sodium citrate
SSPE	Saline sodium phosphate EDTA buffer
sqRT-PCR	Semi-quantitative RT-PCR
TAE	Tris-Acetate-EDTA
TBA	Tertiary butyl alcohol
TEMED	N, N, N', N'-tetramethylethylenediamine
TR-ACO	*Trifolium repens* ACC oxidase
TR-ACS	*Trifolium repens* ACC synthase
Tris	Tris(hydroxymethyl)aminomethane
µg	Microgram
µl	Microlitre
µM	Micromolar
µm	Micrometer
UTR	Untranslated region
UV	Ultraviolet light
v/v	Volume per volume
WT	wild type

w/v	Weight per volume
w/w	Weight per weight
X-Gal	5-Bromo-4-chloro-3-indolyl β-$_D$-galactopyranoside
X-Gluc	5-Bromo-4-chloro-3-indolyl β-$_D$-glucuronide cyclohexylamine salt
YM	Yeast Mannitol

Chapter 1
Introduction

1.1 Overview

Ethylene is a gaseous plant hormone produced in different parts of the plant and is involved in the regulation of various plant developmental processes including seed germination, root elongation, leaf senescence and abscission, as well as fruit ripening. Ethylene is also produced in response to various forms of stress Abeles *et al.*, (1992). These multi-faceted roles indicate the complexity of the mechanisms involved in the synthesis and action of ethylene.

Briefly, ethylene biosynthesis starts from the amino acid methionine which is converted to *S*-adenosyl methionine (SAM) then to 1-aminocyclopropane-1-carboxylic acid (ACC) and finally to ethylene (Adams and Yang, 1979). Within each step, intricate mechanisms are involved which regulate biosynthesis particularly the last two steps involving the two key enzymes, the ACC synthase (ACS) (E.C.4.4.1.14) which is involved in the conversion of SAM to ACC, and the ACC oxidase (ACO) (E.C.1.4.3) which mediates the conversion of ACC to ethylene. Evidence has accumulated that, in many plants, expression of members of the *ACS* and *ACO* gene families are spatially and temporally regulated. For instance, in white clover, both the *ACS* and *ACO* gene families are differentially regulated during leaf developmental stages and in response to environmental cues (Hunter *et al.*, 1999; Gong and McManus, 2000; Murray and McManus, 2005; Chen and McManus, 2006).

The involvement of ethylene in plant responses to changes in phosphorus availability, specifically in the plant roots, has also been investigated in a number of plants (Lynch and Brown, 1997; Borch *et al.*, 1999; Ma *et al.*, 2003; Zhang *et al.*, 2003; Franco-

Zorrilla *et al.*, 2004; Muller and Schmidt, 2004). In *Arabidopsis thaliana*, for example, ethylene is involved in the regulation of root elongation (Ma *et al*. 2003) and increased root hair density (Zhang *et al*. 2003) in response to P deficiency. These findings provide useful leads for investigations of ethylene-phosphate interactions, using white clover as the model plant.

White clover is a low-growing forage legume with a stoloniferous growth habit. In combination with rye grass, it provides an excellent quality pasture for cattle, beef, or sheep (Baker and Williams, 1987), making this legume the most important member of approximately 300 species of the genus *Trifolium*. However, this pasture species generally has a lesser ability to acclimatise to low levels of soil P which makes it less competitive when compared to the companion grasses (Jouany *et al.*, 2004). In order to improve the persistence of white clover in pastures and make production more sustainable, various studies have been undertaken examining the phoshate uptake, transport and utilisation in this pasture legume (Bowling and Dunlop, 1978; Caradus and Snaydon, 1987; Lotscher and Hay, 1996, 1996; Almeida *et al.*, 1999). Aspects of white clover response to low P nutrition have also been characterised. These studies revealed that the white clover leaf is the main sink of the Pi absorbed by the roots (Caradus and Snaydon, 1987), that there is a reduction of photosynthesis at lower concentrations of Pi (Bowling and Dunlop, 1978; Almeida *et al.*, 1999), and that there is an increased secretion and production of phytases as well as acid phosphatases (APases) in the roots during conditions of Pi deficiency (Caradus and Snaydon, 1987, Hayes *et al.*, 1999; Hunter and McManus, 1999; Zhang and McManus, 2000).
However, there have been no studies on the regulation of ethylene biosynthesis by Pi supply in white clover, but given the importance of the hormone in regulating the plant responses to Pi, such a study is warranted.

1.2 The gaseous hormone ethylene in plant development

Ethylene is one of the simplest organic molecules that exhibit significant biological activities. It is a hydrocarbon gas which is produced by different parts of the plant in response to a range of internal developmental cues and external stress factors (Alonso and Stepanova, 2004). This gaseous phytohormone elicits a wide range of physiological phenomena and induces diverse effects in plants throughout their life cycle (Sato and Theologis, 1989; Abeles *et al.*, 1992; Johnson and Ecker, 1998). The most common of these occur during fruit ripening, seed germination, leaf senescence and abscission (Abeles and Rubinstein, 1964; Bleecker and Kende, 2000; Alexander and Grierson, 2002; Adams-Phillips *et al.*, 2004). The role of the hormone in epidermal cell patterning and as a positive regulator for root hair development has also been implicated previously (Heidstra *et al.*, 1997; Michael, 2001).

Transport of ethylene within the plant tissues is largely by diffusion either in the gaseous form or in solution (Johnson and Ecker, 1998). In the root, ethylene passes from the inner root through the apoplast, to the intercellular spaces, and then through the cell wall. From the cell wall, it goes into the rhizodermal cells and depending on the conditions for gas exchange, to the rhizosphere (Michael, 2001). It travels from cell to cell either in the symplast and phloem, or diffuses through the air spaces between the cells (Johnson and Ecker, 1998) .

To better understand how this plant hormone is synthesised and perceived by plants and how it influences plant growth and development, the ethylene biosynthetic pathway, and the characterisation of the key enzymes involved in the pathway are introduced in the subsequent sections.

1.2.1 Ethylene biosynthesis

Ethylene biosynthesis is regulated by environmental and endogenous signals. Plants normally produce basal level of ethylene throughout development (Abeles *et al.*, 1992) but those exposed to biotic and abiotic stressors have been found to generate increased levels of ethylene (Kim *et al.*, 1998).

The biosynthetic pathway of ethylene (Figure 1) begins with the formation of *S*-adenosyl-$_L$-methionine (SAM) which is catalysed by SAM synthetase (E.C.2.5.1.6) from the amino acid methionine (Adams and Yang, 1979) and then to ACC. The participation of ACC in the pathway as the immediate precursor to ethylene was discovered when $_L$-[U-^{14}C] methionine was fed to apple tissue. In these studies, ACC was metabolised to ethylene in air but when incubated in nitrogen, the labeled methionine was only converted to ACC but not to ethylene. The conversion of SAM to ACC is deemed to be the rate-limiting step in the biosynthetic pathway which is mediated by the enzyme ACS (Kende, 1989). Methylthioadenosine (MTA) is a by-product generated along with ACC production (Adams and Yang, 1979; Yang and Hoffman, 1984), and the recycling of MTA back to methionine conserves the methylthio group and, through this process, a constant concentration of cellular methionine is maintained even when ethylene is being rapidly synthesised (Wang *et al.*, 2002).

The second and final committed step in the biosynthetic pathway is the oxidative cleavage of ACC to form ethylene (Figure 1) and this is catalysed by the enzyme ACO, originally known as the ethylene forming enzyme (Hoffman *et al.*, 1982). This step also generates carbon dioxide and cyanide. The genes coding for ACS and ACO can be transcriptionally regulated by various forms of stimuli such as wounding, pathogen

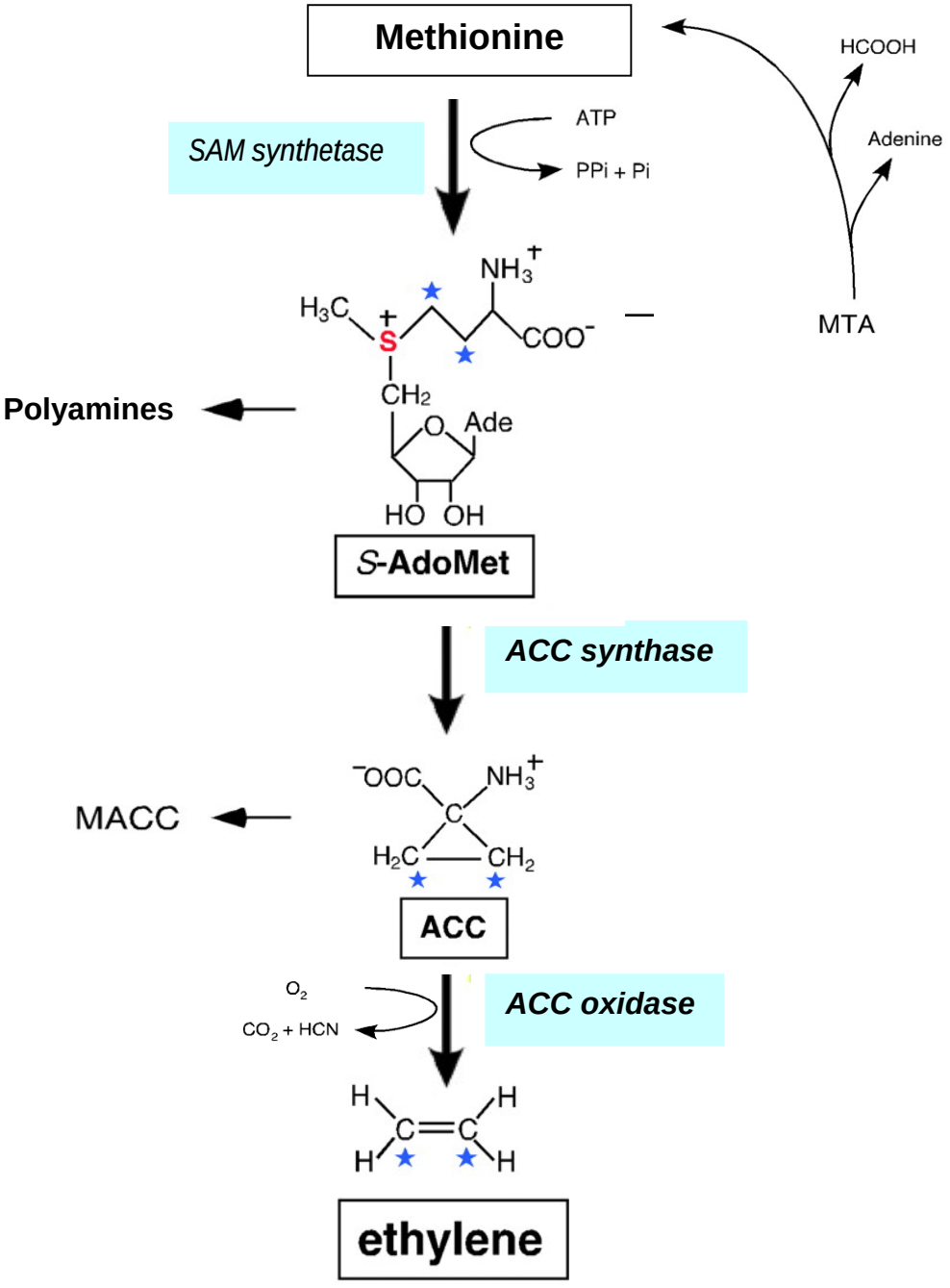

Figure 1. 1 The Ethylene biosynthetic pathway.

ACC = 1-aminocyclopropane-1-carboxylic acid
S-Adomet = S-adenosyl methionine
MTA = 5'methylthioadenosine
MACC = 1-malonylamino cyclopropane-1-carboxylic acid

infection, exposure to UV, and other forms of stress both biotic and abiotic (Kim *et al.*, 1998; Klee, 2002; Wang *et al.*, 2002). Some highlights of studies on the effect of these stimuli on gene regulation as well as the biochemical characterisation of these two enzymes are presented in the subsequent sections.

1.2.2 The enzyme ACC synthase

The first committed step in ethylene biosynthesis is the production of the non-protein amino acid ACC from SAM. This process is mediated by ACS, a pyridoxal-5′ phosphate requiring enzyme, which is present in cytosolic fractions (Adams and Yang, 1979). Like other enzymes requiring pyridoxal 5′-phosphate, ACS is sensitive to inhibitors of pyridoxal 5′-phosphate especially aminoethoxyvinylglycine (AVG) and aminoethoxyacetic acid (AOA) (Buchanan *et al.*, 2000).

With the discovery of ACC as an intermediate in the biosynthetic pathway, subsequent difficulty in the purification of ACS and cloning of the corresponding gene was then a major obstacle to understanding the role of the enzyme in the ethylene biosynthetic pathway in higher plants. This impediment was alleviated by raising antisera against partly purified ACS from zucchini fruit. The ACS antibodies were then used to isolate the first gene encoding the ACS enzyme (Sato and Theologis, 1989). After the gene encoding ACS had been cloned, it was used to express the ACS protein in *E. coli* at high levels and then purified ACS could be isolated in larger amounts (Sato et al. 1991). At the same time, ACS from tomato pericarp was also purified 5000-fold, expressed in *E.coli* and the denatured recombinant polypeptide was also used to raise polyclonal antibodies (Van der Straeten *et al.*, 1990). A full-length cDNA clone encoding ACS was then isolated from tomato pericarp (Van der Straeten *et al.*, 1990). The second isoform with complete nucleotide and derived amino acid sequences of a cDNA encoding ACS

from tomato fruits was reported in the following year (Olson *et al.*, 1991). Expression of transcripts encoding these two ACS isoforms was enhanced under two conditions, namely during fruit ripening and in response to mechanical stress, specifically wounding.

A range of cDNAs encoding *ACS* genes from various plant species and expression studies have now been cloned. Two different *ACS* genes identified as auxin-induced and wound-induced were purified from immature cucumber fruits and these genes were differentially expressed in the fruits (Nakagawa *et al.*, 1991). A year later, five genomic sequences encoding different polypeptides were identified in the *Arabidopsis.* Each of these genes is located on a different chromosome in the genome, and is differentially expressed in response to a variety of stimuli during plant development (Liang *et al.*, 1992). To date, 12 members of the ACS gene family have been isolated from *Arabidopsis* (Peng *et al.*, 2005). These genes have been mostly characterised, and were found to be responsive to a range of stimuli (Yamagami *et al.*, 2003; Peng *et al.*, 2005). For example, four of these genes, the *At-ACS2*, *At-ACS6, At-ACS7*, and *At-ACS9* were induced during hypoxia (Peng *et al.*, 2005).

1.2.3 Regulation of expression of ACC synthase genes

The spatial and temporal expression of the multi gene family of *ACS* has been found to be induced by a diverse group of stimuli such as wounding, pathogen infection and plant hormones particularly auxin and ethylene (Moeder *et al.*, 2002). Some reports showing that pathogen infection causes upregulation of the ACS gene include studies on citrus petals (Lahey *et al.*, 2004), and *Nt-ACS* in the leaves of tobacco infected with cucumber mosaic virus (Knoester *et al.*, 1995; Chaudhry *et al.*, 1998).

Evidence has now accumulated that wounding induces ACS activity and mRNA accumulation in various plants organs. However, differential expression depends on the plant species and the specific gene within a family of ACS. In bamboo shoots, for example, the *pBA-ACS* gene was significantly upregulated within 8 h after cutting and this occurred almost concurrently with an induction in ethylene production (Bhowmik and Matsui, 2005).

A relatively different pattern of ACS gene expression has been noted in Valencia orange. While *CS-ACS2* was constitutively expressed up to six days after detachment of the leaves, *CS-ACS1* was significantly expressed 7–12 d after severing the leaves from the plant (Katz *et al.*, 2005). In mungbean hypocotyls, expression of both *VR-ACS1* and *VR-ACS6* were stimulated by wounding, reaching a peak after about one hour and sustaining that effect for about six hours (Song *et al.*, 2003). In Japanese pear (*Pyrus pyrifolia* Nakai cv. Nijisseiki), activity of *PP-ACS3* was relatively low during ripening but was highly expressed in response to wounding (Itai *et al.*, 2003).

The *ACS* genes in other plants were also highly expressed in response to wounding such as in peach (Jin *et al.*, 2002), potato tubers (Destefanobeltran *et al.*, 1995), winter squash (Kato *et al.*, 2000), broccoli florets (Kato *et al.*, 2002), asparagus (Bhowmik and Matsui, 2004), and in persimmon fruits (Zheng *et al.*, 2005). In contrast, the wound induced upregulation of *DK-ACS2* gene in mature persimmon fruit was negatively regulated by ethylene and *DK-ACS2* gene expression was markedly increased by a treatment with 1-MCP (1-MCP), an inhibitor of ethylene perception (Zheng *et al.*, 2006) indicating that in some plants regulation of ACS can be controlled by ethylene itself.

Exogenous plant hormones have also been found to be inducers of *ACS* gene expression. Some members of the *ACS* gene family in *Arabidopsis* are responsive to

hormone treatment (Wang *et al.*, 2005). For example, treatment with indole-3- acetic acid (IAA) has been reported to induce expression of all three ACS genes in cucumber fruit (Shiomi *et al.*, 1998) and in the hypocotyls of potato (Destefanobeltran *et al.*, 1995). Auxin-inducible expression of *ACS* gene has also been observed in many plants such as mungbean (Yoon *et al.*, 1999; Kim *et al.*, 2001; Song *et al.*, 2005), broccoli (Kato *et al.*, 2002), tobacco (Yoon *et al.*, 1999), and white clover (Murray and McManus, 2005). The enhanced production of ACS by auxin also promotes ethylene synthesis. This induction of *ACS* is inhibited by both protein and RNA synthesis inhibitors, implying that auxin acts to upregulate transcription (Buchanan *et al.*, 2000).

ACS gene appears to be the principal target of ethylene during both autocatalysis and autoinhibition. The gene is upregulated during ripening of climacteric fruits such as tomato (Alexander and Grierson, 2002) and pawpaw (Koslanund *et al.*, 2005). Ethylene itself can also enhance the expression of *ACS* genes in tobacco after pollination (Sanchez and Mariani, 2002; Weterings *et al.*, 2002), in cut flowers of roses (*Rosa hybrida*) (Ma *et al.*, 2005), or during ripening. For example, three days following harvest of persimmon fruit, *DK-ACS2* increased significantly (Zheng *et al.*, 2005)

In white clover, the three members of the *ACS* gene family were found to be developmentally regulated during leaf ontogeny (Murray and McManus, 2005). It is now known that *TR-ACS1* is expressed in the apical structure of the stolon, in mature-green leaf tissue and in leaf tissue at the onset of senescence, and that this gene is regulated by exogenous application of auxin. On the other hand, *TR-ACS2* is expressed in the apical structure of the stolon and in the newly initiated leaf tissue, whereas *TR-ACS3* is predominantly expressed in the senescent leaf tissue (Murray and McManus, 2005).

The expression of *ACS* genes in carnation flower was also found to be differentially regulated in a tissue-specific manner. *DC-ACS2* and *DC-ACS3* were preferentially expressed in styles, whereas *DC-ACS1* mRNA was most abundant in petals (Jones and Woodson, 1999).

While the aforementioned stimuli were found to upregulate *ACS* genes, there are also treatments that can down regulate the gene. For instance, exposure of broccoli florets to high temperature suppresses *ACS* gene expression thereby inhibiting ethylene production (Suzuki *et al.*, 2005).

Taken together, these findings emphasise the complexity of the processes involved in the regulation of *ACS* genes and highlight the significance of the role played by ACS in the regulation of the ethylene biosynthetic pathway.

1.2.4 ACC oxidase: its identification and cloning

The conversion of ACC to ethylene is catalysed by the enzyme ACO, previously referred to as the "ethylene forming enzyme" (EFE). Originally, the activity of the EFE was proposed to be highly regulated in the plant cell and that it was localised in the cell wall-cell membrane complex of plant tissues (Mattoo and Lieberman, 1977). Assays of EFE activity *in vivo* had been carried out successfully in the past decades, but there had been difficulty in conducting the assay *in vitro* since the activity of the enzyme completely disappeared during extraction (Yang and Hoffman, 1984).

While it has been suggested that vacuoles isolated from pea leaves produced 80% of the ethylene evolved by protoplasts (Guy and Kende, 1984), a very small percentage (<5%) of the EFE activity *in vivo* was retained in the protoplast and it appeared that a significant proportion of the activity was unaccounted for (Porter *et al.*, 1986). An early

concept was that the enzyme converting ACC to ethylene was membrane-bound and that its activity required membrane integrity (Kende, 1989). The instability of this enzyme and the difficulty of its purification by conventional techniques was then attributed to the loss of co-factors (Buchanan *et al.*, 2000). This reaction was also shown to be oxygen-dependent and, therefore, under anaerobic conditions ethylene formation was suppressed (Bradford and Yang, 1980; English *et al.*, 1995)

The idea that the EFE enzyme is membrane-bound (Apelbaum *et al.*, 1981) and that EFE activity completely disappears when membrane integrity is lost (Mayne and Kende, 1986; Kende, 1989) remained a proposition until a putative cDNA clone for tomato EFE was identified, purified, and a molecular probe became available. The first cDNA clone for EFE was isolated from ripe tomato and this was designated as pTOM13 (Holdsworth *et al.*, 1987). Several investigations were conducted to confirm that this gene does encode the enzyme which catalyses the last step in ethylene biosynthesis. A significant breakthrough occurred when antisense cDNA of pTOM13 was introduced into tomato, and analysis of transgenic tomato plants showed that the biosynthesis of *ACO* was obstructed and ethylene production was inhibited (Hamilton *et al.*, 1990).

Enzyme activity was further confirmed by heterologous expression of the cloned gene in yeast (*Saccharomyces cerevisiae)* (Hamilton *et al.*, 1991) and *Xenopus* oocytes (Spanu *et al.*, 1991) and, in these studies, it was determined that the characteristics and activities of EFE were similar to the EFE found in plant tissues.

Another significant discovery was when the authentic activity of the EFE was fully recovered *in vitro* from melon (*Cucumis melo)* fruits. In this study, the necessity of adding both Fe^{2+} and ascorbate to the aerobic reaction medium to obtain high EFE activities *in vitro* was first highlighted (Ververidis and John, 1991). Following this

study, ACO from apple fruit was purified and a molecular mass of 35 kDa and 39 kDa was determined by SDS-PAGE and by gel filtration, respectively (Dong *et al.*, 1992). These findings provided significant opportunity for other researchers to conduct various interrelated studies on ACO involving a wide range of plants including fruits (Peck *et al.*, 1992; Ross *et al.*, 1992; Barry *et al.*, 1996; Lasserre *et al.*, 1996; Dunkley and Golden, 1998; Rasori *et al.*, 2003); vegetables (Gomez-Jimenez *et al.*, 1998; Jin *et al.*, 1998; Henzi *et al.*, 1999; Gapper *et al.*, 2002; Gapper *et al.*, 2005); cereals (Lutts *et al.*, 1996; Finlayson *et al.*, 1997; Kruzmane and Ievinsh, 1999; Chae *et al.*, 2000); and flowers (Tang *et al.*, 1994; Bailly *et al.*, 1995; Muller *et al.*, 2001).

There have also been various studies on pasture legumes including white clover (Hunter *et al.*, 1999; Yoo, 1999; Gong and McManus, 2000; Chen and McManus, 2005). These authors focused not only on identification and cloning of the gene but also on biochemical characterisation and regulation of gene expression for different members of the *TR-ACO* gene family.

1.2.5 Biochemical characterisation of ACC Oxidase

The enzyme ACO is known to be a non-heme iron-containing protein. It requires oxygen and a ferrous ion (Fe^{2+}) as co-factors, and a reducing agent, ascorbate, which serves as a co-substrate, for maximal activity *in vitro* (Britsch and Grisebach, 1986; McGarvey and Christoffersen, 1992; McGarvey *et al.*, 1992; Jin *et al.*, 1998).

Studies showed that the optimal activity of ACO in a range of plant tissues varies depending on the concentration of these co-factors and co-substrates. In pear fruit for instance, 15 mM ascorbate and 25 μM Fe^{2+} were shown to be optimal when used as co-substrate and co-factor, respectively (Kato and Hyodo, 1999). In mungbean hypocotyl, inclusion of 100 mM MOPS (pH 7.5), 25 μM $FeSO_4$, 6 mM sodium ascorbate, 1 mM

ACC, 5 mM sodium bicarbonate and 10% (v/v) glycerol in the assay medium enhanced ACO activity (Jin *et al.*, 1998).

Carbon dioxide, which is one of the products of ethylene biosynthesis, has also been shown to enhance ACO activity at a certain level, and is then inhibitory at higher concentrations (Finlayson and Reid, 1996; Buchanan *et al.*, 2000; de Wild *et al.*, 2005). The presence of 5% (w/v) polyvinyl polypyrrolidone (PVPP) in the extraction medium was also deemed essential to obtain an active ACO enzyme from apple tissue (Kuai and Dilley, 1992). In mung bean root tissue, exogenous calcium has been shown to be involved in the activation of ethylene-induced ACO (Jung *et al.*, 2000) .

The inclusion of dithiothreitol (DTT) and sodium bicarbonate in the assay medium was also found to significantly enhance ACO activity in *Carica papaya* and in breadfruit (*Artocarpus altilis*) (Dunkley and Golden, 1998; Williams and Golden, 2002). These findings indicate that the activity of the ACO is influenced by a wide range of inducers. However, there are also reported inhibitors of the ACO enzyme activity, such as cobalt chloride. It was determined that at a concentration of 3 μM, cobalt inhibits ACO activity, and hence lowers ethylene production since cobalt ions compete with iron in the active site of the enzyme (Romera *et al.*, 1996).

Another feature of ACO which has been well studied is the characterisation of its relative molecular mass. Evidence presented shows that the molecular mass of ACO varies slightly among the plant species investigated. In rare cases, the size determined depends upon the method used in characterisation. For instance, the complete coding region of pTOM13 protein, which was isolated from ripe tomato, had a deduced molecular mass of 33 kDa (Holdsworth *et al.*, 1987). By gel electrophoresis, it was found that ACO protein from papaya had a molecular mass of *ca* 28 kDa (Dunkley and

Golden, 1998). This was relatively small when compared with the ACO from pear which is 40 kDa (Kato and Hyodo, 1999) and melon which is 41 kDa (Smith *et al.*, 1992) as determined by SDS-PAGE and gel filtration, respectively.

Most ACOs isolated from other plant species fall within the range of 35 kDa to 39 kDa in size. Examples include an ACO from Arabidopsis which is *ca.* 37 kDa (Gomez-Lim *et al.*, 1993), chick pea at *ca.* 36 kDa (Gomez-Jimenez *et al.*, 1998), turnip at *ca.* 37 kDa (Rodriguez-Gacio *et al.*, 2004), rice seedlings at *ca.* 36 kDa (Chae *et al.*, 2000), and apple cortical tissue at *ca.* 35 kDa (Ross *et al.*, 1992) while an ACO from apricot (*Prunus armeniaca* cv. Bergeron) had a calculated molecular mass of *ca.* 36 kDa (Mbeguie-A-Mbeguie *et al.*, 1999). By immunoblot analysis with monospecific antibodies raised against a tomato ACO expressed in *Escherichia coli,* ACO in tomato (*Lycopersicon esculentum* Mill.) was estimated to have a molecular mass of 36 kDa (Reinhardt *et al.*, 1994). The TR-ACO2 which was isolated from white clover leaf also falls within the range, having a size of 36.4 kDa (Hunter *et al.*, 1999). Similarly, two ACO isoforms purified from mature green leaf tissue (MGI) and senescent leaf tissue (SEII) of white clover, were found to have molecular mass of 37 kDa (MGI) and 35 kDa (SEII), respectively, as determined by SDS-PAGE (Gong and McManus, 2000).

1.2.6 The ACC oxidase gene family and gene structure

Increasing interest in understanding the biochemical and physiological functions of ACO have inspired a number of researchers to characterise *ACO* genes. To date, multi-gene families of ACOs have been identified and characterised in different plants such as in tomato (Barry *et al.*, 1996, Blume and Grierson 1997), melon (Lasserre *et al.*, 1997), sunflower (Liu *et al.*, 1997), *Nicotiana glutinosa* (Kim *et al.*, 1998), apricot (Mbeguie-A-Mbeguie *et al.*, 1999), cucumber (Kahana, 1999), *Rumex palustris* (Vriezen *et al.*,

1999), mungbean (Jin *et al.,* 1999), white clover (Hunter and McManus, 1999; Gong and McManus, 2000; Chen, 2005; Chen and McManus, 2006), and rice (Chae *et al.*, 2000). Further, *ACO* genes have also been characterised in broccoli florets (Kato *et al.*, 2002; Gapper *et al.*, 2005), apple fruit (Chung, 2002), carnation flowers (Kosugi *et al.*, 2002), potato (Zanetti *et al.*, 2002), papaya (Chen *et al.,* 2003, Lopez-Gomez, 2004), peach (Rasori *et al.,* 2003), turnip (Roriguez-Gacio *et al.,* 2004), citrus fruits (Katz *et al.,* 2004), and banana (Pathak *et al.*, 2003).

From among the published reports reviewed in this study so far, it appears that the members of the *ACO* gene family from different plants varied from one to four. In tomato, the three members of the *ACO* gene family, designated as *LE-ACO1, LE-ACO2* and *LE-ACO3*, have been reported to be all transcriptionally active. The protein coding sequences of these three genes are identical and sequence divergence was noted only within the 3′ untranslated regions (Barry *et al.*, 1996). Similarly, there are also three members of the melon *ACO* gene family. The coding region of *CM-ACO1* is organized into 4 exons interrupted by 3 introns while the *CM-ACO2* and *CM-ACO3* genes only have two introns. In relation to *CM-ACO1*, the degree of identity of the other two genes is more than 50% but all the three genes are actively transcribed (Lasserre *et al.*, 1996).

In papaya, at least two members of the *ACO* gene family have been characterised. They share 77% identity over their deduced amino acid sequences. The *CP-ACO2* gene exists as a single copy in the papaya genome and has been shown to be inducible by ethylene and wounding (Chen *et al.*, 2003). There are four members of the *ACO* gene family in petunia, but only three are expressed. These are designated as *PH-ACO1, PH-ACO3* and *PH-ACO4,* and are identical in their promoter sequences. The other gene, designated as *PH-ACO2,* was identified as a pseudogene, being transcriptionally inactive (Tang *et al.*,

1994). There are two members of the *ACO* gene family from peach, *PP-ACO1* which is structured with four exons interrupted by three introns and *PP-ACO2* which has only two introns. These two genes show a high degree of identity to the *ACO* genes of petunia and apple (Ruperti *et al.*, 2001).

1.2.7 Differential expression of ACC oxidase genes and promoter analyses

In an effort to identify the regulatory elements and further study developmental control affecting *ACO* gene expression in various plant species, the 5′ non-coding sequences of the cloned *ACO* genes have been further investigated. Promoter sequences of *ACO* genes from a number of plant species have been characterised through fusion of the various lengths of the 5′ flanking regions to the coding sequence of a reporter gene such as the β- glucuronidase (GUS) gene to study spatial and temporal expression in plants. By the time this study was conducted, functional analysis of the promoter sequences of *ACO* genes from some plants such as tomato (Blume and Grierson, 1997), melon (Lasserre *et al.*, 1997), apple (Atkinson *et al.*, 1998), peach (Rasori *et al.*, 2003) and white clover (Chen and McManus, 2005) had been undertaken.

The temporal and spatial expression patterns of two *ACO* genes isolated from melon was studied by fusing the 726 bp and 2260 bp promoter regions of the *CM-ACO1* and *CM-ACO3* genes, respectively to the GUS reporter gene. These chimeric constructs were introduced into tobacco plants and functional analyses of gene expression using independent transgenic lines was carried out. Results showed that the 726 bp fragment of the *CM-ACO1* promoter was able to drive GUS expression in response to wounding and ethylene treatment, and in response to pathogen infection. In contrast, the *CM-AC03* promoter did not direct any GUS expression in response to infection. Instead, the promoter drove strong GUS expression in green, fully expanded leaves. This gene was

upregulated during flower development and down regulated at the onset of senescence (Lasserre *et al.*, 1997). It was thus suggested that the regulation of expression of *CM-AC01* is stress-related whereas the expression of *CM-AC03* is developmentally regulated (Lasserre *et al.*, 1997).

To further investigate induction of the *CM-ACO1* gene by wounding and ethylene, another chimeric construct carrying a shorter (476 bp) promoter sequence fused to the GUS reporter gene was used (Bouquin *et al.*, 1997). Both constructs (476 bp and 726 bp promoters) were used to transform tobacco. Following wounding and ethylene treatments, induction of promoter-driven GUS activity in transgenic lines harbouring either the longer (726 bp) or shorter (476 bp) promoter was analysed. A 2.7-fold induction of GUS activity was observed in the transgenic line transformed with the 726 bp promoter-GUS fusion whereas the transformed lines with the shorter (476 bp) promoter had no GUS expression (Bouquin *et al.*, 1997). This implies that the wound inducible element is present within the 250 bp deleted region between – 476 and – 726 bp. When the same transgenic lines harbouring 476 bp and 726 bp promoter sequences were subjected to ethylene treatment, GUS activity was increased by 3.3 and 7-fold, respectively. It was also noted that this ethylene-induced GUS activity was strongly inhibited by 1-methylcyclopropene (1-MCP) whereas the wound-induced GUS expression was not. Altogether, these findings indicate that the regulation of the *CM-ACO1* gene in melon by wound and ethylene treatment followed two independent signal transduction pathways (Bouquin *et al.*, 1997).

Using one member of the *ACO* gene family in tomato, Blume and Grierson (1997) investigated how this gene is regulated. Three different chimeric constructs were made consisting of the GUS gene fused to the 97 bp 5′ UTR region plus 124 bp, 396 bp, and

1825 bp of the *LE-ACO1* promoter sequence. These constructs were used to transform tomato (*Lycopersicon esculentum)* and *Nicotiana plumbaginifolia.* The results indicated that the -124 bp to +97 bp region of the *LE-ACO1* gene is sufficient to induce a low level of GUS activity during fruit ripening. When the longer promoter sequence (1825 bp) was used, a strong and more specific GUS activity was observed. A similar pattern of expression as observed in tomato flowers and leaves was noted in *N. plumbaginifolia* (Blume and Grierson, 1997) suggesting that the *LE-ACO1* promoter is able to induce similar expression patterns in a heterologous host.

Promoter activity in an apple *ACO* gene has also been characterised by deletion analysis to investigate how the gene is regulated during ripening (Atkinson *et al.*, 1998). The *ca* 2 kb promoter sequence of *MD-ACO* gene was isolated and sequences of various lengths such as 450 bp, 1159 bp and 1966 bp of the 5′ promoter sequence were fused to the GUS reporter gene. These three different chimeric constructs were then used to transform tomato. Deletion analysis showed that the promoter sequence consisting of the -450 bp region was able to drive GUS expression, but this expression was not specific to the fruit, while the larger fragments of –1159 bp and -1966 bp regions conferred fruit and ripening-specific expression in transgenic tomato. These results suggest that the element that direct ripening-specific gene expression in tomato is located within the –1159 and –450 bp region of the *MD-ACO* promoter.

Recently, the promoter sequences of the four members of *ACO* gene family in white clover have been cloned and characterised by Chen and McManus (2006) and highlights of these results are briefly outlined in Section 1.2.1.6. Altogether, these findings on promoter studies suggest that the *ACO* genes in various plant species are differentially regulated, and while some members of the *ACO* gene family are regulated by different

forms of stressor including ethylene itself, other members of the gene family are regulated by developmental cues.

1.2.8 Localisation of ACC Oxidase

The specific localisation of ACO in the plant cell has been a matter of deliberation for many years. The earliest notion was that ACO was membrane-bound (Yang and Hoffman, 1984). Later, it was proposed that the enzyme was associated with the vacuole and that membrane integrity is required for the enzyme activity, perhaps for a transmembrane ion gradient (Mayne and Kende, 1986). Since the early 1990s, various improved techniques have been used to further examine this issue. Using immunoblot analysis, Peck *et al*. (1992) found that ACO protein is contained in the intact cells and the protoplast. However, there was no evidence that the protein was contained in the vacuole. Further, using cell fractionation techniques followed by immunoblot analysis, Reinhardt *et al.* (1994) determined that the ACO antigen was not present in the vacuole. Instead, most of it was localised in the cytoplasm of the protoplasts without being associated with membranes.

By superimposition of Calcofluor white with immunofluorescence labeling and analysis by optical microscopy, Rombaldi *et al*. (1994) suggested that ACO is located at the cell wall in the pericarp of breaker tomato and climacteric apple fruit. Later, Malerba *et al.* (1995) suggested that ACO was associated with the plasma membrane. To determine the precise location of this enzyme, an immunocytological method was also used by Ramassamy *et al*. (1998) and they demonstrated that apple *ACO* was located on the external face of the plasma membrane. Further, by immunolocalisation experiments in chick-pea with a monoclonal antibody obtained from recombinant ACO, it was

determined that most of the ACO protein was present in the apoplast and not in the vacuole (Gomez-Jimenez *et al.*, 2001).

In apple fruit (var. Golden Delicious), the subcellular localisation of ACO was examined by electron microscopy and immuno-gold-labeled antibodies and it was demonstrated that the location was mainly in the cytosol of the apple fruit pericarp tissue (Chung *et al.*, 2002). Finally, the most recent study confirmed that the ACO of Douglas fir (*Pseudotsuga menziesii*) is a cytosolic protein (Hudgins *et al.*, 2006).

1.2.9 ACC Oxidase in white clover

ACO in white clover (*Trifolium. repens* L.) was not given much attention until Hunter et al.(1999) cloned, characterised and studied the expression pattern of these genes during leaf ontogeny. Three distinct DNA sequences, designated as *TR-ACO1, TR-ACO2,* and *TR-ACO3,* were identified using a combination of reverse transcriptase-polymerase chain reaction (RT-PCR) and 3'- rapid amplification of cDNA ends (RACE). Confirmation that these sequences represent three distinct genes was made through Southern analysis and differential expression was ascertained by northern analysis.

Analyses revealed that *TR-ACO1* was expressed predominantly in the apical structure, *TR-ACO2* was primarily expressed in the newly initiated and mature green leaves, whereas *TR-ACO3* was mainly expressed in the senescing leaves (Hunter *et al.*, 1999). Following the study by Hunter et al. (1999), two isoforms of TR-ACO designated MGI from mature green and SEII from senescent leaf tissues were purified to homogeneity (Gong and McManus, 2000). Studies showed that these isoforms differentially accumulated during leaf development in white clover.

Recently, a fourth member of the *TR-ACO* gene family was isolated and characterised by Chen and McManus (2005). This gene has a very high identity with *TR-ACO3*, displaying 87% similarity when the whole genomic sequence was compared. When all exons of *TR-ACO3* and *TR-ACO4* were compared, the greatest divergences in their coding sequences were found in exon 1 and exon 3. The percentage identites in the sequences in these exons were 89% and 94%, respectively. For exon 2 and exon 4, sequence identities were 99% and 100%, respectively. Both these genes were expressed predominantly in the mature and senescing leaves (Chen, 2005).

Part of the study by Chen and McManus (2006) included cloning and characterisation of the promoter sequences of the four *TR-ACO* genes. Their promoters were designated as *pTR-ACO1 (*1006 bp), *pTR-ACO2* (1510 bp), *pTR-ACO3* (1350 bp), and *pTR-ACO4* (1250 bp). By Southern analysis, it was noted that there are two copies each of the *TR-ACO1* and *TR-ACO2* gene in the genome while each of the *TR-ACO3* and *TR-ACO4* genes exists as a single copy. Analysis *in silico* of each promoter indicated that a high proportion of the domains within the *TR-ACO1* promoter were strongly associated with young developing tissues whereas some domains within the *TR-ACO2* promoter were associated with environmental cues. The other two promoter sequences for the *TR-ACO3* and *TR-ACO4* genes contain domains with a high proportion of wound-associated elements and senescent-related cues such as ethylene response (Chen and McManus, 2006).

All four promoters directed GUS expression in the axillary buds. Tissue-specific expression indicated that the *TR-ACO1* promoter drove GUS expression predominantly in the apex and leaf petiolule in young tissues, the *TR-ACO2* promoter drove expression in mature green tissues, whereas the *TR-ACO3* and *TR-ACO4* promoters directed GUS

expression primarily in the older tissues. Thus it was suggested that the transcriptional regulation of the *ACO* gene family during leaf development in white clover was affected by ontological cues (Chen and McManus, 2006).

Results of these studies on *ACO* genes in white clover further confirm findings of other researches that members of the *ACO* gene family in different plant species are spatially expressed and are primarily regulated by developmental cues. Since these findings were mostly on the leaf and flower developmental stages, it is worthwhile investigating if these genes are also expressed in the roots and if they are differentially regulated by the availability of nutrients, particularly phosphate, which is needed by the plants in relatively large amount.

1.3 Phosphorus: An essential macro nutrient

Phosphorus is an essential nutrient for plant growth and development. It is a key nutrient in the regulation of various plant metabolic processes, both as a reactant and as an effector molecule (Vance *et al.*, 2003; Wasaki *et al.*, 2003). This element plays a significant role in plant energy metabolism and is an important component of the sugar phosphate intermediates of photosynthesis and respiration. It is an important structural constituent of the nucleic acids, and of phospholipids which are vital in the synthesis of plant membranes. Phosphate also plays a very significant role in the activation or inactivation of various enzymes (Buchanan *et al.*, 2000; Raghothama, 2000).

Phosphate is essential both as a substrate and as a regulatory factor in photosynthesis and oxidative metabolism. Evidence has accumulated which suggests that the shortage of P stimulates some adverse effects on cellular metabolism (Shin *et al.*, 2004). Further, this element is known to participate in signal transduction and in the regulation of activities by phosphorylation and dephosphorylation (Buchanan *et al.*, 2000), and

generally, plants exhibit a reduced growth rate when grown at limiting phosphate (Muller *et al.*, 2004).

Phosphorus is taken up and assimilated by plants in the form of orthophosphate (Pi) (Rausch and Bucher, 2002). Although this nutrient is abundant in the rhizosphere, it is one of the least available macronutrients in the soil (Abel *et al.*, 2002). It is often bound in organic esters and a considerable amount interacts with soil constituents such as calcium and aluminum (Vance *et al.*, 2003) making it unavailable for plant use. To offset low P availability in the rhizosphere, plants have evolved an array of morphological, architectural and some biochemical changes in the root system (Figure 1.2). Further, during conditions of low external Pi availability, the Phosphate Starvation Response gene, *PHR1*, which is involved in the induction of Pi starvation inducible (PSI) genes is upregulated (Rubio *et al.*, 2001). These changes occur as a form of coping mechanism in order to maximise efficiency in the acquisition, mobilisation and recycling of Pi, thereby maintaining optimal growth (Abel *et al.*, 2002).

1.3.1 Effect of phosphate on the synthesis of nucleotides and amino acids

P availability strongly affects the synthesis of nucleotides in plant tissues. The cellular levels of ATP and other nucleoside triphosphates are markedly reduced during Pi starvation (Wagner and Backer, 1992). For example, in *Datura* cell cultures deprived of the cellular Pi, the pool of nucleotides was reduced but when the required Pi was added to the cell cultures, nucleotide biosynthesis was re-established (Wylegalla *et al.*, 1985). Similarly, in *Catharanthus roseus* cell cultures, within 24 h after inoculation into a Pi-deficient medium, the ATP, GTP, UTP and CTP pools were reduced by 3- to 5-fold compared with those cells maintained in the Pi sufficient medium (Ashihara *et al.*, 1988).

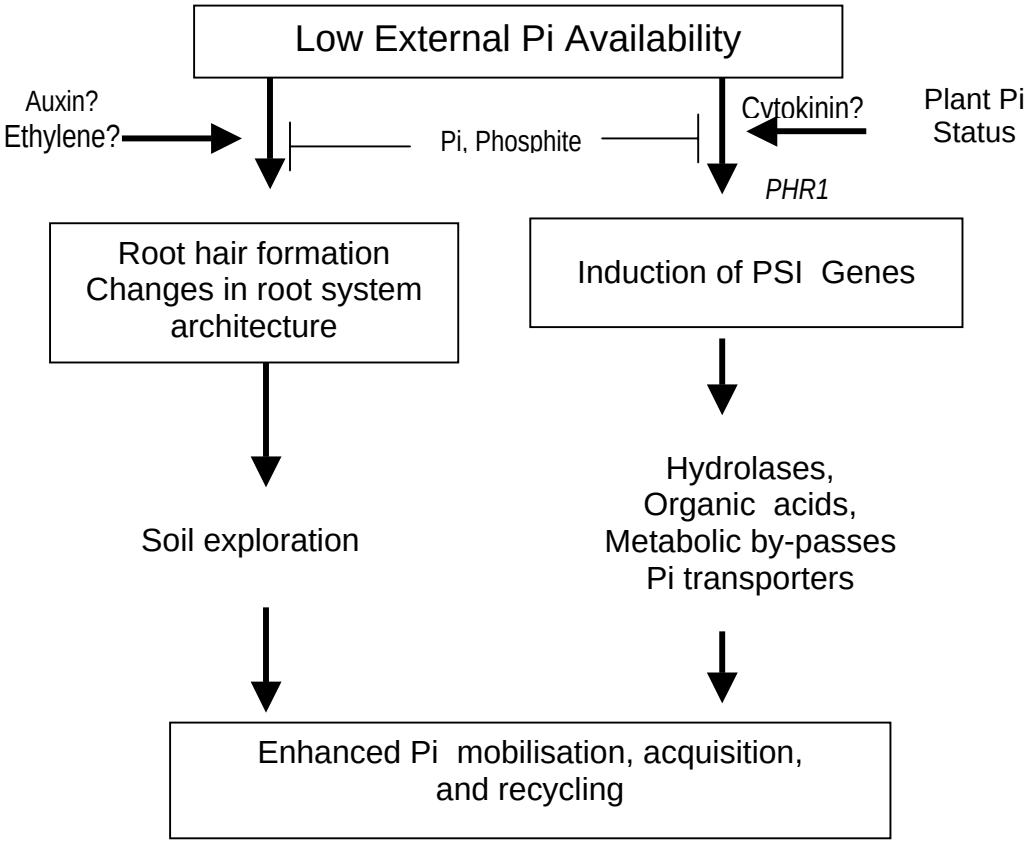

Figure 1.2 Plant responses to phosphate limitation and their regulation. Adapted from Abel *et al.* (2002). *Physiologia Plantarum*. 115:1-8. Low external Pi availability enhances morphological adaptation in plants such as root hair formation and alteration in root system architecture to improve soil exploration and enhance Pi mobilisation, recycling and acquisition. The role of auxin and/or ethylene is implicated although the mechanism involved is still unclear. Low external Pi also induces phosphate–starvation inducible (PSI) genes. This is proposed to be regulated by a transcription factor PHR1 and the regulation is influenced by the Pi status in the plant, possibly mediated by cytokinin.

Recently, in suspension-cultured *C. roseus* cells, Shimano and Ashihara (2006) noted that during prolonged Pi starvation, the levels of the purine nucleotides particularly ATP and GTP were reduced markedly and accumulation of adenosine and guanosine was noted. This phenomenon was attributed to an increase in the activity of RNase, DNase, 5'- and 3'-nucleotidases and acid phosphatase, which are involved in the hydrolysis of nucleic acids and nucleotides to release Pi (Shimano and Ashihara, 2006).

To a certain extent this reduction in the synthesis of nucleotides during Pi starvation was also attributed to the limited availability of the essential phosphorylated intermediates of ATP and phosphoribosyl pyrophosphate, (PRPP) which appeared to be coordinately regulated at the level of gene expression (Hewitt *et al.*, 2005). Regulation of nucleic acids in response to Pi limitation varies within the plant tissues. For instance, total RNA from the roots of *Arabidopsis* seedlings grown in Pi-starved media for 14 d increased by 41%, but the RNA from the shoots decreased by 87% when compared with those grown under Pi sufficiency (Hewitt *et al.*, 2005).

A general decrease in protein accumulation was likewise reported. In suspension cultured cells of *C. roseus* grown in Pi deficient medium, degradation of protein was noted over the 96 h experimental period, causing an increase in the levels of free amino acids in the culture. Levels of glycine, glutamine and arginine in Pi starved cells increased more than 30-fold when compared to cells under Pi sufficiency. Also, under Pi limitation, there was an increase in the level of proteases (endopeptidases), which decreased rapidly when cells were transferred to fresh Pi sufficient medium, accompanied by an increase in the rate of protein synthesis and a corresponding decrease in the levels of free amino acids (Ukaji and Ashihara, 1987).

Taken, together, these studies point to the important role being played by Pi in plant metabolism specifically at the molecular and biochemical level.

1.3.2 Phosphate transport in plants

Acquisition of Pi by the plants generally follows a steep concentration gradient (Raghothama and Karthikeyan, 2005) and transport of Pi into the root cell is an active process (Buchanan *et al.*, 2000). This phenomenon occurs since the concentration of P in the form that is accessible for plant use is usually less than 10 μM in the soil rhizosphere but, in the cytoplasm, the Pi concentration maybe 1000-fold higher (Raghothama, 2000; Muller and Schmidt, 2004). Additionally, in the uptake of Pi and transport across the plasma membrane, the negative membrane potential, which is a characteristic of plant cells (Bieleski, 1973), has to be overcome. The combination of these factors emphasises the plant's requirement for a specific mechanism for extraction of Pi from the soil and transporting it across the membrane and between intracellular compartments.

A number of families of transporter proteins have been reported to mediate the transport of Pi through plant membranes. Kinetic studies showed that, depending upon Pi availability, plants were able to utilize two Pi uptake systems. The first is the high affinity system, in which activity is increased by Pi starvation, and the second is the lower affinity system where activity is constitutive (Schachtman *et al.*, 1998).

Access of Pi into Pi-deficient roots has been associated with high-affinity Pi transporters which are preferentially expressed in the roots (Raghothama and Karthikeyan, 2005). These high affinity Pi transporters are membrane associated proteins with a K_m varying from 1.8 – 9.9 μM Pi (Mimura, 2001). These transporters mediate Pi uptake from the external media with a low Pi concentration into the cytoplasm where the Pi

concentrations are much greater. This type of transporter is rapidly induced when Pi becomes deficient but is reversible upon re-supply of Pi (Raghothama, 2000).

In *C. roseus* suspension-cultured cells, uptake of Pi into the vacuole was highly elicited under low Pi status and this uptake across the membrane was correlated with H^+ pumping and the activities of the vacuolar H^+ pump (Ohnishi *et al.*, 2007). Also in duckweed plants (*Spirodela oligorrhiza),* Pi uptake is energised by the electrochemical proton gradient across the plasma membrane (PM). A more active uptake of Pi occurred in plants grown in Pi deficient medium than in plants grown in a Pi sufficient medium, and the uptake process was significantly stimulated by the induction and accumulation of the high-affinity Pi transporter in the PM. Further, the electrochemical proton gradient across the PM was postulated to be generated by the high-ATP-affinity and energy-efficient H^+ pump in Pi deficient plants. This high affinity H^+ pump normally does not occur in Pi sufficient plants (Hase *et al.*, 2004).

In contrast, the *Arabidopsis Pht2;1,* a low affinity Pi transporter, is constitutively expressed in the green tissues specifically in the leaves, regardless of Pi status. It has an apparent K_m of 0.4 mM for Pi and is possibly involved in the loading of Pi within shoots (Daram *et al.*, 1999).

Pi is able to move radially towards the central stellar region of the root through the apoplast, moving through the walls of root epidermal and cortical cells and their associated intercellular spaces. It moves into the pores of this lattice work in the cell walls until it meets the suberised casparian band around the transverse and radial walls of the endodermal cells that surround the central stele (Smith *et al.*, 2003)

1.3.3 Adaptive strategies of plants to phosphate limitation

Generally, adaptive responses of plants to low P nutrition can be categorised into morphological, physiological, biochemical and molecular changes. Some of these responses are outlined in the following sections.

1.3.3.1 Morphological and physiological changes

During conditions of low Pi availability, plants display some changes in root morphology in order to increase the efficiency of Pi acquisition and mobilisation. These morphological alterations include changes in the primary root length, enhanced production of lateral roots, an increase in root hair density, and the production of proteoid roots (Abel *et al.*, 2002; Sanchez-Calderon *et al.*, 2005).

Changes in root morphology in response to Pi stress vary depending on plant species. For example, some species of temperate pasture grasses such as *Holcus lanatus* L. and *Lolium rigidum* Gaudin, when grown under a limiting amount of Pi, display an increase in root length but a decreased root diameter as compared to those grown under Pi sufficiency (Hill *et al.*, 2006). This observation was the opposite of what has been observed in *Arabidopsis* in which the primary root length significantly decreased in response to limiting Pi (Reymond *et al.*, 2006). To some extent this was attributed to a significant decrease in the size of the mature cortical cells of roots and a significant reduction in the number of cells in the elongation zone (Williamson *et al.*, 2001; Reymond *et al.*, 2006).

Inhibition of primary root growth in *Arabidopsis* during Pi limitation is also attributed to a shift from an indeterminate to a determinate developmental program in the root (Sanchez-Calderon *et al.*, 2005). In the induction of this determinate root developmental

program, the possible role of the quiescent centre (QC) as a sensor of environmental signals has been implicated. Pi deficiency altered the QC. That is, the area usually occupied by the apical meristem when plants were grown in high Pi media became highly vacuolated when plants were grown in low Pi media. No mitosis was observed after 12 h in the Pi deficient media, cell proliferation ceased and cell differentiation started to occur in the region where cell division normally took place, thus leading to an alteration in the normal developmental program in the root (Sanchez-Calderon *et al.*, 2005)

Increased lateral root production and elongation are also significant adaptive responses observed in plant roots grown under Pi deficiency. This mechanism was proposed to increase soil exploration and P solubilization thus contributing to better acquisition of immobile elements such as P (He *et al.*, 2003). However, elongation of lateral roots in response to Pi limitation, depends upon species. For instance, in maize (*Zea mays)* seedlings grown at low P availability, three recombinant inbred lines (RIL) exhibited enhanced lateral rooting with greater relative growth rate (RGR), while two other RILs displayed reduced lateral rooting (Zhu and Lynch, 2004). Also, in *Arabidopsis,* it was reported that under Pi starvation, cell elongation of two RIL populations showed different responses; the cell length of one accession was reduced by 50% while the reduction in cell length of the other RIL was up to 90% (Reymond *et al.*, 2006).

Formation of proteoid roots (clustered tertiary lateral roots) is another form of morphological change noted in response to low Pi availability, specifically in white lupin (*Lupinus albus* L.) and in other old-world lupin species (*L. luteus* L., *L. hispanicus* Boiss. et Reuter and *L. angustifolius* L.) (Johnson *et al.*, 1996; Peek *et al.*, 2003; Hocking and Jeffery, 2004). Proteoid roots are closely spaced lateral rootlets, or groups

of rootlets, that originate from the pericycle opposite the protoxylem poles (Gilbert *et al.*, 2000). These have been associated with efficient production and secretion of organic acids and phosphatases (Johnson *et al.*, 1996; Gilbert *et al.*, 2000) and enhancement of expression of the multidrug and toxin efflux (MATE) genes in Pi deficient lupin (Uhde-Stone *et al.*, 2005). In white lupin plants grown in 1 mM Pi, initiation of clustered tertiary meristems was also noted, but the emergence of these meristems was delayed when compared with Pi starved plants (Johnson *et al.*, 1996). The synthesis and release of carboxylates that mobilise scarcely soluble Pi in the rhizosphere has also been associated with the proteoid root formation in harsh hakea (*Hakea prostata* R.) (Shane *et al.*, 2004).

An increase in root hair density is also observed in Pi deficient roots. This increased root hair density in Pi depleted roots was partly attributed to increased production of trichoblast files in the roots (Ma *et al.*, 2001), and was mainly achieved by the formation of extra hairs over both the tangential and radial walls of the underlying cortical cells in the roots (Muller and Schmidt, 2004). In Arabidopsis grown under limiting Pi conditions, root hair density was about five times greater than plants grown in Pi sufficient (1 mM) media. This increase in root hair density constitutes an important adaptive response of plants since this developmental process increases the competitiveness of plants to absorb more nutrients (Bates and Lynch, 2001). This mechanism increases the effective root surface area thereby maximizing the volume of soil exploited (Ma *et al.*, 2001). The significance of increased root hair production was confirmed when Gahoonia and Nielsen (1998) found that root hairs were able to absorb up to 60% of the total Pi absorbed by the Pi deficient plants.

P deficiency also significantly alters the root anatomy of various crops. For instance, formation of cortical aerenchyma in response to Pi deprivation was observed in rice after 28 d of growth in Pi deficient media (Lu *et al.*, 1999; He *et al.*, 2003). In maize and common bean, intercellular spaces were noted after 12 d of growth in the Pi deficient media (Fan *et al.*, 2003). The development of these gas-filled spaces represent a functional adaptive response to low P availability by reducing the respiratory and P requirement of the roots and by increasing the metabolic efficiency of soil exploration (Fan *et al.*, 2003).

Pi starvation responses are also distinct in different plant organs. For example, a significant drop in cellular Pi is triggered faster in the roots than in the leaves. This was noted in two experiments with *Arabidopsis*, wherein a significant decrease (22%) in Pi concentration was observed in the roots after 24 h of starvation whereas no detectable change in Pi content was noted in the leaves, even after three days of Pi withdrawal (Wu *et al.*, 2003).

It thus appears that changes in the morphological and anatomical features of the root, as influenced by Pi deficiency, is a coordinated response which varies depending on plant species, and such adaptive mechanisms occur for a variety of purposes. In the case of proteoid roots, other than the increase in the absorptive surface area and being involved in the sequestration of scarce nutrient from the root zone, these roots are also implicated in chemically modifying the environment within the root zone; a process which is useful for the improvement of the solubility of nutrients, thus rendering them more available for plant use.

1.3.3.2 Biochemical and molecular adaptations to phosphate limitation

In response to Pi starvation, plants also exhibit a variety of biochemical adaptations. These include increased efficiency of cellular Pi uptake, induction of enzymes involved in scavenging and recycling Pi, as well as induction of alternative pathways of cytosolic glycolysis and of respiratory electron transport system (Plaxton, 2004). Further, some changes in the concentration of Pi in the cytoplasm or in the vacuole trigger the signal transduction pathway which activates the Pi starvation rescue system (Bhadoria *et al.*, 2004)

The combined activities of the phosphoenolpyruvate carboxylase (PEPC), malate dehydrogenase (MDH) and nicotinamide adenine dinucleotide (NAD) malic enzymes can catalyse a by-pass in the glycolytic pathway during Pi stress (Theodorou and Plaxton, 1993). This mechanism can by-pass pyruvate kinase (PK), the enzyme which requires Pi and adenosine diphosphate (ADP). Thus the flow of carbon from glycolysis to the tricarboxylic acid (TCA) cycle is maintained by avoiding the use of ADP but generating free Pi (Theodorou and Plaxton, 1993; Vance *et al.*, 2003).

Transcriptional regulation of PEPC and biosynthesis of organic acids also constitute adaptive mechanisms displayed by white lupin in response to Pi deficiency (Johnson *et al.*, 1996; Vance *et al.*, 2003) . Organic acids enable enhanced mobilisation of available Pi salts and these acids are primarily secreted by the proteoid roots (Watt and Evans, 1999).

The secretion of carboxylates, protons and phosphatases contributes towards efficient acquisition of Pi by proteoid roots and increases the availability of soil Pi immediately adjacent to the rootlets (Smith *et al.*, 2003). These protons and carboxylates which are released from the root hairs, solubilise the P which is bound in other soil constituents

rendering them available for plant use. The P released is then taken up across the plasma lemma through Pi transporters (Vance *et al.*, 2003), thus increasing the amount of Pi for use in various plant metabolic and physiological processes.

Apart from the various biochemical adaptations utilised by plants in response to Pi stress, there are also several Pi starvation inducible (PSI) genes which are regulated during Pi starvation. These PSI genes exhibit distinct or even contrasting expression in leaves and roots. The induction of expression of most genes in the leaves was detected at 24 h with a few others at 72 h after Pi starvation. In root tissues, expression of most genes peaked at 24 h after Pi withdrawal, but some genes exhibited maximal expression after six hours (Wu *et al.*, 2003).

Very recently, in a root transcriptome survey in common bean, 125 genes that were responsive to Pi stress were identified. Of those, 78 were induced either 2-fold or more. Interestingly, one of these genes is *ACO* which was induced *ca* 4-fold under Pi deficiency (Hernandez *et al.*, 2007). In the past couple of years, microarray and macroarray analyses of Pi stress in plants have provided evidence of increased transcript abundance of genes with homology to Pi transporters and acid phosphatases, (Hammond *et al.*, 2003; Uhde-Stone *et al.*, 2003; Vance *et al.*, 2003; Wu *et al.*, 2003), and a sugar-dependent regulation of these genes has been recently postulated (Muller *et al.*, 2007). Involvement of sugar or active photosynthesis was found essential in the expression of the PSI genes under Pi limiting conditions (Muller *et al.*, 2004; Karthikeyan *et al.*, 2007) and these genes were rapidly repressed when plants were replenished with Pi (Muller *et al.*, 2004). On the other hand, expression of some genes, specifically those that encode Rubisco small sub-units and those encoding for key

regulatory enzymes in $C0_2$ assimilation, reduction and regeneration, were repressed maximally at 48 h after the onset of Pi starvation (Wu *et al.*, 2003).

At different stages of proteoid root development in white lupin, expressed sequence tags (ESTs) from cDNA libraries have been isolated. These ESTs which included genes involved in carbon metabolism, secondary metabolism, Pi scavenging and remobilisation, plant hormone metabolism, and signal transduction were noted to be differentially expressed in Pi-deficient proteoid roots when compared with the normal roots of plants grown under Pi sufficiency (Uhde-Stone *et al.*, 2003).

Thus, under limiting Pi conditions, plants adapt not only by alteration in the morphological and anatomical features, but there are also some modifications in the biochemical mechanisms such as secretion of carboxylates and phosphatases. Further, changes at the molecular level such as the coordinated regulation of gene expression which forms part of the plant's Pi starvation rescue system are also observed.

.

1.4 Regulation of root growth by ethylene and phosphate availability

The involvement of the phytohormone ethylene in some responses to stress was proposed many years ago (Torrey, 1976). It is known that ethylene is involved in generating a range of the morphological and physiological responses of plants to nutrient deficiencies, such as alteration of primary root growth, and promotion of root hair and lateral root formation (Lynch and Brown, 1997; Lynch and Brown, 2001; Schmidt, 2001), as well as inhibiting primary root elongation (Dolan, 1997). These findings confirmed previous observations by Borch *et al*. (1999) that, under P deficiency, ethylene is involved in the regulation of main root extension and lateral root spacing in common bean (*Phaseolus vulgaris*).

Recent findings show that in Pi deficient *P. vulgaris* (L), ethylene participates in the formation of root growth angle but this involvement is dependent on the genotype grown. When genotypes with shallow or deep basal roots were compared, ethylene sensitivity was greater for shallow-rooted than for deep-rooted genotypes (Basu *et al.*, 2007). Further, plants grown in low P conditions were more affected when compared to those plants grown under a high P condition. Also, a strong correlation between ethylene sensitivity and root growth angle was observed more commonly in shallow than in deep-rooted genotype (Basu *et al.*, 2007).

In the study by Ma *et al.* (2003) in Arabidopsis, it was deduced that Pi limitation altered the signal transduction pathway that linked ethylene levels to root development. Findings showed that ethylene limited primary root growth under P sufficiency, but tended to maintain it under P deficient conditions. In plants grown under Pi sufficiency, root hairs start to develop further from the tip, whereas under Pi deficiency with ethylene action inhibited, root hairs initiated closer to the tip and further from the end of the growth zone. (Ma *et al.*, 2003).

1.5 Aerenchyma formation as affected by ethylene and phosphate availability

Formation of aerenchyma in plant roots is reported to be due in part to P deficiency and to some extent to the presence of ethylene. For example, in maize root, cell lysis and aerenchyma formation in the cortical cells had been associated with increased ethylene sensitivity which was enhanced by the limiting P (He *et al.*, 1992). When the ethylene action inhibitor (Ag^+) was added at a low concentration (0.6 μM), the formation of gas spaces in the root cortex of Pi-deficient plants was inhibited (He *et al.*, 1992).

The involvement of ethylene in the formation of cortical aerenchyma in response to Pi deficiency has also been reported in peas wherein the plants exposed to low Pi showed an increased formation of intercellular spaces (Lynch and Brown, 1997).

The aerenchyma formation in the root cortex is one of the plant's mechanisms to prevent accumulation of ethylene within the tissue (Drew *et al.*, 2000). These intercellular spaces are actually gas transport ducts that can enhance the ventilation system by facilitating gas diffusion between the roots and the aerial environment (Bragina *et al.*, 2001; Visser and Pierik, 2007).

The formation of cortical aerenchyma has been observed in the roots of various plants such as *Arabidopsis* (Lynch and Brown, 1997; Ma *et al.*, 2001; Schmidt, 2001; Lopez-Bucio *et al.*, 2002; Muller and Schmidt, 2004), common bean (Liao *et al.*, 2001; Lynch and Brown, 2001), tomato (Schikora and Schmidt, 2001) and rice (Visser and Pierik, 2007).

Aerenchyma formation initiated by ethylene appears to be a form of programmed cell death that shows characteristics, resembling in part both apoptosis and cytoplasmic cell death (Gunawardena *et al.*, 2001).

Taken together, these results seem to suggest that the formation of these large intercellular spaces may be caused by a number of factors such as Pi stress or increased levels of ethylene. The possibility of these being caused by interaction between P and ethylene can also be considered.

1.6 Aims of the project

Expression of *ACO* genes in the stolon and leaves of white clover has been well studied. Evidence has shown that each member of the gene family is differentially expressed

during leaf development and in response to environmental cues (Hunter *et al.*, 1999; Chen and McManus, 2006). In the roots, an initial study on the expression of the *TR-ACO* genes has been carried out by Yoo (1999). Using northern analysis, Yoo showed that both *TR-ACO1* and *TR-ACO2* genes were expressed in the roots. However, the expression of *TR-ACO3* was not examined, and a detailed analysis on the expression of *TR-ACO1* and *TR-ACO2* was also not conducted.

Further, based on the results of previous studies, it has been postulated that ethylene is also involved in the adaptive mechanisms of plant roots to low P availability. In those studies, however, the regulation of the ethylene biosynthetic genes was not examined. Therefore, this thesis has sought to examine, in more detail, the differential expression of the *TR-ACO* gene family in roots, and then to use this as basis to examine the influence of Pi supply on this expression.

To do this, three major aims were addressed.

- First, the expression pattern of the *TR-ACO* genes in the roots of white clover was investigated to determine if these genes were differentially expressed
- Secondly, changes in the expression of the *TR-ACO* gene family were examined, as was the accumulation of the TR-ACO proteins in the roots in response to changes in Pi supply, and
- Thirdly, tissue specific activity of the *TR-ACO1* promoter in white clover roots using a *TR-ACO1p::mGFP-5 ER* gene fusion in transgenic white clover was characterised, and any changes in the pattern of activity in response to Pi availability were determined.

Chapter 2

Methods and Materials

2.1 Plant material

Wild type white clover (*Trifolium repens* L.) cultivar Grasslands challenge, genotype 10F (Agresearch Grasslands, Palmerston North, New Zealand), and transgenic lines, either *TR-ACOp::GUS* or *TR-ACO1p::mGFP5 ER* were used in this study. The transgenic plants harbouring either the *TR-ACO1, TR-ACO2* or *TR-ACO3* gene promoters fused to the β-Glucuronidase (GUS) reporter gene (*TR-ACOp::GUS*) in the binary vector PRD410 were originally produced by Dr Balance Chen, and were generated at IMBS, Massey University (Chen and McManus, 2006). The *TR-ACO1* promoter-*mGFP5 ER* fusion (*TR-ACO1p::mGFP5 ER*) was in the *pBIN* vector. The introduction of the chimeric gene into the white clover was conducted through *Agrobacterium*-mediated transformation using the strain LBA4404 (Section 2.6.2), as part of this thesis.

2.1.1 Maintenance of stock plants of white clover

Stock plants of wild type white clover (Figure 2.1) were first rooted in medium-sized vermiculite (2-4 mm, Nuplex Industries, Ltd., Auckland, NZ), then transferred into a horticultural grade potting mix (Oderings, Palmerston North, NZ) and allowed to develop a sufficient number of stolons for use in various experiments. These were grown either in a glasshouse in the Plant Growth Unit (PGU), Massey University, Palmerston North or in the Ecology Glasshouse at Massey University. The temperature in the PGU glasshouse was set at a minimum of 12^{o}C during the night and at 20^{o}C during the day, with venting once the temperature reached 25^{o}C. Plants were watered manually everyday.

Figure 2.1 White clover stock plants grown in the glasshouse

2.1.2 Experimental plants

Four-node stolon cuttings (Figure 2.2) were used in various experiments. These cuttings were set in vermiculite then acclimatised in Hoagland's solution (Table A.1) at varying number of days depending on the purpose for which the experiments were conducted. For root morphological and anatomical studies, stolon cuttings were set in vermiculite for two weeks then transferred to Hoagland's solution for three days before starting the phosphate experiment. At this stage, roots were still relatively short, and stolon cuttings with more or less similar root lengths were used in the experiment. For confocal microscopy, stolon cuttings were set in vermiculite for two weeks then transferred to Hoagland's solution for one week before starting the experiment. For the biochemical and molecular studies, stolon cuttings were rooted in vermiculite for two weeks then acclimatised in Hoagland's solution for another two weeks before starting the experiment in order to have sufficient root materials for various analyses. The concentrations of Pi used to constitute the +P and –P treatments are provided in the description of the experiments in the Results section, as appropriate, and/or in the Figure legends, as appropriate.

2.1.3 Root growth measurements

The length of the main root was measured using a standard ruler. To do this, the sample plant was quickly lifted out from the Hoagland's solution, roots aligned onto a flat surface and the length was measured in centimetres. The number of lateral roots was determined while in the Hoagland's solution to prevent the roots from adhering to each other. The root biomass represents the pooled roots of the sample plants and the biomass was determined both in fresh weight and dry weight

2.2 Microscopy techniques

2.2.1 Fixation of plant tissue materials

Formaldehyde, acetic acid and alcohol (FAA) at a final concentration of 60% (v/v) ETOH, 5% (v/v) glacial acetic acid, and 2% (v/v) formaldehyde was used as tissue fixative. Root tissues were immersed in FAA soon after being excised, vacuum

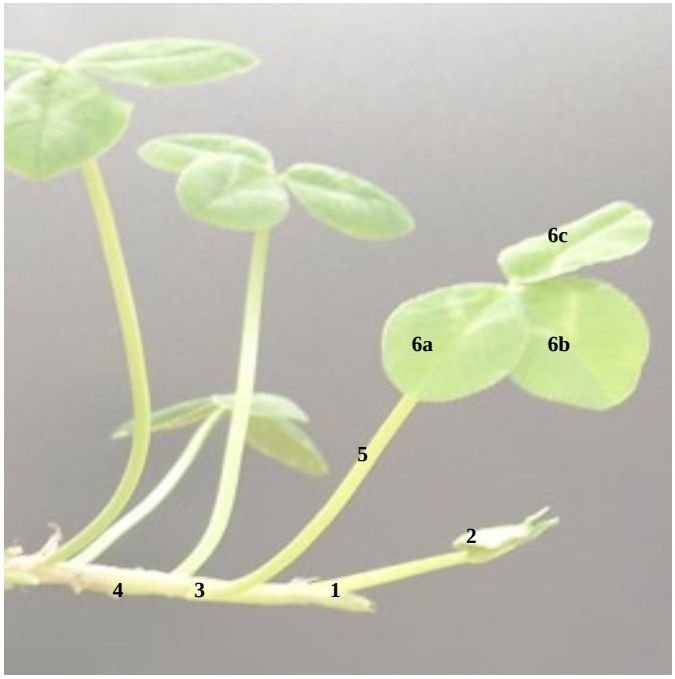

Figure 2.2 A white clover stolon showing the apex (1), an unexpanded leaf (2), node (3), internode (4), petiole (5), and a trifoliate leaf (6), each unit joined by a petiolule is termed a leaflet (a-c). In preparation for rooting, the fully expanded trifoliate leaves were trimmed off from the base of the petiole and the four-node stolon cutting with the apex and an unexpanded leaf was placed in vermiculite wetted in Hoagland's solution.

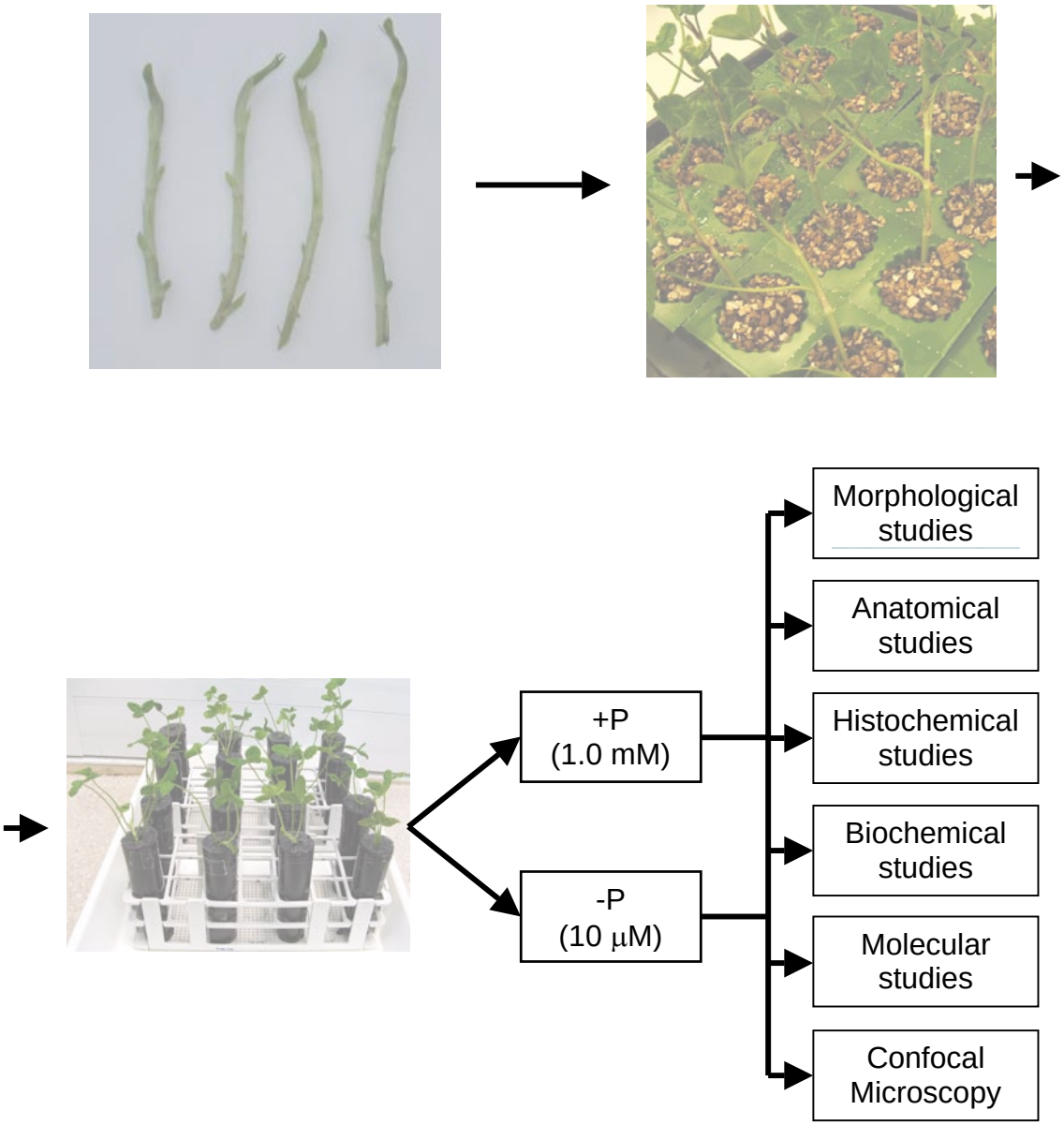

Figure 2.3 Flow diagram for setting up the experiments for various analyses. Four node stolon cuttings were rooted in vermiculite for 14 d, acclimatised in Hoagland's solution for 14 d before setting up a Pi experiment. Containers for growing individual cuttings were 50-mL Falcon tubes wrapped with black polyethylene plastic sheet.

infiltrated at *ca.* 35 kPa for 15 min and then fixed at room temperature for 3 h. In some instances, tissues were left in FAA overnight if vacuum infiltration was not conducted. After fixation, the roots were rinsed with 50% (v/v) ethanol and then passed through a series of dehydration steps.

2.2.2 Dehydration

Dehydration was achieved with a series of ethanol solutions. After rinsing with 50% (v/v) ethanol, tissues were passed on to 70% (v/v), 85% (v/v), 95% (v/v) and 100% ETOH for a minimum of 1 h for each step. To visualise the tissues within the wax block, roots were stained with erythrosine B (0.1% (w/v) in 95% (v/v) alcohol) for 3 min. Sample tissues were then rinsed twice with 100% ETOH for 2 h per rinsing and then left immersed in ETOH.

2.2.3 Clearing, wax infiltration and embedding

Clearing of the fixed and dehydrated tissues was conducted using Histochoice® (Sigma-Aldrich, USA). To allow gradual clearing and appropriate wax infiltration, tissues in 100% ETOH were incubated in a solution of 25% (v/v) Histochoice-75% (v/v) ETOH for 2 h. The percentage of Histochoice in the solution was then increased to 50% (v/v), then 75% (v/v) and then 100% with 2 h incubation at each step. This was followed with three changes of the 100% Histochoice for 2 h at each step. If more convenient, at any step in 100% Histochoice, tissues were left to incubate overnight.

Wax infiltration was initiated by adding paraplast chips (TYCO Healthcare, Mansfield, MA, USA) to the 100% Histochoice to give a final ratio of 50% paraplast-50% Histochoice and the mixture left for 24 h at 37^{o}C with gentle shaking. After this period, more paraplast chips were added and the mixture again left overnight in a shaking incubator. To melt the wax, tissues in paraplast were transferred to a 60^{o}C oven. Once

the paraplast was thoroughly melted, tissues were transferred to fresh paraplast. Six changes of pure melted paraplast were made twice per day until the tissues were ready to be embedded into the wax blocks.

Wax blocks were then prepared using a histochemical embedder (Leica., Bensheim, Germany). Pre-warmed embedding boats were half-filled with melted wax and after placing the tissue into the bottom of the boat in the correct orientation, an embedding cassette was placed on top and then filled with wax. To hasten setting of wax the embedded boats were placed onto a cold plate. Once set, the wax blocks were stored in 4^{o}C room until used for sectioning.

2.2.4 Sectioning

In preparation for sectioning, the wax blocks were trimmed to leave an *ca.* one cubic centimetre with the tissue at the centre. Waxed tissues were then sectioned at 10-12 μm using a Leica microtome (Leica, Bensheim, Germany) fitted with disposable microtome blades. Ribbons of desired length were then floated on water at 42^{o}C, captured onto precoated polysine microscope slides (BDH) and then placed on top of a slide warmer (Agar Scientific, UK) at 42^{o}C overnight.

2.2.5 Staining

Tissues on slides were stained with 0.1% (w/v) safranin in 70% ETOH and 0.2% (w/v) fast green as illustrated in Figure 2.4 before conducting light microscopy.

2.3 Histochemical assays

2.3.1 GUS staining

Reagents:

- 50 mM sodium phosphate buffer, pH 7.2

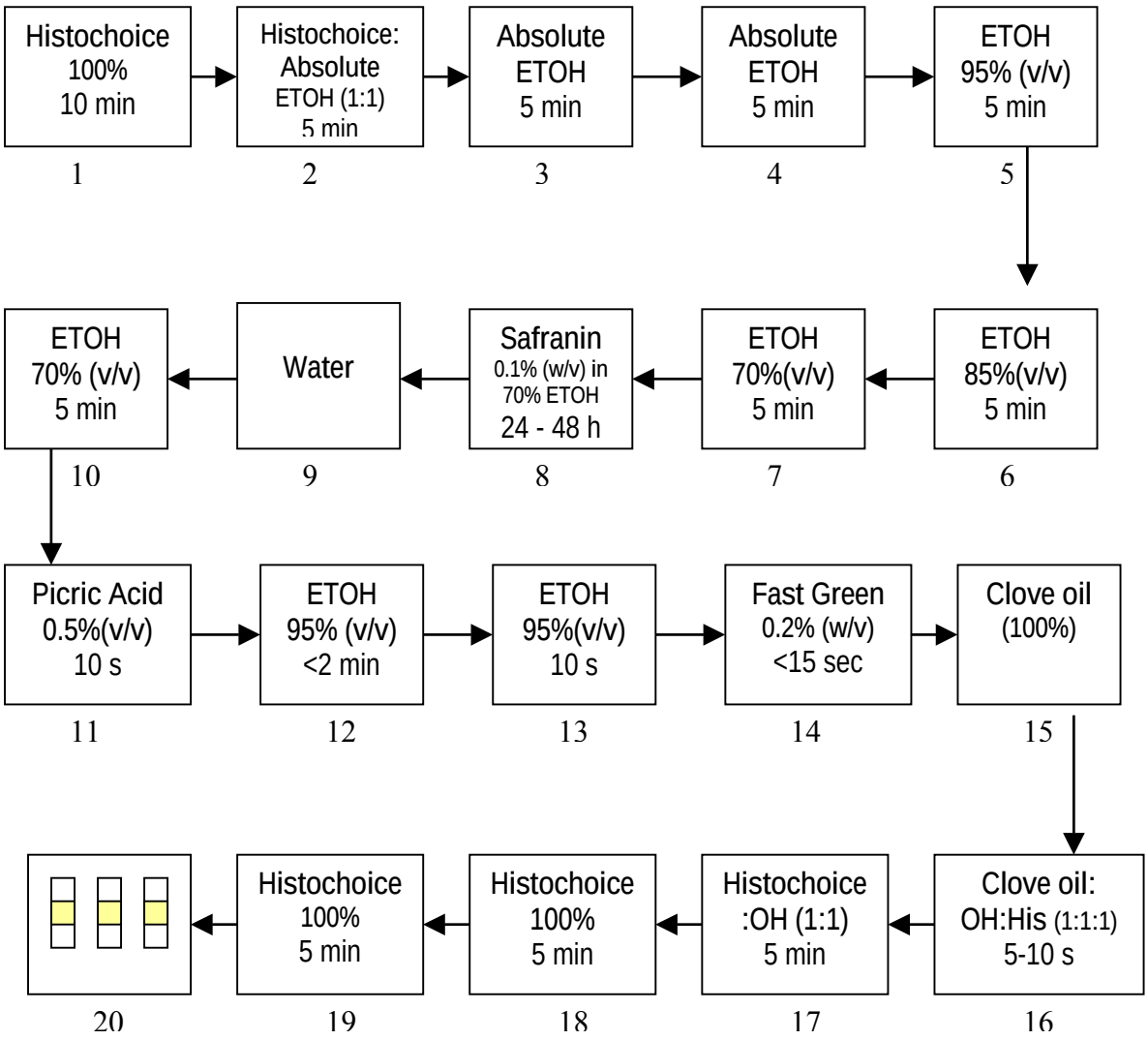

Figure 2.4 Staining schedule with safranin and fast green. Tissues on slides were dewaxed using Histochoice, immersed in ethanol series in preparation for staining with safranin and fast green, and destained with clove oil. After two rinses with 100% Histochoice, the slides were layered with DPX, and covered with glass slips. (Modified from Nickless, L., IMBS, Massey University, pers. comm.).

- X-Gluc substrate: 2 mM 5-bromo-4-chloro-3 indolyl β-$_D$-glucuronide cyclohexylamine salt (Sigma) diluted in 50 mM sodium phosphate buffer, pH 7.2 containing 0.1% (v/v) Triton X-100, and 0.1% (v/v) 2-β-mercaptoethanol

Root tissues for analysis were excised fresh and placed on ice. These were then dipped in ice-cold acetone for *ca.* 10 min and then rinsed twice with 50 mM sodium phosphate buffer pH 7.2. Following the second rinse, tissues were immersed into the X-Gluc substrate, vacuum infiltrated at *ca.* 50 kPa for 20 min, wrapped in tin foil, and then incubated at 37^{o}C overnight.

2.3.2 Preparation of GUS stained tissues for microscopy

After incubation in the X-Gluc solution, root tissues with GUS activity normally display a blue precipitate at the site of enzyme activity. To prepare for further analysis, tissues were destained in 30% (v/v) ethanol for 30 min. This was followed by fixation with FAA overnight, using the methods as described (Section 2.2.1). Dehydration was then conducted by immersing the tissues in a series of ETOH solutions ranging from 70% (v/v), 85% (v/v), 95% (v/v) and 100% for 1 h at each step. Tissues were immersed twice in fresh 100% ETOH for 2 h, and then kept in 100% ETOH in 4^{o}C until required for further analysis.

For further examination of the specific localisation of GUS activity in sectioned tissues, de-stained tissues were cleared with a series of Histochoice:ETOH solution starting with 25% Histochoice to 75% ETOH for 1 h. The tissues were then transferred every hour to fresh clearing solution with the percentage of Histochoice gradually increased from 50% (v/v), to 75% (v/v) and finally to 100%. At the conclusion of the clearing step, tissues were incubated for another 1 h in fresh 100% Histochoice and then paraplast chips were gradually added to commence the gradual infiltration process. These methods were similar to the protocol described in Section 2.2.3 except that the duration

of incubation for each step was shortened to *ca.* 1 h each step so as not to significantly reduce the blue staining in the tissues.

The embedding and sectioning procedures were as described in Section 2.2.4 After mounting and warming the waxed tissue sections, the slides were de-waxed by dipping in 100% Histochoice, three times for 15 min for each dip, and then layered with DPX before placing the glass cover slips.

2.4 Biochemical Analyses

2.4.1 Analysis of leaf phosphate content

The phosphate (Pi) content in white clover leaves was analysed using a Phosphate Fluorometric (resorufin) Assay Kit, PiPer™ (*Molecular Probes* Invitrogen Detection Technologies). With this method, the amount of Pi in the sample is measured based on the resulting increase in fluorescence in the reaction mixture, which is measured at excitation and emission maxima of 563 and 587 nm, respectively.

2.4.1.1 Extraction of leaf phosphate

The first fully expanded leaf (typically 30 –35 mg fresh weight) was powdered in liquid nitrogen in a 2-mL Eppendorf tube using a plastic pestle. Following the addition of 100 μL of the reaction buffer (0.1M Tris-HCl, pH 7.5), the mixture was vortexed for 1 min and then diluted with a further 1 mL of reaction buffer. After vortexing for 30 s, the slurry was centrifuged at 13,000 x g for 3 min at 4^{o}C and then the supernatant was transferred to a fresh Eppendorf tube for leaf Pi assay.

2.4.1.2 Leaf phosphate assay

Reagent

- **Amplex Red Reagent solution**: 4 $U.mL^{-1}$ maltose phosphorylase, 0.4 mM maltose, 2 $U.mL^{-1}$ glucose oxidase, 0.4 $U.mL^{-1}$ HRP, 100 μM Amplex Red reagent, 1x reaction buffer
- **Reaction buffer:** 0.1 M Tris-HCl, pH 7.5.

Ten microlitres of the sample extracts (Section 2.4.1.1) were diluted to 50 μL with 0.1 M Tris-HCl, pH 7.5, and then pipetted into designated wells of the microtitre plate. At the same time, a Pi standard curve was also prepared with varying Pi concentrations ranging from 0 to 120 μM dissolved at 0.1 M Tris-HCl, pH 7.5. The reaction was started by the addition of 50 μL of Amplex Red Reagent solution, the microtitre plate covered with tin foil to exclude light and then incubated at 37^{o}C for 30 min. Finally, fluorescence units (FU) were read using a Fluorostar plate reader (Fluostar/Polarstar Galaxy, BMG Technologies GmbH, Germany) with the filters set for absorption and fluorescent emission maxima of *ca.* 563 nm and 587 nm, respectively.

The amount of Pi in the sample was then calculated corresponding to the given FU in comparison with the standard curve (Figure 2.5). The background fluorescence was corrected by subtracting the values obtained from the control (0 Pi) from that of the sample reading.

2.4.2 Analysis of acid phosphatase activity

Root acid phosphatase activity was examined in both water soluble and cell wall associated root fractions.

2.4.2.1 *Extraction of the soluble and ionically-bound cell wall proteins*

The soluble and ionically-bound cell wall proteins from white clover roots were extracted following the protocol of Hay *et al*. (1998) Root tissues were washed with

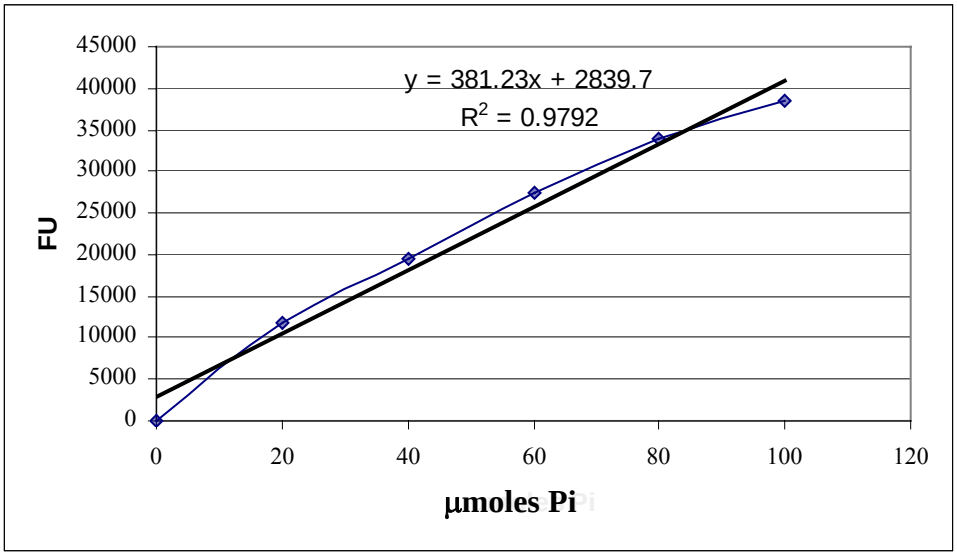

Figure 2.5 A typical standard curve for the phosphate assay. The dots connected by a line are the actual data points while the solid straight line represents the regression line

water, blot dried and powdered in liquid nitrogen. The water soluble protein was extracted using 1mM DTT whilst the cell wall associated protein was extracted using 1 M NaCl.

Aliquots of powdered roots in liquid nitrogen were suspended in 3 volumes of 1 mM Dithioethritol (DTT) and the slurry was kept on ice for 30 minutes. After centrifugation at 12,000 x g for 10 min at 4^{o}C, the supernatant was transferred to a fresh tube and stored at 4^{o}C. This was designated the soluble extract. The extraction procedure of the pellet with 1 mM DTT was carried out three more times, followed by a further seven washes with water. A centrifugation step (12,000 x g for 10 min at 4^{o}C) was used to collect the pellet after each wash. After the final wash, the remaining water was removed from the pellet by two successive centrifugations.

The pellet was then resuspended in one volume of 1.0 M NaCl, incubated at 37^{o}C for 1 h, and the slurry centrifuged at 12,000 x g. After transfering the supernatant to a fresh labeled tube, the pellet was again resuspended in 1 M NaCl and incubated at 4^{o}C overnight. After centrifugation, the supernatant was pooled with the first 1.0 M NaCl supernatant and designated the ionically-bound cell wall protein extract.

2.4.2.2 *Acid phosphatase assay*

Reagents:

- 50 mM sodium citrate buffer, pH 5.6
- Substrate solution (8 mM ρNPP in 50 mM citrate buffer, pH 5.6)
- 1.0 M NaOH

In the activity assay, ρ-nitrophenol phosphate (ρNPP) is used as substrate and acid phosphatase (APase) activity measured based on the amount of liberated ρ-nitrophenol (ρNP). Finally, the activity was determined by comparing values against a ρNP standard curve (Figure 2.6).

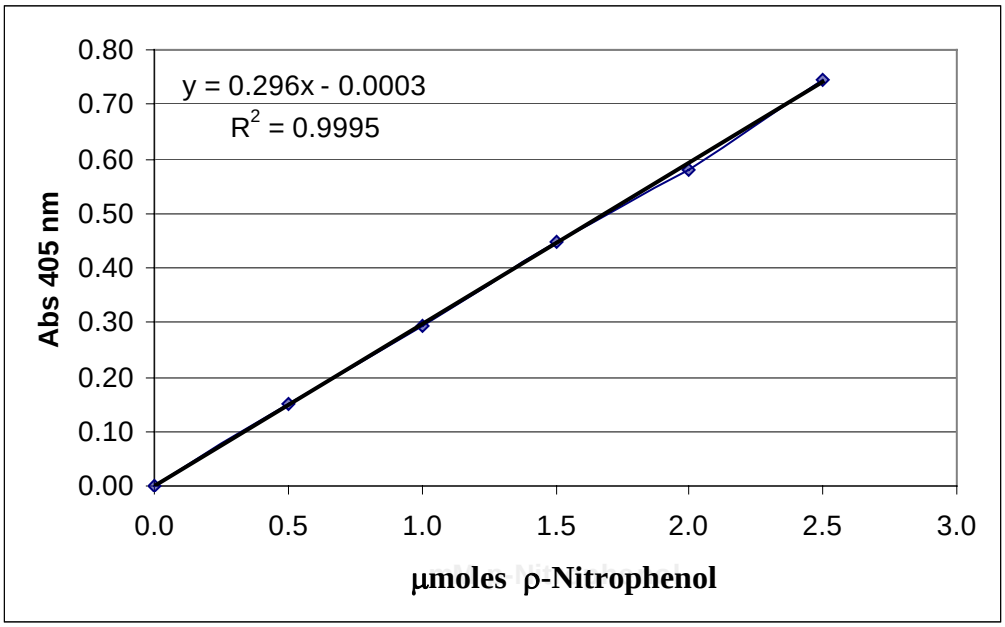

Figure 2.6 A typical ρ-nitrophenol (ρNP) standard curve for the determination of acid phosphatase activity in white clover roots

Twenty microlitres of either water soluble or ionically-bound cell wall extracts were pipetted, in triplicate, into wells of microtiter plates, and following the addition of 30 μL of 50 mM sodium citrate buffer, pH 5.6, the mixture was incubated at 37^{o}C for 5 min. Following the addition of 200 μL of substrate solution, pre-warmed at 37^{o}C, the reaction mixture was incubated at 37^{o}C for 10 min. After this time, 50 μL of reaction mixture was pipetted into a fresh well in the microtitre plate and 50 μL of 1.0 M NaOH was added to terminate the reaction. Absorbance was then read using the Anthos HTII plate reader (Anthos Labtech Instruments, Salzburg, Austria) at 405 nm and the amount of liberated ρNP by acid phosphatase was determined by comparison of the absorbance against the ρNP standard curve. APase activity is expressed in terms of the liberated ρNP per minute per gram of root fresh weight.

2.4.3 Protein and immunological analyses

2.4.3.1 Protein extraction

Reagent:

- Extraction buffer: 100 mM Tris-HCl, pH 7.5, containing 10% (v/v) glycerol, 1 mM DTT

Root tissues which were required for analysis were washed, blot dried, then weighed and frozen in liquid nitrogen. The required aliquots of tissues were ground using a previously chilled mortar and pestle, and then immediately scraped directly into chilled extraction buffer. For every gram of root tissues, 3.0 mL of extraction buffer was used. The solution was vortexed until a fine slurry was produced and then centrifuged at 14,000 rpm for 5 min at 4^{o}C. The supernatant was transferred to a fresh labelled microfuge tube and kept at –20^{o}C until used in a protein assay or for western analysis.

2.4.3.2 Protein quantitation

The protein concentration was measured using commercially available Bio-Rad protein dye. Aliquots (10 μL) of the protein extract were pipetted into wells of a microtitre plate, 20 μL of protein dye added, and the mixture made up to 100 μL with distilled water. Each sample was prepared in triplicate. After standing for 5 min, the absorbance at 595 nm was determined using an Anthos Labtech HTII plate reader. To determine the protein concentration, a standard curve of 0 - 5.0 μg of BSA (Figure 2.7)was constructed using the same procedure.

2.4.3.3 SDS-PAGE of Protein

Sodium dodecyl sulfate polyacrylamide gel electrophoresis (SDS-PAGE) was conducted as described by Laemmli (1970) to separate protein on the basis of molecular mass using the mini-PROTEAN II slab cell system.

Reagents:

- 40% (w/v) acrylamide (Bio-Rad)
- 4x separating buffer (1.5M Tris-HCl, pH8.8, containing 0.4% (w/v) SDS)
- 2x stacking buffer (0.25M Tris-HCl, pH6.8, containing 0.4% (w/v) SDS)
- 10% (w/v) ammonium persulfate (APS), prepared fresh
- (N,N,N', N- tetramethylethylenediamine) TEMED
- 10x SDS running buffer (0.25 M Tris, 1.92 M glycine, 1% (w/v) SDS, water to 1L), stable at room temperature at pH 8.3
- 2x SDS gel loading buffer (100mM Tris-HCl pH 6.8, 20% (v/v) glycerol, 5% (w/v) SDS, 5% 2-mercaptoethanol, (0.01% (w/v) bromophenol blue) (stable for weeks in the refrigerator or months at –20^{o}C).

To prepare the separating gel solution, the different components were mixed in the order as outlined in Table 2.1. The solution was then poured into a previously assembled acrylamide gel sandwich up to *ca.* 0.5 cm lower than the level where the bottom of the

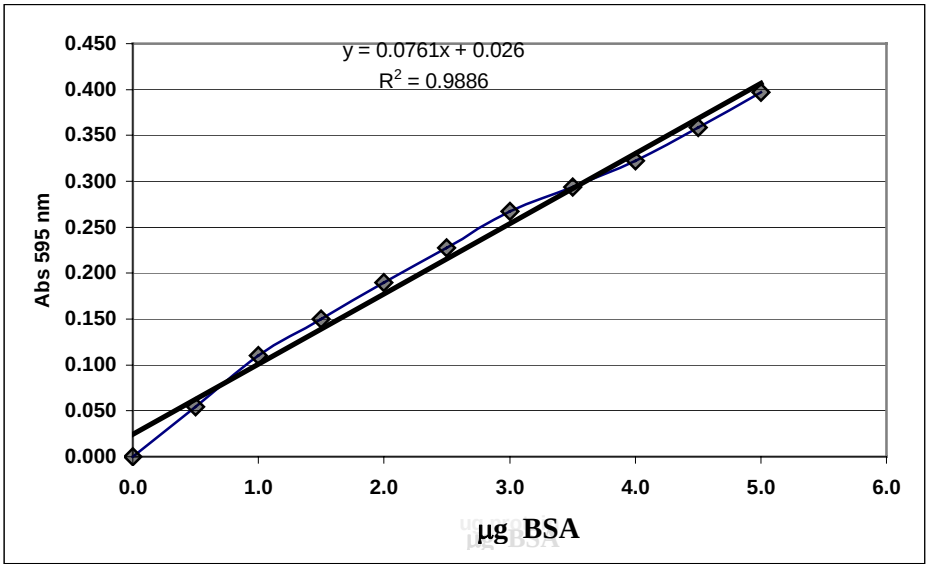

Figure 2.7 Typical standard curve for the Bio-Rad protein assay. The dots connected by a line are the actual data points while the solid straight line represents the regression line

Table 2.1 Composition of separating and stacking gel solutions for SDS-PAGE using Mini-Protean II apparatus

Order of addition	Component	1x separating gel	1x stacking gel
1	water	2.25 mL	1.25 mL
2	4x separating buffer	1.25 mL	
	2x stacking buffer		1.25 mL
3	40% acrylamide	1.50 mL	0.25 mL
4	TEMED	5.0 μL	2.5 μL
5	10% Ammonium persulphate (APS)	50 μL	25 μL

well-forming comb sits. To protect the gel surface from atmospheric oxidation, water was then pipetted on top and the gel was allowed to set for *ca.* 30 min. Prior to addition of stacking gel, the layer of water was discarded, the top of the gel rinsed with stacking buffer, and the well-forming comb inserted.

The stacking gel was allowed to polymerise for *ca.* 10 min and when set, the sandwich apparatus was transferred to the electrophoresis apparatus. Finally, the running buffer was added to the inner and outer compartment of the assembly until the buffer reached *ca.* 1 cm from the lid, and the well-forming comb removed in preparation for loading of the protein extracts.

Protein extracts were prepared for loading by adding an equal amount of 2 x SDS gel loading buffer to each sample, boiling for 5 min, and then the samples were collected by pulse centrifugation. Routinely, 5 to 10 μg of denatured protein was loaded into each sample well. For each gel, one lane was reserved for the prestained molecular marker

(Bio-Rad) where 5 μL was routinely loaded. SDS-PAGE was carried out at 150 V for 1 h and 15 min.

2.4.3.4 Staining of gels after SDS-PAGE

Reagents:

- CBB stain : 0.1% (w/v) Coomassie Brilliant Blue R-250, 40% (v/v) methanol, 10% (v/v) acetic acid)
- CBB destain: (30% (v/v) ethanol)

To determine the loading control, staining was conducted by immersing the SDS-PAGE gels in Coomassie Brilliant Blue (CBB) stain for 20 to 30 min with gentle agitation. To destain, the gel was rinsed with CBB destain until the gel background became relatively clear.

2.4.3.5 Western analysis of SDS-PAGE gels

2.4.3.5.1 Transfer of proteins from the SDS-PAGE gel to a PVDF membrane

After separation of protein by SDS-PAGE, the protein was transferred to a Polyscreen polyvinylidene difluoride (PVDF) (PerkinElmer™ Life Sciences, Inc, Boston, USA) transfer membrane using the mini-trans blot cell system. To do this, the gel was removed from the electrophoresis apparatus and equilibrated in transfer buffer (25 mM Tris, 190 mM glycine) for *ca.* 15 min. At the same time, the PVDF membrane was soaked in 100% methanol for *ca.* 15 s, then in transfer buffer for *ca.* 15 min. Simultaneously, pre-cut 3 MM papers and the fibre pads were soaked in transfer buffer. The gel sandwich was assembled in a transfer cassette holder in the order outlined in Figure A.1 and, to avoid air bubbles, the assembly was set up while partially immersed in the transfer buffer. Further, each layer was rolled gently with a glass tube in order to roll out any bubbles trapped in between layers. After assembly, the cassette was placed into the transfer device and placed into the electrophoresis gear with pre-chilled transfer

buffer. Transfer was conducted at 100 V for 1 h at 4^{o}C, with continuous stirring of buffer. At the conclusion of the transfer, the gel was stained with Ponceau S solution for 5 min whenever necessary to confirm full transfer and to detect equal loading of protein. The membrane was then destained with 30% (v/v) ethanol before conducting the next step.

2.4.3.5.2 Immunodetection of some proteins

Reagents:

- Phosphate buffer saline (PBS): (50 mM sodium phosphate buffer, pH 7.4, containing 250 mM NaCl)
- PBS: Tween 20 (0.05% (v/v) Tween 20 in 1 x PBS
- Blocking buffer: (50 mL 1x PBS, 12.5% (w/v) skimmed powder milk)
- Primary antibody (α-TR-ACO1 and α-TR-ACO2)
- Secondary antibodies (α-rabbit IgG conjugate to alkaline phosphatase, α-rabbit IgG horse radish peroxidase(HRP) conjugate, and α -mouse peroxidase conjugate)

At the conclusion of the transfer, the blotting apparatus was disassembled, the PVDF membrane placed in blocking buffer, and either incubated at room temperature for 1 h, or at 4^{o}C overnight. After three washes with PBS-Tween with 3 min per wash, the membrane was incubated in primary antibody (1:500 dilution in 1x PBST) at 37^{o}C for 1 h, or at 4^{0}C overnight with gentle agitation. Subsequently, the membrane was incubated in a 1:10,000 dilution of secondary antibody (anti-rabbit IgG conjugated to alkaline phosphatase) for 1 h at room temperature. In between each antibody incubation, the membrane was washed five times with PBS-Tween for *ca.* 5 min each wash.
For immunodevelopment of membrane using the chemiluminescent substrate, different concentrations of primary and secondary antibodies were used.

2.4.3.5.3 Immunodevelopment of membranes using alkaline phosphatase conjugates

Reagents:

- Substrate buffer: (100 mM Tris HCl, pH 9.6, containing 100 mM NaCl)
- Developing solution: (10 mM $MgCl_2$, 0.01% (w/v) BCIP, 0.02% (w/v) NBT)

A colorimetric detection of alkaline phosphatase activity using 5-bromo-4-chloro-3-indolyl-Phosphate (BCIP) in conjunction with Nitro Blue Tetrazolium chloride (NBT) was used.

After the final wash with PBS-Tween (Section 2.4.3.5.2), the membrane was neutralised by washing with substrate buffer twice. Following the neutralisation step, the developing solution was poured onto the membrane and once the blue precipitate appeared as a clear band, the membrane was washed several times with distilled water. The membrane was then dried in between layers of paper towels, and stored until further analysis.

2.4.3.5.4 Immunodevelopment of membrane using chemiluminescent substrate

Reagent:

- Blot rinse solution: (10 mM Tris HCl, pH 7.4, containing 150 mM NaCl, 1.0 mM EDTA, and 0.1% (w/v) Tween 20)
- Substrate solution: (1:1 ratio of Luminol and hydrogen peroxide)

The Supersignal West Pico chemiluminescent substrate (PIERCE, Rockford, IL) which is composed of a stable luminol with enhancer and a stable peroxide solution was used for detecting HRP immobilised on PVDF membrane. Luminol is a chemiluminescent substrate, which when oxidised by peroxide creates a product known as 3-aminophthalate which is in an excited state. Upon its decay to a lower energy state, the product releases photons of light. Immunodevelopment of blots was carried out following the manufacturer's instruction.

After the final wash with PBS Tween (Section 2.4.3.5.2), the membrane was washed twice with a blot rinse solution for *ca.* 5 min each wash. Immediately prior to development of the membrane, a substrate working solution was pipetted on the surface of the membrane. For each cm^2 area of the membrane, *ca.* 50 μL of the substrate solution was used. The membrane was incubated in the solution for 5 min, the excess reagent drained off and the membrane wrapped in clear plastic sheet (Glad wrap), ensuring any trapped bubbles was removed.

To develop the image, the membrane was exposed to an X-ray film (Kodak) at a designated time and finally the protein blot was developed using an automatic X-ray film processor (100Plus™, All Pro Image, Hickville, NY, USA).

2.4.3.5.5 Titration of primary and secondary antibodies for the chemiluminescence method

Titration of the primary (1^oAb) and secondary (2^oAb) antibodies was conducted in order to determine the optimal dilution, and to obtain a minimal signal to noise background. The three primary antibodies used in this thesis, α-GFP, α-TR-ACO1 and α-TR-ACO2 were titrated against two secondary antibodies, a α-mouse- peroxidase conjugate and a α-rabbit- HRP conjugate. For each antibody, four dilutions were tested.

Results of titration of the α-GFP showed that the putative optimum combination for the recognition of GFP protein was either 1:5,000 dilution for the 1^oAb and 1:40,000 for the 2^oAb, or 1:10,000 for the 1^oAb and 1:20,000 for the 2^oAb (Figure 2.8). For TR-ACO1 protein, the combination of antibodies used for the subsequent analysis was 1:5,000 for 1^oAb and 1:50,000 for the 2^oAb (Figure 2.9). Similarly, for the TR-ACO2 protein, the combination of 1:5000 for the 1^oAb and 1:50,000 for the 2^oAb (Figure 2.10) was also used for the subsequent analyses.

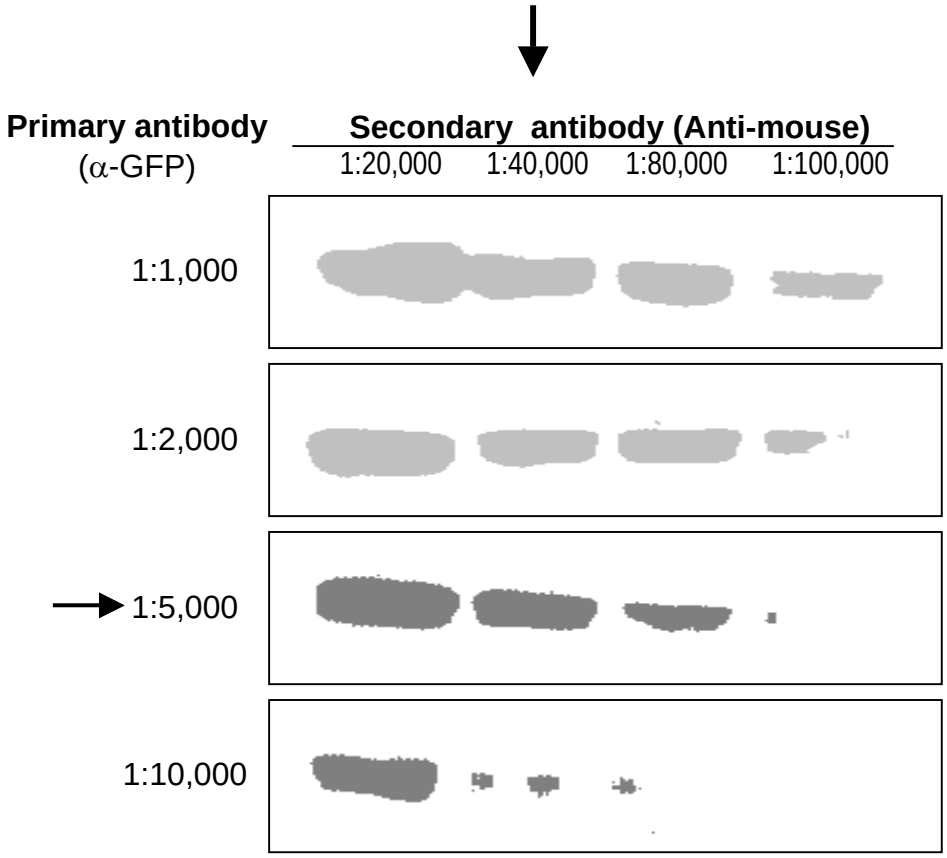

Figure 2.8 Immunodetection of GFP protein at varying dilutions of α-GFP (1^{o}Ab) and α-Mouse (2^{o}Ab). Five μg of protein from white clover root extract were separated by SDS-PAGE at 150 V for 1.5 h and blotted onto PVDF at 100 V for 1 h, incubated with the α-GFP (1^{o}Ab), as indicated, for 1 h at 37^{o}C and with the α-mouse IgG HRP conjugate (2^{o}Ab), as indicated, for another 1 h at room temperature. Immunodevelopment of the blot was carried out using the Supersignal West Pico chemiluminescent substrate. Membrane was exposed to X-ray film (Kodak) for 2 min. Arrows indicate the antibody dilution used in the subsequent analyses

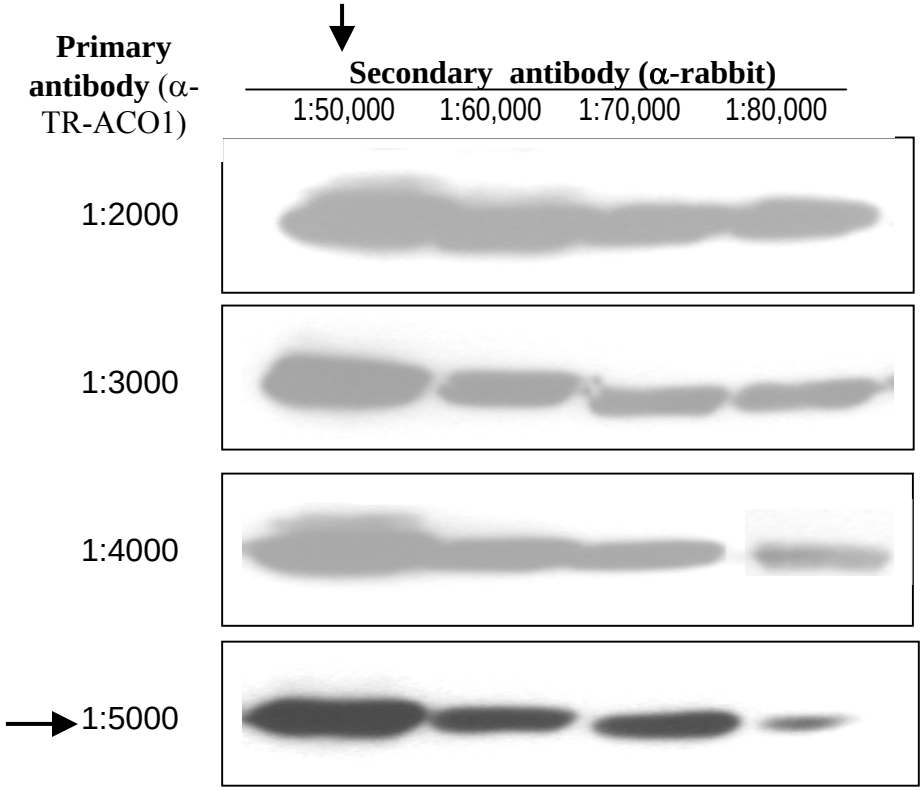

Figure 2.9 Immunodetection of TR-ACO1 protein at varying dilutions of α-TR-ACO1 antibody (1°Ab) and α-Rabbit IgG HRP conjugate (2°Ab). Five μg of protein from white clover root extracts were separated by SDS-PAGE at 150 V for 1.5 h, blotted onto PVDF at 100 V for 1 h, incubated with the α-TR-ACO1 (1°Ab), as indicated, for 1 h at 37°C, and with an α-Rabbit IgG HRP conjugate (2°Ab), as indicated, for another 1h at room temperature. Immunodevelopment of the blot was carried out using Supersignal West Pico chemiluminescent substrate. Membrane was exposed to X-ray film (Kodak) for 1 min. Arrows indicate the antibody dilution used in the subsequent analyses

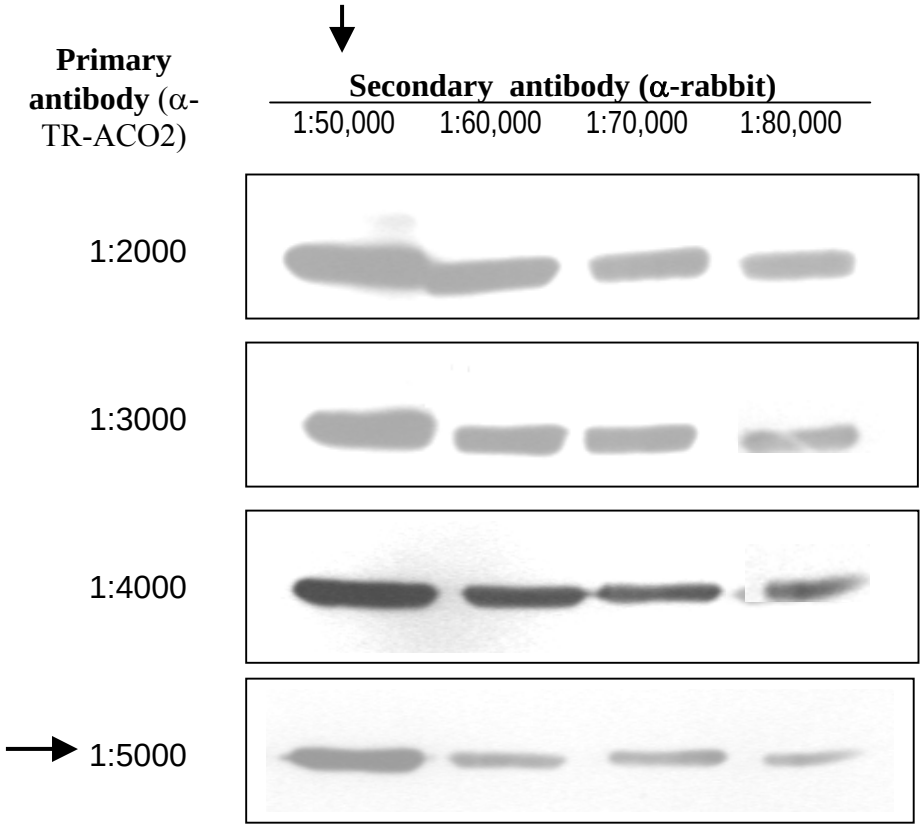

Figure 2.10 Immunodetection of TR-ACO2 protein at varying dilutions of α-TR-ACO2 antibody (1°Ab) and α-Rabbit IgG HRP conjugate (2°Ab). Five μg of protein were separated by SDS-PAGE at 150 V for 1.5 h, blotted onto PVDF at 100 V for 1 h, incubated with the α-TR-ACO2 antibody (1°Ab), as indicated, for 1 h at 37°C and with the α-Rabbit IgG HRP conjugate (2°Ab), as indicated, for another 1 h at room temperature. Immunodevelopment of the blot was carried out using the Supersignal West Pico chemiluminescent substrate. Membrane was exposed to X-ray film (Kodak) for 30 s. Arrows indicate the antibody dilution used in the subsequent analyses

2.5 Molecular Methods

2.5.1 Preparation of Plasmid DNA and cloning procedures

2.5.1.1 Plasmid DNA isolation

Two methods of plasmid DNA extraction, both relying on the alkaline lysis of bacterial cells, were routinely used in this study. The first is the rapid mini preparation method while the second is the column mini preparation method, which uses a commercially available Pure Plasmid Isolation Kit (Roche diagnostic, GmbH, Mannheim, Germany).

2.5.1.1.1 Alkaline lysis mini prep method

Reagents and culture medium:

- Lauria Bertani (LB) broth: [1% (w/v) tryptone, 0.5% (w/v) yeast extract, and 1% (w/v) NaCl, pH 7.5]
- Solution A: (25 mM Tris-HCl, pH 8.0, containing 50 mM glucose, and 10 mM EDTA)
- Solution B: (0.2 M NaOH, 1% (w/v) SDS)
- Solution C: (3 M potassium acetate, 11.5% (v/v) glacial acetic acid)

E. coli cells were grown for approximately 16 h at 37^{o}C in 5 –10 mL of LB broths with appropriate antibiotic for selection. The cells were pelleted at 10,000 x g for 5 min, the supernatant discarded and the pellets resuspended in 100 μL of freshly prepared alkaline lysis Solution A, mixed by vortexing, and then transferred to an 1.5-mL Eppendorf. Alkaline lysis Solution B (400 μL) was then added, the solution mixed by slow inversion 5-6 times, then the mixture was kept on ice for 10 min. After this, 300 μL of Solution C was added, the mixture shaken quite vigorously, then kept on ice for 15 min followed by centrifugation at 20,000 x g for 5 min. Supernatant (500 μL) was then transferred to a new tube, 1 mL of isopropanol added, the contents mixed by gentle inversion and the precipitated DNA collected by centrifugation at 20,000 x g for 5 min at 4^{o}C. The pellets were then washed with 70% (v/v) ethanol, and after air drying for *ca.*

5 min, the DNA was resuspended in 50 μL sterile distilled water or TE buffer (10 mM Tris, 1 mM EDTA, pH 7.5).

2.5.1.1.2 Column miniprep method

This method was carried out following the manufacturer's instruction and the reagents used were those included in the Plasmid Isolation kit

Reagents:

- Suspension buffer
- Lysis buffer
- Binding buffer
- Wash buffer I
- Wash buffer II
- Elution buffer

Overnight culture of *E.coli* cells (Section 2.5.1.1.1) were pelleted by centrifugation at 9,000 x g for 5 min at room temperature (RT). After discarding the supernatant, the pellet was resuspended in 250 μL of suspension buffer with RNase. Following centrifugation at 9,000 x g for 1 min, the supernatant was again discarded and 250 μL of lysis buffer was added, the suspension mixed gently before incubation for 5 min at room temperature. After addition of chilled binding buffer (350 μL), the suspension was mixed gently and incubated on ice for 5 min, then pelleted by centrifugation at 20,800 x g for 10 min. The supernatant was then carefully transferred to High Pure Filter Tube (Roche Diagnostics GmbH, Mannheim, Germany), centrifuged at 20,800 x g for one min at room temperature, and the flow through discarded. The column was washed with 500 μL of Wash Buffer 1, followed by 700 μL of Wash Buffer II, with each flow through discarded after centrifugation at 13,000 x g for 1 min. The column was then centrifuged for additional 1 min and the final flow through discarded before 100 μL of elution buffer was passed through the column to elute the purified plasmid DNA which was collected by centrifugation at 20,800 x g for one min at room temperature.

2.5.1.2 Polymerase chain reaction (PCR)

Routinely, PCR was carried out either in a Palm-Cycler Thermocycler version 2.2 (R.Corbett Life Sciences, Australia) or in a ***T***Gradient Thermoblock (Biometra®, Germany). The standard PCR reaction mixture (50 μL) was normally composed of DNA template (5-10 ng plasmid DNA or 50-100 ng genomic DNA), 2 μL of each primer (10 μM), 25 μL of 2x PCR Master mix (Promega) and the remaining volume was made up of sterile distilled water. In some instances, the PCR mix was made up to a total volume of 25 μL, using only one-half of the contents mentioned previously. The PCR conditions varied , and depended on the primers used in the reaction (Table 2.4) and on the expected product size.

2.5.1.3 Precipitation of nucleic acid

Routinely, nucleic acid was precipitated by adding 0.1 volume of 3 M sodium acetate and 2.5 (for DNA) or 3 (for RNA) volumes of ice-cold 100% ethanol. The length of time for precipitation varied depending upon the calculated concentration of the nucleic acid. If the concentration was considered to be lower than 0.5 $\mu g.mL^{-1}$, the nucleic acid was incubated overnight either at 4°C or –20°C for maximal yield. However, if the concentration was estimated to be 1 $\mu g.mL^{-1}$ or greater (commonly observed for plasmid preparations), then the nucleic acid was collected by centrifugation immediately. The precipitated nucleic acid was pelleted by centrifugation at 20,000 x g for 15 min either at room temperature or at 4°C. After discarding the supernatant, the pellet was washed with 80% (w/v) ethanol, the nucleic acid pellet air dried for *ca.* 5 min, and then suspended in sterile distilled water or in TE buffer. RNA pellet was resuspended in sterile water treated with 0.1% (v/v) diethyl pyrocarbonate (DEPC, Sigma) and kept at –80°C until future use.

Table 2.2. Primer sequences used in this study

Primer name	Sequence
mGFP-seq-F1	5′- CCCA.GGCTTTACACTTTA- 3′
mGFP-seq-R1	5′- GCCCA.TTAACA.TCACCA.T –3′
ACO1p-mGFP5-F1	5′-TCTCCTTCTGATCGCA.GCTGC –3′
ACOp-mGFP5-R1	5′-GCTGCTGGGATTACACA.TGGC–3′
Actin F	5′- GCGAATTCTTCACCACYACHGCYGARCG 3′
Actin R	5′- GCGGATCCCCRATCCA.RACACTGTAYTTCC 3′
mGFP-probeF	5′-CCTATCA.TTATCCTCGGCCG–3′
mGFP-probeR	5′-GTCGGCCA.TGATGTATACGTTG–3′
TR-110 forward	5′-GACGACA.AGCTTAAATATTATTCTTACTGCTTATT–3′
TR-110 Reverse	5′-GACGACGGATCCTTTGCTTCTTTCA.ATTTTCT –3′
TR-ACO1For	5′-CTT TGA GTT GGT GAA CCA. TGGA –3′
TR-ACO1Rev	5′-GTT ATG ACT TCA. AGT TGA TCA. CC –3′
TR-ACO2 For	5′-CTT TGA GC T GG T GAA TC A TGG –3′
TR-ACO2Rev	5′-GTT ATT ACC TCG AGT TGG TCA. –3′
TR-ACO3 For	5′-GGA TTC TTT GAG CTG GTG AAT C –3′
TR-ACO3Rev2	5′-TTCTGCTAGCTTCTCTAACCTCA.A–3′
TR-ACO4For	5′-GAT TCT TTG AGC TGG TGA ATC –3′
TR-ACO4Rev2	5′-GGTTCTCTTCCCTAACA.GAAA–3′

2.5.1.4 Determination of DNA quantity and purity

DNA was quantified by absorbance at 260 nm using a spectrophotometer (Ultrospec 3000, Pharmacia Biotech). An optical density (OD) of 1.0 at 260 nm corresponds to approximately 50 $\mu g.mL^{-1}$ of double stranded DNA. DNA was diluted 100-fold with water and placed in a 1 mL quartz cuvette, and the OD reading at 260 nm was compared against a water blank.

DNA was calculated using the formula:

$$\text{Concentration of DNA } (\mu g.mL^{-1}) = \frac{OD_{260} \text{ x } 50 \text{ x dilution factor}}{1000}$$

The purity of the DNA was resolved by determining the OD_{260}/OD_{280} ratio. Typically, a pure DNA has a ratio of $OD_{260}/_{280}$ equivalent to 1.8. A ratio which is lower than 1.8 indicates possible presence of protein contaminants (Sambrook *et al.*, 1989) whereas a ratio higher than 2.0 suggests that the sample may be contaminated with chloroform (Chawla, 2003).

2.5.1.5 Dephosphorylation of linearised plasmid DNA

Dephosphorylation of linearised plasmid vector was undertaken prior to the ligation reaction to inhibit or ensure very minimal occurrence of self-ligation of the vector and allowing better chance of ligation of the insert to the vector. Shrimp Alkaline Phosphatase (SAP) was used to dephosphorylate either the 5′ overhangs or 5′ recessive ends of the linearised plasmid DNA. The appropriate amount of 10x reaction buffer and 1 μL of SAP were added to the DNA dissolved in sterile distilled water to a final volume of 50 μL and then the reaction incubated at 37^{o}C for 60 min. Following the dephosphorylation reaction, the SAP was deactivated by heating at 65^{o}C for 15 min and the dephosphorlated DNA was then used for ligation without further purification.

2.5.1.6 DNA ligation

DNA ligation was carried out using a 1:3 molar ratio of vector:insert. The molar ratio was calculated using the equation below:

$$\frac{\text{Amount of vector(ng)} \times \text{size of insert (kb)}}{\text{Size of vector (kb)}} \times \text{molar ratio of } \frac{\text{insert}}{\text{vector}} = \text{amount of insert (ng)}$$

The ligation reaction was carried out using 1 unit of T4 DNA ligase (Promega, Madison, USA) per 50 ng vector and the calculated amount of DNA insert, with the appropriate volume of 2x T4 DNA ligation buffer supplied by the manufacturer. The ligation reaction was made up to a final volume of 20 μL with sterile distilled water and incubated at 25^{o}C overnight.

2.5.1.7 Preparation of E. coli (strain DH5-α) competent cells

LB broth was inoculated with *E. coli* cells of strain DH5-α (GIBCO BRL) and incubated overnight at 37^{o}C, with shaking at 180 rpm. From this overnight culture, 400 μL of broth was transferred to a fresh 40 mL of LB broth and the culture was allowed to grow for 2–2.5 h at 37^{o}C until the OD_{600} reached approximately 0.40. The cell culture was then poured into a sterile, pre-chilled centrifuge tube and centrifuged at 3000 x g for 5 min at 4^{o}C. The supernatant was discarded and the pellet gently re-suspended in 10 mL of ice-cold 60 mM $CaCl_2$ before an additional 10 mL of 60 mM $CaCl_2$ was poured into the tube and the mixture incubated on ice for 30 min. After centrifugation for 5 min at 3000 x g at 4^{o}C, the supernatant was poured off and the pellet gently re-suspended in 4 mL of 60 mM $CaCl_2$ containing 15% (v/v) glycerol. Aliquots (300 μL) of the competent cells were then snap frozen in liquid nitrogen and stored at –80^{o}C until required.

2.5.1.8 Bacterial transformation using the heat shock method

Competent cells were thawed on ice for *ca.* 5 min, then 50 µL to 100 µL aliquots were added to 2.5 µL to 5.0 µL of ligation reaction, the suspension gently mixed and incubated on ice for *ca.* 20 min. The suspension was heat shocked at 42°C for 30 s, then returned to ice for 2 min. A 500 µL aliquot of LB was added immediately, followed by incubation at 37°C for 1 h with shaking at 180 rpm. The putative transformed cells were then spread onto LB plates with the appropriate antibiotic (typically 50 $\mu g.mL^{-1}$ Kanamycin). The LB^{Kan50} plates were left for *ca.* 5 min to allow drying, then sealed with parafilm and placed in an inverted position and incubated at 37°C overnight to allow the colonies to grow.

2.5.1.9 Selection of putative transformants

Following transformation, random colonies were grown in 10 mL of LB^{Kan50} broth and after DNA isolation (Section 2.5.1.1.1) putative transformants were screened by PCR (Section 2.5.1.2) using appropriate primers (Table 2.4). Further screening was also conducted by restriction digestion using enzymes *Hind* III and *Bam* H1 following the protocol outlined in Section 2.6.1.9.

2.5.1.10 *Electrotransformation of Agrobacterium tumefaciens*

2.5.1.10.1 Preparation of electrocompetent cells

Culture media:

- Yeast Mannitol (YM) Broth, pH 7.0, containing 0.04% (w/v) yeast extract, 1% (w/v) mannitol, 0.01% (w/v) NaCl, 0.01% (w/v) $MgSO_4$, and 0.50% (w/v) $KH_2PO_4.3H_20$
- YM agar: 1.5% (w/v) agar in YM broth

A colony from a 48 h culture of *A. tumefaciens* strain LBA 4404 plated on YM agar was cultured for *ca.* 16 h in YM broth. An aliquot (3 mL) from the log phase culture was then inoculated into 1.5 L of YM broth, incubated overnight at 30°C, with shaking at

300 rpm until the OD_{550} = 0.70. The cultured cells were then decanted into sterile 500 mL centrifuge tubes and pelleted by centrifugation at 3000 x g for 10 min at 4°C. The supernatant was carefully poured off and discarded, and the cell pellets kept on ice. To maintain highly competent cells, all manipulations were carried out on ice and all buffers used were ice-cold. Further, because the cells are particularly susceptible to shearing, pipetting of cell suspensions was minimised and, whenever necessary, large-bore pipette tips were used.

Into each centrifuge tube containing cell pellets, sterile, ice-cold 10% (v/v) glycerol (50 mL) was added and the tube vortexed to re-suspend the cell pellets. An additional 450 mL of sterile, ice-cold 10% (v/v) glycerol was then added to each tube to wash the cells followed by centrifugation at 3000 x g for 10 min at 4°C. The supernatant was carefully discarded and the cells were washed again as before. The resulting cell pellets were again resuspended in 5 mL of cold 10% (v/v) glycerol, transferred to 30 mL Oakridge tubes (Nalgene®, Rochester, NY, USA) and pelleted at 3,000 x g for 5 min. After discarding the supernatant, cell pellets in each tube were re-suspended in 0.5 mL of sterile, ice-cold 1 M sorbitol, and a 200 µL aliquots of competent cells were dispensed into 1.5 mL microfuge tubes, snap frozen in an isopropanol-dry ice bath, and stored at –80°C until required.

2.5.1.10.2 Electroporation procedures

Electrotransformations were performed in a microelectroporation chamber using a MicroPulser™ electroporation apparatus (BIORAD, Life Technologies Inc., Gaithersburg, Md.). Electrocompetent *Agrobacterium* cells were transformed following the manufacturer's instructions.

In preparation for electrotransformation, the electroporation cuvettes were pre-cooled on ice, the YM broth (1 mL per DNA sample to be electroporated) was pipetted in separate microfuge tubes, and the required electrocompetent *Agrobacterium* (2.5.2.1) cells were thawed on ice. The required DNA (5 μL, ~0.5 μg) was pipetted into sterile pre-chilled 1.5 mL-capacity microfuge tubes and following the addition of 20 μL of electro-competent cells, the tubes were gently tapped to mix. After setting the electroporation apparatus to ”Agr” (which refers to *Agrobacterium)*, the DNA samples were immediately transferred to the pre-cooled electroporation cuvettes, and the cuvettes gently tapped so that the suspension was gravitated to the bottom. The cuvette was quickly placed into the chamber slide, and the pulse button pressed once to provide a 5 milliseconds pulse of ~400 V. Immediately, the cuvette was removed from the chamber and the ice-cold 1 mL YM broth was used to transfer the cells from the cuvette to the tube. The electroporated cells were then incubated at 28^{o}C for 3 h, with shaking at 250 rpm, and aliquots were then plated onto YM^{Kan50} agar plates and then incubated for 48 h at 28^{o}C.

2.5.1.10.3 Confirmation of the transformation of A. tumefaciens

The colonies from putative electrotransformed cells (2.5.2.2) were re-inoculated into 10 mL YM ^{Kan50} broth (Section 2.5.2.1) and incubated at 28^{o}C for 2 d with shaking at 180^{o}C before the plasmid DNA was isolated as described in Section 2.5.1.1.1. To confirm that transformation to *A. tumefaciens* occurred, the extracted DNA was digested with appropriate restriction enzymes (Section 2.5.1.11) and the insert resolved by gel electrophoresis (Section 2.5.1.13). Further confirmation was carried out by PCR (Section 2.5.1.2) using the appropriate primers. All plasmid DNA was stored at –20^{o}C or at 4^{o}C until required.

2.5.1.11 Restriction digestion of plasmid DNA

Restriction digestion of plasmid DNA was carried out using Roche restriction enzymes (Roche) and 10x reaction buffer (Roche). The volume of the digestion reaction varied from 10 – 50 μL and the reaction mixture was incubated at either 25^{o}C (for *Agrobacterium)* or 37^{o}C (for *E. coli*) for between 1 h to 16 h. Digestion of small plasmids, such as pGEM was routinely undertaken with short incubation times (1-3 h). For large plasmids (such as *pBIN19*), restriction digestion was allowed to occur for approximately 16 h. To check if the digestion had progressed to completion, an aliquot (2 μL) of each digestion mix was separated by gel electrophoresis through a 1% (w/v) agarose (Ultrapure^{TM} agarose, GIBRO BRL, Grand Island, NY, USA) gel. When restriction digests had been completed, the DNA fragments were again separated, routinely through a 1% (v/v) agarose gel (2.6.1.10).

2.5.1.12 Restriction digestion of genomic DNA

Restriction endonuclease enzymes were used in separate reaction mixes to digest genomic DNA. Each reaction mixture consisted of 30 μg DNA, 80 units of restriction enzyme, 20 μL of 10 x restriction buffer and sterile distilled water to make a final volume of 200 μL. After gently mixing the components, the samples were incubated overnight at either 37^{o}C or 25^{o}C depending on the temperature requirement of the restriction enzyme for optimum activity. On the following day, a further 30 U of each enzyme was added into the reaction mixture and the DNA further digested for 3 to 5 h. To degrade contaminating RNA, RNAse (0.5% (v/v) of the reaction mixture) was added to each sample mixture and incubated for 1 h at 37^{o}C. The DNA was then precipitated with ethanol (Section 2.5.1.3) and resuspended in 20 μL of sterile distilled water. Samples were then resolved by 1.0% agarose gel electrophoresis (Section 2.5.6).

2.5.1.13 Agarose gel electrophoresis

The dimensions of agarose gels used for electrophoresis varied depending upon the purpose for which the gel was required. The mini gel was routinely used for resolving the fragment size of DNA after PCR or restriction digestion. For Southern blotting, larger agarose gels (150 mm x 150 mm) were routinely prepared.

The composition of the agarose gels as well as the length of running time during electrophoresis generally varied depending on the expected size of the DNA fragment. Generally, from 1.0 to 2.0% (w/v) agarose in 1x tris acetate EDTA (TAE) was used and the gels were routinely run at 50-100 V for 1-2 h. For Southern blotting, the DNA separation was normally conducted at 22 V for *ca.* 18-20 h. To visualise the DNA, the gel was soaked in ethidium bromide solution (10 $\mu g.mL^{-1}$) for 10 – 30 min followed by destaining for *ca.* 10 - 20 min in distilled water. The destained gel was then viewed under UV light using the gel documentation system. To estimate fragment size, DNA markers (Invitrogen LIFE TECHNOLOGIES) were used at 0.7 μg per lane.

2.5.1.14 DNA purification from agarose gels

The QIAquick Gel Purification Kit (QIAgen Pty Ltd, CA., USA) was used to recover and purify DNA from agarose gels following the manufacturer's instructions. DNA inserts and vectors for cloning were gel cut under the UV transilluminator and the excised gel was added to 3 volumes of Buffer QG (QIAGEN). The gel was incubated at $50^{o}C$ for 10 min or until completely solubilised. During the incubation, the tube was vortexed every 2 to 3 min to help dissolve the gel. If the DNA fragments to be recovered were 500 bp or > 4 kb, one gel volume of isopropanol was added to the sample in order to increase the DNA yield. The dissolved gel slurry was pipetted into

the QIAquick column seated in a 2 mL collection tube and the flow through was discarded after centrifugation for 1 min at room temperature. For plasmid DNA to be used for direct sequencing, 0.5 mL of Buffer QG was added and the column centrifuged for 1 min to remove all traces of agarose. The column was then washed with 0.75 mL of Buffer PE (QIAGEN), and allowed to stand for 2-5 min before spinning for 1 min. After discarding the flow through, an additional centrifugation step of ~17,000 x g for 1 min was undertaken to eliminate residual ethanol. The plasmid DNA bound to the QIAquick column was then eluted by adding 50 μL of Buffer EB (QIAGEN) to the centre of the membrane column, and the pure plasmid DNA collected in a 1.5 μL microfuge tube by centrifugation at 17,000 x g for 1 min at RT.

2.5.1.15 DNA sequencing and purification procedures

DNA sequencing was carried out for either plasmid or linearised DNA templates recovered from agarose gels. For plasmid DNA, *ca.* 0.5 – 1.0 μg of DNA was used in the sequencing reaction and usually 50–100 ng of the linearised DNA fragment was used. The sequencing reaction was normally composed of 2 μL of Big Dye Terminator (Version 3.1, Applied Biosystems, CA., USA), 3 μL of sequencing buffer (Applied Biosystems), 3.2 pmol of the appropriate primer, the estimated amount of DNA template, and PCR water (filter sterilised distilled water) to make a final volume of 20 μL. The reaction was routinely ran in 27 cycles of 96^{o}C for 30 s, 50^{o}C for 15 s, and 60^{o}C for 4 min using a one-step reaction programme in a Thermal Cycler.

At the termination of the programme, the reaction was transferred to a microfuge tube, and following the addition of 2 μL of 125 mM EDTA (pH 8.0), 2 μl of 3M sodium acetate (pH 5.2) and 50 μL of 100% ethanol, the solution was mixed by inversion 5 times. After incubation for 15 min at 4^{o}C, the samples were centrifuged at 17,000 x g

for 30 min at 4°C and the supernatant was discarded immediately. The DNA pellet was washed twice with 70 μL of 70% (v/v) ethanol and the supernatant discarded after centrifugation for 10 min. At the conclusion of the washing procedure, the DNA was air dried for *ca.*1 min, and the sample submitted to the DNA sequencing laboratory, Allan Wilson Centre, Institute of Molecular BioSciences, Massey University, Palmerston North, NZ for automated sequencing using ABI PRISM® Big Dye™ Terminator Cycle Sequencing (Applied Biosystems).

2.5.2 Southern analysis procedures

2.5.2.1 Isolation of genomic DNA

Genomic DNA was extracted from young leaves using the protocol modified from Keb-Llanes et al (2002).

Reagents and Buffers:

- Extraction Buffer A - 100 mM Tris-HCl, pH 8.0 containing 2% (w/v) hexadecyltrimethylammonium bromide (CTAB), 20 mM EDTA, 1.4 M NaCl, 4% (w/v) polyvinylpyrrolidone (PVP), 0.1% (w/v) ascorbic acid, 10 mM β-mercaptoethanol (BME)
- Extraction Buffer B - 100 mM Tris-HCl, pH 8.0 containing 50 mM EDTA, 100 mM NaCl, 10 mM β- mercaptoethanol
- TE Buffer - 10 mM Tris-HCl, pH 8.0, 1 mM EDTA
- Other reagents:

  20% (w/v) Sodium dodecyl sulphate (SDS)

  5 M Potassium acetate (stored at –20°C)

  3 M Sodium acetate (pH 5.2)

  70% (v/v) ethanol

  Absolute isopropanol, stored at -20°C

Frozen tissues (typically 0.3 g) were ground to a fine powder in liquid nitrogen and after transfer of the cold powder to 2.0 mL-capacity Eppendorf tubes, 300 μL of extraction

buffer A, 900 µL of extraction buffer B, and 100 µL of 20% (w/v) SDS were added and the mixture was vortexed for 30 s. The slurry was then incubated at 65^{o}C for 10 min, and after the addition of 410 µL of ice-cold 5 M potassium acetate, the suspension was mixed thoroughly by inversion. After centrifugation at 15,300 x g for 15 min at 4^{o}C, 1.0 mL of the supernatant was transferred to a clean Eppendorf tube, 1.0 mL of cold isopropanol added and the mixture incubated on ice for 20 min to precipitate the genomic DNA. Following centrifugation at 9,600 x g for 10 min at 4^{o}C, the supernatant was discarded, and the DNA pellet washed with 500 µL of 70% (v/v) ethanol followed by another centrifugation for 5 min at 4^{o}C. The pellet was re-suspended in 600 µL of TE buffer, and 60 µL of 3M sodium acetate (pH 5.2) and 360 µL of cold isopropanol added. Following incubation on ice for 20 min, the suspension was pelleted by centrifugation at 9600 x g for 10 min at 4^{o}C, the supernatant discarded, and the DNA pellet washed with 70% (v/v) ethanol. To further purify the DNA, the pellet was again re-suspended in 600 µL of TE buffer and a second precipitation step was conducted, by adding 60 µL of 3M of sodium acetate and 360 µL of ice-cold isopropanol followed by another wash with 70% (v/v) ethanol. After the last wash, pellets were air dried for 5 min and then re-suspended in 100 µL of TE buffer. The DNA concentration was quantified as outlined in Section 2.5.1.4.

2.5.2.2 DNA blotting onto the nylon membrane

The method for the downward alkaline capillary transfer by Chomczynski (1992) was used to transfer genomic DNA fragments into the positively charged nylon membrane (Roche Diagnostics GmbH, Mannheim, Germany).

Reagents:

- Depurination solution: (0.25 M HCl)
- Denaturation solution: (1.5 M NaCl, 0.4 M NaOH)

- Transfer solution: (3 M NaCl, 8 mM NaOH, pH 11.4 -11.45)
- 5 x SSPE: (50 mM $Na_2PO_4.2H_2O$, pH 7.7, 0.9 M NaCl, 5 mM EDTA)

Following electrophoresis (Section 2.5.6), the resolved DNA fragments were viewed under UV in a gel documentation system, and the gel was immersed in the depurination solution (0.25 M HCl) with gentle agitation for 7 min. After decanting the acid solution, the gel was rinsed twice with distilled water, then placed in the denaturation solution for 1 h. After which, the gel was rinsed in water three times then immersed in transfer solution for 15 min.

While the gel was still in the transfer solution, the blotting system (Figure 2.10) was prepared. Two pieces of 3 MM Whatman® chromatography paper (Whatman®, Whatman International Ltd, Maidstone, England), cut slightly bigger than the gel size, were placed onto a glass plate, with the one on top pre-soaked in the transfer solution. The positively charged nylon membrane, cut to the same dimension as the gel, and with the upper left corner nicked for later identification, was also pre-soaked for 5 min in transfer solution then laid on top of the 3 MM Whatman® chromatography paper. After sufficient incubation in the transfer solution, the gel was placed face-up on top of the membrane, gently rolled with a test tube to exclude air bubbles that may hinder direct contact of the gel with the membrane. The edge of the gel was surrounded with strips of glad wrap film to ensure that the transfer solution would pass through the gel. For the next layer, 3 pieces of 3 MM Whatman® paper, pre-wetted in transfer solution were laid one after another, again ensuring no air bubbles were trapped in between. The whole assembly was transferred onto the 3 MM paper which sat on a stack of paper towels *ca.* 5 cm high. Two sets of 3 MM paper, cut gel-width but *ca.* 40 cm long (two pieces per set) were soaked in transfer solution and used as a capillary wick, with the

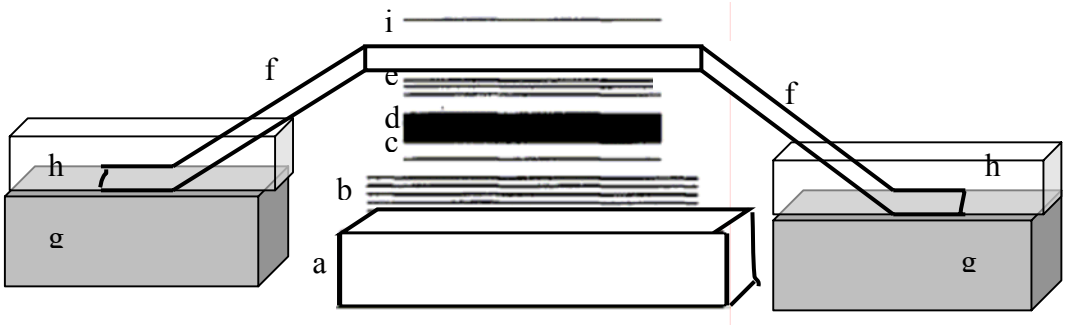

Figure 2.11 Schematic presentation of the blotting assembly for the downward alkaline capillary transfer of DNA from gel to positively charged nylon membrane. DNA transfer was allowed to occur for 4 – 6 h.

a - paper towels in a plastic box (*ca.* 5 cm stack)
b - 3 MM blotting paper (5 layers)
c - positively charged nylon membrane (Roche diagnostics, GmbH)
d - DNA gel
e - pre-wet 3 MM blotting papers (3 layers)
f - wick - 3 MM paper - 2 strips on both sides
g - support
h - tray with transfer buffer solution
i - plastic cover

distal end dipped into the transfer solution and other end covering the surface of the blotting assembly (Figure 2.11). The entire wick and transfer solution were covered with cling wrap to avoid evaporation of liquid, and then the transfer of DNA was allowed to occur for 4-6 h. At the conclusion of blotting, the membrane was neutralised in a solution of 0.2 M $Na_2PO_4.2H_20$, pH 7.2 for 10 min, then post-fixed by UV cross linking at 12,000 μjoules for 1.2 min using a UV Stratalinker® 2400 (STRATAGENE, La Jolla, Ca. USA), and finally sealed in a plastic bag and stored at 4^oC until required. The same procedure was also used to transfer the sqRT-PCR products onto the positively charged nylon membrane, except that the depurination and denaturation steps were not carried out.

2.5.2.3 Labelling DNA with [α-^{32}P]–dCTP

A Ready-To-Go DNA labelling kit (Amersham) was used to incorporate [α-^{32}P]–dCTP into the DNA probe. To do this, a 25 ng aliquot of DNA was diluted with 45 μL of sterile water, denatured in a boiling water bath for 2 min, then immediately chilled on ice for another 2 min.

The denatured DNA was collected by pulse centrifugation, added to the Ready-to-go reagent beads, mixed by pipetting up and down gently, and then 5 μL of [α-^{32}P]–dCTP (3,000 Ci.mmol^{-1}) added. The reaction was incubated at 37^oC for 15 min, after which the labelled DNA was layered onto a ProbeQuant™ Sephadex G-50 mini-column which was seated in a microfuge tube, and the assembly centrifuged at 1,200 x g for 1.5 min at room temperature. The labelled DNA probe was then denatured in a boiling water bath for 2 min and then added to the hybridisation solution which was pre-equilibrated at 65^oC with the transfer membrane (Section 2.5.2.2).

2.5.2.4 Hybridisation and washing of DNA blots

Reagents:

- Church hybridisation solution: (0.25 M $Na_2PO_4.2H_2O$, pH 7.2 containing 7% (v/v) SDS, 1.0% (w/v) BSA fraction V, 1 mM EDTA, pH 8.0)
- Hybridisation wash solution: (20 mM $Na_2PO_4.2H_2O$, pH 7.2 containing 5% (v/v) SDS, 0.5% (w/v) BSA fraction V, 1 mM EDTA, pH 8.0)
- 20x SSPE: (0.2 M $Na_2PO_4.2H_2O$, pH 6.5, 3.6 M NaCl, 20 mM EDTA)
- 2x SSPE wash: (2x SSPE pH 6.5, 0.1% (w/v) SDS)
- 1x SSPE wash: (1 x SSPE, pH 6.5, 0.1% (w/v) SDS)
- 0.2 SSPE wash: (0.2x SSPE, pH 6.5, 0.1% (w/v) SDS)
- 0.1 SSPE wash: (0.1x SSPE, pH 6.5, 0.1% (w/v) SDS)

The hybridisation and washing of DNA blots was carried out as described by Church and Gilbert (1984). In a Hybaid^{TM} glass tube, the blotted membrane (Section 2.5.2.2) was rolled up with the nucleic acid facing upwards, placed inside, and then 25 ml of Church hybridisation solution was poured in and the tube pre-warmed in a rotary oven at 65^{o}C. The denatured labelled probe (Section 2.5.2.3) was then added to the hybridisation solution and allowed to circulate over the membrane overnight at 65^{o}C. On the following day, the membrane was washed at 65^{o}C, first with 100 mL of hybridisation wash solution for 30 min, then with 2X SSPE, 1x SSPE (for 30 min each), 0.2 SSPE (for 45 min), and finally 0.1x SSPE for 1.5 h.

After washing, the membrane was sealed in cling wrap and placed immediately in a phosphorimaging cassette (Fujifilm, Tokyo, Japan) for varying exposure times and then the image was developed in a FUJI Film developing machine (FLA-5000). For autoradiography, the membrane was placed in X-OMATIC cassette with a single X-OMATIC intensifying screen with X-Ray film (Kodak) and exposed at –80^{o}C for 1 to 3 weeks. The film was then developed using an automatic X-ray film processor.

For developing RT-PCR blots, a shorter exposure of the membrane to the X-ray film was performed, usually ranging from 20 min to 2 h.

2.5.3 RNA extraction

The modified hot borate method as previously described by Hunter and Reid (2001) was used for the isolation of total RNA.

Reagents:

- Extraction buffer: (0.2 M sodium borate decahydrate containing 0.03 M EGTA, 1.0% (w/v) SDS, 1.0% (w/v) sodium deoxycholate salt, 10 mM DTT, 1.0 % (v/v) nonidet P-40 (IGEPAL), and 2% (w/v) polyvinylpyrrolidone-40 (PVP-40)
- Proteinase K: (20 $mg.mL^{-1}$ in DEPC-treated water)
- 2 M KCl
- 0.4 M LiCl

The extraction buffer was pre-equilibrated at 80^{o}C before use. Plant tissue was powdered in liquid nitrogen and added to the hot extraction buffer at a ratio of 5 mL buffer to 1 g tissue powder and the mixture vortexed for 30 s. An aliquot (37.5 μL) of Proteinase K was added per gram fresh weight of tissue and the suspension was incubated, with shaking at 42^{o}C for 1.5 h. After this period, an 0.08 volume of 2 M KCl was added and the solution swirled gently on ice for 30 min, centrifuged at 15,000 x g for 20 min at 4^{o}C and the supernatant transferred to a fresh tube. After carefully determining the volume of the supernatant, one volume of 4 M LiCl was added, mixed gently and RNA allowed to precipitate overnight at 4^{o}C. On the following day, the precipitate was collected by centrifugation at 15,000 x g for 30 min at 4^{o}C. After discarding the supernatant, the remaining LiCl was carefully drained on absorbant paper and the pellet was resuspended in 500 uL of sterile DEPC-treated water and 50 μL of 3 M sodium acetate, pH 5.2 added. The suspension was then pipetted to microfuge tubes, followed by the addition of 500 μL of chloroform/ isoamyl alcohol (24:1). After

vortexing for 30 s, centrifugation was conducted at 15,000 x g for 5 min at 4°C, and 400 µL of the supernatant again transferred to a new tube. A second 400 µL aliquot of water was added to the chloroform extract, and after centrifugation, another 400 µL of supernatant was collected. After combining the two supernatants, 30 µL of 3 M sodium acetate, pH 5.2 and 800 µL of isopropanol were added, the contents mixed by inversion, incubated on ice for 1 h and centrifuged at 20,800 x g for 30 min at 4°C. The pellet was washed with 80% (v/v) ethanol and then re-suspended in 50-500 µL of water. RNA was quantified using an Ultrospec 3000 spectrophotometer as described in Section 2.5.1.4.

2.5.4 Semi-quantitative reverse transcriptase - Polymerase chain reaction

The semi-quantitative RT-PCR was conducted using the two-step ThermoScript™ RT-PCR System (Invitrogen) following the manufacturer's instruction. The first step comprised cDNA synthesis from total RNA and the second step constitutes the amplification by PCR using gene-specific primers (Table 2.2). For cDNA synthesis, 3 µg of total RNA was routinely used which was combined with 1 µL of 50 µM Oligo $(dT)_{20}$ primer, 2 µL of 10 mM dNTP mix and the volume adjusted to 12 µL with RNase-free water. The combined RNA and primer was denatured by incubating at 65°C for 5 min and then placed on ice.

For each reverse transcription reaction, the following components of the reaction mix were prepared into another tube: 4 µL of the 5x cDNA synthesis buffer, 1 µL of 0.1 M DTT, 1 uL of RnaseOUT™ (40 U/µL), 1 µL of Rnase-free water provided in the kit, and 1 µL of ThermoScript™ RT (15 U/µL). The mixture was vortexed gently, added into the reaction tube containing the RNA and primer, and incubated at 55°C for 60 min. At the conclusion of this step, the mixture was incubated at 85°C for 5 min to terminate the

reaction. To prevent RNA – DNA complex formation, 1 μL of RNase H (provided in the kit) was added and the mixture was incubated at 37^{o}C for 20 min.

For the amplification of the synthesised cDNA, the following components were mixed: 10 μL of the PCR Master mix, 1 μL each of the 10 μM gene-specific forward and reverse primers, 1 μL of the cDNA synthesis reaction and 7 μL of PCR water. The PCR programme setting varied depending on the primers used and the expected PCR product size.

2.6 White clover Transformation

2.6.1 Cloning *TR-ACO1* promoter to *GFP*

The cloning of *TR-ACO1* promoter into GFP reporter gene (Figure 2.12) was conducted with assistance from Miss Susanna Leung, Massey University. This was achieved by the replacement of the CaMV35S promoter in the *pBIN19-mGFP5-ER* plasmid with the *TR-ACO1* promoter. The *TR-ACO1* promoter was obtained from the *TR-ACO1p::GUS* construct in PRD410 (Chen and McManus, 2006).

2.6.2 Transformation and regeneration of *Trifolium repens*

2.6.2.1 Seed sterilisation and germination

The required amount of seeds (normally 0.20 g, which is equivalent to *ca.* 300 seeds) were weighed out, placed in a 15 ml centrifuge tube and rinsed with 70% (v/v) ethanol for 1 min followed by sterilisation with 3.0 % (v/v) sodium hypochlorite (NaOCl) for 7-8 min in a circular mixer. After draining the solution, the seeds were rinsed with sterile distilled water four times. After the last rinse, seeds were emptied into a petri dish, covered with sterile water, wrapped in tin foil and incubated at room temperature overnight. On the following day, water was drained off and the imbibed seeds were

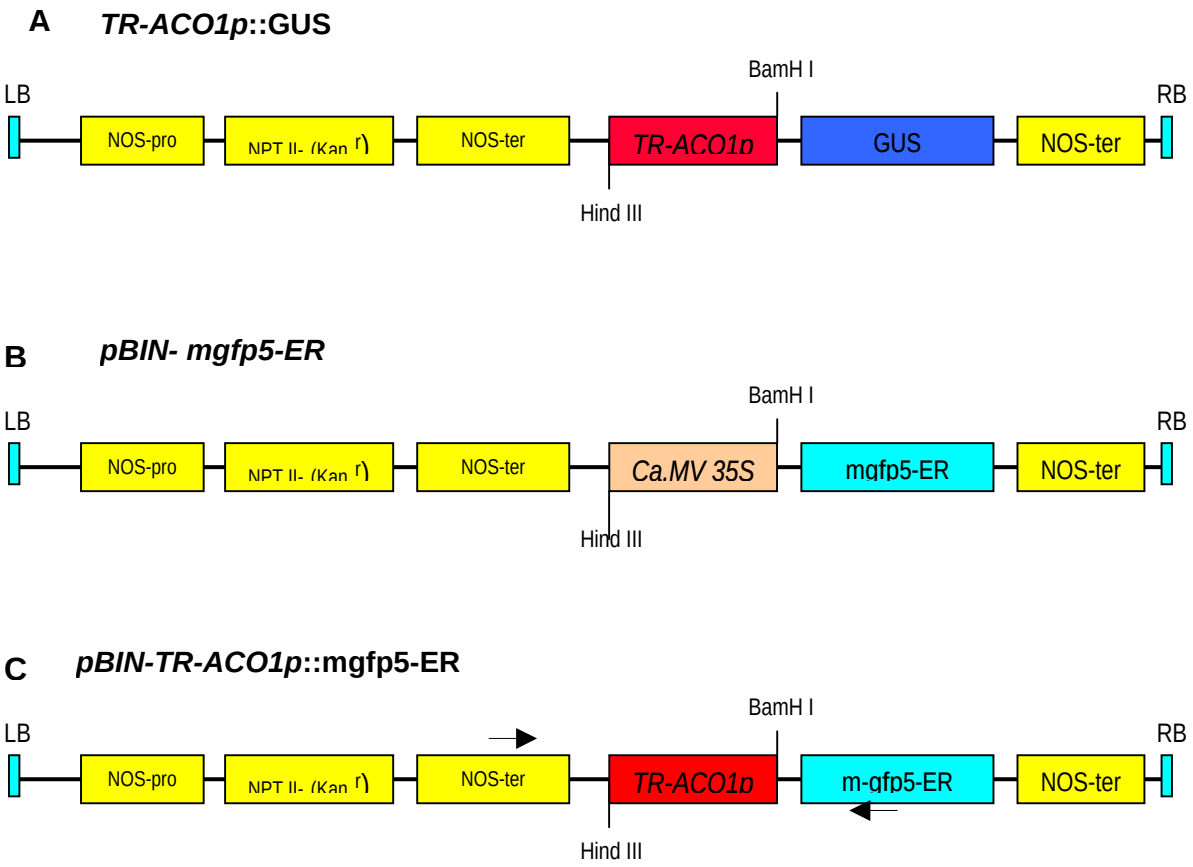

Figure 2.12 Schematic representation of the T-DNA regions of the binary vectors used in cloning (not to scale). LB, left T-DNA border; RB, right T-DNA border; NOS, promoter and terminator from the nopaline synthase gene from *Agrobacterium tumefaciens,* NPT II, neomycin phosphotransferase II gene for Kanamycin resistance; *TR-ACO1p,* 1.006 kb ACC oxidase 1 promoter from *Trifolium repens*; GUS, β-Glucoronidase reporter gene; *mgfp5-ER*, modified green fluorescence protein. Arrows indicate the location of the forward and reverse primers used in PCR to check for the presence of the insert.

covered with 6% (v/v) hydrogen peroxide for 3 min, with occasional stirring. After draining off the hydrogen peroxide solution, the seeds were washed five times with sterile distilled water. After the final wash, seeds were covered with sterile water until dissection of cotyledons.

2.6.2.2 *Inoculation and co-cultivation with A. tumefaciens*

Under the dissecting microscope, the seed coat and the endosperm of the imbibed seeds were removed, the radicle cut, and the two cotyledons carefully separated. The dissected cotyledons were then aligned on dampened sterile filter paper placed on CR7 media (MS Media [Table A.2], containing 1 $mg.L^{-1}$ 6-benzylaminopurine (BAP, Sigma), 0.05 $mg.L^{-1}$ 1-naphthalene acetic acid (NAA, Sigma) 0.8% (w/v) Phytoagar (*Duchefa Biochemie)*, pH adjusted to 5.7 with 1.0 M KOH).

An overnight culture of *A. tumefaciens* (Section 2.5.2.2) was centrifuged at 5,000 x g for 5 min at room temperature and the collected cells resuspended in 5 mL of sterile 10 mM $MgSO_4$. Three microlitres of the suspension was then pipetted onto each cotyledon. The plates were sealed with parafilm and then incubated at 23^{o}C under continuous lights in the growth chamber

2.6.2.3 *Regeneration and growth of transgenic white clover*

After co-cultivation with *A. tumefaciens* for 4 d, the cotyledons were transferred onto CR7 selection media (150 $ug.mL^{-1}$ kanamycin, 300 $ug.mL^{-1}$ cefotaxime) and moved to fresh media every 14 d. Regenerating cotyledons were shifted to $CR5^{Kan100, Cef300}$ (MS media containing 0.1 $mg.L^{-1}$ BAP, 0.05 $mg.L^{-1}$ NAA, 0.8% (w/v) Phytoagar; pH adjusted to 5.7 with 1 M KOH, 100 $ug.mL^{-1}$ kanamycin, 300 $ug.mL^{-1}$ cefotaxime) when starting to form shoots and transferred onto fresh selection medium every two weeks. Kanamycin resistant plantlets were moved onto hormone-free $CR0^{Kan50}$ (MS media, pH

5.7, containing 0.8% (w/v) Phytoagar, 50 ug.mL^{-1} kanamycin) rooting media. Clumps of plantlets were subdivided and planted onto fresh media. Plantlets with well established roots and shoots were exflasked, transferred to sterile potting mix (ODERINGS) and maintained in a Physical Containment 2 (PC2) GMO Glasshouse, with 75% relative humidity and a day and night temperature of 22^{o}C and 16^{o}C, respectively. The schematic diagram of the regeneration and growing of transgenic white clover is presented as Figure 2.13.

Putative transgenic plants were screened by PCR (Section 2.5.1.2) and gene copy number was examined by Southern analysis (Section 2.5.2).

2.7 Confocal microscopy

Root samples for confocal microscopy were prepared immediately before examination in order to obtain more accurate analysis of gene expression. Excised roots were washed with distilled water then stained with 10 ng.µL^{-1} propidium iodide for *ca.* 10 s. Destaining was done with three washes with distilled water before mounting the root in 50% (v/v) glycerol on microscope slides before covering with a glass slip.

A Leica Confocal Microscope (Mannheim, Germany) equipped with Leica Application Suite Advanced Fluorescence (LAS-AF) software was used to collect images of the root sections. Dual scanning was routinely conducted with the filter set for the excitation and emission of the green fluorescent protein at 477 nm and 510 nm, respectively, while for the propidium iodide, the filter was set at an excitation and emission maxima of 540 nm and 610 nm, respectively.

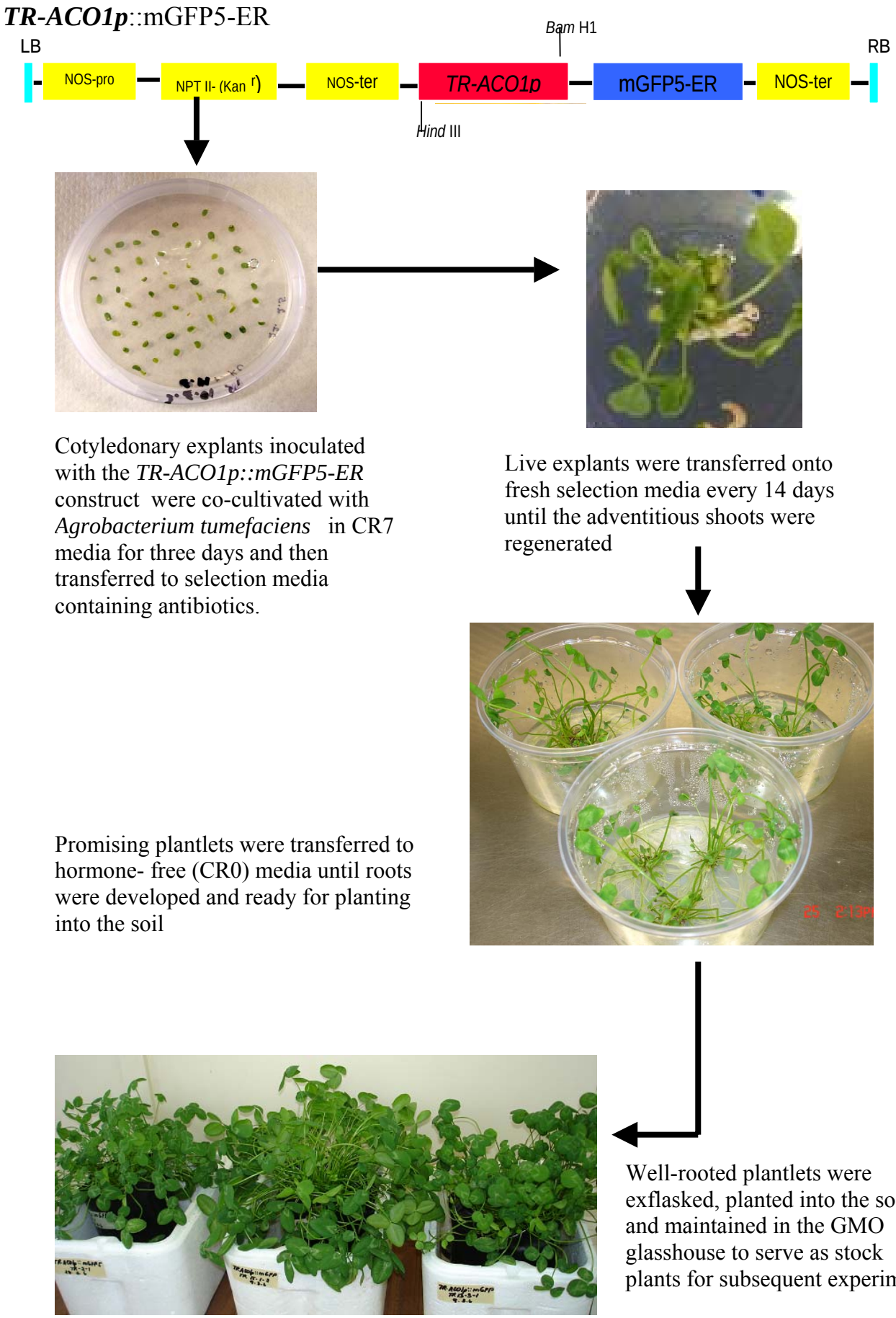

Figure 2.13 Flow diagram of the white clover transformation

2.8 Replication of experiment and statistical analysis

All experiments were conducted with two treatments, so simple statistical analyses of data were carried out using the Microsoft Excel program. Data on root morphology as well as on leaf Pi content and acid phosphatase activity were summarised as the mean and the standard error of the sample mean, and difference between sample means were analysed using a *t*-test for 2 independent samples.

To confirm results obtained, two biological replicates were conducted separately for each experiment, and for each western analysis and sqRT-PCR, aside from the two biological replicates, at least two technical replicates were carried out both for the wild type and for the transgenic white clover.

Chapter 3 - Results

3.1 Differential accumulation of the TR-ACO proteins and differential expression of *TR-ACO* gene family in roots of white clover

3.1.1 Accumulation of TR-ACO1 and TR-ACO2 protein in roots of white clover

The pattern of accumulation of TR-ACO1 and TR-ACO2 protein in the roots of white clover plants grown in Pi sufficient media (1.0 mM) was determined by western analysis. When protein extracts (Section 2.4.3.1) were challenged with the α-TR-ACO1 antibody, there was a greater recognition of the ACO protein in the lateral roots when compared with the main roots (Figure 3.1), suggesting greater accumulation of TR-ACO1 protein in the lateral roots relative to the main roots.

Similarly, when an aliquot of the same protein extract was challenged with the α-TR-ACO2 antibody, there was also greater band intensity (as antibody recognition) in the lateral roots when compared with the main roots. However, the difference in accumulation between the main and lateral roots were not as marked as for TR-ACO1 Figure 3.1).

3.1.2 Expression pattern of members of the *TR-ACO* gene family in the roots of wild type white clover

The expression pattern of the *TR-ACO* genes in the main roots and lateral roots was investigated using semi-quantitative reverse transcriptase-polymerase chain reaction (sqRT-PCR). The transcripts (as cDNA) of each gene were amplified using forward and reverse primers specific for the *TR-ACO1*, *TR-ACO2* and *TR-ACO3* genes. Sequences of these primers are provided in Table 2.2. The ethidium bromide stained fragments generated after amplification are shown in Figure 3.2. For *TR-ACO1* and *TR-ACO2*, there was greater transcript abundance in the lateral roots when compared to the main

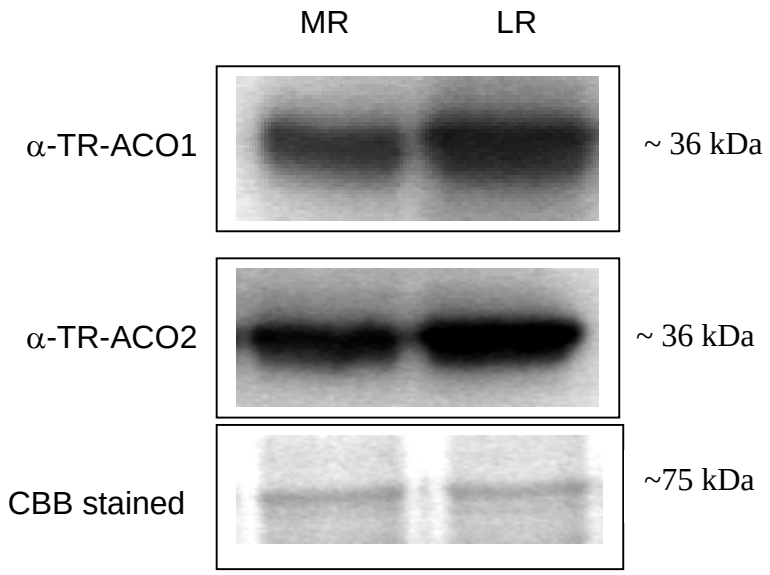

Figure 3.1 Accumulation of the TR-ACO1 and TR-ACO2 protein in the main root and lateral roots of wild type white clover using western analysis. Total protein was extracted from the main roots (MR) and lateral roots (LR) of white clover grown in Pi sufficient media for 15 d. Five μg of the crude protein extract was separated using SDS-PAGE at 150 V for 75 min, and electroblotted onto PVDF membrane at 100V for 1 h. Blot development was conducted using the West Pico Supersignal kit. The figure shown is a representative of two technical replicates performed on each of two biological replicates.

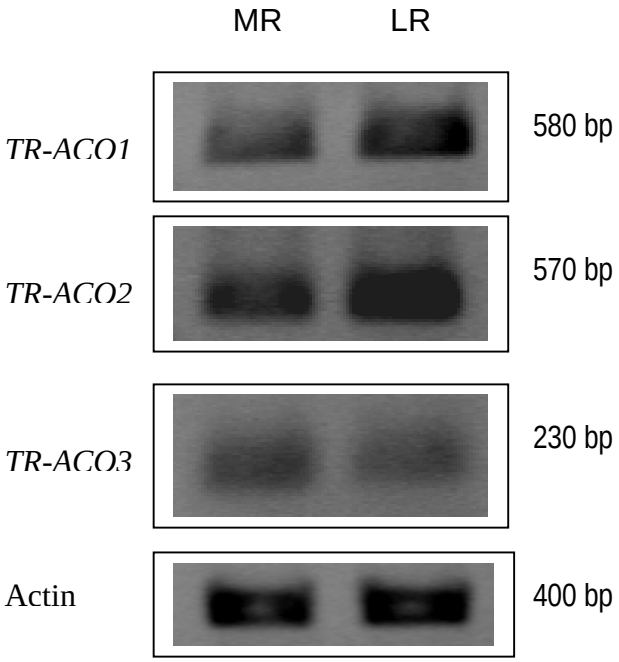

Figure 3.2 Analysis of the *TR-ACO* gene expression, as indicated, in the roots of wild type white clover using sqRT-PCR and ethidium bromide staining. Three micrograms of total RNA was used for reverse transcription and 1 μL of cDNA was used for each PCR reaction. Amplified fragments were electrophoresed through a 1.5% (w/v) agarose gel in 1x TAE for 2 h at 50V . MR = main roots, LR = lateral roots. The figure shown is a representative of two technical replicates performed on each of two biological replicates.

roots, while for *TR-ACO3* there was a lower transcript abundance in the lateral roots when compared with the main roots.

3.1.3 Localisation of *TR-ACO* promoter activity in the roots of *TR-ACOp::GUS* transformed white clover

3.1.3.1 Primary GUS staining pattern in the roots of TR-ACO1p::GUS transformed plants

Roots of eight stolon cuttings from single genotype of *TR-ACO1p::GUS* transformed white clover (designated as TR110-1, the high GUS expressing line), were GUS stained (Section 2.3.1) and the staining pattern analysed. Seven out of eight roots had GUS staining, and the staining was predominantly in the lateral roots. In less intensely staining roots, where only a few lateral roots had detectable blue staining, the stain was mostly located towards the younger part of the roots (indicated by the arrow in Figure 3.3A). In well stained roots, almost all the lateral roots had blue dye while the main root had lesser staining or none at all (Figure 3.3B).

Longitudinal sections of GUS stained roots showed predominant staining in the lateral root primordium as indicated by the arrow in the example shown in Figure 3.3C. There was also light staining in the cells extending from the outer to inner cortical cells but not as intense as the signal in the lateral root primordium. In the developing lateral root (Figure 3.3D), the primary staining was also in the meristem. Further, there was also greater staining in the stele and in the pericycle with less staining in the cortical cells. Since the GUS reporter gene is driven by the *TR-ACO1* promoter, these results suggest that *TR-ACO1* is predominantly expressed in the lateral roots with more preferential staining in the apical meristem.

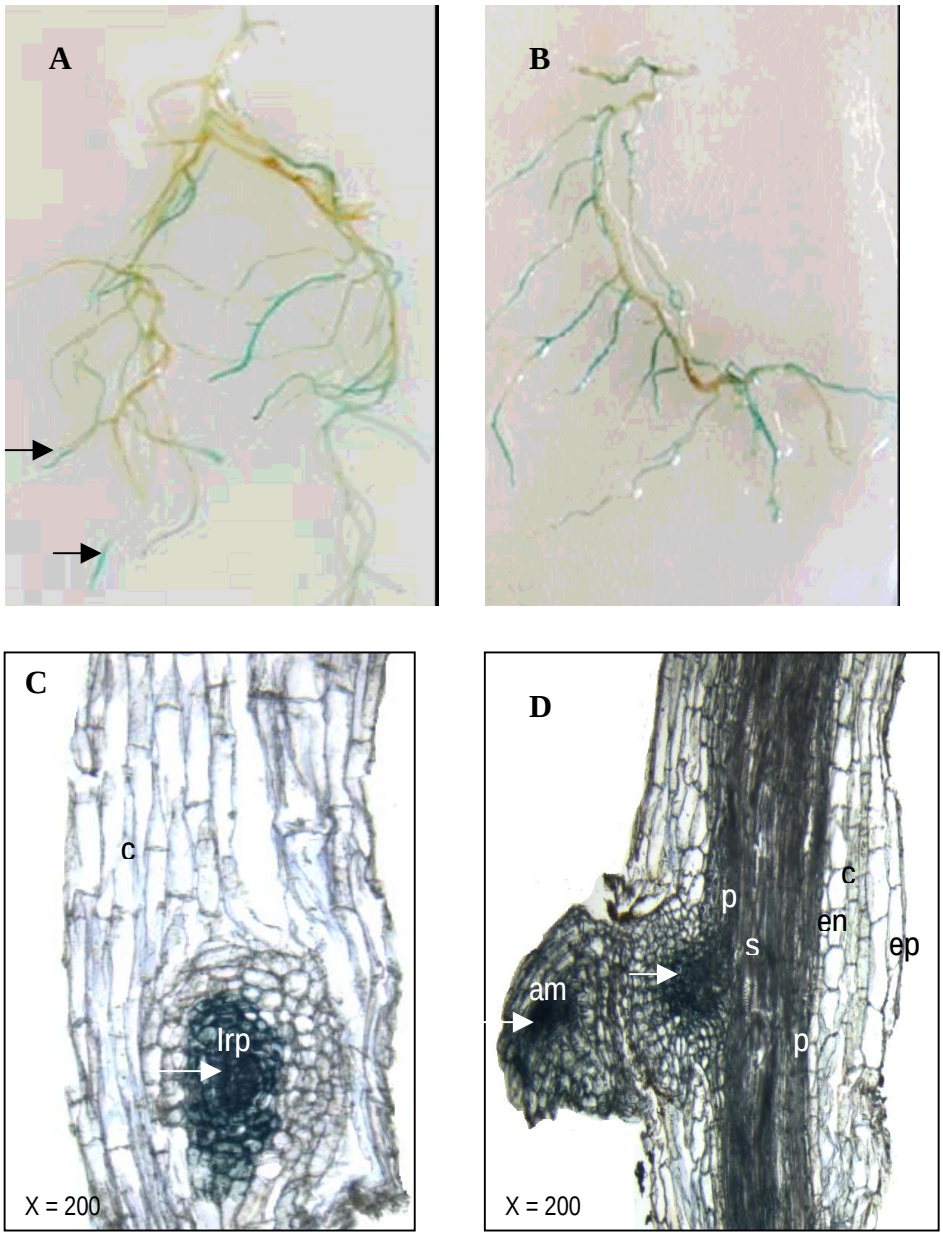

Figure 3.3 Whole roots of *TR-ACO1p::GUS* transformed white clover after GUS staining (A,B) and longitudinal sections (C,D) of GUS stained roots. The roots were immersed in 90% (v/v) cold acetone, and incubated in ice for 15 min. Tissues were immersed in X-Gluc staining solution (2 mM X-Gluc, 50 mM Na_2HPO_4, pH 7.2) and incubated at 37^{o}C overnight. Stained tissues were wax embedded and sectioned at 10 μm thickness. Longitudinal sections of the main root showed predominant GUS staining in the lateral root primordial (lrp) and in the apical meristem of the newly developing lateral root (arrow in D).
The figure shown is representative of two biological replicates. In both replicates, seven out of eight roots displayed GUS activity mostly in the lateral roots

am = apical meristem, lrp = lateral root primordium, c = cortex,
en = endodermis, ep = epidermis, p = pericycle, s = stele

3.1.3.2 Primary GUS staining pattern in the roots of TR-ACO2p::GUS transformed plants

Roots of eight stolon cuttings from a single genotype of *TR-ACO2p::GUS* transformed white clover (designated TR214-1) were used for GUS staining. Six roots showed GUS staining both in the main and lateral roots (Figure 3.4). In roots where the staining was less intense (data not shown), light blue staining was localised only in some areas in the lateral or in the main roots. In roots where staining was more intense, the intensity of blue colour was more noticeable both in the lateral roots and in the main roots (Figure 3.4A). Unlike the *TR-ACO1p::GUS* transformed plants where there was none or very slight staining in the main roots, the TR-ACO2p roots had some staining in both main and lateral roots. This pattern of staining was more marked when the GUS stained root was examined under the light microscope, and the blue dye was observed in the main and in the lateral roots (Figure 3.4B). Examination of longitudinal sections of GUS stained roots under the light microscope showed blue staining in both the lateral root primordia and the adjacent tissues such as in the cortical cells, pericycle and even up to the outer cells in the epidermis in the example shown (Figure 3.4C). The staining was not just confined to the meristem.

3.1.3.3 Primary GUS staining pattern in the roots of TR-ACO3p::GUS transformed plants

Eight stolon cuttings from one high expressing line of *TR-ACO3p::GUS* transformed white clover (designated TR313-1) were also used for the experiment. From the roots of these cuttings five were GUS stained and displayed predominant staining in the main roots (Figure 3.5). In the young roots, the blue deposit was noted mostly in the basal and mid portion of the roots which then disappeared towards the root tip (Figure 3.5A).

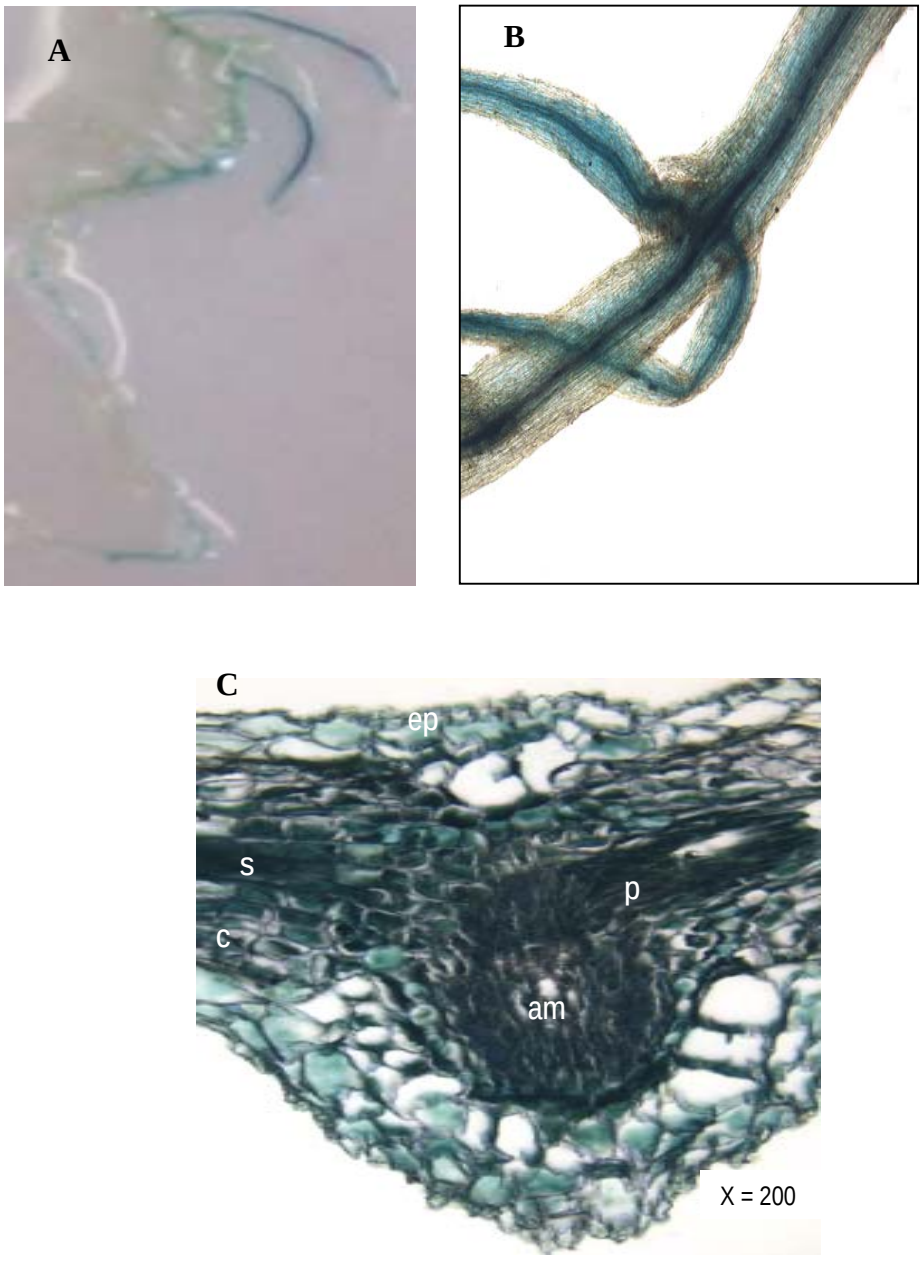

Figure 3.4 Whole roots of *TR-ACO2p::GUS* transformed white clover after GUS staining (A,B) and a longitudinal section (C) of GUS stained roots. The root samples were immersed in 90% (v/v) cold acetone, and incubated in ice for 15 min. Tissues were then rinsed with 50 mM Na_2HPO_4 buffer (pH 7.2), then immersed in X-Gluc staining solution (2 mM X-Gluc, 50 mM Na_2HPO_4, pH 7.2) and incubated at 37^{o}C overnight. Stained tissues were fixed, wax embedded and sectioned at 10 μm thickness. The figure shown is representative of two biological replicates. In both replicates, at least six out of eight roots were stained in both the main and lateral roots.

am = apical meristem, c = cortex, ep = epidermis, p = pericycle, s = stele

In a more intensely stained root (Figure 3.5A, right hand side image), the dye was also noted towards the root tip but GUS staining was relatively faint or nil in the lateral root. In more mature roots which had quite well developed lateral roots (Figure 3.5B), the pattern of GUS staining was more distinct. The blue staining was observed mostly in the main root and staining was markedly reduced towards the lateral roots. These observations suggest that *TR-ACO3* is expressed predominantly in the main roots with less expression in the lateral roots.

In longitudinal sections (Figure 3.5 C,D), the blue staining was noticeable in the epidermis through to the cortical cells and into the pericycle. There was not much GUS staining in the lateral root primordium (Figure 3.5C) and in the meristem of the developing lateral roots (Figure 3.5D), again indicating that *TR-ACO3* is expressed less in the lateral roots when compared with the main root.

3.2 Morphological and anatomical changes in the roots of white clover in response to changes in phosphate supply

The main focus of this study was to investigate the expression of members of *TR-ACO* gene family and accumulation of TR-ACO proteins. However, prior to examination of these parameters, some responses of white clover to Pi availability were also monitored over a time course. This included changes in the root morphology, root anatomy, leaf Pi content and root acid phosphatase activity. Stolon cuttings subjected to Pi treatment were designated as either Pi sufficient (+P) when grown in media with 1.0 mM Pi, or Pi depleted (-P) when grown in media with 10 μM Pi.

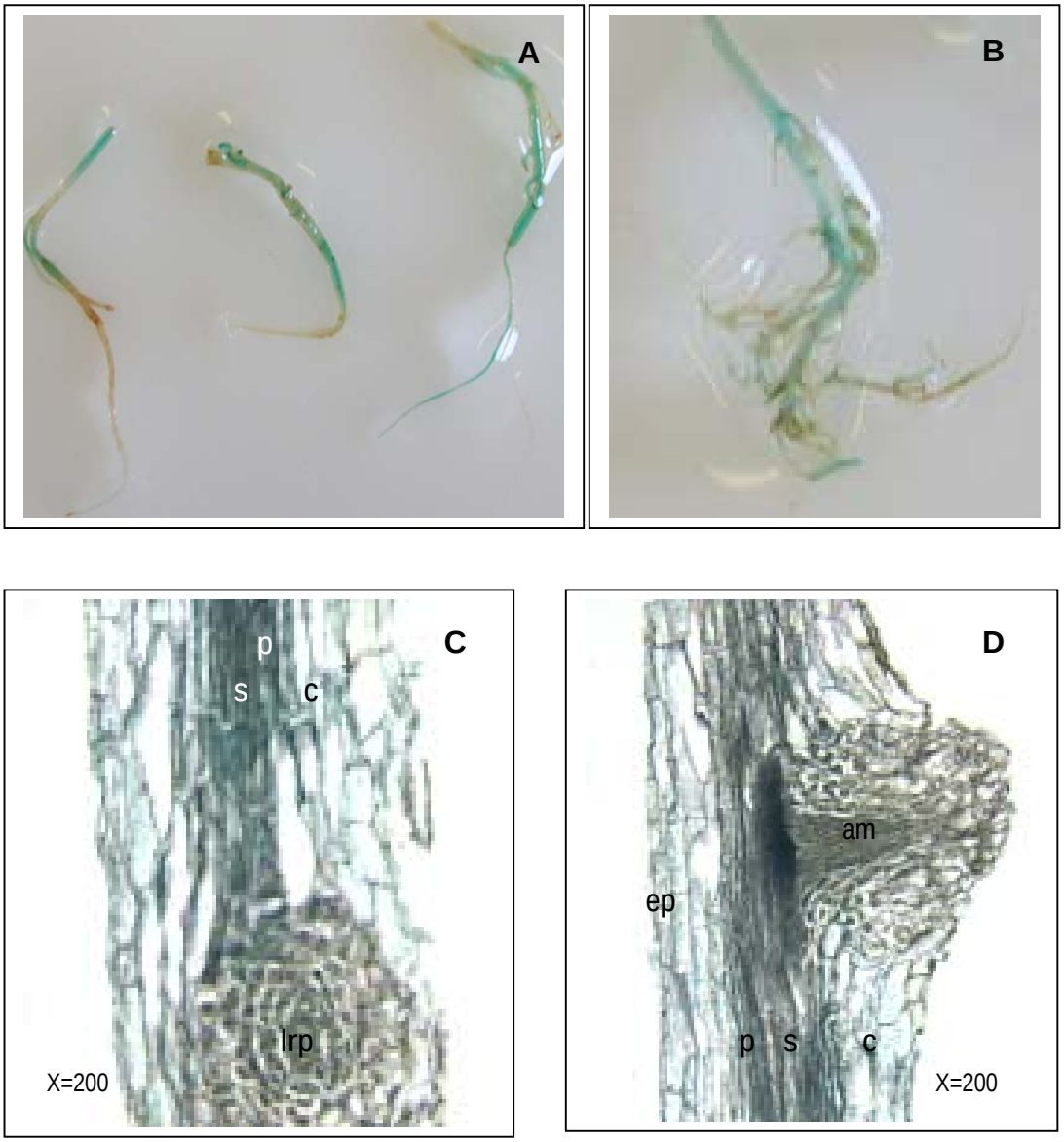

Figure 3.5 Whole roots of *TR-ACO3p::GUS* transformed white clover after GUS staining (A,B) and longitudinal sections (C,D) of GUS stained roots.
The root samples were immersed in 90% (v/v) cold acetone, and incubated in ice for 15 min. Tissues were immersed in X-Gluc staining solution (2 mM X-Gluc, 50 mM Na_2HPO_4, pH 7.2) and incubated at 37^{o}C overnight. Stained tissues were fixed, wax embedded and sectioned at 10 μm thickness, and viewed under the light microscope. The figure shown is representative of two biological replicates.. In both replicates, at least five out of eight roots showed staining in the main roots.

am = apical meristem, c = cortex, ep = epidermis, lrp = lateral root primordium
p = pericycle, s = stele

3.2.1 Morphological changes in roots in response to changes in phosphate supply

The morphological features of the roots which were examined in response to Pi supply included number of main roots, number of lateral roots, length of main roots and weight of biomass. These were monitored at three day intervals over a time course starting from day 0 [the time of transfer to the Pi depleted media (-P), or the continued maintenance in the Pi sufficient (+P) media] to 18 d after transfer to the Pi treatments. This experiment was conducted twice in order to confirm the reproducibility of the plant responses.

3.2.1.1 Number and length of main roots in response to phosphate supply

Results of the assessment on the number and length of main roots are shown in Figure 3.6. Stolon cuttings in both Pi sufficient and Pi depleted media did not vary significantly in terms of the number of main roots produced within the observation period. The number of roots increased over time but did not differ significantly between treatments (Figure 3.6A), as analysed using a t-test for independent samples.

In terms of the length of roots, plants differed significantly between treatments (Figure 3.6B). The Pi depleted (-P) plants generally produced longer main roots when compared with Pi sufficient (+P) plants. At day 0, the mean length of roots under Pi sufficiency and Pi deficiency was 1.0 cm and 0.76 cm, respectively and the very slight difference was insignificant at P = 0.05 level. By the 3rd day after Pi depletion, the mean length of the Pi depleted roots was 3.0 cm while for those under Pi sufficiency the mean length was 2.28cm. The greatest rate of increase occurred between the 6th and 9th day. By the 6th day, roots of Pi depleted plants had a mean length of 4.0 cm whereas Pi sufficient roots was 3.7 cm in length, a 7.5% difference.

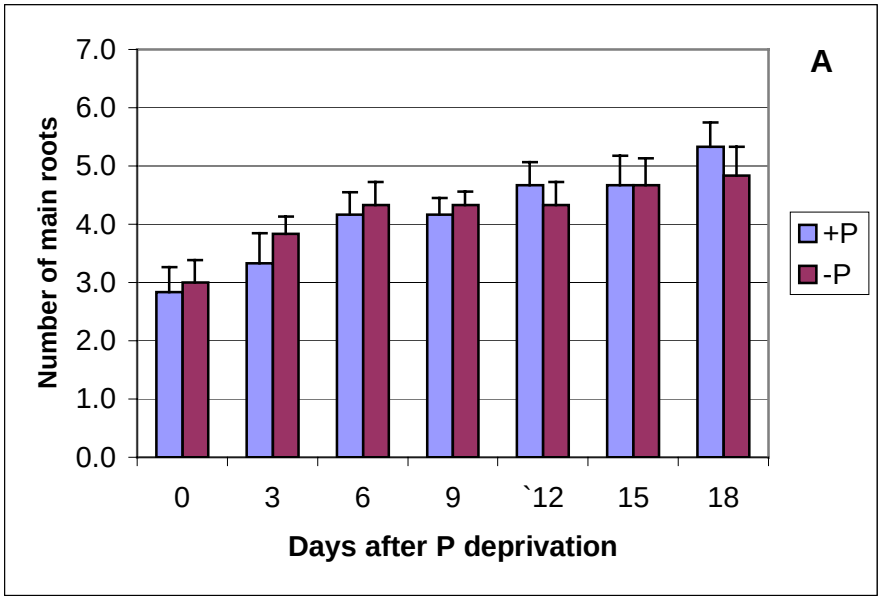

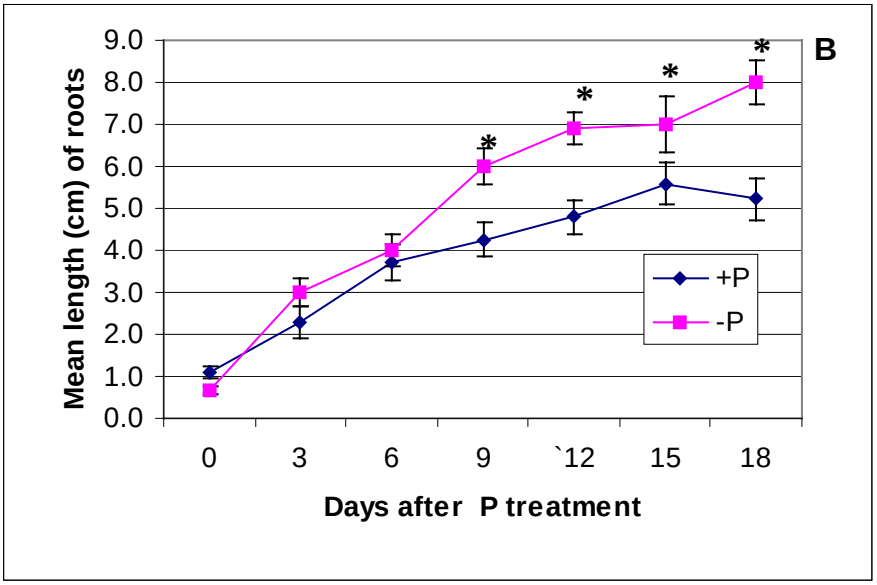

Figure 3.6. Effects of Pi sufficiency (+P; 1.0 mM) and Pi depletion (-P; 10 μM) on the number of main roots (A) and mean length of main roots (B) of wild type white clover plants (Genotype 10F). Values are means of six sample plants, bars represent standard error of the sample mean (s.e.), *****- indicates significant difference between treatments at P = 0.05, using a t-test for independent samples. The figures shown are representative of two biological replicates.

This difference increased to 29.0% on the ninth day, where the –P plants had a mean length of 6.0 cm as compared to 4.26 cm in Pi sufficient roots, and was significant at the P = 0.05 level. This significant difference continued over the remaining time course, such that after 18 d, the mean root length was 8.0 cm in the –P plants, compared to 5.23 cm in the +P plants.

3.2.1.2 Number of lateral roots and weight of biomass in response to phosphate supply

The production of lateral roots in response to changes in Pi availability is shown in Figure 3.7. This parameter followed the same trend as observed in the length of roots such that there were more lateral roots produced in the Pi depleted plants when compared to those grown in Pi sufficient conditions. At the start of the experiment no plants had lateral roots but on the third day, three out of six Pi sufficient plants had developed lateral roots while in the Pi depleted plants, only one out of six plants had developed lateral roots. By day 6, the Pi depleted plants had an average of six lateral roots per plant while the Pi sufficient plants had an average of five, but the difference between treatments was insignificant. The difference between treatments became significant at day 9 and continued to day 18 with Pi depleted roots having a greater number of lateral roots. By day 9, the Pi depleted plants had a mean of 10 lateral roots per plant and this was greater by 2.2 when compared to Pi sufficient plants. By day 12, the average number of lateral roots increased to 11 for Pi sufficient roots or an average increase of one lateral root per day, whereas the Pi depleted roots increased to a mean of 17 lateral roots per plant. This translates to an increase of two lateral roots per day in Pi depleted plants. This trend was also noted for the subsequent observations. At the conclusion of the experiment (18 d after Pi depletion), the Pi sufficient plants had a mean of 16 lateral roots per plant whereas the Pi depleted plants had an average of 24

lateral roots. The mean difference between treatments was statistically significant at the P= 0.05 level, at days 9, 12, 15 and 18.

During this time course, in addition to having a greater number of secondary roots, tertiary roots were also well developed on plants grown under Pi depletion by day 15. In contrast, tertiary roots were just starting to form in Pi sufficient roots (Figure 3.8). However, any difference was not quantified as part of this study.

Plants under Pi sufficiency and Pi deficiency did not show any significant difference in terms of total root biomass at the end of the time course (day 18) (Figure 3.9). This was observed in terms of both fresh weight and dry weight. By day 18, the mean fresh weights were 387 mg and 462 mg for Pi sufficient and Pi deficient roots, respectively, while dry weights of Pi sufficient and Pi depleted roots were 21.8 mg and 25.39 mg, respectively. These results suggests that although the Pi depleted white clover plants had a greater number of lateral roots and relatively longer main roots, the difference was due to changes in root morphology in response to the limiting supply of phosphate rather than an actual increase in the root biomass.

3.2.2 Anatomical changes in roots in response to phosphate supply

Roots of plants subjected to either Pi sufficiency or Pi depletion were collected at various time points from 0 to 4 d, dehydrated, fixed with FAA, wax infiltrated and then sectioned for microscopy in order to analyse any changes in the anatomical features (Section 2.5). Both longitudinal and transverse sections of the roots were examined.

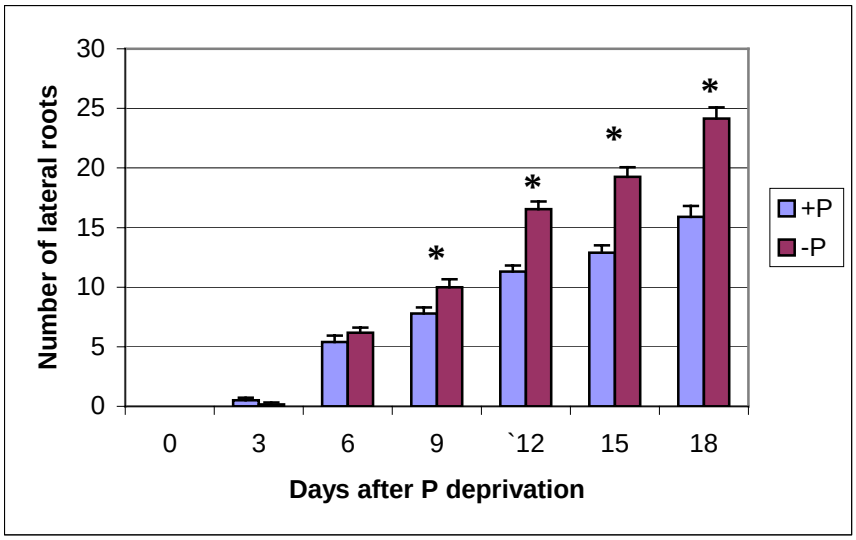

Figure 3.7 Effects of Pi sufficiency (+P; 1.0mM) and Pi depletion (-P; 10 µM) on the number of lateral roots of wild type white clover (Genotype 10F). Values are means of six sample plants, bars represent standard error of the sample mean (s.e.), ***-** indicates significant difference between treatments at P= 0.05, using a t-test for independent samples. The figure shown is representative of two biological replicates.

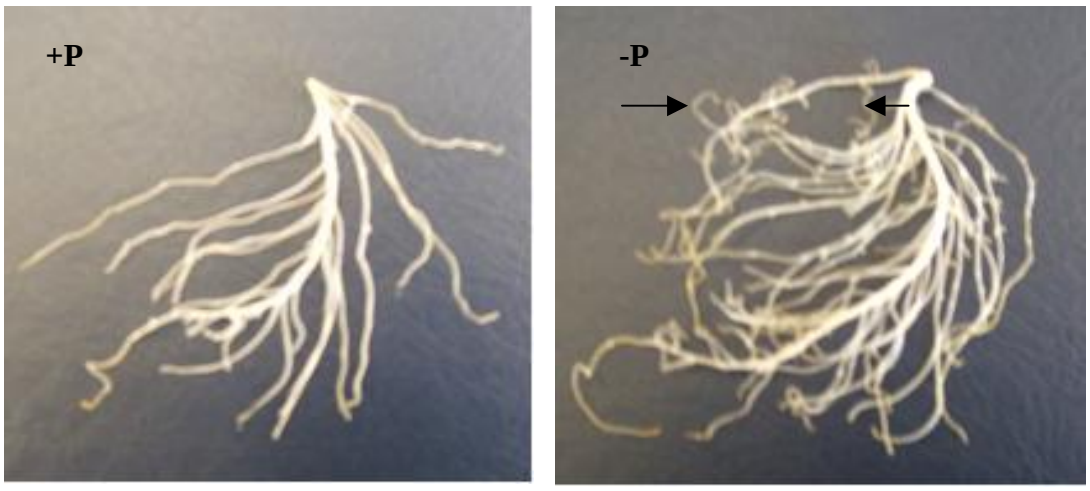

Figure 3.8 Roots of wild type white clover (genotype10F) grown under Pi sufficiency (+P; 1.0mM) or Pi depletion (-P; 10 µM) for 15 days. Four node stolon cuttings were rooted in vermiculite for 14 d then acclimatised in Hoagland's solution for another 14 d before starting the experiment. Arrows indicate some tertiary roots. The figure shown is representative of two biological replicates. In each replicate, at least four out of six sample plants displayed increase in lateral roots in –P treatment.

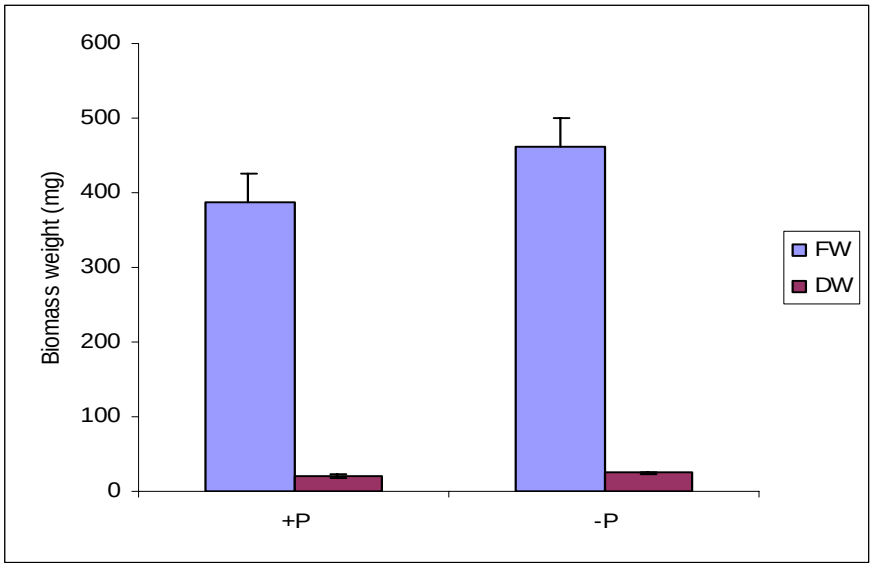

Figure 3.9 Effects of Pi sufficiency (+P; 1.0mM) and Pi depletion (-P; 10 µM) on the weight of root biomass of wild type white clover Genotype 10F. FW- fresh weight; DW- dry weight, oven dried at 80^{o}C for 24 h. Values are means of six sample plants per replicate, bars represent standard error of the sample mean (s.e.). The figure shown is representative of two biological replicates.

There were no noticeable changes in root tissues after the first two days of Pi depletion (data not shown). The epidermis, cortex and pericycle of the root, and the root tip up to the maturation zone in both Pi sufficient and Pi depleted roots, comprised intact cells, indicating that as early as two days there were no detectable anatomical effects of Pi depletion on root tissues. At 3 d after Pi depletion, root cells were still intact, at 4 d after Pi depletion, intercellular spaces were observed (Fig 3.10).

In the transverse sections (Figure 3.11), cells were also intact up to 3 d after Pi depletion, but at 4 d, tissues in the Pi depleted roots were relatively difficult to section. Further, the inner cortex and the pericycle showed some indication of the formation of intercellular spaces.

3.3 Changes in selected physiological responses as affected by phosphate supply

3.3.1 Leaf phosphate content as influenced by phosphate supply

For the determination of the leaf phosphate content, extracts from the first fully expanded leaf on each stolon were used in the assay, and the results shown in Figure 3.12. At the start of the experiment, the phosphate level was at 0.05% per g fresh weight of the leaf sample. The Pi content remained at this level for up to 5 d after Pi depletion, and so there was no significant difference between the leaf Pi content of Pi sufficient and Pi depleted plants.

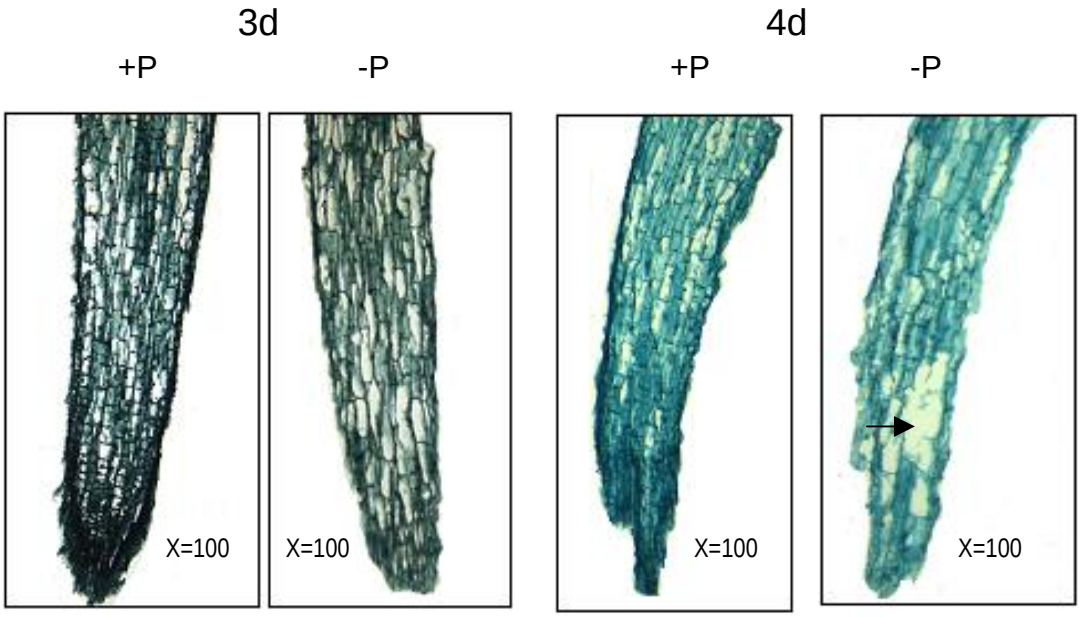

Figure 3.10 Longitudinal sections of wild type white clover roots grown in +P (1.0 mM) or –P (10 μM) for the times indicated. Root tissues were dehydrated in an ethanol series, fixed with FAA, and wax infiltrated with paraplast for at least 48 h before embedding. Tissues were sectioned at 10 μm, dewaxed, stained with 0.1% (w/v) safranin for 24 h and 0.2% (w/v) fast green for less than 15 s, then rinsed with clove oil and finally with Histochoice®. The arrow points to the intercellular gas space in the root grown in Pi depleted media. The figure shown is representative of two biological replicates, with three sample roots sectioned per replicate, with each showing intercellular spaces at 4 d after Pi depletion in –P roots.

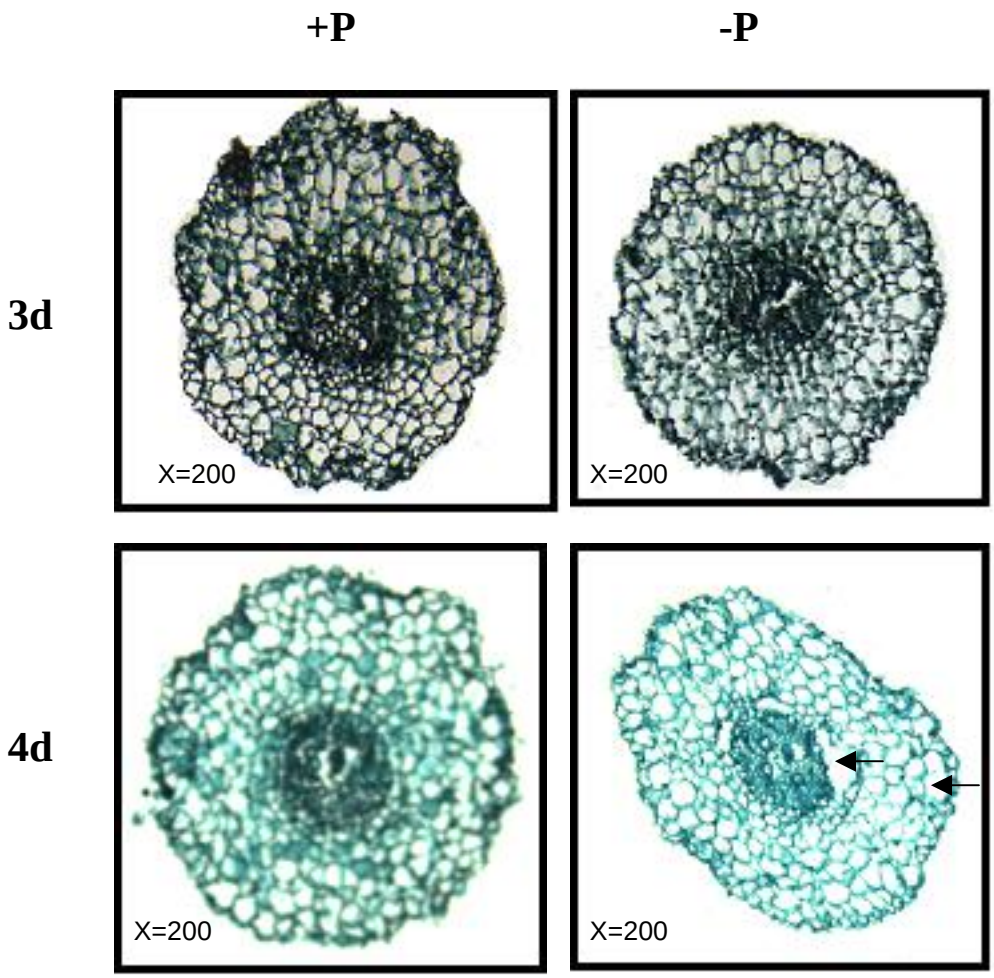

Figure 3.11 Transverse section of the root elongation zone of wild type white clover plants grown under +P (1.0 mM) or –P (10 µM) for the time indicated. Root tissues were dehydrated in an ethanol series, fixed with FAA, and wax infiltrated with paraplast for at least 48 h before embedding. Tissues were sectioned at 10 µm, dewaxed, stained with 0.1% (w/v) safranin for 24 h and 0.2% (w/v) fast green for less than 15 s, then rinsed with clove oil and finally with Histochoice®. The arrow points to the intercellular gas spaces close in the outer and inner cortex of the Pi depleted root 4 d after Pi depletion. The figure shown is representative of two biological replicates, with three sample roots sectioned per replicate, with each showing intercellular spaces in the cortex of –P root at 4 d after Pi depletion.

However, from day 7, a decline in Pi level in the Pi depleted plants was detectable with a mean level of 0.048% per g fresh weight. The difference of 0.004% Pi between the Pi depleted and the Pi sufficient leaves was not significant at the P=0.05 level. By day 8, the Pi level in Pi depleted plants decreased to 0.039% per g fresh weight whereas the Pi content in Pi sufficient plants remained at a steady level of *ca.* 0.052% Pi per g fresh weight. This difference gives a mean decrease of 0.013% in the leaf Pi content of the Pi depleted plants when compared to those under Pi sufficiency, and this difference was significant at the P= 0.05 level.

3.3.2. Acid phosphatase activity in response to phosphate supply

The activity of root acid phosphatase (APase) was examined in conjunction with the leaf Pi assay from the samples collected at 1 d to 8 d after Pi depletion. Both water soluble and cell wall associated protein extracts from the roots were used in the assay and APase activity monitored over the designated time course. In the activity assay, ρ-nitrophenol phosphate (ρNPP) was used as substrate and the APase activity was measured based on the amount of liberated ρ-nitrophenol (ρNP). The amount of product liberated was calculated using a ρNP standard curve (Figure 2.6).

Analysis of the water soluble extract between treatments showed no significant difference in APase activity up to 5 d after Pi depletion (Figure 3.13A). In both Pi sufficient and Pi depleted roots, the activity rate ranged from 9 to 16 μmoles/min/g root FW. The greatest rate of increase occurred between day 7 and day 8 where there was a sudden increase in the APase rate measured in the Pi depleted extracts. APase activity in the Pi depleted root extracts significantly increased by 2.0-fold on day 7 and by 3.5-fold

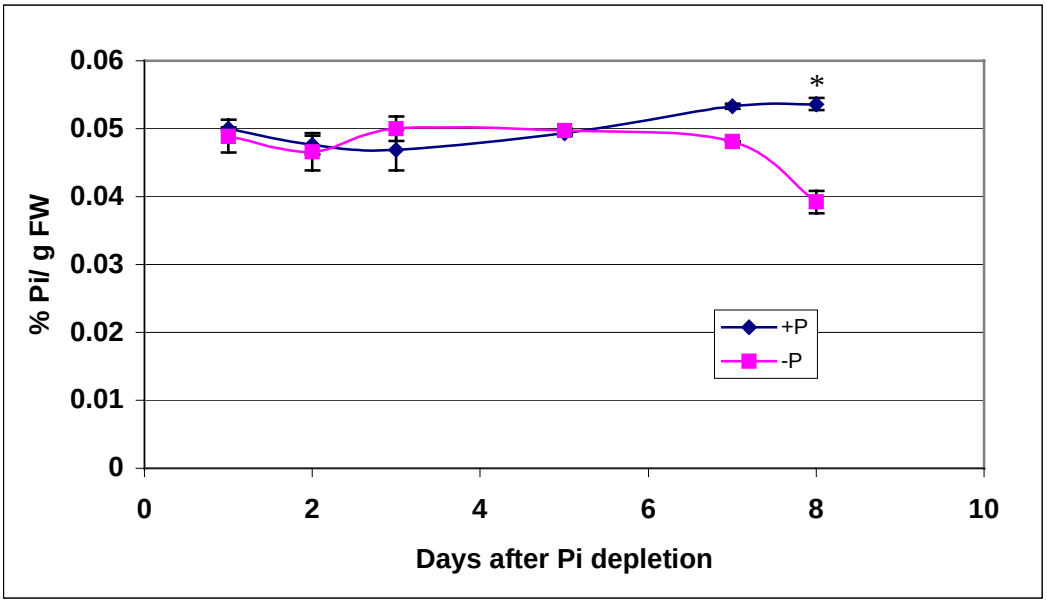

Figure 3.12 Phosphate content in white clover leaves as influenced by Pi supply. Leaf Pi from *ca.* 30 mg tissue of the first fully expanded leaf was extracted using 1.0 mL of 0.1M Tris-HCl, pH 7.5. For each assay, 10 μL of the supernatant was used and the Pi content was calculated against a Pi standard curve using potassium di-hydrogen orthophosphate. Values are means ± s.e., n = 3; ***-** indicates significant difference between treatments. The figure shown is representative of two biological replicates.

on day 8 when compared with the Pi sufficient samples. This increase coincided with the period of time after Pi depletion in which levels of leaf Pi in the same extracts also started to significantly decline (day 8; see Figure 3.12).

When the high salt extractable cell wall proteins were analysed, there was also an increase in the APase activity in the extract derived from the Pi depleted roots (Figure 3.13B). A gradual increase in the APase activity started from day 2 after Pi depletion, but the significant difference commenced only at day 5 where the APase activity in the Pi depleted extracts was almost double the activity level measured in the Pi sufficient extracts. This activity further increased by day 7. By day 8, the activity rate measured for Pi depleted root extracts was 2.6 fold higher when compared with the rate measured in extracts from Pi sufficient roots.

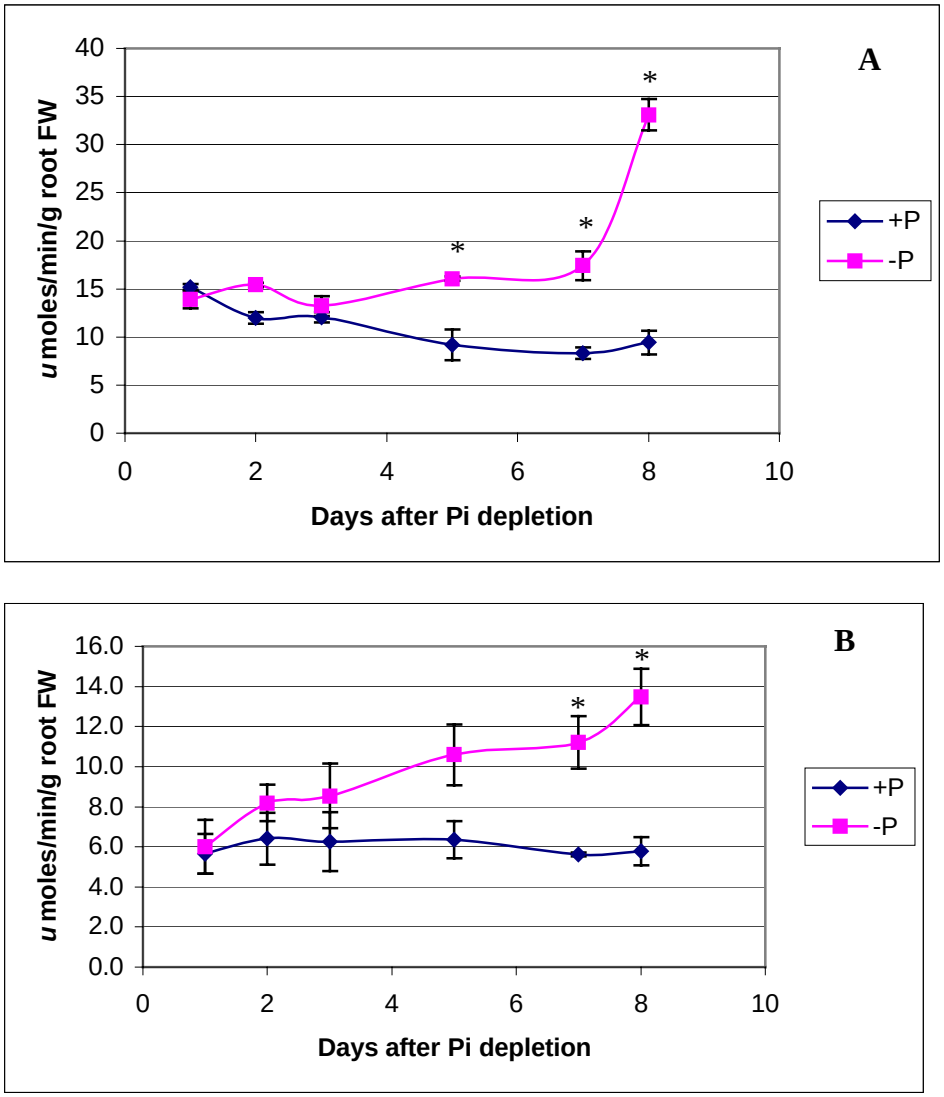

Figure 3.13 Acid phosphatase activity measured in water soluble (A) and ionically bound (high salt extractable) (B) cell wall proteins extracts from the roots of wild type white clover grown in either Pi sufficient (1.0 mM) or Pi depleted (10 μM) Hoagland's solution for the number of days indicated. Values are means ± SE, n = 3. ***-**indicates significant difference between treatments at P = 0.05. The figure shown is representative of two biological replicates.

3.4 Differential accumulation of TR-ACO proteins and expression of *TR-ACO* genes in wild type white clover roots in response to phosphate supply

3.4.1 Accumulation of TR-ACO proteins in the roots in response to phosphate depletion

The pattern of accumulation of the TR-ACO proteins in white clover roots in response to changes in Pi availability was analysed in three different experiments conducted over varying time durations. At least two biological replicates for each experiment were conducted with at least four samples per replicate. At each time point, the roots of all the four samples were pooled to make one sample for the extraction of total protein.. For each replicate, two to three technical repeats of the gel were conducted to confirm the results obtained.

Results of both replicates showed similar pattern of TR-ACO protein accumulation, and an example is shown. The first experiment was relatively long term wherein the plants were subjected to Pi depletion for 21 d, whereas the second experiment was conducted for seven days and the final experiment was conducted over a 12 h time course. Aliquots of protein extracts were challenged with α-TRACO1 and α-TRACO2 antibodies and the results are presented as western blots with the relative density of each image analysed using a gel doc image quantification system. Values generated, expressed in arbitrary units (Au), correspond to the relative signal intensity (RSI) and are presented as a histogram to accompany each blot.

3.4.1.1 Changes in TR-ACO1 protein accumulation as influenced by phosphate supply

The accumulation of TR-ACO1 protein in the roots of white clover increased slightly in response to a relatively long-term Pi depletion (Figure 3.14). Using the α-TRACO1

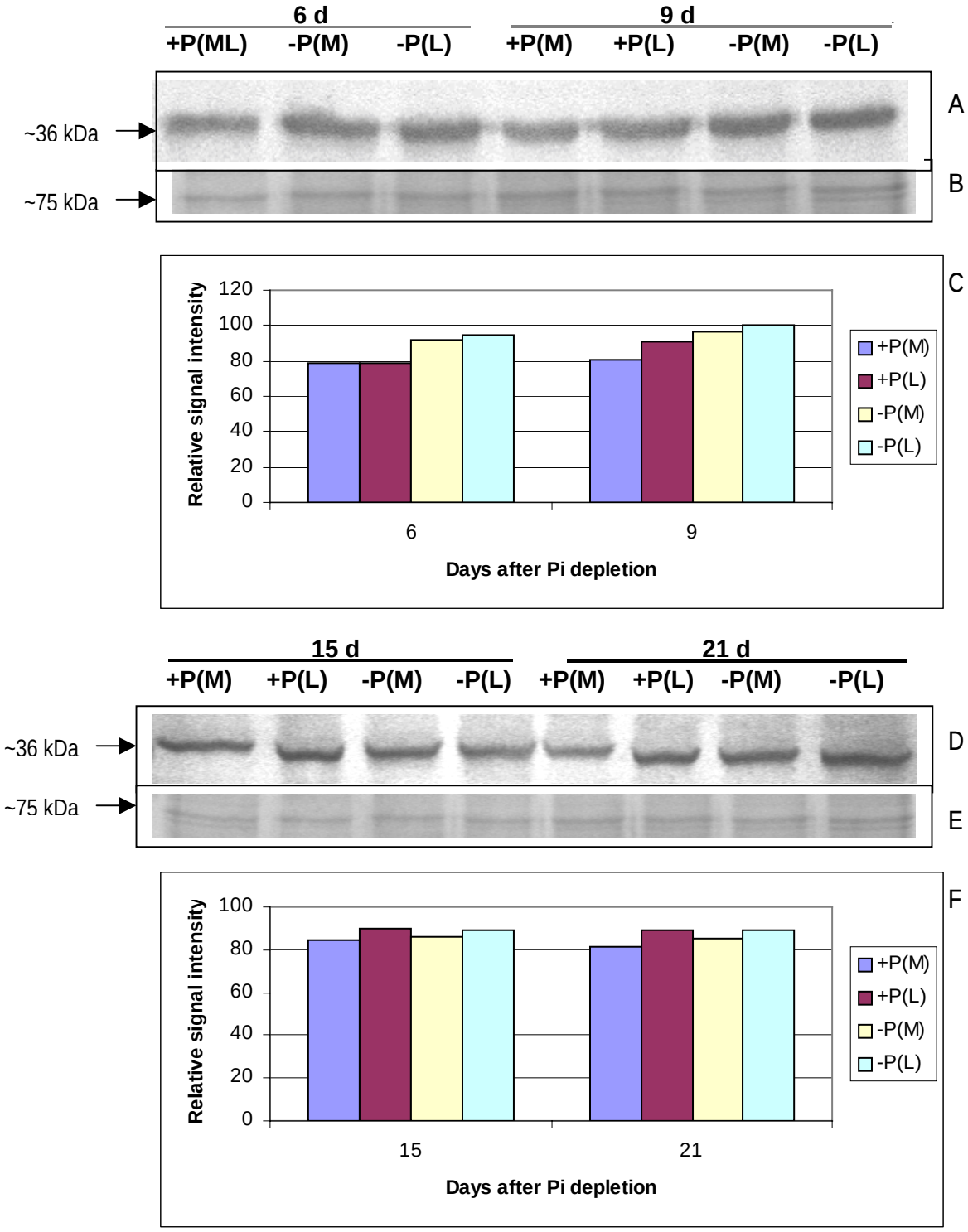

Figure 3.14 Western analyses to detect TR-ACO1 protein in the roots collected at the days indicated after +P or –P treatments. Aliquots (10 ug) of protein were separated using 12.5% SDS-PAGE, electroblotted onto PVDF membrane and challenged with α-TR-ACO1 antibody (A,D). Blot development was conducted using the alkaline phosphatase conjugates. Relative quantification of the blots are shown in histograms (C,F). +P, 1.0 mM; -P, 10 μM, Coomassie Brilliant Blue staining (B,E) is shown as a loading control (M) – main roots, (L) – lateral roots, (ML) – combined main roots and lateral roots

antibody, recognition of a protein of *ca.* 36 kDa in size was slightly greater in Pi depleted roots on the 6th day after Pi depletion. The RSI value for Pi depleted main and lateral roots was 91 Au and 94 Au, respectively, while in the pooled main and lateral roots (roots were pooled since there were only few lateral roots) under Pi sufficiency, the RSI was lower with 79 Au. By day 9, the RSI in Pi sufficient roots were 81 Au for the main root and 91 Au for the lateral root, while for the Pi depleted roots the RSI were 96 Au and 100 Au for the main roots and lateral roots, respectively (Figure 3.14A,C). On the 15th day, there were no marked difference in the RSI values between +P and –P but rather the very slight difference was noted only between the main root and lateral roots, both under +P and -P. This trend was also noted on day 21, with a slightly greater TR-ACO1 protein accumulation in the lateral roots when compared to the main roots but between +P and –P, there was no significant difference in the RSI values (Figure 3.14D,F).

In the second experiment, conducted over a 7-day period, the difference in the accumulation of TR-ACO1 protein was more noticeable between Pi treatments. Over the period of seven days, there were not enough lateral roots for analysis and therefore the TR-ACO protein accumulation was analysed using extracts from the pooled main and lateral roots. Generally, there was greater recognition of TR-ACO1 protein in Pi depleted roots when compared with those grown under Pi sufficiency (Figure 3.14A,C). By day 1, the RSI of the immunoblot for the –P roots was greater by 16 Au when compared to the +P roots. The relative difference increased to 24 Au by day 4, and on the 7th day, the RSI for the -P roots was greater by 29 Au when compared to +P (Figure 3.14A,C).

These results indicate that the extent of recognition by the α-TR-ACO1 antibody was greater in Pi depleted roots, and further indicate an early onset of the response in terms of TR-ACO1 protein accumulation due to Pi limitation.

To further investigate the early response to Pi limitation, western analysis of samples collected over a 12 h period was conducted (Figure 3.15). At 1 h after P treatment, the values indicate that the extent of protein recognition by the α-TR-ACO1 antibody was slightly higher for –P extracts with a RSI value of 120 Au as compared to 111 Au for +P. By 6 h, the relative intensity value for +P was 132 Au while for –P the RSI value was 134 Au, suggesting that as early as 6 h, the TR-ACO1 protein accumulation in the roots was not significantly affected by phosphate limitation. At 12 h after Pi depletion, protein accumulation was greater for –P with a RSI value of 145 Au and this was greater by 25.4 Au when compared to the RSI value for +P (Figures 3.14C,F).

The results of the three experiments indicated that the TR-ACO1 protein started to accumulate more in Pi depleted roots 12 h after Pi depletion, and that up to 9 d after Pi depletion, there were greater accumulation of TR-ACO1 protein in Pi depleted roots. At 1 h after Pi depletion there was also greater RSI value in Pi depleted extracts but this result was not observed at 6 h.

3.4.1.2 Changes in TR-ACO2 protein accumulation as influenced by phosphate supply

Changes in the accumulation of TR-ACO2 protein was first examined over the relatively long term of 21 days and western analysis was conducted using protein extracts from 6 d, 9 d, 15 d and 21 d after Pi depletion (Figure 3.16). At 6 d after Pi depletion, there was no significant difference in the TR-ACO2 protein accumulation in response to Pi treatments. For +P roots, the RSI was 88 Au while for the –P, the RSI

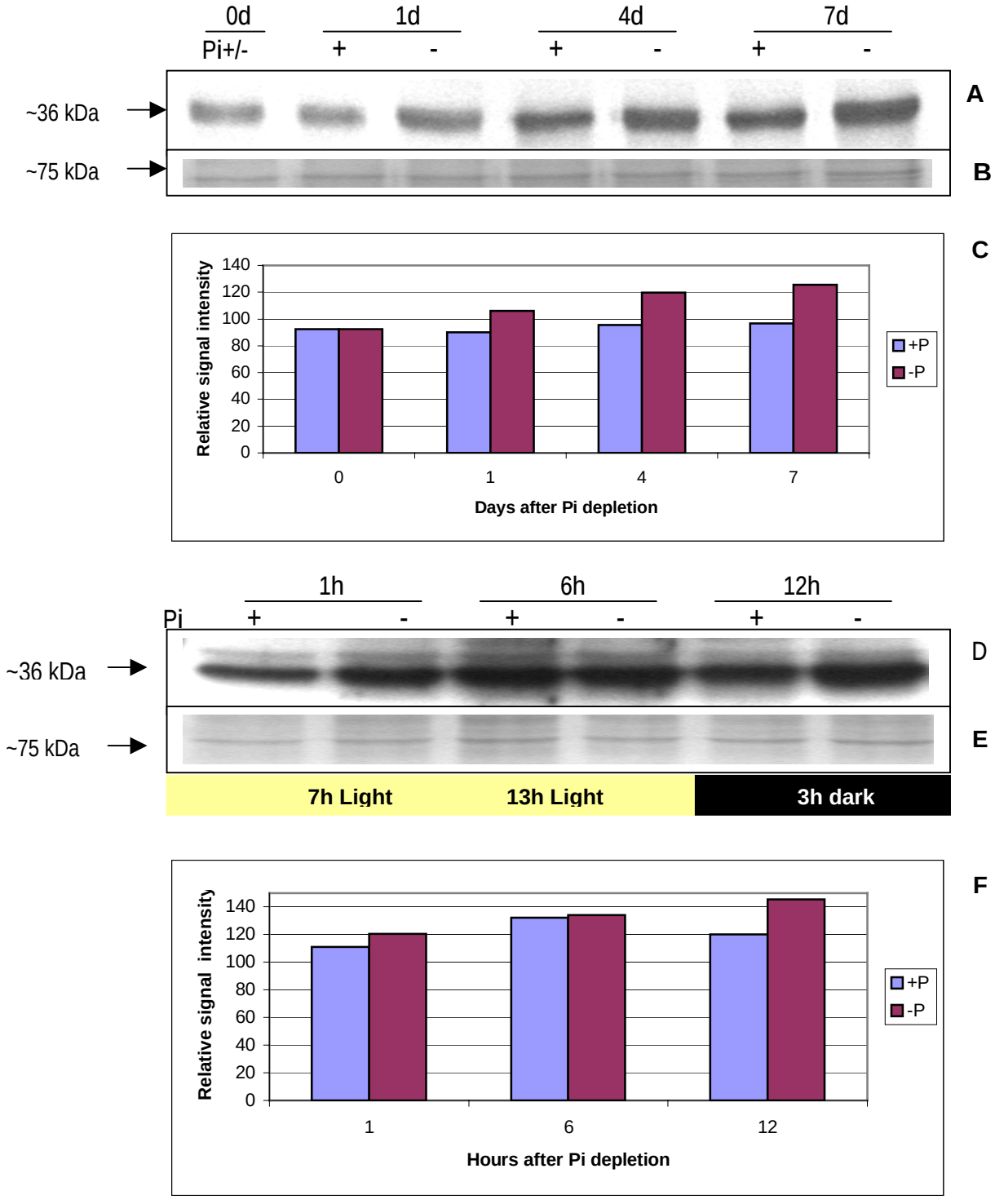

Figure 3.15 Western analyses to detect TR-ACO1 in the roots of wild type white clover collected at the hours/days indicated after +P or –P treatments. Aliquots (10 ug) of protein from each observation point after P treatment were separated using SDS-PAGE, electroblotted onto PVDF membrane and challenged with α-TR-ACO1 antibody (A,D). Coomassie staining of protein was used as a loading control (B,E), Relative values of quantified blots are shown in the histograms (C, F).

was 92 Au and 96 Au for the main roots and lateral roots, respectively. By day 9, the RSI for the main roots was 64 Au for +P and 101 Au for –P. For the lateral roots, the RSI was 101 Au for +P and 102 Au for –P (Figure 3.16A,C), indicating that the difference in the protein accumulation between +P and –P existed only in the main roots.

A more noticeable change in the band intensity in the lateral roots occurred starting on the 15th day after Pi depletion wherein the extent of recognition by the α-TR-ACO2 antibody was greater in the Pi depleted roots, both for main and lateral roots. For the main roots the RSI value for the Pi sufficient roots was 75 Au and 94 Au for the Pi depleted roots. For the lateral root, the RSI for Pi sufficient extract was 96 Au while for the Pi depleted extract, the intensity value was 121 Au, giving a difference of 25 Au. There was again greater accumulation of protein in the Pi depleted extracts on the 21st day after Pi depletion with RSI value of 77 Au for Pi sufficient and 108 Au for Pi depleted roots, showing significant difference in protein accumulation between +P and –P (Figure 3.16 D,F). For the lateral roots, the RSI value was 110 Au for +P and 118 Au for –P.

A further investigation into the response of TR-ACO2 protein was made over the shorter time course experiment, with a 7 d observation period. Over the whole time duration of 7 d there was no difference between Pi sufficient and Pi depleted roots in terms of the extent of recognition of protein when the α- TRACO2 antibody was used (Figure 3.17A,C). Within the time-course, the band intensity appeared to be similar. When the blot was quantified, the RSI values ranged from 94 Au to 98 Au in both Pi sufficient and Pi depleted extracts, thus indicating no difference in the accumulation of TRACO2 protein in the roots within the 7 d experiment.

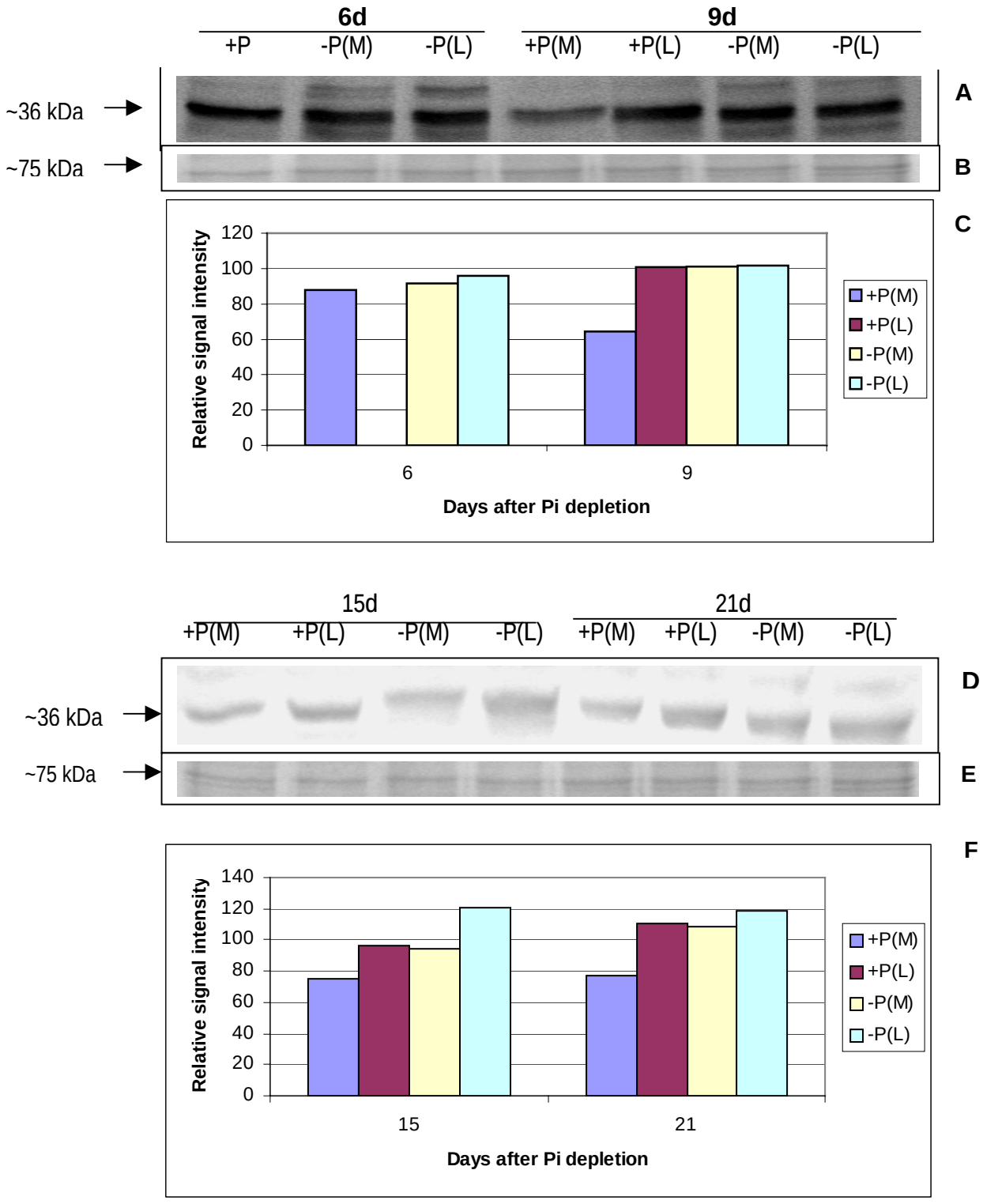

Figure 3.16 Western analyses to detect TR-ACO2 in the roots of wild type white clover collected at the days indicated after +P or –P treatments. Aliquots (10 ug) of protein from each observation point after P treatment were separated using SDS-PAGE, electroblotted onto PVDF membrane and challenged with α-TR-ACO2 antibody (A,D). Coomassie staining is indicated as a loading control (B,E). Relative values of quantified blots are shown in the histograms (C, F).

To further characterise the response of TR-ACO2 protein to changes in Pi supply, a third experiment which examined protein changes over 12 h was also conducted. Over this time duration the pattern of accumulation of TR-ACO2 protein from both Pi depleted and Pi sufficient roots was again very similar. The RSI values for the Pi sufficient and Pi depleted extracts ranged from 90 Au to 93 Au, indicating that the accumulation of TR-ACO2 protein was not significantly affected by Pi supply within a time course of 12 h (Figure 3.17 D,F).

3.4.2 Differential expression of *TR-ACO* genes in response to phosphate supply

With the findings that at least one member of the TR-ACO gene family (*TR-ACO1)* responded to changes in the Pi availability in the roots within 12 h after Pi depletion, and that the previous investigation was made at the protein level, analyses at the transcriptional level were also conducted to gain an understanding as to when this regulation was stimulated. To do this, sqRT-PCR was used on cDNA templates which were reverse transcribed from RNA isolated from roots subjected to different Pi treatments for 24 h. In order to exclude genomic contamination, each of the forward and reverse primers of the four *TR-ACO* genes was designed from the junction of two exons (Section 2.5.1.2). As such, the PCR product sizes corresponding to each mRNA were 581 bp, 577 bp, 232 bp, and 222 bp for *TR-ACO1*, *TR-ACO2*, *TR-ACO3* and *TR-ACO4*, respectively.

Each experiment was conducted as two biological replicates with at least four sample plants for each time point per treatment per replicate. Throughout the time course, the roots of the four sample plants per time point were pooled to make one sample for the extraction of RNA. For each experiment, at least two technical repeats of the sqRT-PCR were carried out to confirm the results obtained.

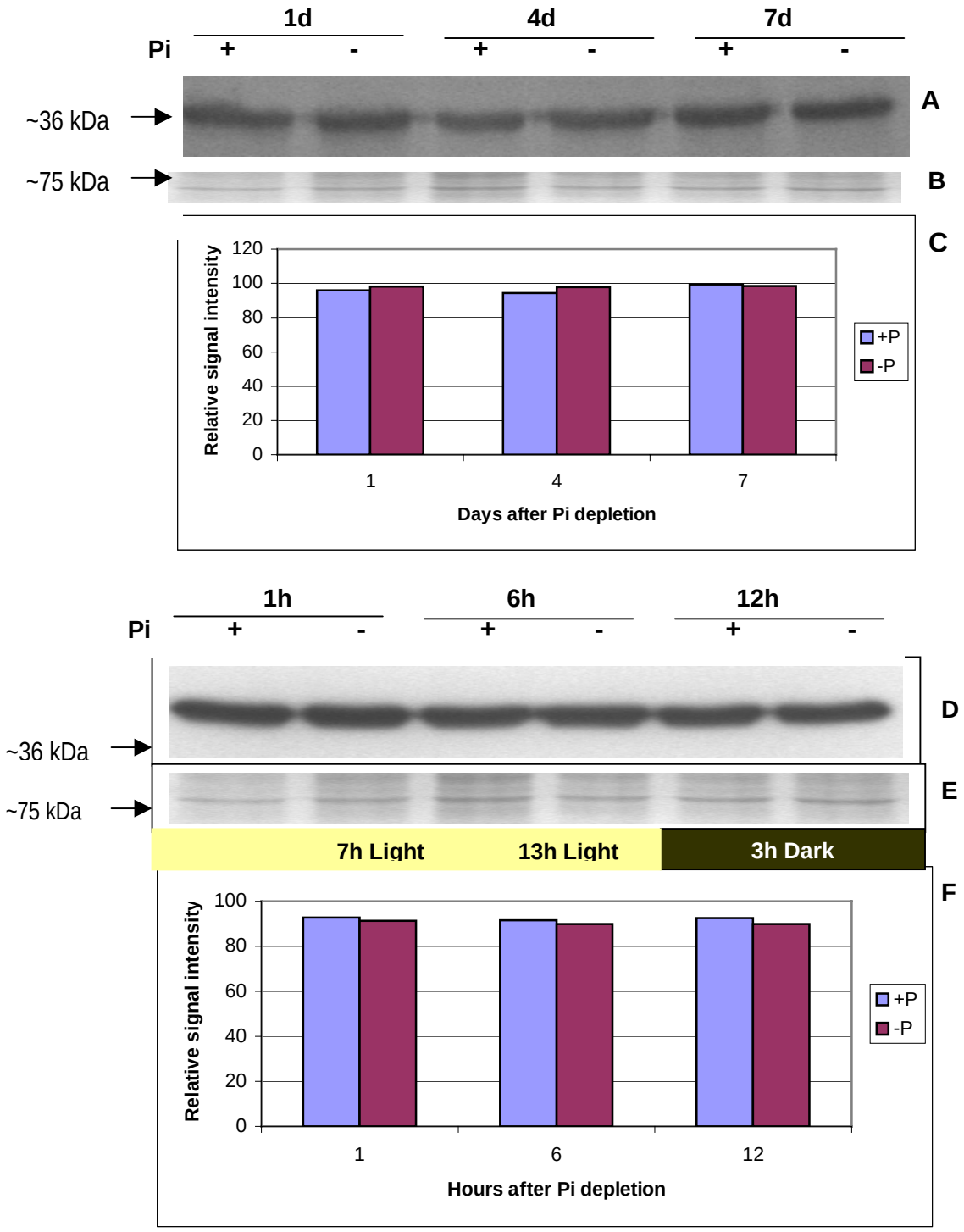

Figure 3.17 Western analyses to detect TR-ACO2 protein in the roots of wild type white clover collected at the days/hours indicated after +P or –P treatments. Aliquots (10 ug) of protein from each observation point after P treatment were separated using SDS-PAGE, electroblotted onto PVDF membrane and challenged with α-TR-ACO2 antibody (A,D). Coomassie staining is indicated as a loading control (B,E) The relative values of quantified blots are shown in the histograms (C, F).

For each member of the *TR-ACO* gene family, the first analysis was conducted by ethidium bromide staining of the sqRT-PCR products which were separated in an agarose gel. In the preliminary experiment, a varied number of cycles were used for the PCR as a linearity check using the +P root extracts. The relative quantification of gene expression was made using a Gel Doc system. Analysis was conducted by a photo-metric interpretation of the band intensity of the specific gene relative to the band intensity of the actin. Following this analysis, another set of products corresponding to each gene was amplified with a reduced number of cycles and, following the separation of the amplified fragments using agarose gel, the products were blotted onto a positively charged nylon membrane using the downward alkaline capillary transfer method (Chomcznski, 1992). The blots were then hybridised with [α-^{32}P]-dCTP labelled gene-specific probes. To further analyse the amount of transcript that hybridised to each of the labelled probes, the radioactivity level in the blot was quantified using the Image Gauge Version 4.0 on the Phospho Imager (FUJIFILM FLA-5000). The extent of hybridisation of the labelled probe to the gene transcript was given as radioactivity level and values are expressed as photo-stimulated luminescence per unit area (PSL/mm^2).

3.4.2.1 Expression of the TR-ACO1 gene in response to changes in phosphate supply

The expression profile of the *TR-ACO1* gene in response to changes in phosphate availability was analysed in two distinct experiments and a similar pattern of expression was noted in both. The first major indication of change was recognisable at 12 h after Pi depletion with an increase in the transcript accumulation in Pi depleted roots (Figure 3.18A,C). At this time point, the expression level of the *TR-ACO1* gene, relative to the expression of actin, for Pi sufficient and Pi deficient roots was 0.65 and 0.942, respectively (Fig 3.18C). At 18 h after Pi depletion, the Pi sufficient roots had relatively greater amount of *TR-ACO1* transcript when compared to the roots under Pi

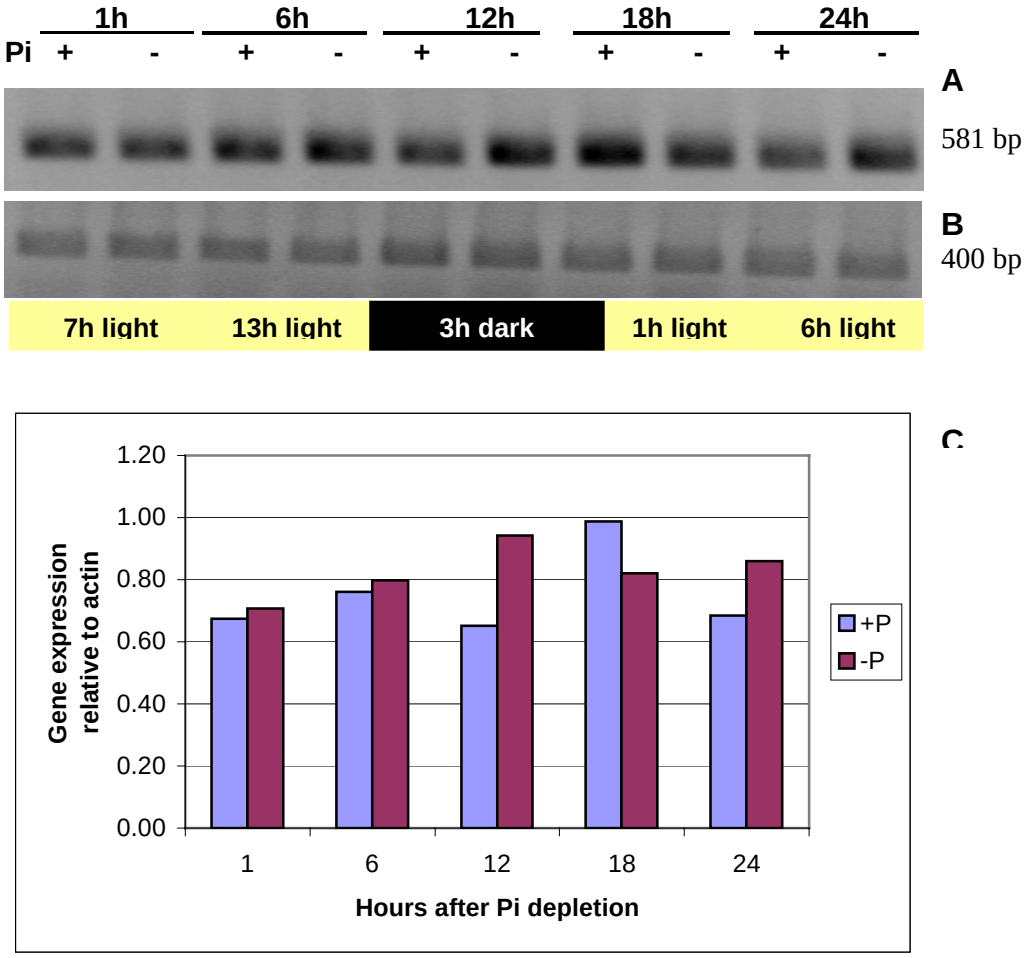

Figure 3.18 Expression of the *TR-ACO1* gene in the roots of wild type white clover collected at the number of hours indicated after Pi depletion. Primers used were specific for *TR-ACO1* gene (A), and actin (B), and gene expression was quantified relative to actin (C). Three micrograms of total RNA was used for reverse transcription and 1 μL of cDNA was used for each PCR reaction. Annealing temperature was set at 60^{o}C for 45 s and amplification was carried out at 35 cycles. Amplified fragments were electrophoresed through a 1.5% agarose gel in 1x TAE for 2 h at 60 V. The gel was then stained with ethidium bromide.

deficiency, but by 24 h the expression level was 0.69 for Pi sufficient and 0. 86 for Pi deficient roots giving a relative difference of 0.17.

When the blot was hybridised with a [α-^{32}P] dCTP labelled *TR-ACO1* gene probe and analysed by autoradiography, the hybridisation of transcripts to the labelled probe was generally greater in Pi depleted roots when compared to those under Pi sufficiency (Figure 3.19). The up regulation of the *TR-ACO1* gene in Pi depleted roots appeared to start from the first hour after Pi depletion but the greatest expression occurred 12 h after Pi depletion.

Analysis of the photo-stimulated luminescence (PSL/mm^2) values revealed that at 1h after Pi depletion, a 16% increase in the Pi depleted roots was detected when compared with the Pi sufficient roots. This value increased to 26% after 6 h and the greatest difference occurred at the 12 h with an increase of 74% compared to the Pi sufficient roots. At 24 h, the increase in PSL values in Pi depleted roots was 29%.

3.4.2.2 Expression of TR-ACO2 gene in response to phosphate availability

The *TR-ACO2* gene was constitutively expressed in white clover roots over the 24 h period (Figure 3.21). In both Pi sufficient and Pi deficient roots, the band intensity of the ethidium bromide stained sqRT-PCR products was relatively similar. Further, when the blot was hybridised with [α-^{32}P]-dCTP labelled *TR-ACO2* gene probe, generally, there was no significant difference in the amount of transcript that hybridised to the labelled probe when the Pi sufficient samples were compared with those under Pi deficiency (Figure 3.21A).

The quantified blot expressed in PSL/mm2 also showed very slight differences in the PSL values between treatments (6-12%) (Figure 3.21B). In the two separate

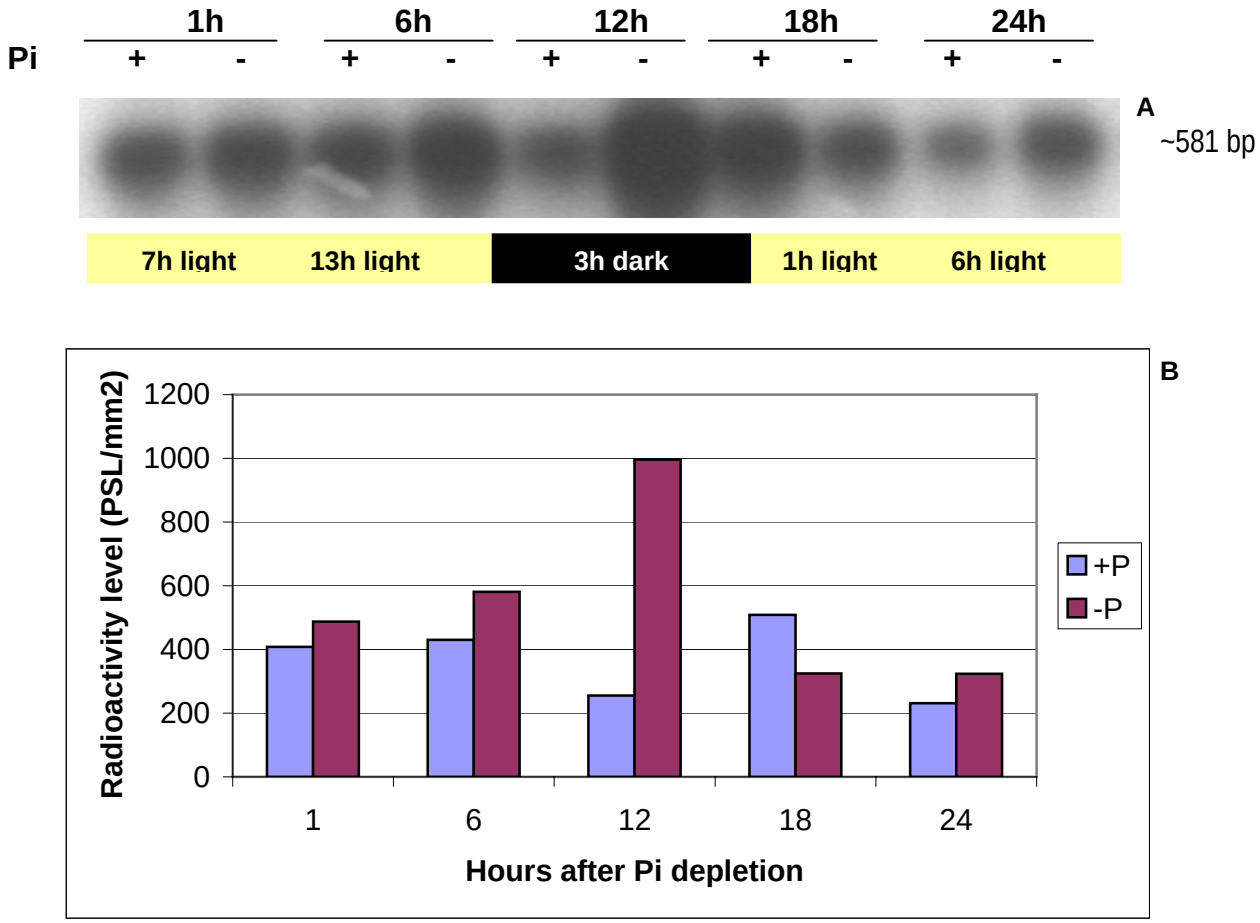

Figure 3.19 Southern hybridisation (A) and phosphorimage quantification (B) to analyse expression of the *TR-ACO1* gene in the roots of wild type white clover collected at the number of hours indicated after Pi depletion. Transcripts of *TR-ACO1* gene were amplified by 25 cycles of PCR, separated through a 1.5% agarose gel for 2 h at 60 V, blotted onto positively charged nylon membrane by downward alkaline capillary transfer for 3 h, and hybridised with [α-^{32}P]-dCTP labelled *TR-ACO1* gene probe. Washing was carried out at high astringency at 65^{o}C to remove non-specific binding of nucleotides. The Phosphorimage was quantified using a FLA-5000 Image Gauge version 4.0.

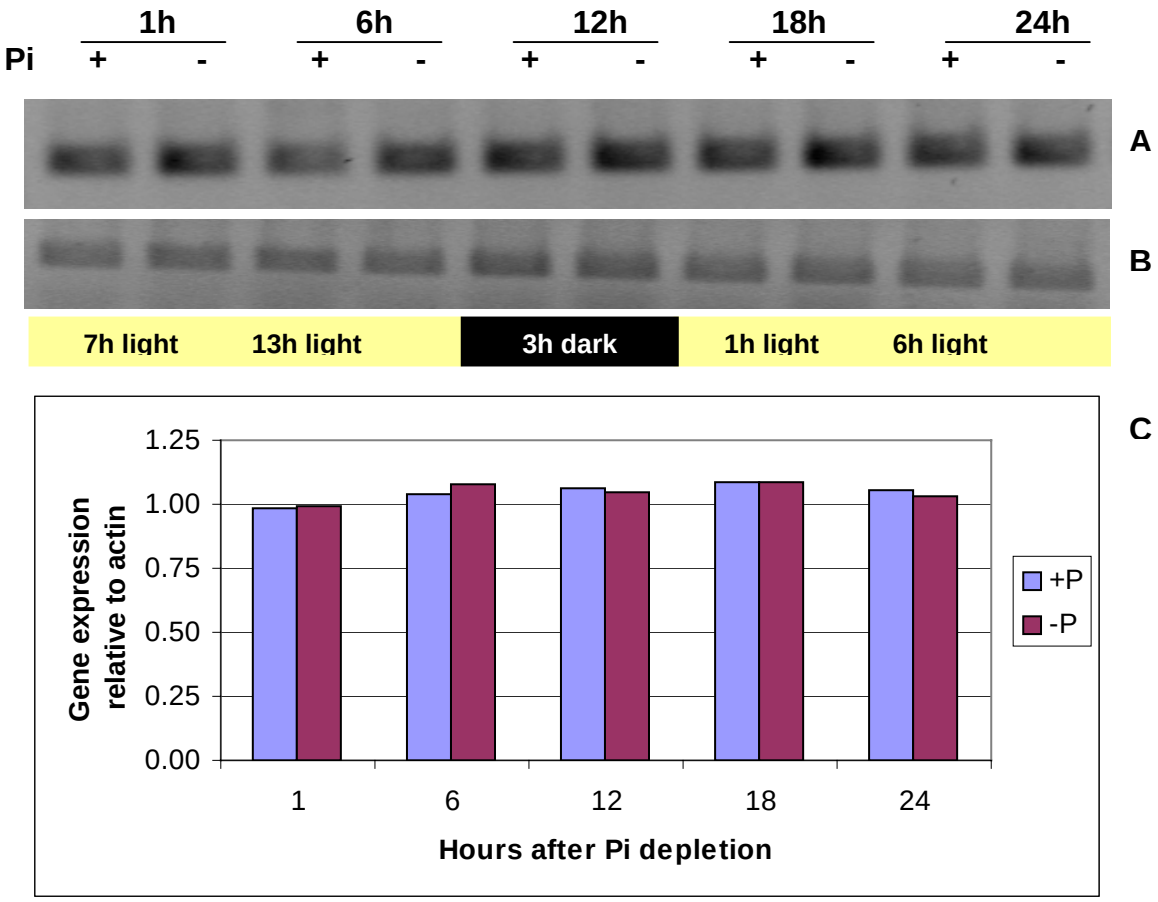

Figure 3.20 Expression of the *TR-ACO2* gene in the roots of wild type white clover collected at the number of hours indicated after Pi depletion. Primers used were specific for *TR-ACO2* gene (A), actin (B), and gene expression was quantified relative to actin (C). Three micrograms of RNA was used for reverse transcription and 1 μL of cDNA was used for each PCR reaction. Annealing temperature was set at 58^{o}C for 45 s and amplification was carried out at 30 cycles. Amplified fragment was electrophoresed at 1.5% agarose gel in 1x TAE for 2 h at 60V. The gel was then stained with ethidium bromide.

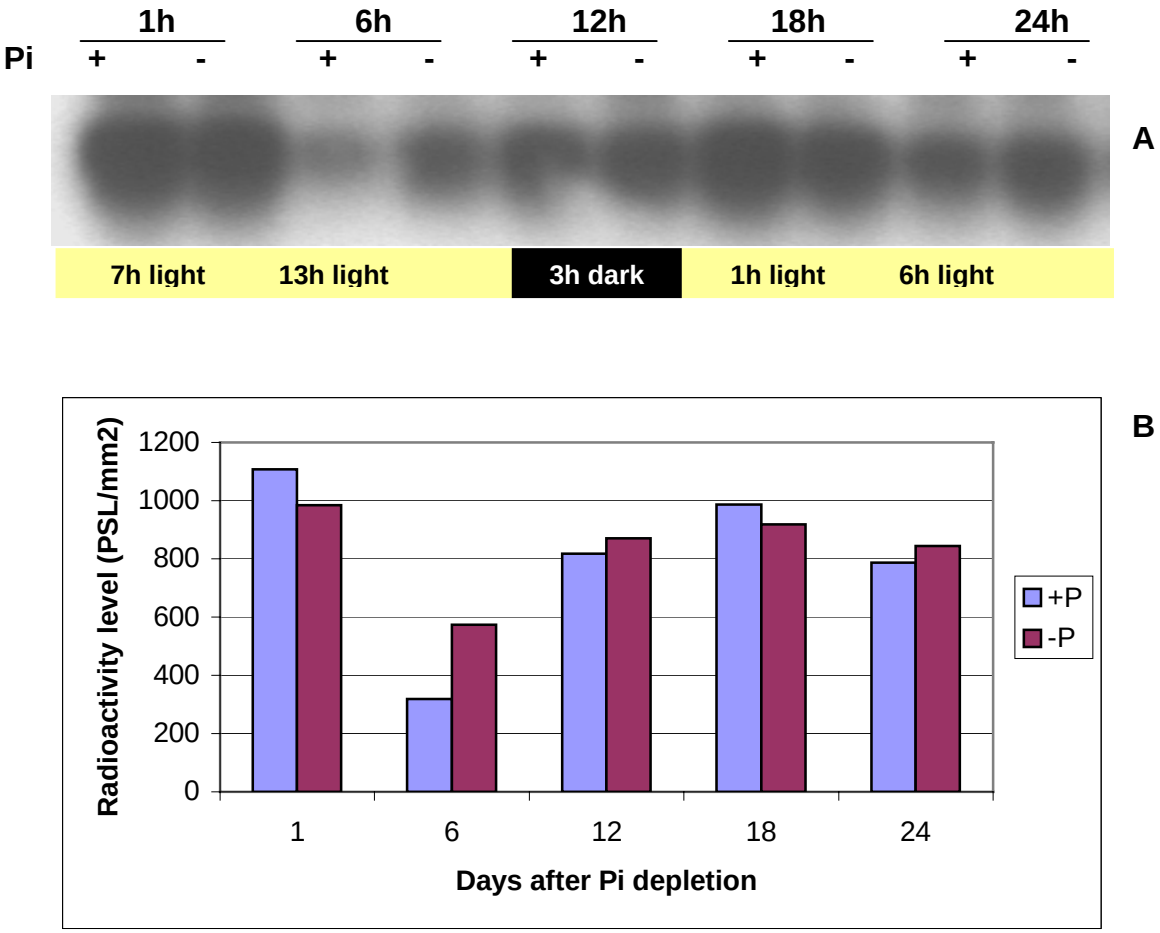

Figure 3.21 Southern hybridisation (A) and phosphorimage quantification (B) to analyse expression of *TR-ACO2* gene in the roots of wild type white clover collected at the number of hours indicated after Pi depletion. Transcripts of *TR-ACO2* gene were amplified by 25 cycles of PCR, fragments separated at 1.5% agarose gel in 1x TAE for 2 h at 60V, blotted onto positively charged nylon membrane by downward alkaline capillary transfer for 3 h, and hybridised with [α-^{32}P]-dCTP labelled *TR-ACO2* gene probe. Washing was carried out at high astringency at 65^{o}C to remove non-specific binding of nucleotides. The phosphorimage was quantitated using a FLA-5000 Image Gauge version 4.0.

3.4.2.3 Expression of the TR-ACO3 gene in response to changes in phosphate supply

experiments in wild type white clover, the same trend was observed, which implies that over a 24 h period, expression of the *TR-ACO2* gene in the roots of white clover was not significantly affected by changes in the availability of Pi. The decrease in the gene expression in samples at 6 h can possibly be due to factors other than the availability of Pi, as it happened to both, and this will be discussed later.

The effect of Pi supply on the expression of *TR-ACO3* gene is shown in Figure 3.22. There was a considerable decrease in the transcript level of *TR-ACO3* gene in Pi depleted roots at 1 h, 12 h and 24 h after Pi depletion. However, this observation did not hold through at 6 h and 18 h after Pi depletion, where there was a greater amount of transcript in Pi depleted roots.

Analysis of the blotted transcript that hybridised to the [α-^{32}P]-dCTP labelled *TR-ACO3* gene probe showed that at 1 h after Pi depletion, the PSL values in Pi depleted sample decreased by 40% when compared to the Pi sufficient sample, and at 12 h and 24 h, the decreases were 55% and 59%, respectively (Figure 3.23). However, the opposite was the case at 6 h and 18 h, where transcript abundance in Pi depleted roots was greater by 43% and 11%, respectively, when compared to the Pi sufficient extracts.

3.4.2.4 Expression of TR-ACO4 gene in response to changes in phosphate supply

The expression profile of the *TR-ACO4* gene in response to Pi supply is presented in Figure 3.24. Starting at 1 h after Pi depletion a greater transcript accumulation occurred in Pi depleted samples. This level was maintained up to 12 h and then declined at 18 h and 24 h. On the other hand, the accumulation of transcript in Pi sufficient samples generally remained at a relatively low level throughout the 24 h experiment.

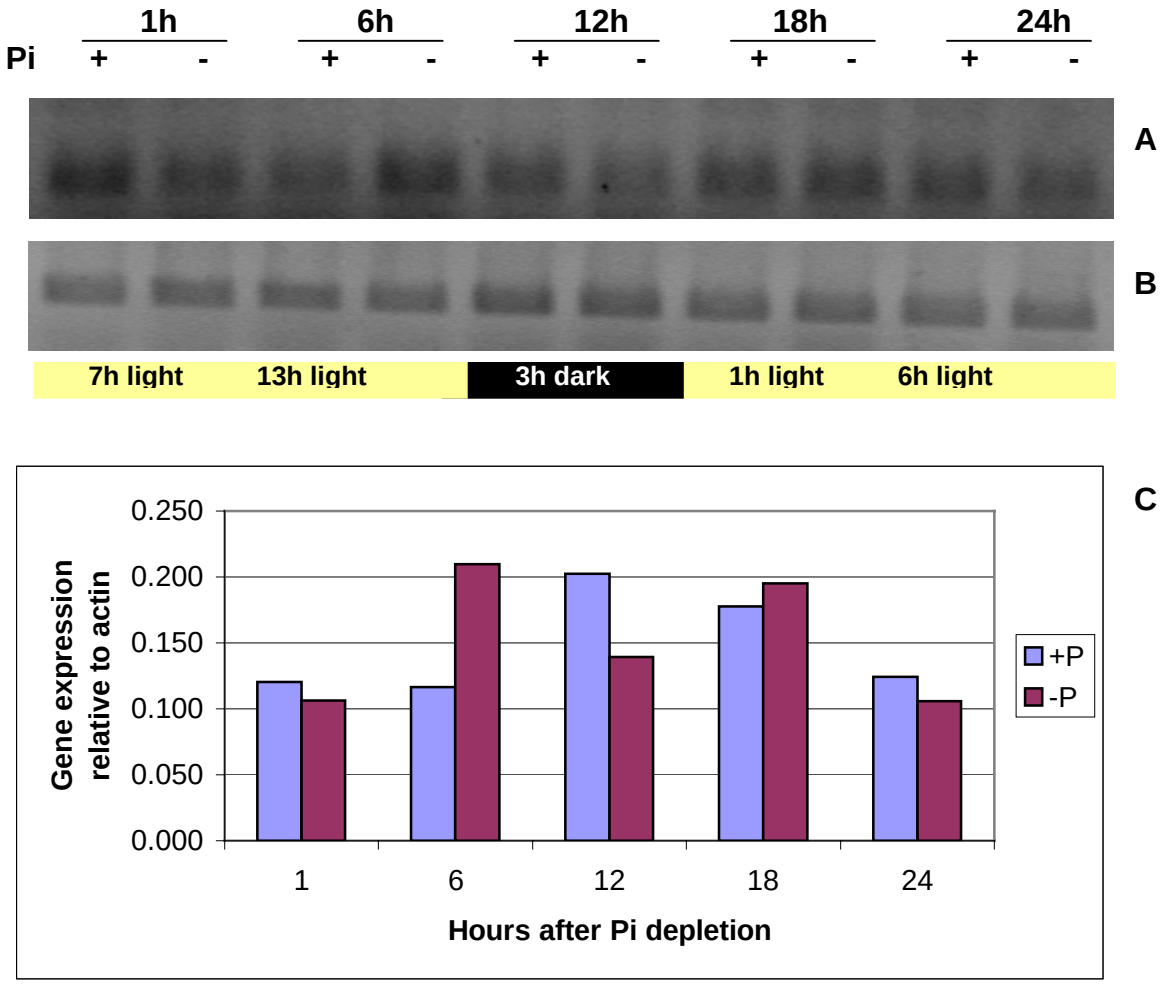

Figure 3.22 Expression of the *TR-ACO3* gene in the roots of wild type white clover collected at the number of hours indicated after Pi depletion. Primers used were specific for *TR-ACO3* gene (A) and actin (B), and gene expression was quantified relative to actin (C). Three micrograms of RNA was used for reverse transcription and 1 μL of cDNA was used for each PCR reaction. Annealing temperature was set at 55^{o}C for 45 s and amplification was carried out at 40 cycles. Amplified fragment was electrophoresed at 1.5% agarose gel in 1x TAE for 2 h at 50V. The gel was then stained with ethidium bromide.

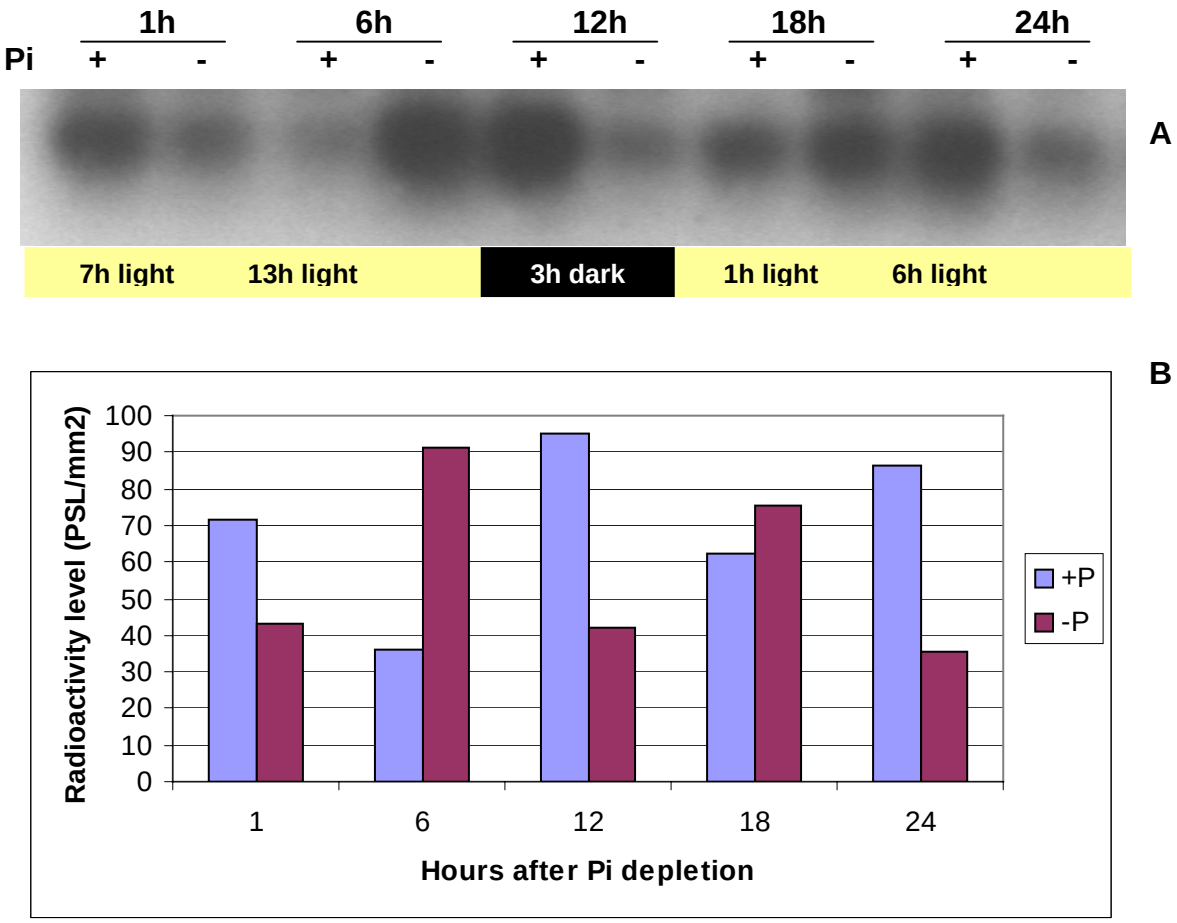

Figure 3.23 Southern hybridisation (A) and phosphorimage quantification (B) to analyse expression of *TR-ACO3* gene in the roots of wild type white clover collected at the number of hours indicated after Pi depletion. Transcripts of *TR-ACO3* gene were amplified by 25 cycles of PCR, fragments separated by a 1.5% agarose gel, blotted onto positively charged nylon membrane by downward alkaline capillary transfer for 3 h, and hybridised with [α-^{32}P]-dCTP labelled *TR-ACO3* gene probe. Washing was carried out at high astringency at 65^{o}C to remove non-specific binding of nucleotides. The phosphorimage was quantitated using the FLA-5000 Image Gauge version 4.0. PSL = Photo stimulated luminescence.

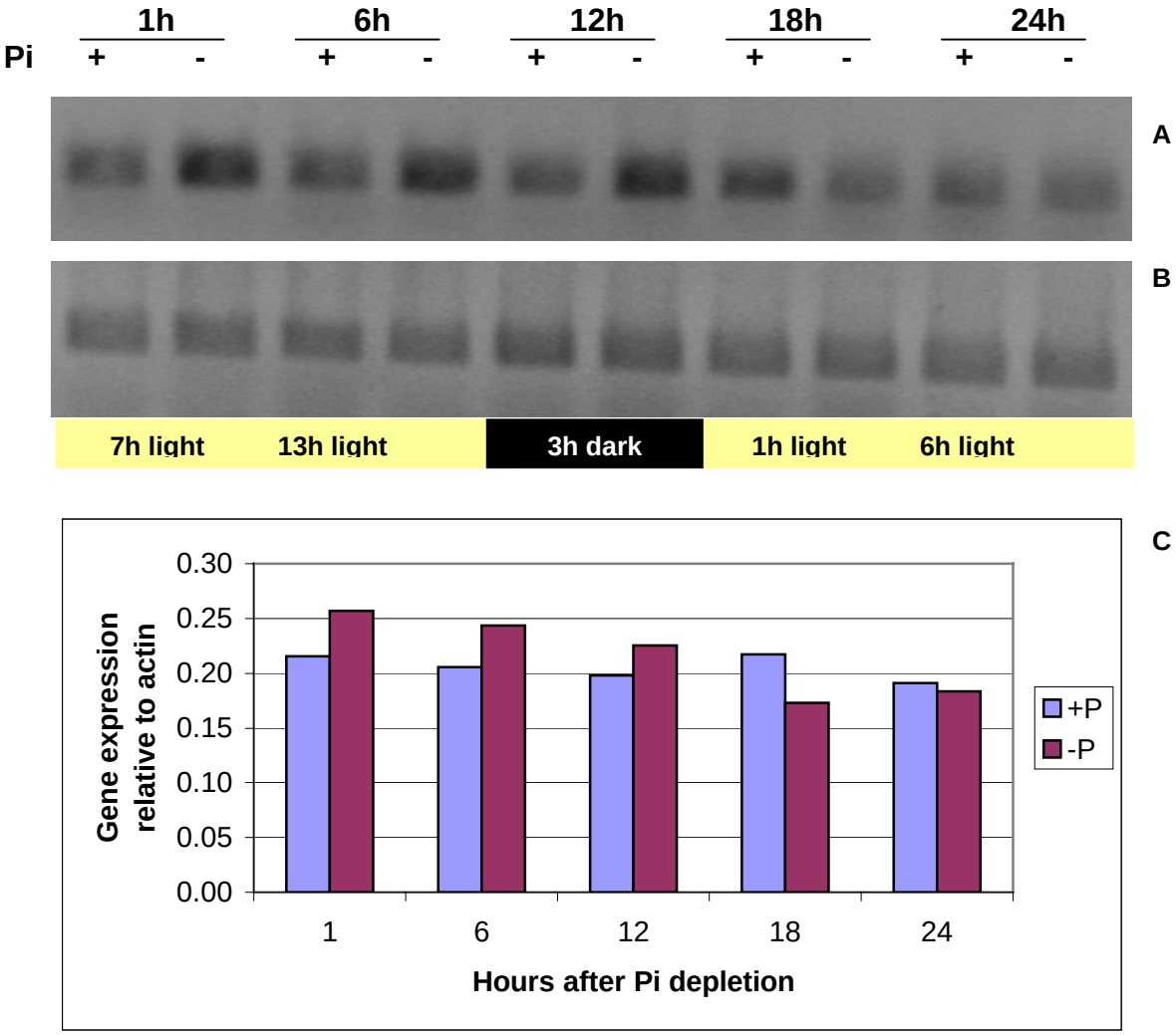

Figure 3.24 Expression of the *TR-ACO4* gene in the roots of wild type white clover collected at the number of hours indicated after Pi depletion. Primers used were specific for *TR-ACO4* gene (A), and actin (B), and gene expression was quantified relative to actin (C). Three micrograms of RNA was used for reverse transcription and 1 μL of cDNA was used for each PCR reaction. Annealing temperature was set at 55^{o}C for 45 s and amplification was carried out at 40 cycles. Amplified fragment was electrophoresed at 1.5% agarose gel in 1x TAE for 2 h at 50V. The gel was then stained with ethidium bromide.

Chapter 4

4.1 Transformation of white clover with *TR-ACO1p::mGFP5 ER*

4.1.1 Confirmation of the transformation of *Agrobacterium tumefaciens* LBA 4404 with *TR-ACO1p:: mGFP5-ER*

The gene construct *TR-ACO1p::mGFP5-ER* inserted into pBIN19 and transformed into *E. coli* strain DH5-α was obtained from Miss Susanna Leung (IMBS, Massey University). The isolated plasmid was transformed into *A. tumefaciens* strain LBA 4404 by electroporation using a Micropulser™ electroporation apparatus in preparation for its introduction into the white clover. After transformation, the *A. tumefaciens* culture was plated onto YM agar plates and allowed to grow for *ca.* 48 h. Eight colonies containing the putative *TR-ACO1p::mgfp5-ER* insert were screened by PCR using the forward primer, mGFP-seq-F1 (Table 2.2), designed from the NOS terminator upstream of the *TR-ACO1* promoter, and the reverse primer mGFPseq-R1 (Table 2.2), located downstream of the promoter (See Figure 2.12).

Seven colonies (#1 to #6 and #8) contained insert as detected by PCR which corresponded to the expected size of the positive control, a PCR fragment amplified from a *TR-ACO1p-mGFP5-ER* plasmid isolated from *E. coli*, (lane 9) (Figure 4.1). Plasmid DNA from colonies #1 to 4 was also digested with *Bam*H1 and *Hind*III, and bands corresponding to the expected size of 1200 bp were observed (data not shown). The PCR products obtained from colonies #1 and #4 were sequenced, and the results indicated a 90% and 98% similarity, when aligned with the original sequence of the *TRACO1* promoter. Plasmid DNA from colony # 4 which had the higher percentage of similarity with the original *TR-ACO1* promoter sequence was then used in the transformation of white clover (See Materials and Methods, Section 2.6.2).

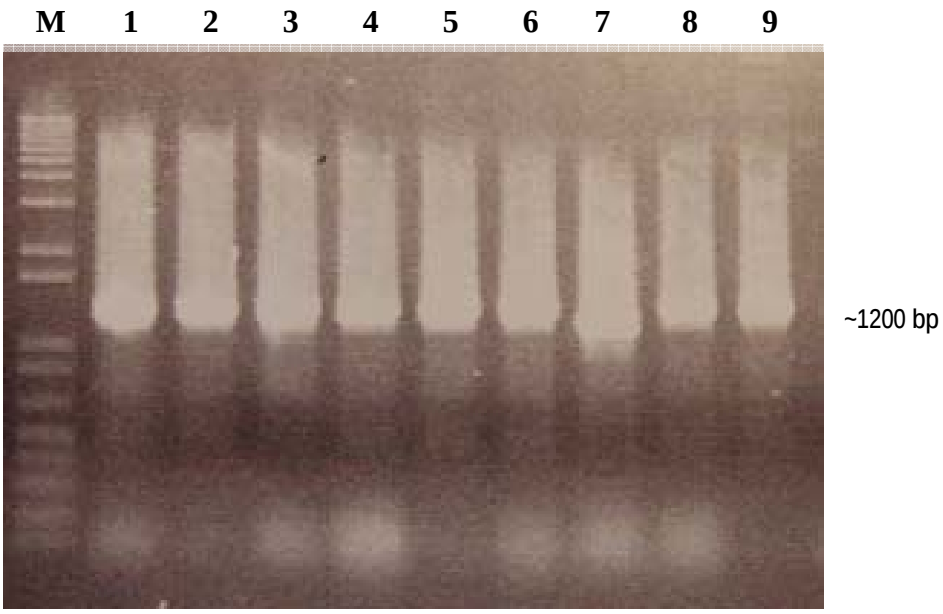

Figure 4.1 PCR of *A. tumefaciens* colonies putatively harbouring a pBIN plasmid with a *TR-ACO1p::mGFP5-ER* insert. The primers mGFP-seq-F1 and mGFP-seq-R1 were used for the PCR. DNA was stained with ethidium bromide following separation in a 1% (w/v) agarose gel. Lane numbers 1 to 8 were amplified products of plasmid DNA from each colony, as indicated; Lane # 9 is the positive control (amplification from *TR-ACO1p-mgfp5-ER* plasmid isolated from *E.coli*); M = 1kb+ DNA marker.

4.1.2 Transformation and regeneration of white clover transformants

White clover cotyledons, inoculated with a suspension of *A. tumefaciens* containing the *TR-ACO1p::mGFP5-ER* gene, were co-cultivated on CR7 media (See Section 2.6.2.2) for 3 d. After this period, approximately 80% of the cotyledons started to swell and turn green indicating an initiation of growth. However, after transferring to the selection media ($CR7^{Kan200, Cef300}$) an increasing number of cotyledons started to turn whitish, and then eventually turned necrotic. Any remaining green cotyledons (typically *ca.* 1300 from *ca.* 2500 cotyledons) were subsequently transferred to fresh $CR7^{Kan150, Cef300}$ media every two to three weeks. After two months, there were only *ca.* 50 growing cotyledons starting to produce adventitious shoots. Shoots which had developed two to three leaves were transferred to $CR5^{Kan150, Cef300}$ media (Section 2.6.2.3) and allowed to root. By weeks 12 to 15 after inoculation, 20 plantlets had rooted. These plantlets were initially screened by confocal microscopy (Section 2.7). Thirteen lines were identified as containing the *TR-ACO1p: :mGFP5ER* transgene, and these were exflasked and planted into potting mix. These plants were grown in the GMO glasshouse and were further screened by PCR and Southern hybridisation.

4.1.3 Confirmation of the incorporation of the *TR-ACO1p: :mGFP5-ER* transgene into the white clover genome

To confirm the presence of the transgene, PCR was conducted using the mGFP5-probe forward primer and mGFP5 probe reverse primer (Table 2.2), giving an expected amplified fragment of *ca.* 490 bp (Figure 4.2).

A total of 11 putative transformants were identified although line TR9-1 only had a very faint band. These plants, however, had a poor survival rate when transferred to the GMO glasshouse. Despite efforts to rescue these, only six plants survived (designated as TR2-1, TR9-1, TR31-3, TR15-1, TR22-1, and TR22-2). DNA isolated from these plants was used in Southern analysis to further confirm incorporation of the transgene and to determine the gene copy number in the genome. The first Southern analysis was conducted on three putative lines (Figure 4.3A) and showed that the pattern of hybridisation of two of the lines, TR2-1 and TR22-1, to the [α-^{32}P]-dCTP labelled mGFP5-ER probe was similar. In the *Kpn*1 digested lane, only one fragment which was more than 12 kb in size hybridised to the labelled probe. In the *Eco*RV digested lane four fragments of *ca.* 11 kb, 7 kb and 3 kb in size hybridised to the probe. Using the *Xba*1 restriction enzyme, there were three fragments which hybridised to the probe. One clear band was larger than 12 kb in size, whereas the other two bands of less intensity were approximately 12 kb and 5 kb in size. For the third line, TR9-1, no fragment hybridised to the labelled probe.

Following these results, further Southern analysis was conducted using only one restriction enzyme, *Hind*III. In this analysis, lines TR2-1, TR22-1, TR22-2 and TR31-1 gave the same size of fragments with a similar pattern of hybridisation to the probe (Figure 4.3B). In the digested lane, there were at least six fragments which hybridised to the labelled probe. There was one intense band of *ca.* 5 kb, two bands of lesser intensity which were close to 12 kb, and another two smaller bands that had sizes of *ca.* 2 kb and 1.8 kb.

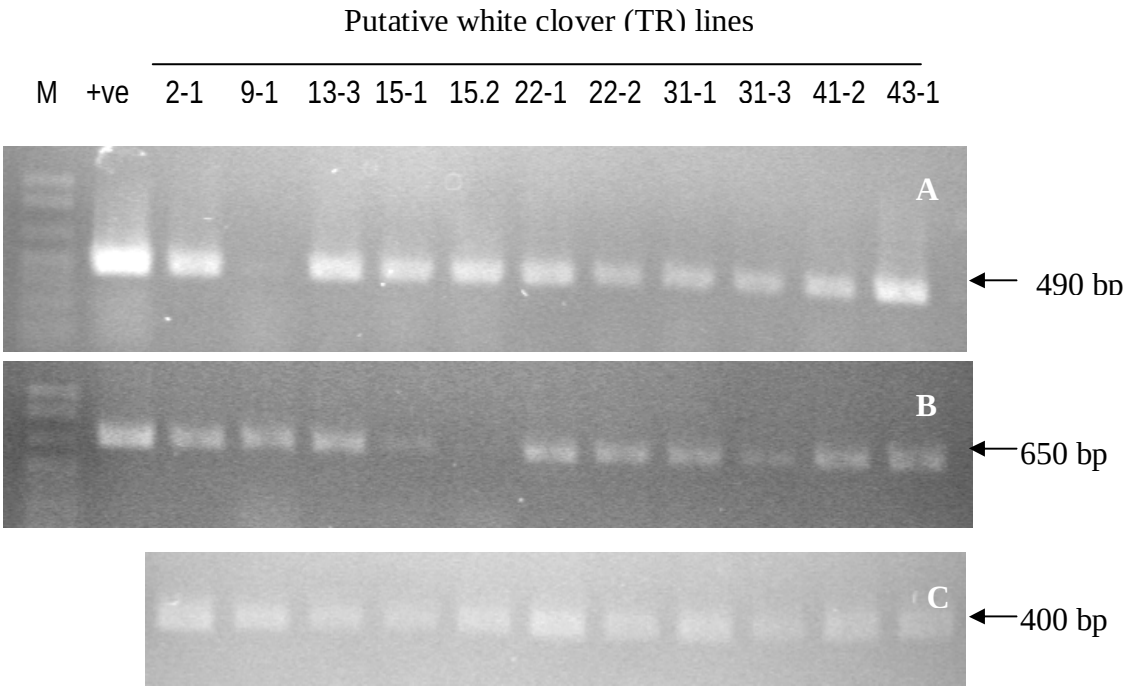

Figure 4.2 PCR screening of putative white clover transformants harbouring the *TR-ACO1p::mGFP5-ER* gene insert. PCR was conducted using primers to amplify the *mGFP5-ER* gene (A) or the *TR-ACO1* promoter (B). PCR products of genomic DNA using actin primers are shown in panel C. The relative sizes of generated PCR products are indicated on the right.
M = 1 Kb+ DNA marker;
+ve = positive control, using the *TR-ACO1p::mGFP5-ER* plasmid as template

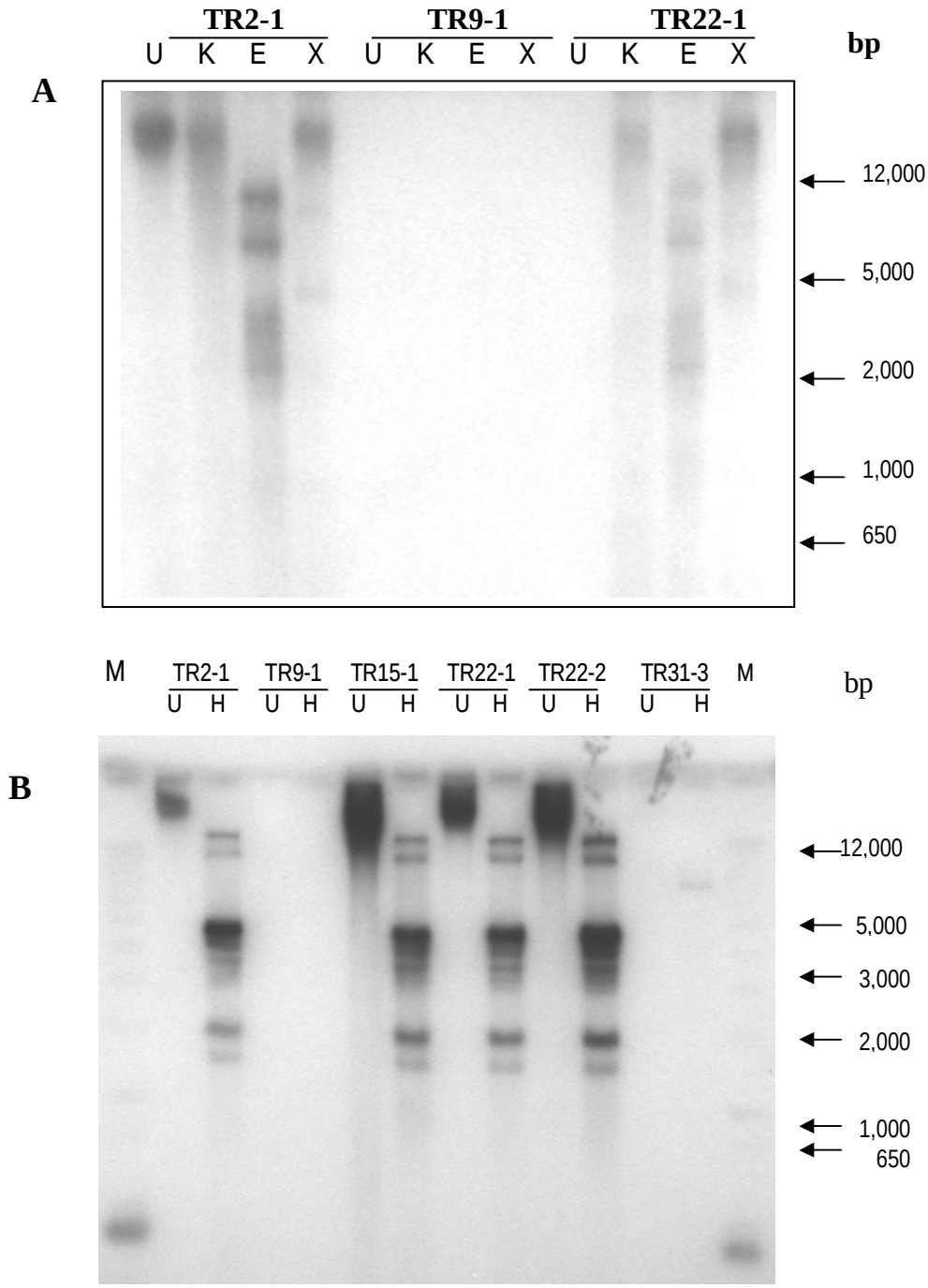

Figure 4.3 Southern hybridisation of [α-^{32}P]-dCTP labelled mGFP5-ER probe to digested and undigested genomic DNA from the putative white clover transformants harbouring the *TR-ACO1p::mGFP5-ER* gene insert. Genomic DNA (20 μg) was separated on a 1% (w/v) agarose gel and blotted onto nylon membrane. The membrane was hybridised with [α-^{32}P]-dCTP labelled mGFP5-ER probe and washed at high astringency (0.1x SSPE, 0.1% (w/v) SDS at 65^{o}C) to remove unincorporated nucleotides. The relative sizes are indicated on the right. Panel A: U = undigested; K = digested with *Kpn*1, E = digested with *Eco*RV; and X = digested with *Xba*1; Panel B: U= undigested, H = digested with *Hind*III, M =1 kb+ DNA ladder.

These results indicate that these transformants may have been derived from only one transformation event. The line TR31-3 had only one fragment of *ca.* 8 kb that hybridised to the probe, but this band was very faint. From this analysis, it appeared that there were only two genetically independent lines in this transformation, TR2-1 and TR31-3. However, the TR31-3 line appeared quite weak and did not grow very well in the glasshouse. Hence, TR2-1 was used as a stock plant for the subsequent biochemical and molecular studies.

As there was a concern as to the reliability of results in the use of only a single transgenic line, another transformation of white clover was undertaken. This was conducted in order to obtain more genetically-distinct transgenic lines. In doing this, 12 new putative transgenic lines were identified by PCR screening using the mGFP5-ER gene primers (Figure 4.4A) and *TR-ACO1p* primers (Figure 4.4B).

Southern analysis was conducted on nine putative transgenic lines (designated TR-1, TR-2, TR3, TR-6, TR-7, TR-8, TR-12, TR-13, and TR-20) using a [α-^{32}P]–dCTP labelled mGFP5-ER gene probe. The results showed a different hybridisation pattern for each line indicating that these nine lines were from different transformation events and were genetically-distinct. Three independent lines had one copy number of the gene (Figure 4.5). These were TR-7 in which the mGFP5-ER gene probe hybridised to a fragment of *ca.* 4 kb in size, to a *ca.* 5 kb fragment in TR-8, and a *ca.* 3 kb fragment in TR-12. TR-20 had putatively two gene copy numbers, with two hybridisation fragments at *ca.* 11.5 kb in size and the other fragment at *ca.* 5 kb.

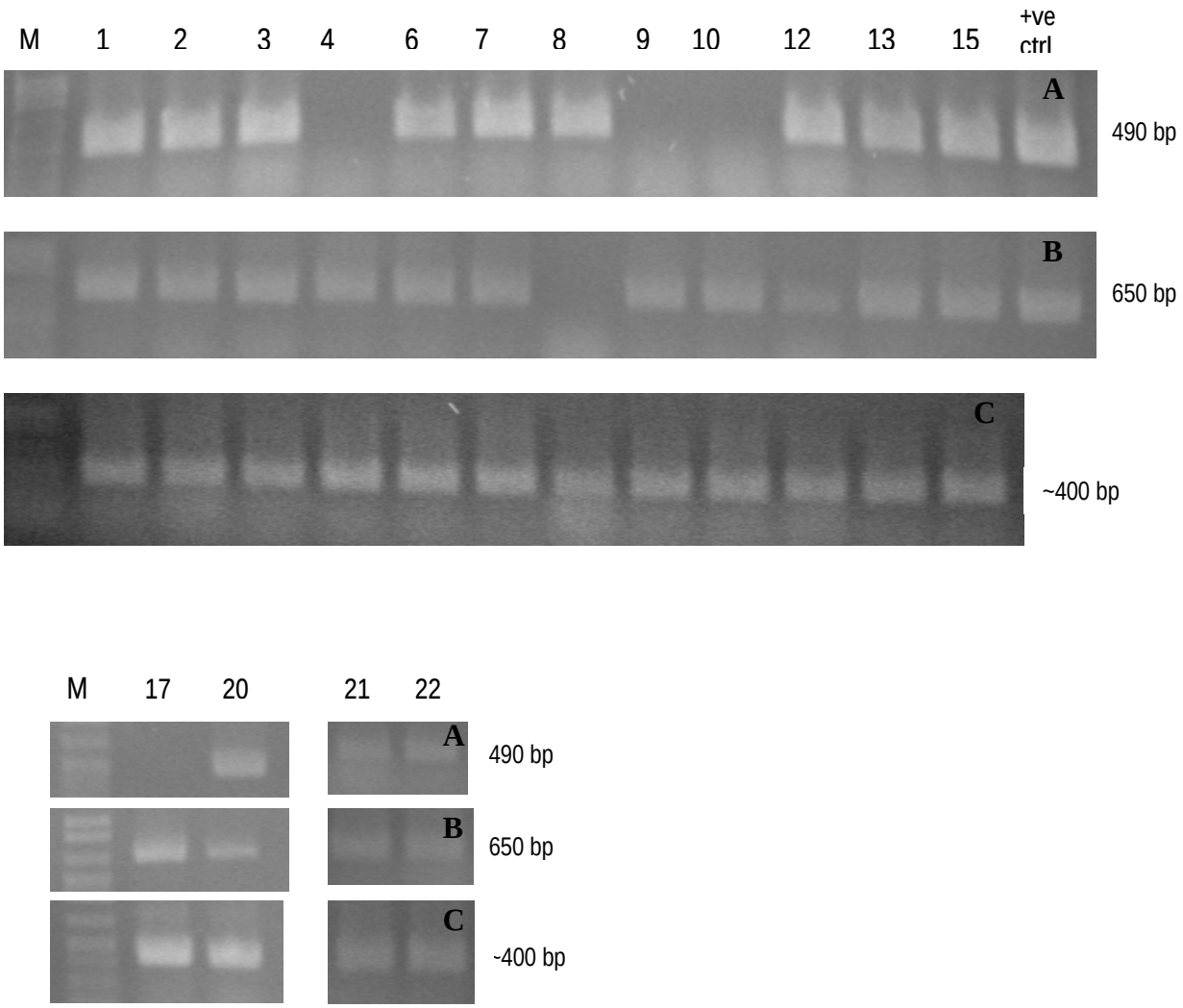

Figure 4.4 PCR screening of a set of putative white clover transgenic lines harbouring the *TR-ACO1p::mGFP5-ER* gene insert using primers to amplify the *mGFP5-ER* gene (A) or the *TR-ACO1* promoter (B), and actin (C). PCR products were electrophoresed in a 1.0% (w/v) agarose gel and visualised with ethidium bromide. The relative size of the generated fragments are indicated on the right. The numbers on top of panel A correspond to the lines of the putative white clover transformants. M=1kb+ DNA marker.

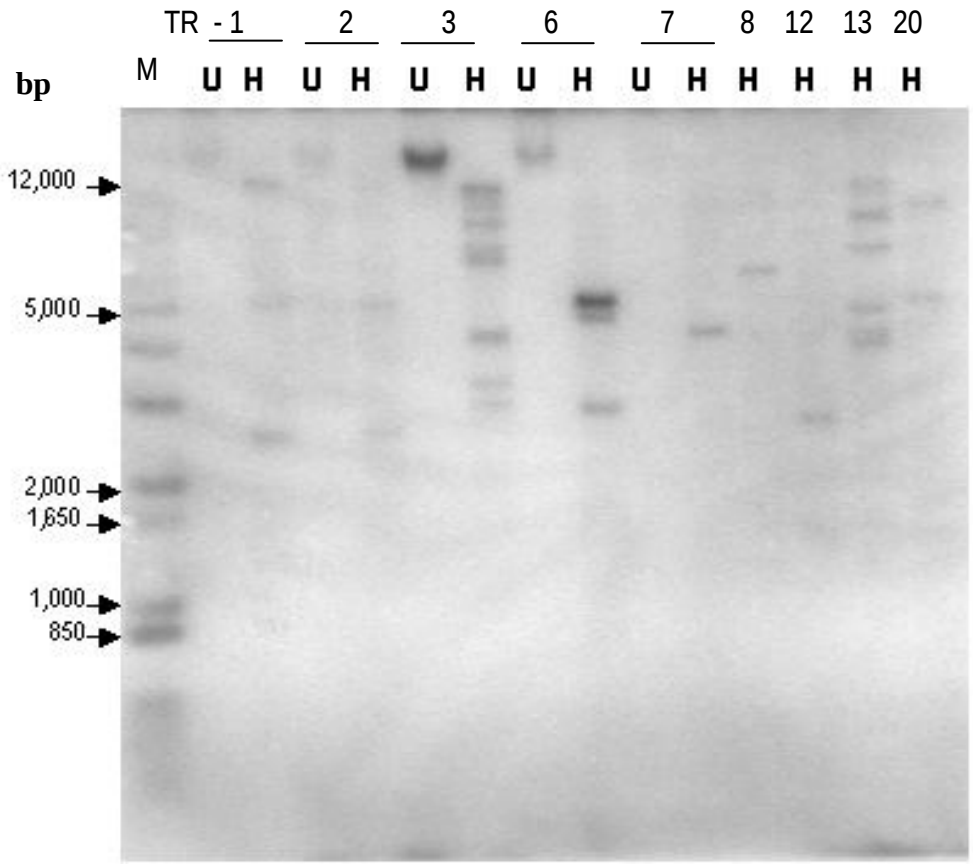

Figure 4.5 Southern hybridisation of a [α-^{32}P]–dCTP labelled mGFP probe to the *Hind*III digested genomic DNA from nine putative white clover transformants harbouring a *TR-ACO1p: :mGFP5-ER* gene insert. Digested genomic DNA (20 μg) was separated on a 1% (w/v) agarose gel at 26 V for 16 h and blotted onto nylon membrane using the downward alkaline capillary transfer. The membrane was hybridised with [α-^{32}P]–dCTP labelled mGFP5-ER probe overnight followed by high astringency washing (0.1x SSPE, 0.1% SDS at 65^{o}C) to remove non-specific binding of nucleotides. Numbers on top of the panel represent the individual transgenic lines; M=1 kb+ DNA marker; U= undigested; H= digested with *Hind*III restriction enzyme.

The lines designated as TR-1, TR-2, and TR-6 had putatively three gene copy numbers each. The largest molecular mass hybridization fragment for TR-1 and TR-2 was *ca.* 12 kb and the smallest was *ca.* 2.5 kb. For TR-6, the largest molecular mass hybridisation fragment was *ca.* 5 kb followed by *ca.* 4.8 kb fragment and the smallest was *ca.* 3 kb. TR-13 had putatively five copies, while TR-3 had at least eight copies of the gene as determined by hybridisation of the labelled mGFP5-ER probe.

4.2 Analysis of TR-ACO protein accumulation and *TR-ACO* gene expression in TR-ACO1p::mGFP5-ER transformed white clover

4.2.1 Accumulation of TR-ACO protein in the roots of transgenic (line TR2-1) white clover

To analyse protein accumulation in the roots of theTR2-1 transgenic line, stolon cuttings were grown in liquid media (Hoagland's solution) with a sufficient amount (1.0 mM) of Pi (see Section 2.1.2). After acclimatisation in the Pi sufficient media for two weeks, cuttings were allowed to grow for a further 15 days prior to root sample collection for western analysis. Crude protein extracts from the main roots and the lateral roots were challenged with either the α-TR-ACO1 or the α-TR-ACO2 antibody. When the extract was challenged with the α-TR-ACO1 antibody, greater band intensity and hence a greater recognition of TR-ACO1 protein occurred in the lateral roots when compared to the main roots. Similarly, when the α-TR-ACO2 antibody was used, it also recognised more protein in the lateral roots relative to the main roots, indicating greater TR-ACO2 protein accumulation in the lateral roots (Figure 4.6). This result was confirmed in a separate analysis (data not shown).

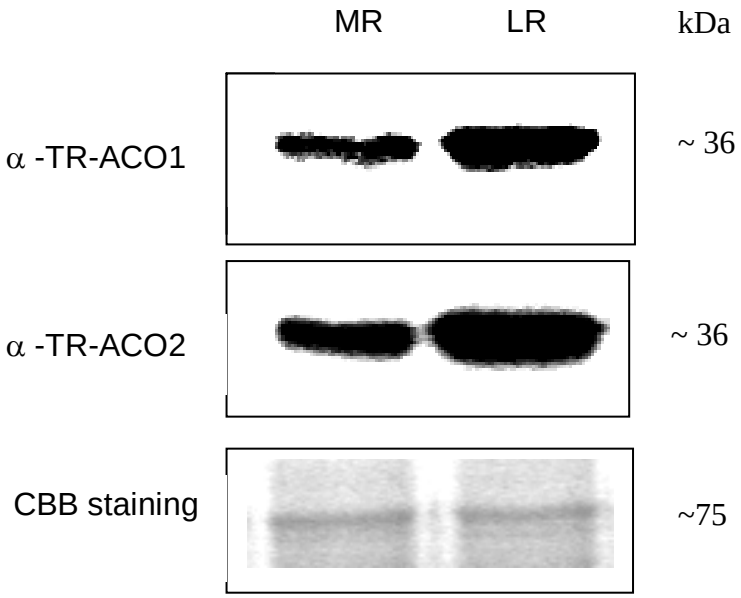

Figure 4.6 Accumulation of the TR-ACO1 and TR-ACO2 protein in the main root and lateral roots of the TR2-1 transgenic white clover line using western analysis. Total protein was extracted from the main roots (MR) and lateral roots (LR), 5 μg of the crude protein extract was separated in SDS-PAGE at 150 V for 75 min, and electroblotted onto PVDF membrane at 100V for 1 h. Blot development was conducted using West Pico Supersignal kit. MR = main roots; LR = lateral roots. The figure shown is representative of two technical replicates performed on each of two biological replicates.

4.2.2 Differential expression of the *TR-ACO* gene family in the roots of transgenic (line TR2-1) white clover

Representative root samples collected from the same experiment used for western analysis were also used to analyse the pattern of expression of the *TR-ACO* gene family in both the main and lateral roots. Analysis was conducted by the semi-quantitative Reverse Transcriptase-Polymerase Chain Reaction (sqRT-PCR). RNA extracted from these samples were used for cDNA synthesis and the extent of transcript accumulation was examined by amplification using *TR-ACO* gene specific primers. Using these primers, the fragment sizes for *TR-ACO1, TR-ACO2* and *TR-ACO3* were 580 bp, 570 bp, and 230 bp, respectively. The amplified fragments which were separated and stained with ethidium bromide (Figure 4.7) shows the expression pattern of each gene.

For *TR-ACO1,* there was greater band intensity, indicating greater transcript accumulation in the lateral roots when compared with the main roots. Similarly for *TR-ACO2*, transcript accumulation was also greater in the lateral roots and less in the main roots. Using the *TR-ACO3* primers, the pattern of transcript accumulation appeared different from *TR-ACO1* and *TR-ACO2*, wherein greater band intensity was noted in the main roots. In the lateral roots, there was a very faint band which was barely detectable, suggesting that the gene was less expressed in these roots. These results were confirmed in a separate experiment. To indicate a loading control, the cDNA was also amplified using actin primers.

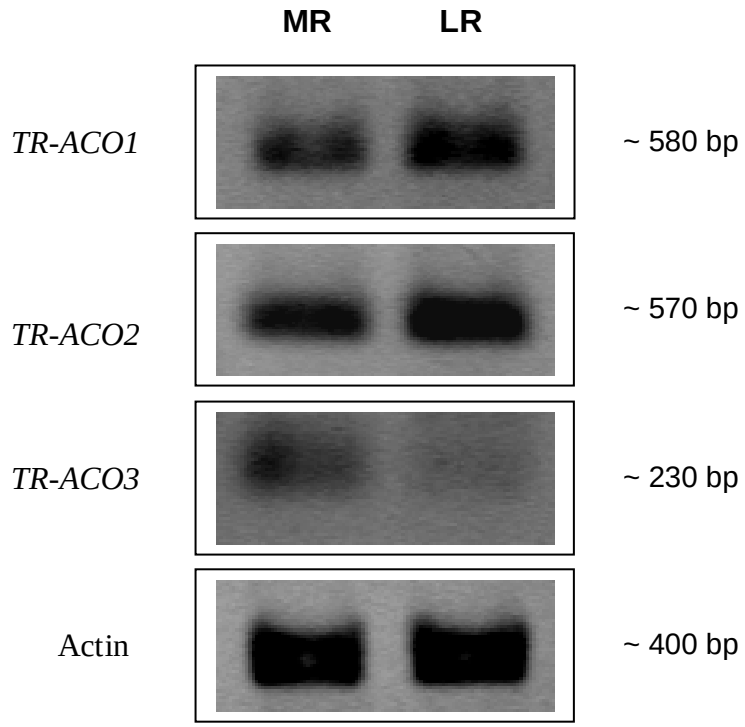

Figure 4.7 Analysis of the expression of the *TR-ACO* genes, as indicated, in the roots of the *TR2-1* transgenic white clover line using sqRT-PCR and ethidium bromide staining. Three micrograms of total RNA was used for reverse transcription and 1 μL of cDNA was used for each PCR reaction. Amplified fragments were electrophoresed through 1.5% (w/v) agarose gel in 1x TAE for 2 h at 50 V . MR = main roots; LR = lateral roots. The figure shown is representative of two technical replicates performed on each of two biological replicates.

4.3 Changes in selected physiological responses as affected by phosphate supply

4.3.1 Leaf phosphate content in transgenic (TR2-1) white clover in response to phosphate supply

The leaf Pi content of the TR2-1 transgenic white clover line was analysed in the same way as that for wild type plants (Section 2.5.1), where the first fully expanded leaf from each of four replicates was collected at 1 d, 4 d, 7 d, 14 d and 21 d after Pi depletion. Over the time course, the leaf Pi content of plants supplied with sufficient Pi ranged from 0.0424% to 0.0506% per gram fresh weight, whereas for the Pi depleted plants, the leaf Pi content was significantly reduced from 0.0496% to 0.025% Pi per gram fresh weight (Figure 4.8). By day 1, the leaf Pi content of the Pi sufficient plants averaged 0.048% $Pi.g^{-1}$ fresh weight (FW) whereas the Pi depleted plants was 0.046% $Pi.g^{-1}$ FW, and the slight difference between treatments was insignificant. After 4 d, the mean leaf Pi content of the Pi sufficient and Pi depleted plants were 0.0506% $Pi.g^{-1}$ FW and 0.0496% $Pi.g^{-1}$ FW, respectively. Again the difference was insignificant at the $P = 0.05$ level. By day seven, a significant decrease in the Pi content of the Pi-depleted plants was noted.

By day 14, the mean leaf Pi content were 0.0441% $Pi.g^{-1}$ FW and 0.0311% $Pi.g^{-1}$ FW for Pi sufficient and Pi depleted plants, respectively. Again the difference of 0.013% $Pi.g^{-1}$ FW was significant. The leaf Pi continuously declined significantly in the Pi depleted plants such that by day 21, the Pi content was reduced to 0.025% $Pi.g^{-1}$ FW whereas for the Pi sufficient plants, although there was a very slight decline, the Pi content was still within the 0.04% $Pi.g^{-1}$ FW level.

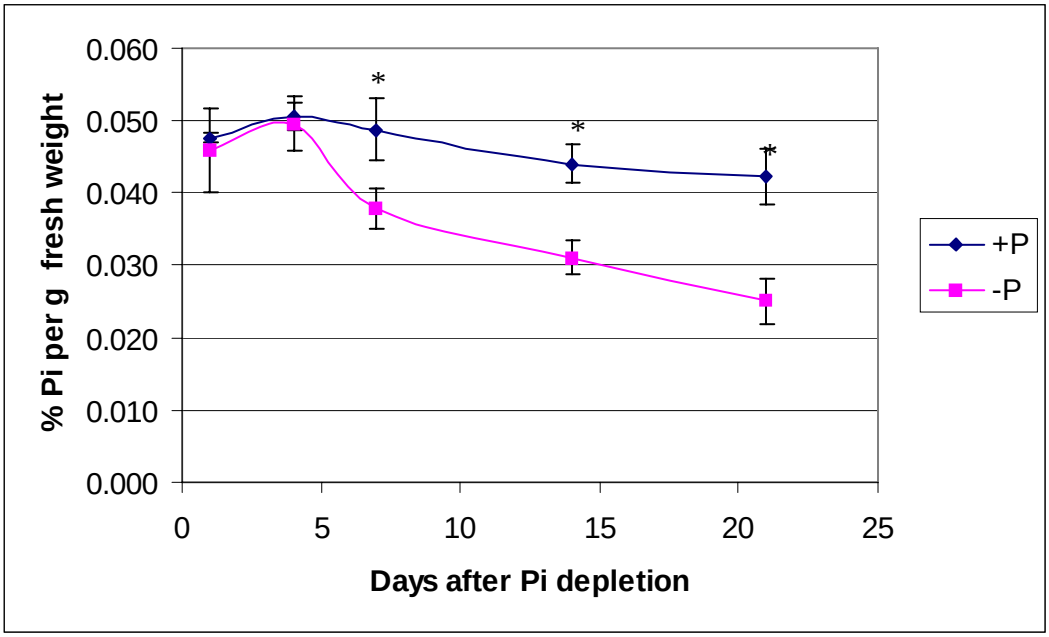

Figure 4.8 Leaf phosphate content in transgenic white clover (TR2-1) as influenced by changes in phosphate supply. Leaf Pi from *ca.* 30 mg tissue of the first fully expanded leaf was extracted using 1.0 mL of 0.1 M Tris-HCl, pH 7.5. For each assay, 10 µL of the supernatant Pi extract was used and the Pi content was calculated against a Pi standard curve using potassium di-hydrogen orthophosphate. Values are means ± SE, n = 3; ***** - indicates significant difference between treatments at the P = 0.05. The figure shown is representative of two biological replicates.

4.3.2 Root acid phosphatase activity in response to phosphate supply

The activity of acid phosphatase (APase) in the roots in response to changes in the availability of Pi was examined in conjunction with the analysis of leaf Pi content. Samples were collected over a time course from the same experimental plants as those used for the Pi assay. Both water soluble and ionically-bound cell wall proteins were analysed (Section 2.5.2) for APase activity.

For the water soluble protein, the APase activity for +P and –P one day after Pi depletion averaged 20.6 μmoles/min/g root FW. Four days after Pi depletion, the mean APase activity was 18.1 and 17.6 μmoles/min/g root FW for +P and –P roots, respectively. For both day 1 and day 4 measurements, differences between treatments were insignificant at the P = 0.05 level. By day 7, the mean APase activity for +P was 20.6 μmoles/min/g root FW whereas for –P, the mean increased to 29.4 μmoles/min/g root FW, a significant difference. By day 14, the difference between treatments became greater. The APase activity in +P roots was 23.5 μmoles/min/g root FW whereas the measurements for the –P roots was 52.7 μmoles/min/g root FW. By day 21, the APase activity of both the–P and +P roots roots had stabilised (Figure 4.9A). From day 7 to day 21, the differences between the two treatments were significant at the P=0.05 level.

When the ionically bound cell wall protein was assayed for APase activity, relatively lower values for both the +P and –P were obtained when compared to the values for the soluble extracts throughout the time course. However, changes in activity in response to Pi supply followed the same trend (Figure 4.9B). By day 1, APase activity in +P extracts was measured at 11.2 μmoles.min.g^{-1} FW, with the activity in –P extracts at

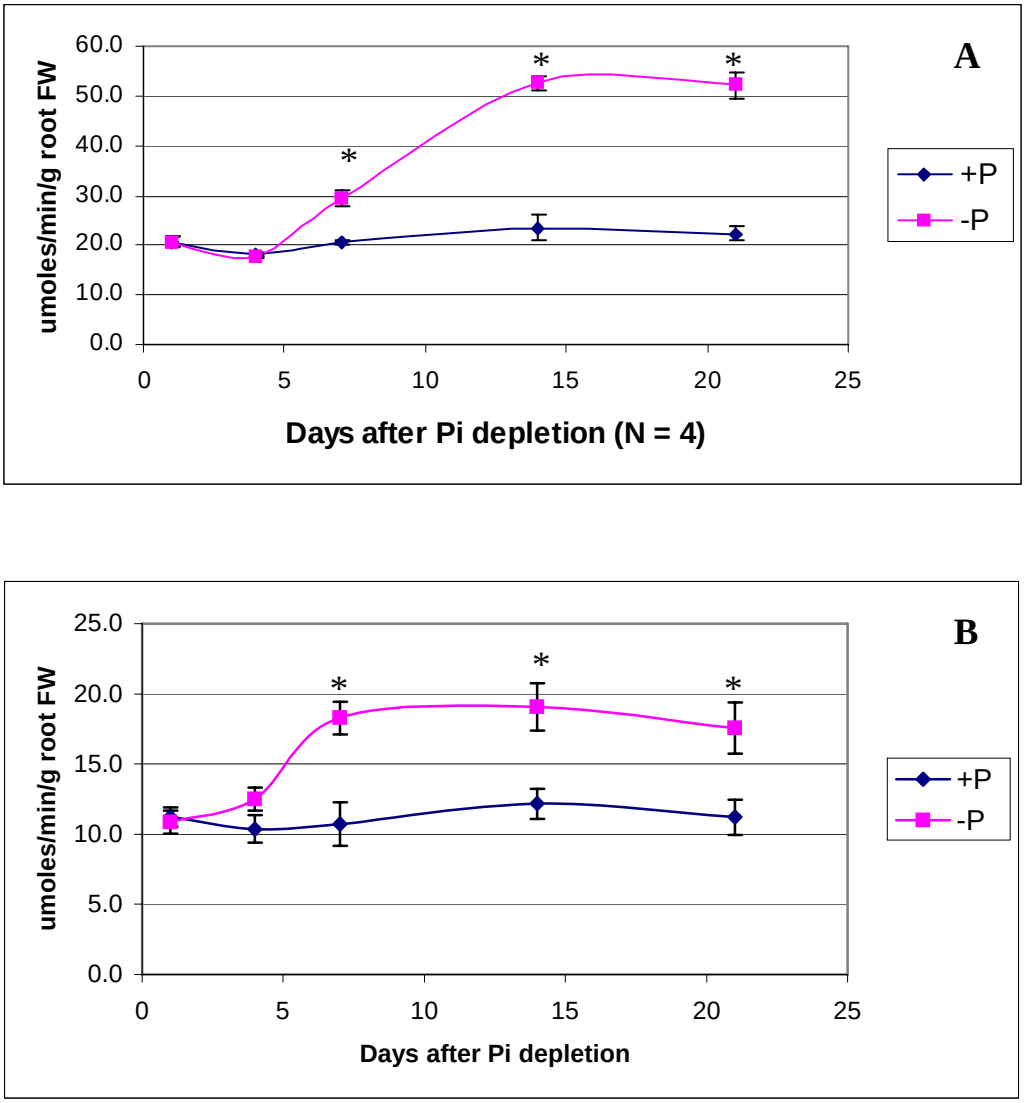

Figure 4.9 Acid phosphatase activity detected in water soluble (A) and ionically bound (high salt extractable) (B) cell wall protein extracts from the roots of the transgenic (TR2-1) line of white clover grown in either Pi sufficient (1.0 mM) or Pi depleted (10 μM) Hoagland's solution for the number of days indicated. Values are means ± SE, n = 4. *****=indicates significant difference between treatments at the P=0.05 level. The figure shown is representative of two biological replicates.

11 μmoles.min.g^{-1} FW. By day 4, the activity in +P extracts was 10.4 μmoles.min.g^{-1} FW whereas that measured in the –P extract was12.49 μmoles.min.g^{-1}FW. Although the activity measured in the –P extracts was higher at 2.09 μmoles.min.g^{-1} FW, this difference was insignificant at the P=0.05 level.

By day 7, a greater difference was noted: an activity of 10.7 μmoles.min.g^{-1} FW was measured in the +P extracts while the –P extracts had 18.27 μmoles.min.g^{-1}FW. The difference of 7.57 μmoles.min.g^{-1}FW in the APase activity was significant. While the APase activity measured in +P extracts remained at a steady level, the activity in –P extracts continued to increase. By day 14, the activity in the +P extracts was 12.2 μmoles.min.g^{-1}FW while the activity in the –P extracts was 19.05 μmoles.min.g^{-1}FW On the last day of the time course (21 days after Pi depletion), the activity in the +P extract was 11.2 μmoles.min.g^{-1}FW while the activity in the –P was 16.57 μmoles.min.g^{-1}FW (Figure 4.9B). The mean differences of 6.85 μmoles.min.g^{-1}FW and 5.37 μmoles.min.g^{-1}FW between treatments on day 14 and day 21, respectively, were both significant at the p= 0.05 level.

4.4 Changes in the accumulation of the TR-ACO proteins in response to phosphate supply

With the aim of obtaining a comprehensive analysis of the temporal accumulation of TR-ACO1 and TR-ACO2 proteins in the roots of transgenic white clover in response to changes in the Pi availability, three separate experiments of varying time-duration were conducted. The first experiment was a time course analysis of TR-ACO1 and TR-ACO2 protein accumulation from root samples collected at 6 d, 9 d, 15 d and 21 d after Pi depletion.

In the second experiment, samples for analysis were collected at 1 d, 4 d and 7 d after Pi depletion; while the last trial was an analysis over a short time period of 12 h. To confirm the results obtained, each experiment was conducted twice, and the western blots for each experiment repeated at least twice. For each time point four sample plants were collected, and the roots pooled for the extraction of total protein.

4.4.1 Changes in the accumulation of the TR-ACO1 protein in roots in response to phosphate supply

Results of analysis of TR-ACO1 protein accumulation over a 21-day time course is shown as Figure 4.10. Root samples were first collected 6 d after Pi depletion, and for Pi sufficient roots, the main and lateral roots were pooled as there was not enough lateral roots for analysis. By day 9 after Pi depletion, a slight difference in the accumulation of TR-ACO1 protein between treatments was observed. Comparing the protein extracts from main roots alone, a slightly greater intensity of band was noticeable in Pi depleted extracts when compared to the Pi sufficient extract, indicating a slightly greater recognition of protein by the α-TR-ACO1 antibody. When lateral roots from both treatments were compared, a greater accumulation of TR-ACO1 protein was again detected from extracts of Pi depleted roots when compared with the extracts from Pi sufficient roots. Further, a more noticeable difference in band intensity was distinguished between the main root and the lateral roots with greater TR-ACO1 protein accumulation in the lateral roots (Figure 4.10A). When the blots were quantified using the Gel Doc system, the relative signal intensity (RSI) for the main roots on day 9 were 85 arbitrary units (Au) and 95 Au for Pi sufficient and Pi deficient roots, respectively. For the lateral roots, the RSI values were 100 Au and 105 Au for Pi sufficient and Pi deficient roots, respectively (Figure 4.10C), suggesting a slightly greater accumulation of TR-ACO1 in the lateral roots.

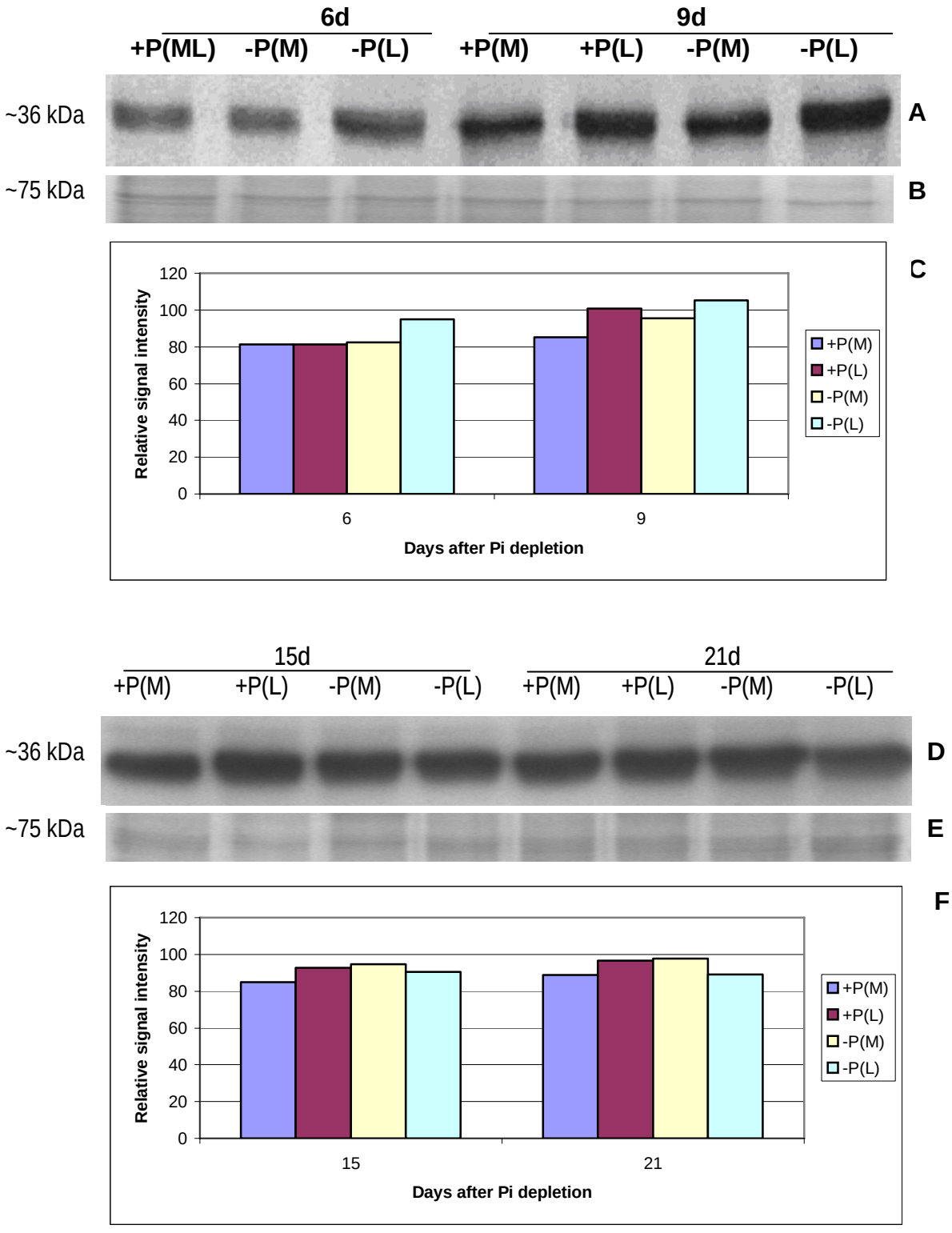

Figure 4.10 Western analyses to detect TR-ACO1 protein accumulation in the roots of transgenic white clover line TR2-1 (transformed with *TR-ACO1p::mGFP5-ER)* collected at the number of days indicated after Pi deprivation. Aliquots (10 ug) of protein extract from roots collected at each observation point after P treatment were separated using SDS-PAGE, electroblotted onto PVDF membrane and challenged with the α-TR-ACO1 antibody (A,D). Coomassie Brilliant Blue staining are shown (B,E) as loading control. Relative quantification of blots are presented in the histograms (C,F).

Western analysis of protein extracts collected at 15 d and 21 d also showed slightly greater accumulation of TR-ACO1 protein in Pi depleted main roots compared to the Pi sufficient main roots. This slight increase was not noted in the Pi depleted lateral roots (Figure 4.10F).

In the second experiment, which was conducted over the shorter time-course of seven days, the difference in the accumulation of the TR-ACO1 protein between treatments was more apparent. When the protein extract was challenged with an antibody raised against the TR-ACO1 protein there was greater protein recognition in the Pi depleted samples starting on day 1 and the trend was consistent up to day 7 (Figure 4.11A). The RSI during the first day was 66 Au for +P roots, and 98 Au for –P roots. By day 7, +P roots had a RSI of 62 Au while the –P roots had 96 Au, or adifference in protein accumulation in Pi depleted roots of 34 Au. When the protein was challenged with a commercially available α-GFP antibody, recognition of protein was also greater in the –P extracts from day 1 to day 7 (Figure 11 D,E), suggesting greater TR-ACO1 and GFP protein accumulation in the –P extracts.

With the observation that even after one day, accumulation of TR-ACO1 protein was greater in the Pi depleted samples (Figure 4.11A), a shorter time-course experiment was conducted and root samples were collected at 1 h, 6 h and 12 h after Pi depletion. Results of western analysis revealed that accumulation of TR-ACO1 protein was greater in Pi depleted extracts when compared with those under Pi sufficiency within 6 h after Pi depletion. The same observation was also noted at 12 h (Figure 4.12), suggesting a relatively rapid increase of TR-ACO1 protein in response to Pi stress.

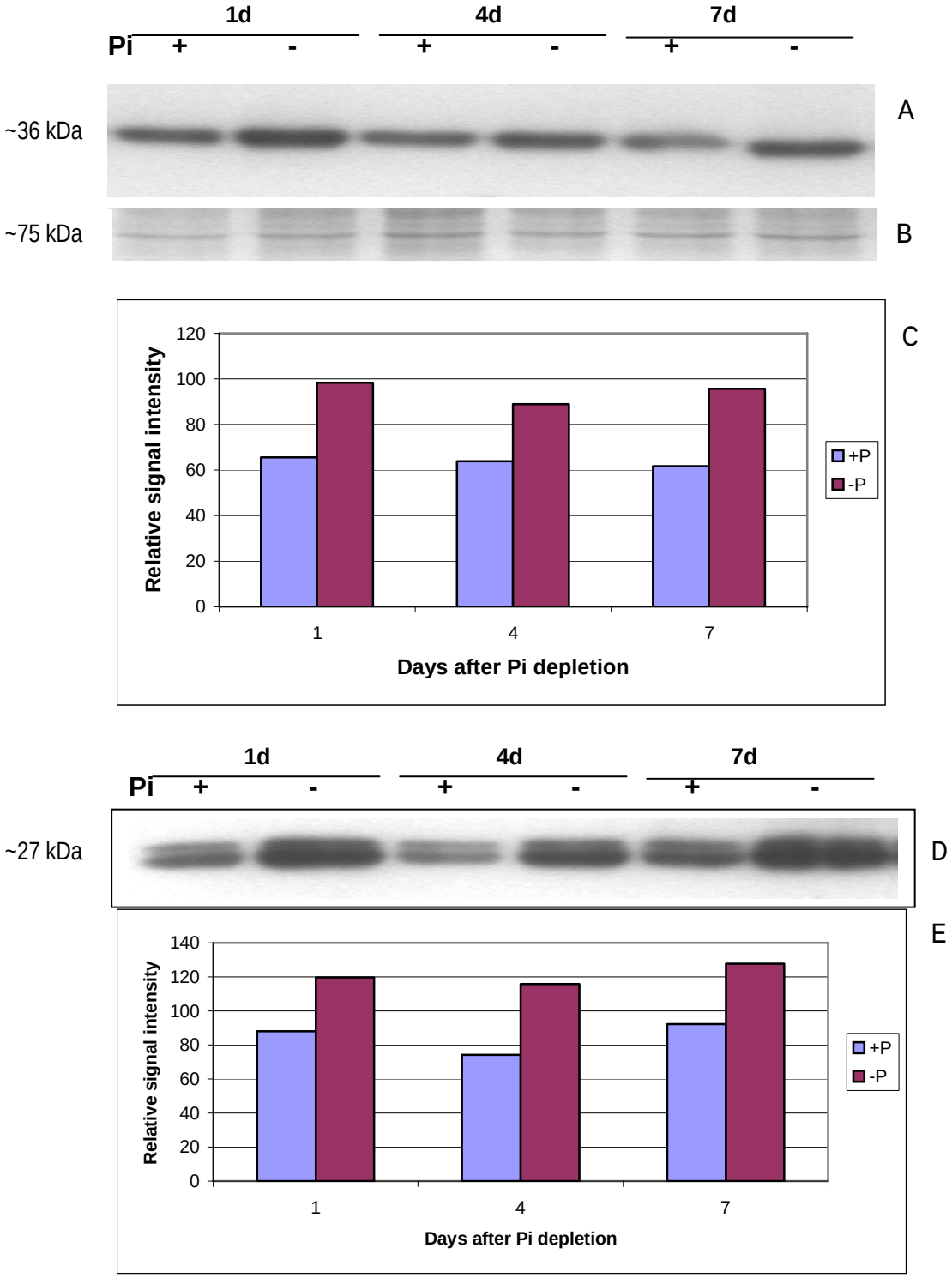

Figure 4.11 Western analyses to detect TR-ACO1 protein accumulation in the roots of transgenic white clover line TR2-1 (transformed with *TR-ACO1p::mGFP5-ER)* collected at the number of days indicated after Pi deprivation. Aliquots (10 μg) of protein extract from roots collected at each observation point after P treatment were separated using SDS-PAGE, electroblotted onto PVDF membrane and challenged with the α-TR-ACO1 (A) and α GFP (D) antibodies. Coomassie Brilliant Blue staining is shown (B) as a loading control. Relative quantification of blots are presented in the histograms (C,E).

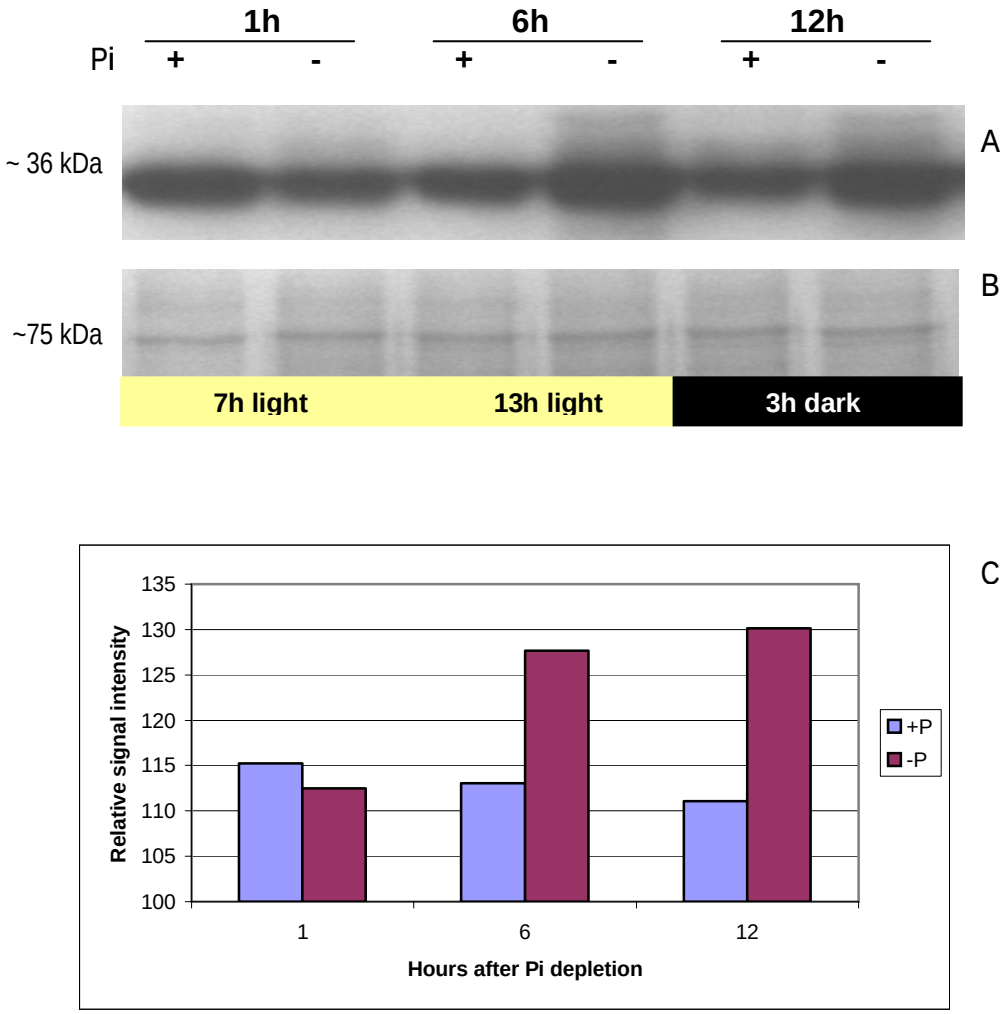

Figure 4.12 Western analyses to detect TR-ACO1 protein accumulation in the roots of transgenic white clover line TR2-1 (transformed with *TR-ACO1p: :mGFP5-ER)* collected at the number of hours indicated after Pi depletion. Aliquots (10 μg) of protein extract from roots collected at each observation point after P treatment were separated using SDS-PAGE, electroblotted onto PVDF membrane and challenged with the α-TR-ACO1 antibody (A). Coomassie Brilliant Blue staining is shown (B) as a loading control. Relative quantification of blot is presented in the histogram (C).

4.4.2 Changes in the accumulation of TR-ACO2 protein in the roots in response to phosphate supply

Results of western analysis using TR-ACO2 over a time course of 21 days revealed that by day 6 after Pi depletion, there was no significant difference in the amount of protein accumulation when extracts collected from Pi sufficient and Pi depleted roots were compared (Figure 4.13A). There was a relatively low amount of protein recognised by the α-TR-ACO2 antibody in the Pi depleted main root [-P(M)] when compared to extracts from Pi sufficient roots (+P) on day 6. However, it is difficult to compare since in the Pi sufficient extracts, the main and the lateral roots were not separated. The recognition of TR-ACO2 in Pi depleted lateral root, however, on the same day was almost the same as with the extracts from Pi sufficient roots. By day 9, there was some evidence of difference in the accumulation of TR-ACO2 protein when the extracts from Pi sufficient and Pi deficient roots were compared. A higher level of protein recognition was observed in the –P main roots when compared with the +P main roots. However, from the lateral root, this difference was reversed. This may indicate that the accumulation of TR-ACO2 protein in the roots of transgenic (TR2-1) white clover was not consistently affected by changes in the availability of phosphate during the first week after Pi depletion.

The first noticeable change was evident from extracts of root samples collected at 15 d after Pi depletion. During this time, accumulation of protein was greater in the Pi depleted samples. When the extracts from Pi sufficient and Pi deficient main roots were compared, there was greater TR-ACO2 protein accumulation in the Pi depleted extracts. Also, when the extracts from Pi sufficient and Pi depleted lateral roots were compared, there was also greater accumulation of TR-ACO2 protein in Pi depleted lateral root extracts (79 Au for -P, and 50 Au for +P) (Figure 4.15D). The same trend occurred on

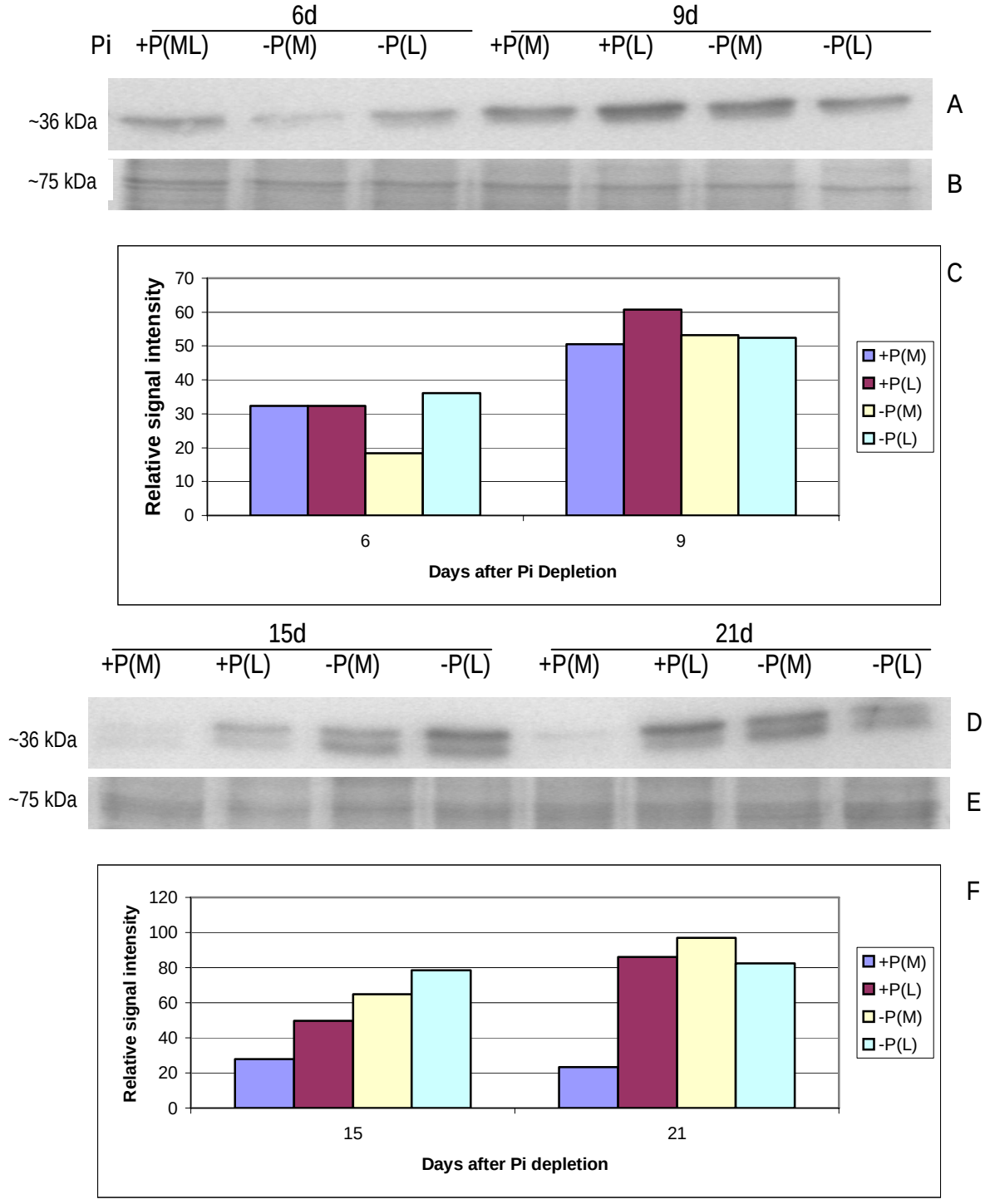

Figure 4.13 Western analyses to detect TR-ACO2 protein accumulation in the roots of transgenic white clover line TR2-1 (transformed with *TR-ACO1p::mGFP5-ER)* collected at the number of days indicated after Pi depletion.
Aliquots (10 μg) of protein extract from roots collected at each observation point after P treatment were separated using SDS-PAGE, electroblotted onto PVDF membrane and challenged with α-TR-ACO2 antibody (A,D). Coomassie brilliant blue staining (B,E) are shown as loading control. Relative quantification of the signal intensity are presented in the histograms(C,F).

the 21st day, with greater protein accumulation in the Pi main depleted roots and not in the lateral roots. It was also interesting to note that by 15 d (and also observed at 21 d), the protein recognised by the α-TR-ACO2 antibody now appears as a clear doublet.

In the experiment over 7 d, where root samples were collected at 1 d, 4 d and 7 d after Pi depletion, there was no marked difference in the protein accumulation between treatments (Figure 4.14A). From day 1 to day 7, the extent of protein recognition by the α-TR-ACO2 antibody was relatively similar. Inspection of the band intensity (Figure 4.14 A) and comparison of the signal intensity in terms of Au units did not support a significant difference. When the protein extracted from samples collected from a 12 h experiment was also challenged with α-TR-ACO2 antibody, results revealed that recognition of protein was of a similar extent (Figure 4.14D), indicating no consistent difference in protein accumulation between treatments. This result indicates that TR-ACO2 did not respond rapidly to phosphate stress.

4.5 Changes in *TR-ACO* gene expression in response to changes in phosphate supply

Expression of members of the *TR-ACO* gene family in the TR2-1 white clover transgenic line in response to Pi supply was examined using the samples collected over a time-course of 1 h to 24 h. The first analysis was conducted using ethidium bromide stained product generated by the semi-quantitative Reverse Transcription - Polymerase Chain Reaction (sqRT-PCR). This experiment was conducted twice, with at least four sample plants per treatment for each time point. Roots of the sample plants per treatment, collected at each time point, were pooled into one sample for RNA extraction. The gels and the Southern blots were conducted at least twice to confirm the results obtained.

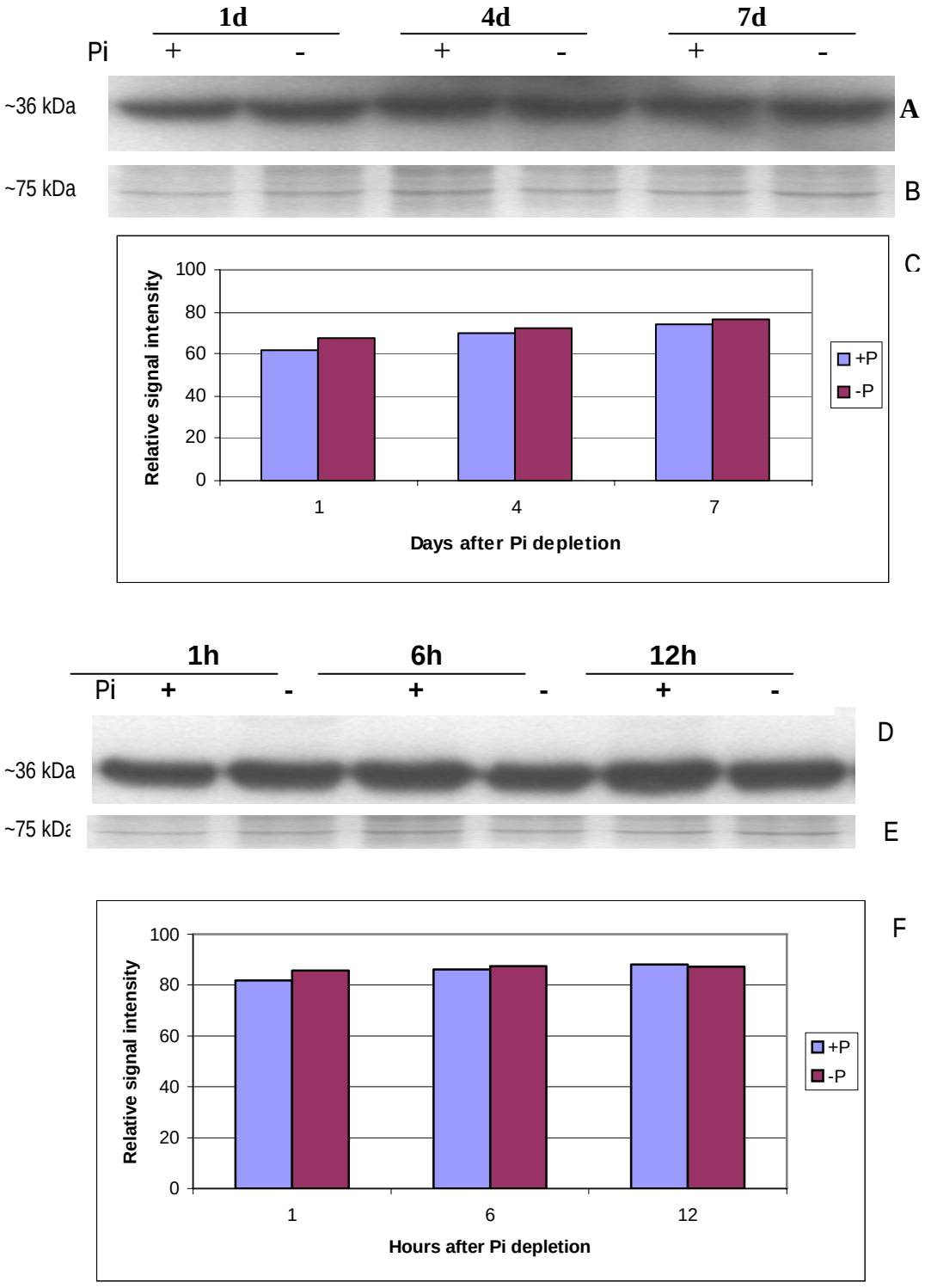

Figure 4.14 Western analyses to detect TR-ACO2 protein accumulation in the roots of transgenic white clover line TR2-1 (transformed with *TR-ACO1p::mGFP5-ER)* collected at the number of days/hours indicated after Pi depletion. Aliquots (10 μg) of protein extract from roots collected at each observation point after P treatment were separated using SDS-PAGE, electroblotted onto PVDF membrane and challenged with α-TR-ACO2 antibody (A,D). Coomassie Brilliant Blue staining is shown (B,E) as a loading control. Relative quantification of blots are shown in the histograms (C,F).

In the sqRT-PCR, gene specific primers were used which were designed from the junction between two exons with the aim of excluding PCR products amplified from genomic DNA contamination. Prior to the actual experiment, a linearity check was conducted to find out the appropriate number of PCR cycles for each gene which is within the slope. The amount of transcript abundance for each treatment during the time course was quantified relative to the abundance of the amplified actin fragment and the expression of a specific gene relative to actin is presented in histogram form.

A further investigation on the extent of gene expression was carried out by expression Southern analysis of the amplified fragment. The amount of hybridisation of the transcript to the [α-^{32}P]-dCTP labelled *TR-ACO* gene probe was examined by phosphorimaging and by autoradiography. By autoradiography, membranes were exposed to the x-ray film for 1 h to overnight depending on the extent of the signal.

By phosphorimaging, the radioactivity corresponding to the amount of transcript that hybridised to the labelled probe was detected by placing the membrane in contact with the phosphorimaging plate from 15 min to 1 h depending upon the intensity of the signal. Following this contact, the IP was laser scanned into the phosphorimager, thus producing bands with intensities that corresponded to the amount of transcript that hybridised to the labelled probe. These images were then quantified using the Image Gauge Version 4.0 quantification tool. Corresponding values were expressed in photo stimulated luminescence per mm^2 (PSL/mm^2).

4.5.1 Expression of the *TR-ACO1* gene in response to changes in phosphate supply

For *TR-ACO1,* there was a greater transcript abundance in extracts from roots under Pi deficiency when compared to those collected from Pi sufficient roots (Figure 4.15).

Starting from 1 h after Pi depletion there was a consistent greater transcript abundance of *TR-ACO1* gene in Pi depleted samples and this trend continued up to 24 h after Pi limitation.

Using autoradiography, results also showed a greater accumulation of *TR-ACO1* transcript that bound to the labelled probe in the Pi depleted samples when compared to those under Pi sufficiency starting from one hour after Pi depletion (Figure 4.16A). This trend continued up to 24 h after Pi depletion.

The quantified transcript that hybridised to the *TR-ACO1* gene labelled probe is shown in Figure 4.16B. An increase in the amount of transcript that hybridised to the labelled probe occurred in Pi depleted samples starting at 1 h after Pi depletion. As indicated, there was a 5-fold increase in transcript abundance at 1 h in the Pi depleted roots when compared to those under Pi sufficiency. There was a slight decrease in values both of Pi sufficient and Pi deficient samples at 6 h but transcript accumulation in the Pi depleted samples was still higher. After 12 h of Pi depletion, the hybridisation of transcript to the labelled probe was even greater. The greatest transcript hybridisation to labelled probe was noted at 18 h after Pi depletion (Figure 4.16B) with 158 $PSL.mm^{-2}$ in Pi depleted samples compared with only 22 $PSL.mm^{-2}$ for Pi sufficient roots, indicating an over 7-fold increase in transcript abundance in response to Pi limitation.

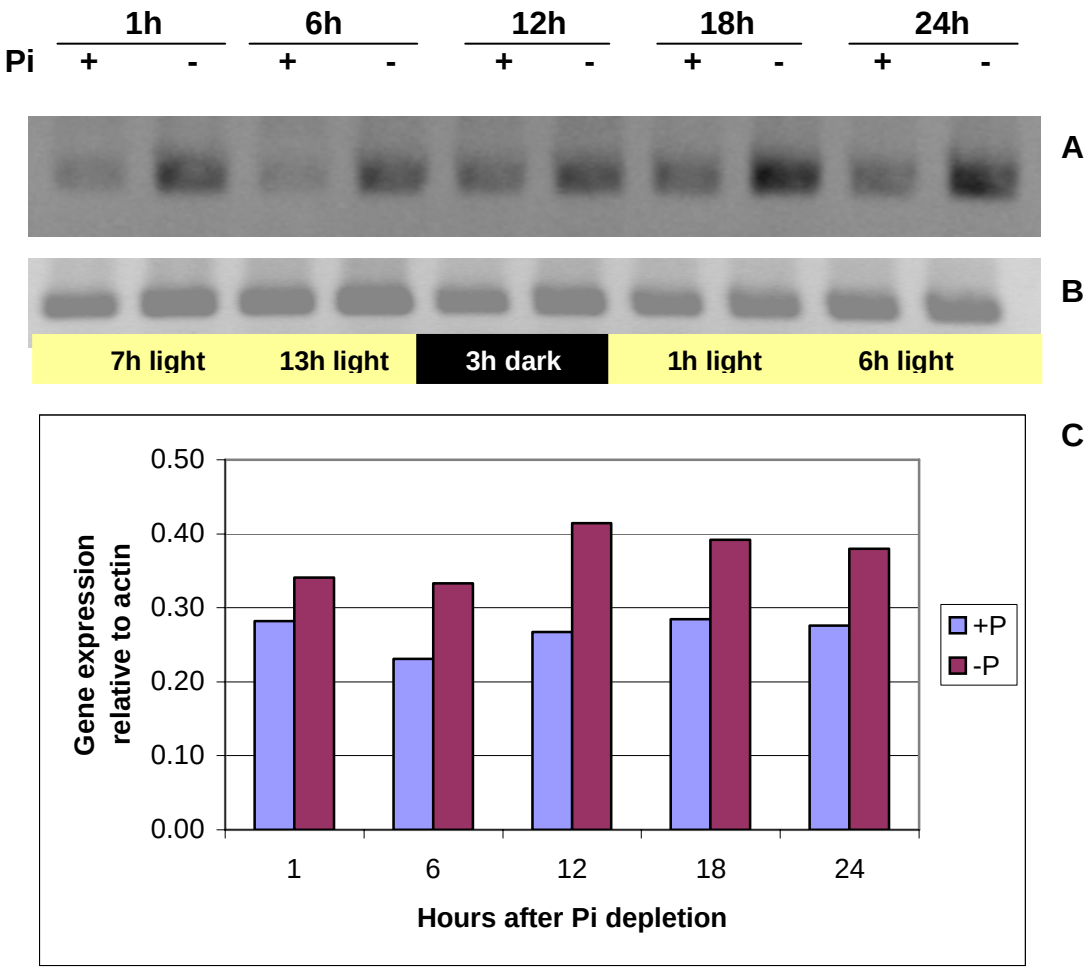

Figure 4.15 Expression of the *TR-ACO1* gene in the roots of TR2-1 white clover transgenic line collected at the number of hours indicated after Pi depletion. Primers used were specific for *TR-ACO1* gene (A), and Actin (B). Three micrograms of RNA was used for reverse transcription and 1 μL of cDNA was used for each PCR reaction. Annealing temperature was set at 60^{o}C for 45 s and amplification was carried out over 35 cycles. Amplified fragment was electrophoresed at 1.5% (w/v) agarose gel in 1x TAE for 2 h at 60V. The gel was then stained with ethidium bromide. The quantification of gene expression relative to actin is shown in histogram (C).

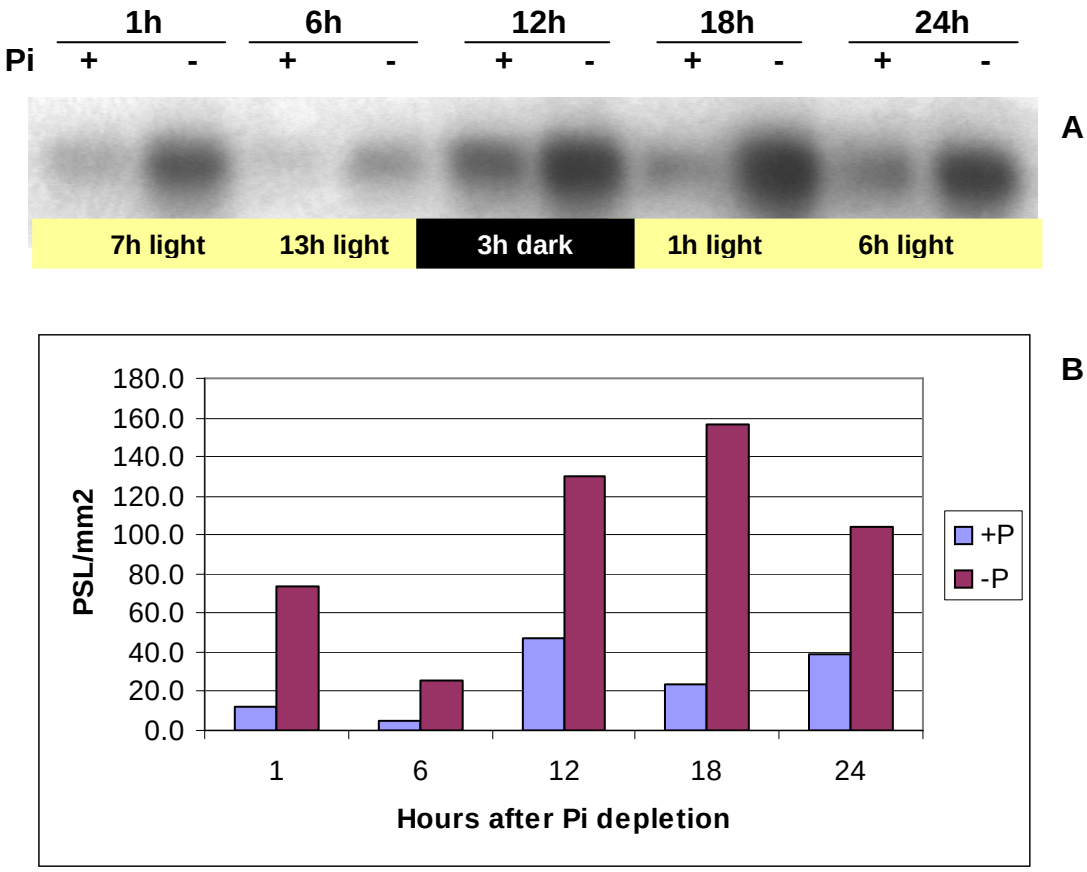

Figure 4.16 Southern hybridisation (A) and phosphorimage quantification (B) to analyse expression of *TR-ACO1* gene in the roots of TR2-1 white clover collected at the number of hours indicated after Pi depletion. Transcripts of *TR-ACO1* gene were amplified by 25 cycles of PCR, blotted onto positively charged nylon membrane by downward alkaline capillary transfer for 3 h, and hybridised with [α-^{32}P]-dCTP labelled *TR-ACO1* gene probe. High astringency washing (0.1x SSPE, 0.1% (w/v) SDS at 65^{o}C) was carried out to remove non-specific binding of nucleotides. Phosphorimage was quantitated using the FUJIFILM FLA-5000 Image Gauge version 4.0.
PSL – Photo stimulated luminescence

4.5.2 Expression of *TR-ACO2* gene in transgenic (TR2-1) white clover in response to changes in phosphate supply

Over the 24 h duration of the experiment, the transcript abundance of the T*R-ACO2* gene was not consistently affected by Pi depletion (Figure 4.17). Apart from Pi depleted samples at 6 h, accumulation of transcripts throughout the time course was comparable for both Pi depleted and Pi sufficient roots. This result was confirmed in Figure 4.18A when the amplified fragments were hybridised with the [α-^{32}P]-dCTP labelled *TR-ACO2* gene probe where the amount of transcript that hybridised to the probe was almost similar in both treatments at 1, 12, 18 and 24 h.

The result of phosphorimage quantification showed that generally, the radioactivity level expressed in PSL.mm^{-2} values was almost the same throughout the time course. This excluded the observation at 6 h where the relative value was very low at 6 h after Pi depletion. This general observation suggests that there was no significant difference in the transcript abundance between Pi depleted and Pi sufficient roots and further indicates that the expression of the *TR-ACO2* gene within a short duration of 24 h was not significantly influenced by Pi availability.

4.5.3 Expression of *TR-ACO3* gene in transgenic (TR2-1) white clover in response to changes in phosphate supply

Expression of the *TR-ACO3* gene in transgenic white clover was relatively weak when compared to expression of the *TR-ACO2* and *TR-ACO1* genes (Figure 4.19). Although the same amount of cDNA was used in the PCR reaction mixture, with the same number of cycles of PCR in the amplification as in *TR-ACO1* (35x) (and 5 cycles more than that of *TR-ACO2*), the bands of the amplified fragments appeared quite weak indicating that the gene may not be highly expressed in the roots.

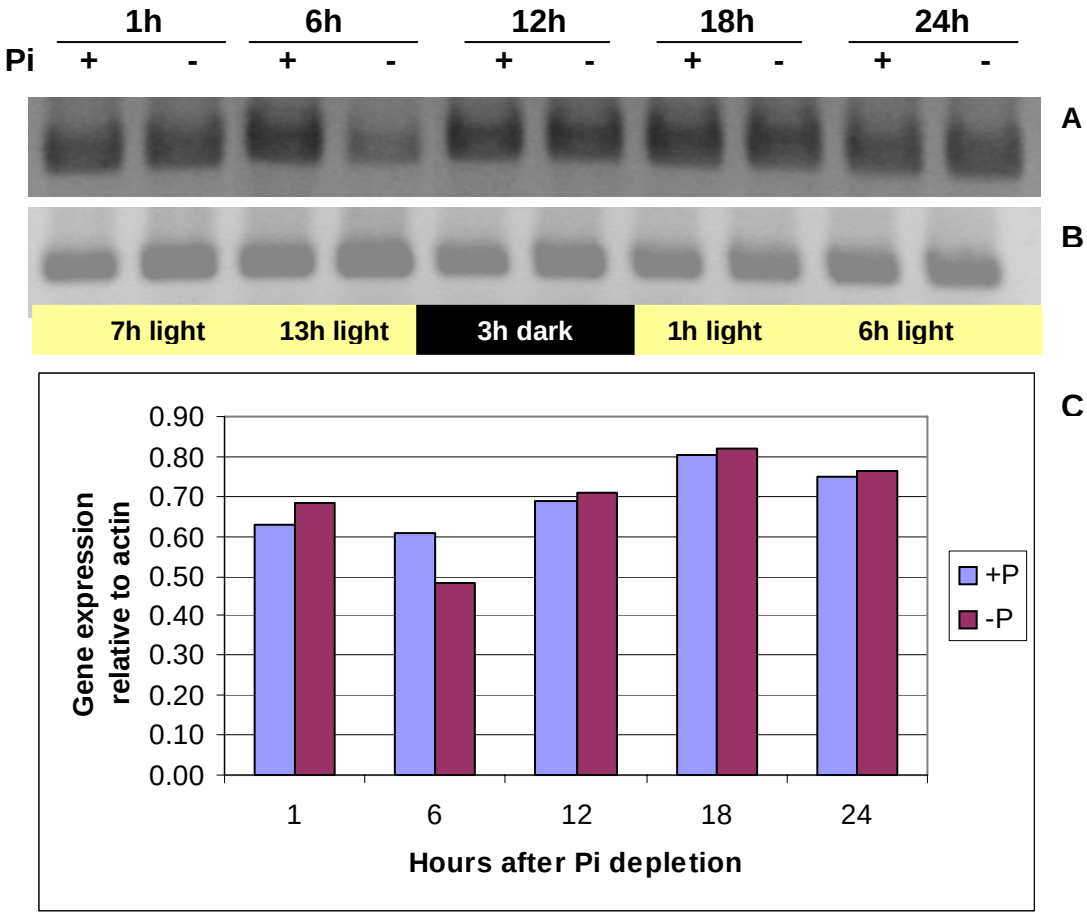

Figure 4.17 Expression of the *TR-ACO2* gene in the roots of TR2-1 white clover transgenic line collected at the number of hours indicated after Pi depletion. Gene specific primers for TR-ACO2 (A), and Actin (B) were used. Three micrograms of RNA was used for reverse transcription and 1 µL of cDNA was used for each PCR reaction. Annealing temperature was set at 55^{o}C for 45 s and amplification was carried out over 30 cycles. Amplified fragment was electrophoresed at 1.5% agarose gel in 1x TAE for 2 h at 60V. The gel was then stained with ethidium bromide.

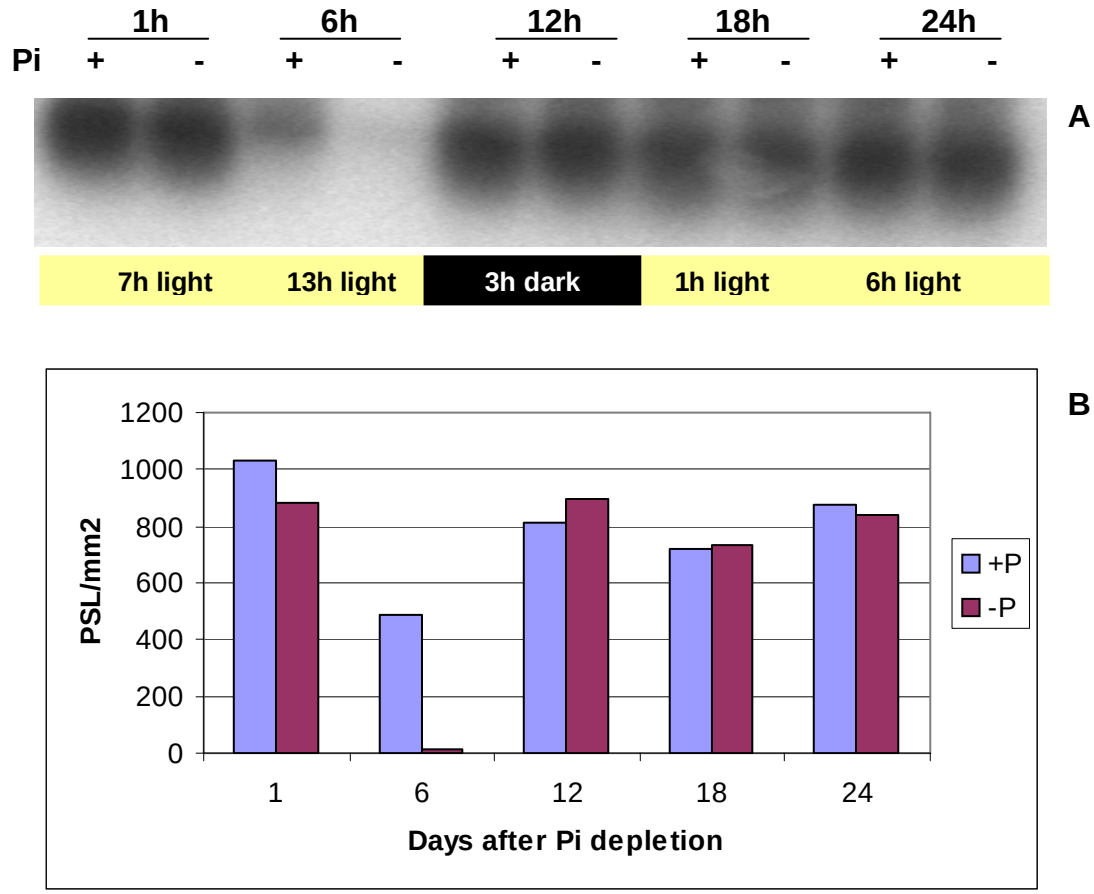

Figure 4.18 Southern hybridisation (A) and phosphorimage quantification (B) to analyse expression of the *TR-ACO2* gene in the roots of TR2-1 white clover transgenic line collected at the number of hours indicated after Pi depletion. Transcripts of *TR-ACO2* gene were amplified by 20 cycles of PCR, blotted onto positively charged nylon membrane by downward alkaline capillary transfer for 3 h, and hybridised with [α-^{32}P]-dCTP labelled *TR-ACO2* gene probe overnight. High astringency washing (0.1x SSPE, 0.1% (w/v) SDS at 65^{o}C) was carried to remove non-specific binding of nucleotides. Phosphorimage was quantified using the Image Gauge version 4.0. PSL – Photo stimulated luminescence

Further, if there was a response to changes in Pi supply, this was not consistent. There was a lower amount of transcript abundance in Pi depleted roots at 1 h, 12 h and 24 h after Pi depletion when compared to those under Pi sufficiency. However, at 6 h after Pi depletion, a greater accumulation of transcript was noted in Pi depleted roots.

Further, any response to changes in Pi supply can be hardly detected since the trend was quite erratic. There was a lower amount of transcript abundance in the Pi depleted roots at 1 h, 12 h and 24 h after Pi depletion when compared to those under Pi sufficiency. However, at 6 h, a greater accumulation of transcript was noted in Pi depleted roots.

Further analysis of gene expression was conducted by Southern hybridisation of amplified fragments using the [α-^{32}P]-dCTP labelled *TR-ACO3* gene probe. The results showed a general decrease in the hybridisation of the transcripts to the labelled probe in Pi depleted samples starting at 1 h after Pi depletion (Figure 4.20A). Apart from the samples collected at 6 h after Pi depletion, this decrease in transcript accumulation was observed in other time points.

Analysis of the quantified phosphorimage, as shown in Figure 4.20B, showed that at 1 h after Pi depletion there was a more than 60% decrease in *TR-ACO3* gene expression in Pi depleted samples when compared with the Pi sufficient roots. At 24 h after Pi depletion, the decrease in transcript abundance that hybridised to the labelled probe was more than 40%.

4.6 Anatomical comparison between roots of wild type and transgenic (TR2-1) white clover

Representative root samples of both wild type and transgenic (TR2-1) white clover were sectioned for anatomical studies (Section 2.3). Longitudinal sections were examined

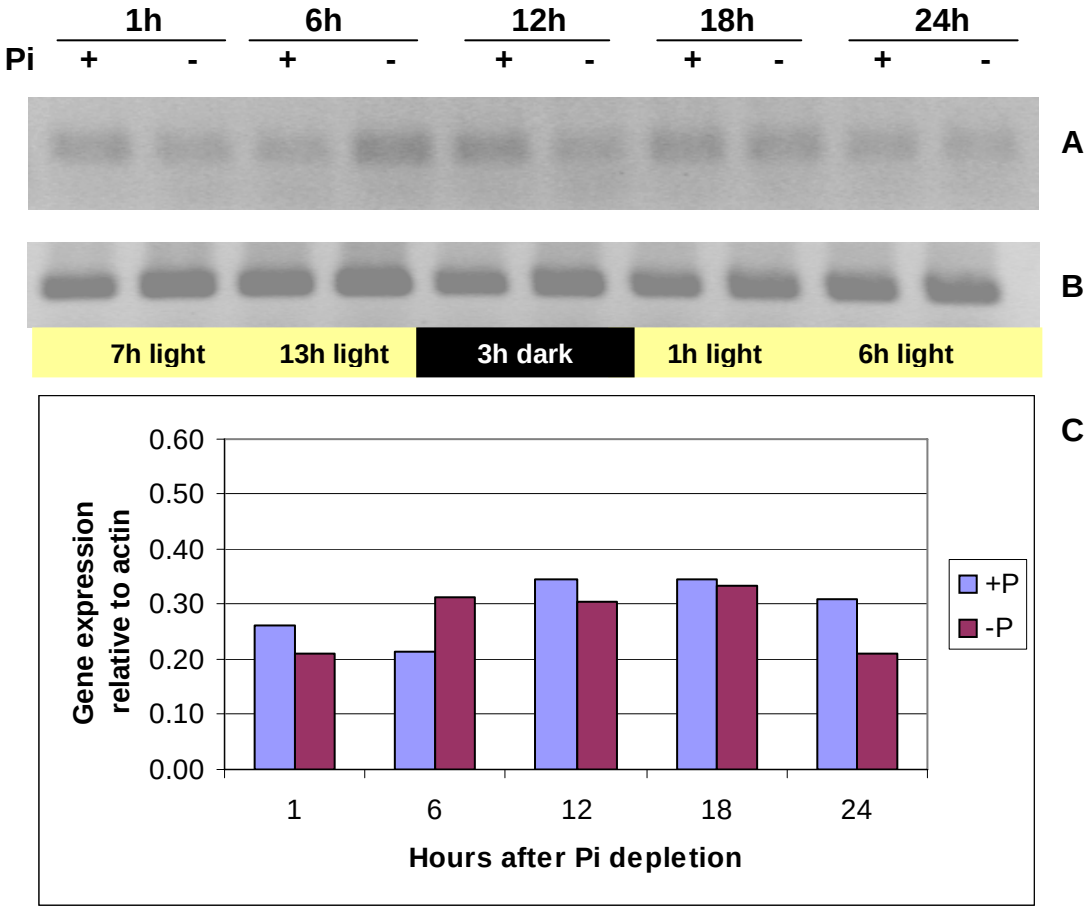

Figure 4.19 Expression of the *TR-ACO3* gene in the roots of TR2-1 white clover transgenic line collected at the number of hours indicated after Pi depletion. Primers used were specific for *TR-ACO3* gene (A), and Actin (B). Three micrograms of RNA was used for reverse transcription and 1 μL of cDNA was used for each PCR reaction. Annealing temperature was set at 62^{o}C for 45 s and amplification was carried out at 35 cycles. Amplified fragment was electrophoresed at 1.5% (w/v) agarose gel in 1x TAE for 2 h at 60V. The gel was then stained with ethidium bromide.

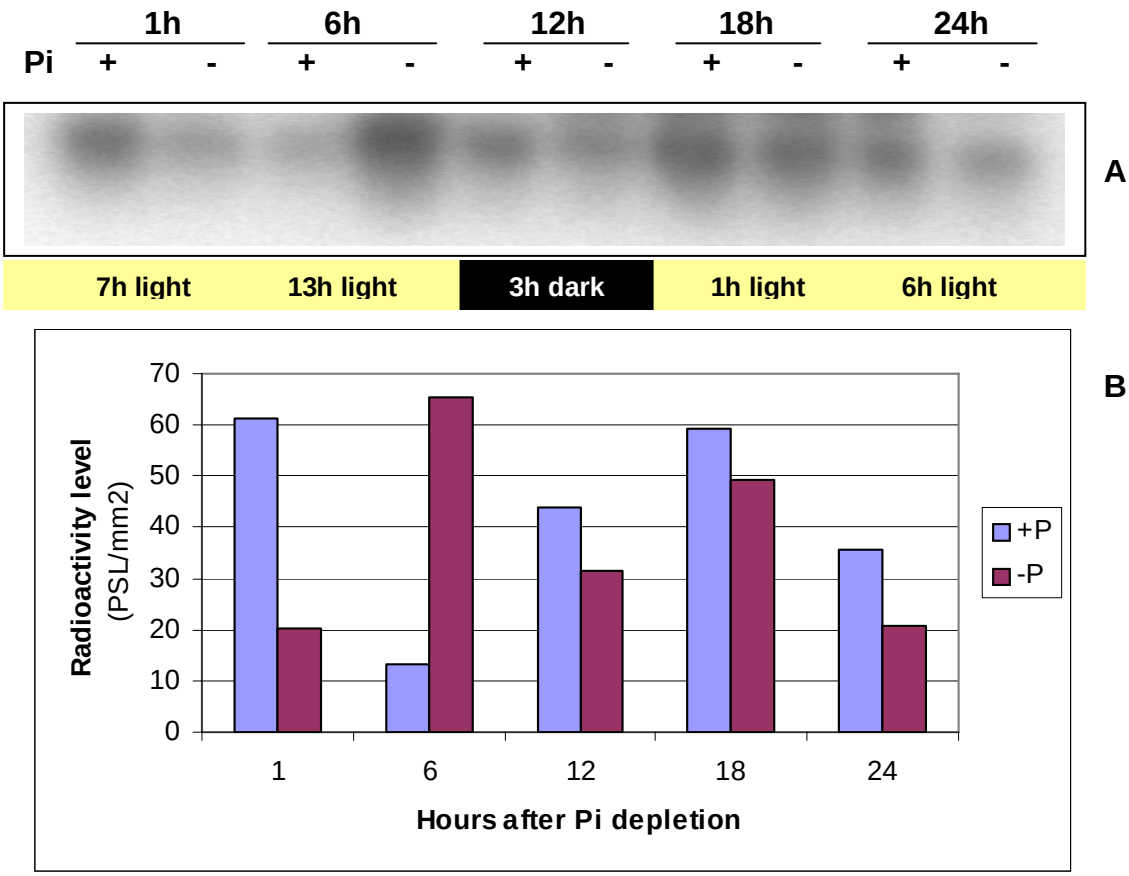

Figure 4.20 Southern hybridisation (A) and phosphorimage quantification (B) to analyse expression of the *TR-ACO3* gene in the roots of TR2-1 white clover transgenic line collected at the number of hours indicated after Pi depletion. Transcripts of *TR-ACO3* gene were amplified by 25 cycles of PCR, blotted onto positively charged nylon membrane by downward alkaline capillary transfer for 3 h, and hybridised with [α-^{32}P]-dCTP labelled *TR-ACO3* gene probe. High astringency washing (0.1x SSPE, 0.1% (w/v) SDS at 65^{o}C) was carried out. Phosphorimage was quantitated using the Image Gauge version 4.0. PSL = Photo stimulated luminescence.

using a light microscope to identify cell types and to compare cell arrangements between wild type and transgenic plants. A longitudinal section of the root of wild type white clover showing the root cap, the region of cell division, the region of elongation, and the region of maturation is shown as Figure 4.21.

Sections of the elongation zone (Figure 4.22A,B) and maturation zone (Figure 4.22 C,D) of the wild type and TR2-1 roots are presented. In these sections, no significant difference in the root anatomy between the wild type and TR2-1 was detected. In the region of the root elongation, all cells appeared intact from the epidermis and cortex to the inner cells in the pericycle and vascular tissue. Further, there were no intercellular spaces noted in all sections examined.

In the region of maturation, the area of root investigated included a lateral root primordium. Again, there was no significant difference noted between the wild type and the transgenic white clover. The lateral root primordia, which have arisen from the pericycle, have started to push through the cortical cells with the newly formed cells, and will exit through the epidermis. The transverse sections of the roots of wild type (Figure 4.23A) and TR2-1 (Figure 4.23B) white clover are also shown. The different cells such as the epidermis, cortex, endodermis, pericycle, phloem and xylem are indicated.

4.7 Tissue-specific localisation of *TR-ACO1* promoter-driven GFP accumulation in the roots of TR2-1 white clover using *TR-ACO1p::mGFP5 ER* gene construct

As noted in Chapter 3, using wild type and transgenic (*TR-ACOp::GUS*) white clover, members of the *TR-ACO* gene family were differentially expressed in the roots. The

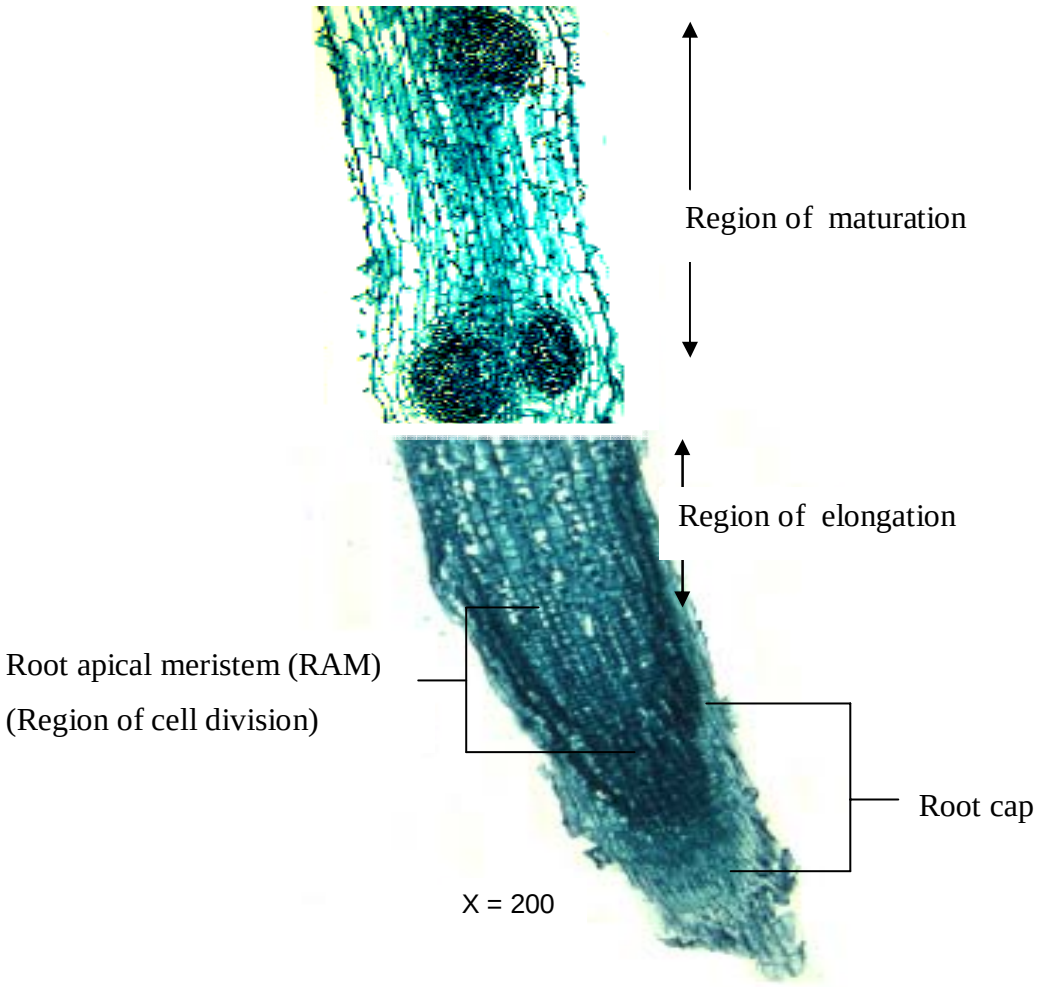

Figure 4.21 Longitudinal section of a wild type white clover root showing the different regions. Roots were sectioned at 12 μM thickness and were stained with 0.1% (w/v) safranin and 0.2% (w/v) fast green**.** For details of procedures see Section 2.2.

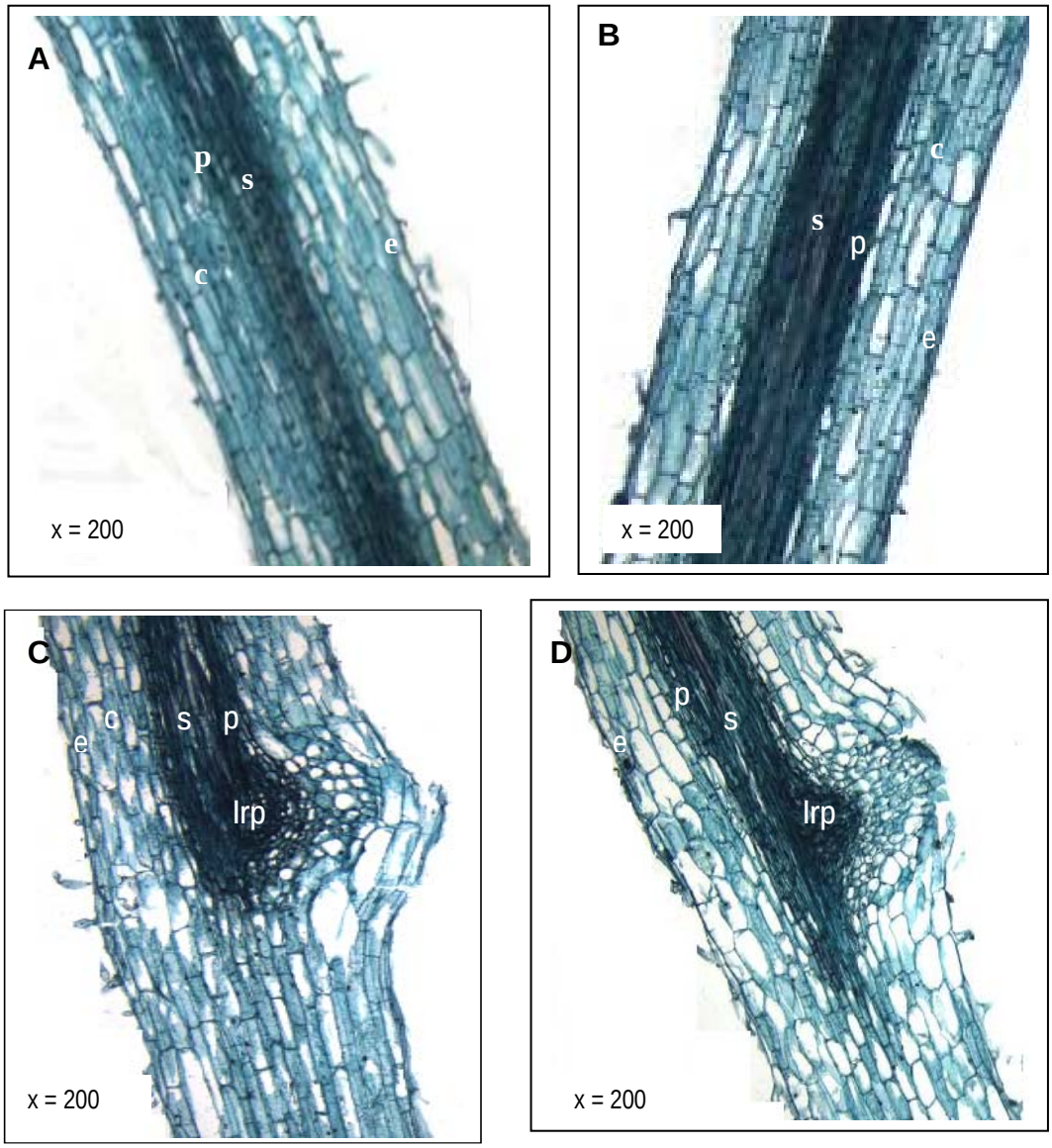

Figure 4.22 Longitudinal sections of the elongation zone (A,B) and maturation zone (C,D) of the roots of wild type (A,C) and transgenic line, TR2-1 (B,D) white clover. Roots were sectioned at 12 μm and were stained with safranin and fast green**.** For details of procedures see Section 2.3. The figure shown is representative of two biological replicates. The main roots of three sample plants per replicate were used for the light microscopy.

c = cortex, e = epidermis, p = pericycle, s = stele
lrp = lateral root primordium

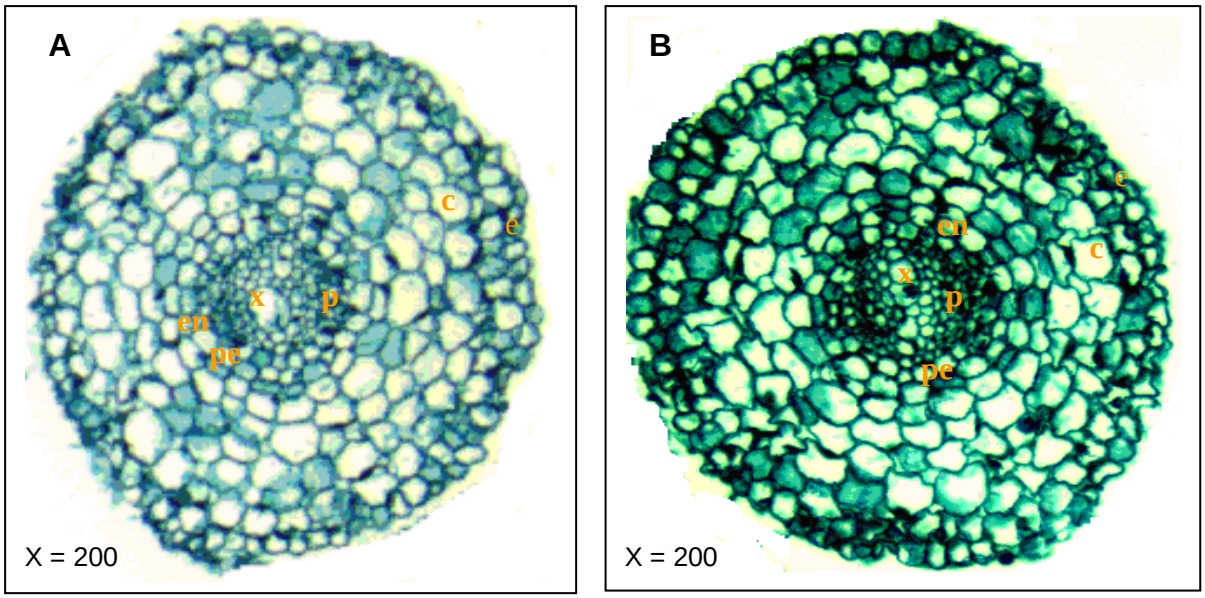

Figure 4.23 Transverse section of a wild type (A) and transgenic, TR2-1 (B) white clover root. Roots were sectioned at 12 μm thickness and were stained with safranin and fast green**.** For details of procedures see Section 2.2. The figure shown is representative of two biological replicates. The main roots of three sample plants per replicate were used for the light microscopy. Section was taken from the elongation zone.

e = epidermis, c = cortex, p = phloem, x = xylem, pe= pericycle, en = endodermis

TR-ACO1 promoter-driven GUS expression was predominantly in the lateral roots with less expression in the main root. From the results presented in Section 3.2.1, it appeared that the increase in number of lateral roots is a major response to Pi depletion.

Further, western analyses (Section 3.4.1.1 and Section 4.4.1) and the sqRT-PCR experiments (Section 3.4.2.1 and 4.5.1) have shown that *TR-ACO1* gene expression and protein accumulation were upregulated in response to Pi depletion. To further this investigation, the tissue-specific activity of the *TR-ACO1* gene promoter was determined. To do this, white clover was transformed with a green fluorescent protein (GFP) reporter gene driven by the *TR-ACO1* promoter. The use of GFP allows non-destructive monitoring of GFP fluorescence directly in living cells, and thus can be used to indicate the specific localisation of the induction of *TR-ACO1* gene expression in living tissue. Unless otherwise indicated, the plants used for the examination of tissue specific localisation of the *TR-ACO1* promoter activity in the roots were grown in Pi sufficient (1.0 mM) liquid media.

Confocal microscopy showed that in the main root of the TR2-1 plant, GFP fluorescence was predominant in the cells of the cell division zone in the root apical meristem (RAM) (Figure 4.24B). In the root samples examined, the green fluorescence was present in at least three to four rows of cells including the ground meristem tissue (the primary meristem that develops into cortex) and partly in the procambium (the primary meristem that differentiates into the vascular tissues). In some roots examined, there were also very low fluorescence in the protoderm (primary meristem that gives rise to the epidermis) and in the outermost layer of cells of the root cap (data not shown). To ensure that the green fluorescence was caused by the accumulation of the GFP protein and not due to autofluorescence, roots of wild type white clover (grown

simultaneously with TR2-1 cuttings) were also stained with propidium iodide and used as a control in the microscopy. Using the same filter set as for the transgenic roots, no green fluorescence was noted in the root tips of wild type white clover (Figure 4.24A), indicating that the fluorescence in the TR2-1 roots was due to the presence of the transgene.

From the RAM, GFP fluorescence significantly decreased towards the region of elongation where GFP staining was only observed in at least one or two rows of the outer cortical cells (Figure 4.24D). Although present in only one or two rows of cells, such green fluorescence was relatively bright. In some TR2-1 roots which were examined, very light *TR-ACO1p*-driven GFP expression was observed in a few cells in the epidermis, occasionally diffusing into the next one or two adjacent rows of the cortical cells (data not shown). Generally, GFP fluorescence in these cells was very weak. A confocal image of the elongation zone in a root of wild type white clover is presented in Figure 4.24C which displays no green fluorescence in any of the cells.

Strong GFP fluorescence was also noted in the root maturation zone. In almost all roots examined, bright fluorescence was located mainly in the pericycle with nodes of expression corresponding to a developing lateral root (arrowed in Figure 4.24F). Apart from the pericycle, GFP staining were also observed in the inner cortical cells, and some in the stele (data not shown).

TR-ACO1 promoter-driven GFP expression was stronger in the lateral root primordium (Figure 4.25A) and in the meristem of the developing lateral roots (Figure 4.25B). The whole lateral root primordium in Figure 4.25A showed intense GFP staining, with relatively weak fluorescence in the pericycle where the lateral root initiated.

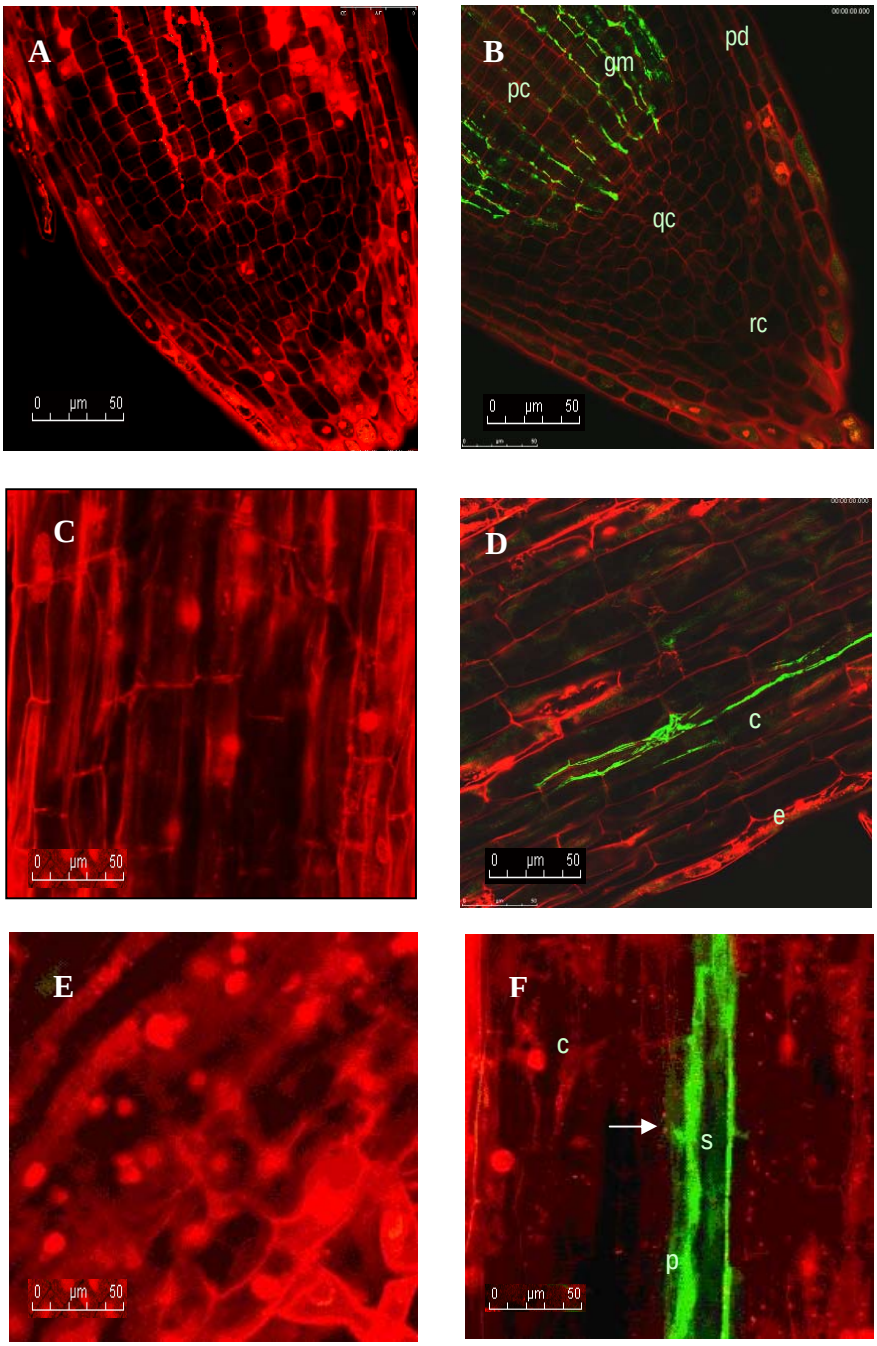

Figure 4.24 *TR-ACO1* promoter-driven GFP expression, determined using confocal microscopy in roots of either the transgenic line TR2-1 (B,D,F) or wild type white clover (A,C,E). Root tissues were stained for 10 s with 10 ng.µL^{-1} propidium iodide prior to microscopy. Dual scanning was conducted with the filter for the excitation and emission of propidium iodide set at *ca.* 540 nm and *ca.* 610 nm, respectively. For GFP excitation and emission, the filter was set at *ca.* 480 nm and *ca.* 510 nm, respectively. A,B = root cell division zone, C,D = elongation zone, E,F = maturation zone, gm = ground meristem, pc= procambium, pd = protoderm, qc = quiescent center, rc = root cap, e = epidermis, c = cortex, p = pericycle, s = stele

GFP fluorescence was very intense in the meristem up to the epidermis within the periphery of the lateral root primordium.

In the inner cortical cells and in the epidermis of the main root some hint of GFP staining was also noticeable, while the rest of the tissue displayed no GFP fluorescence but appeared reddish due to the propidium iodide staining.

In the developing lateral root (Figure 4.25B), predominant GFP staining was also in the apical meristem. There was an intense GFP staining in the root apex which included the tissue forming the root cap. This signal was significantly reduced just basal to the meristem region towards the base of the lateral root. The GFP signal in the pericycle however was still evident although not very strong, and this fluorescence crept through to the tip of the developing lateral root. When the lateral roots began to elongate, it appeared that the GFP fluorescence was concentrated in the meristem (Figure 4.25C) and putatively in the cells of the root cap. There was little or no signal towards the base of the lateral root.

In some developing lateral roots there were also some GFP fluorescence detected towards the base approaching the pericycle of the main root. (Figure 4.25B). This pattern was also noted in well developed lateral roots (Figure 4.25D) where the signal just basal to the meristem also decreased further as it approached the region of elongation. These results clearly indicate the tissue-specific localisation of *TR-ACO1* promoter activity in the roots of white clover and that this gene is expressed predominantly in the root meristem and in the pericycle of the root maturation zone.

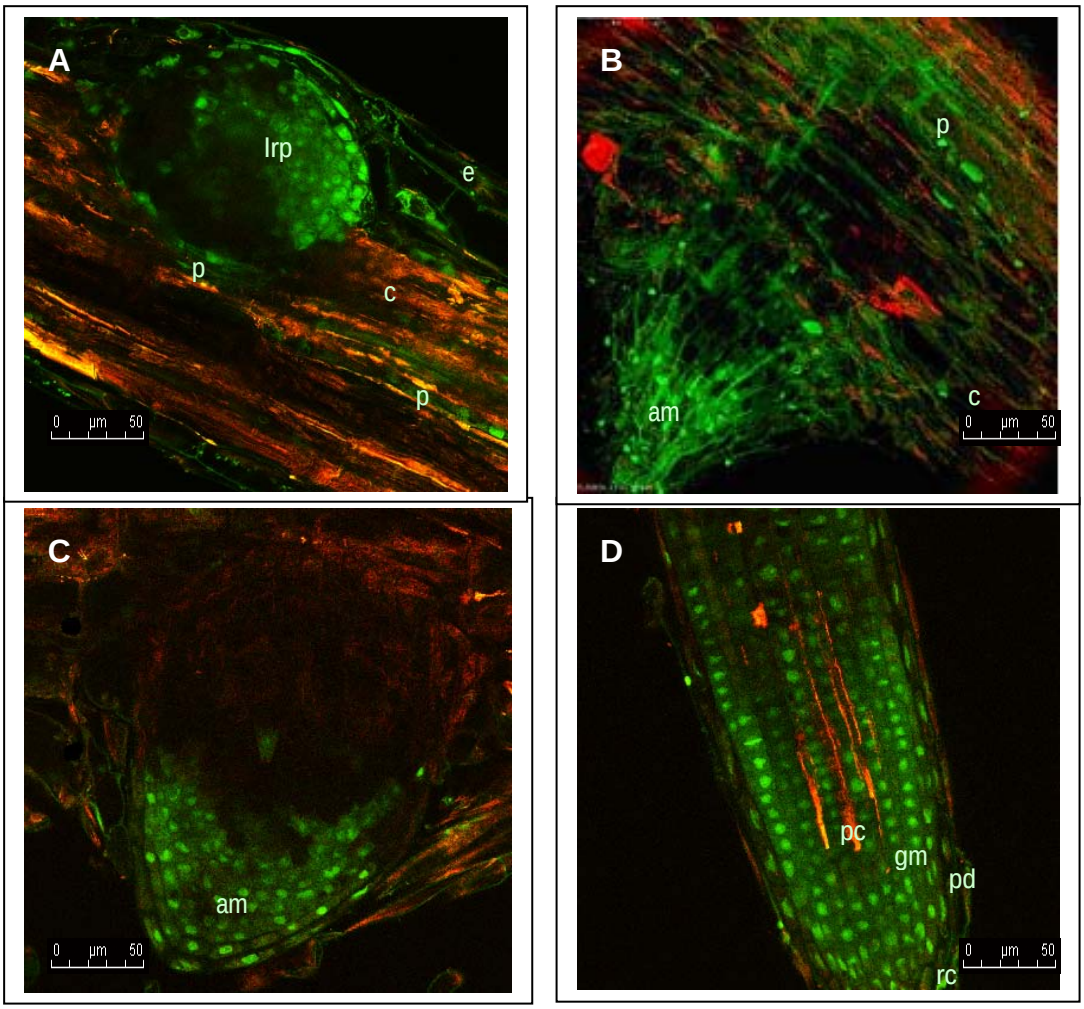

Figure 4.25 GFP expression in the lateral root primordium (A), developing lateral roots (B,C), and developed lateral root (D), showing the tissue-specific localisation of *TR-ACO1p*-driven GFP accumulation using *TR-ACO1p: :mGFP5-ER* transformed white clover. Root tissues were stained for 10 s with 10 ng.µL^{-1} propidium iodide prior to microscopy. Dual scanning was conducted with the filter for the excitation and emission of propidium iodide set at *ca.* 540 nm and *ca.* 610 nm, respectively. For GFP excitation and emission, the filter was set at *ca.* 480 nm and *ca.* 510 nm, respectively.

am = apical meristem, lrp = lateral root primordium, e = epidermis, c = cortex, p = pericycle, pc = procambium, gm = ground meristem, pd = protoderm, rc = root cap

4.7.1 Tissue-specific localisation of the *GFP* in the roots of different white clover lines harbouring the *TR-ACO1p::mGFP5-ER* gene construct

In the previous section, observations on the localisation of *TR-ACO1* promoter-directed expression in the roots was noted using one white clover transgenic line, TR2-1. However, a wider confirmation of the pattern of GFP expression was deemed essential. Therefore, examination of roots of at least ten different lines of newly transformed *TR-ACO1p::mGFP5-ER* white clover was carried out to confirm the observed tissue-specific localisation of *TR-ACO1* promoter activity. The presence of the transgene in the genome of each of the putative transgenic lines was confirmed by PCR and Southern hybridisation analysis as shown in Figures 4.4 and 4.5. Observations on the localisation of the gene in the roots of at least six independent lines are presented in Figures 4.26 and 4.27. All roots were stained with propidium iodide before undertaking confocal microscopy in order to ensure good contrast, and to reduce the signal to noise ratio.

For the comparison of GFP fluorescence in the roots of different lines, observation was made in similar tissues. Specific parts of the roots examined for this purpose were the meristem of both lateral and main roots, as well as the pericycle of the maturation zone since these were the specific tissues where *TR-ACO1p*-driven GFP expression was observed in the TR2-1 roots.

Generally, GFP was expressed highly in the pericycle of at least six independent lines harbouring the *TR-ACO1p::mGFP5-ER* gene (Figure 4.26). Some fluorescence is also detectable in the stele particularly in the Lines TR-2A, TR-7 and TR 20, and in the cortex, as in Line TR-8 and TR-12.

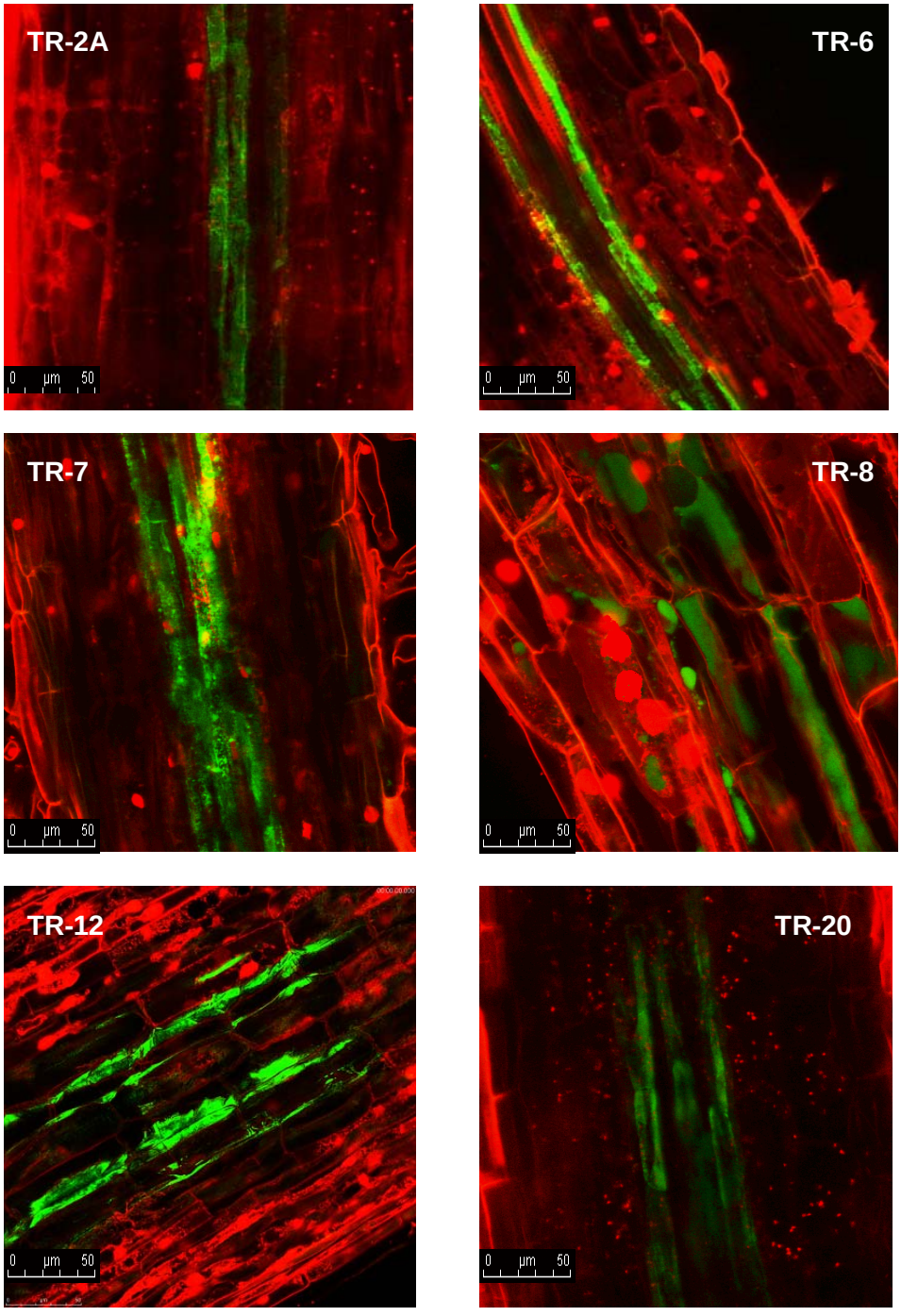

Figure 4.26 GFP expression, using confocal microscopy, in the pericycle of the roots of newly transformed white clover lines harbouring the *TR-ACO1p::mGFP5-ER* gene. Root tissues were stained for 10 s with 10 ng.µL^{-1} propidium iodide prior to microscopy. Dual scanning was conducted with the filter for the excitation and emission of propidium iodide set at *ca.* 540 nm and *ca.* 610 nm, respectively. For GFP excitation and emission, the filter was set at *ca.* 480 nm and *ca.* 510 nm, respectively.

Images presented in Figure 4.27 were all from the developing lateral roots of the same transgenic lines examined for GFP fluorescence in the pericycle. These lines generally showed the same pattern of GFP fluorescence in the lateral roots. As in the TR2-1 line, predominant GFP staining was in the root meristem, which abruptly decreased towards the base of the lateral root. In the TR-2A line, aside from the intense GFP staining in the meristem, there was also strong GFP fluorescence in some epidermal cells of the main root at the junction basal to the lateral roots. There were relatively weak signals in the root cap which envelopes the meristematic tissue.

For the TR-6 line, GFP was mainly in the cells of meristematic tissue. For TR-7, there was a relatively weaker signal compared to other lines and these were mostly in the two to three layers of cells surrounding the root apical meristem, putatively in the protoderm and in the ground meristem. There was also strong GFP fluorescence in the apical meristem of TR-8, with lower expression basal to the lateral root. A similar expression pattern was noted in line TR-12 and expression was relatively weaker in line TR-20, where GFP was again localised predominantly in the apical meristem of the developing lateral root.

4.7.2 Expression pattern of GFP in the roots of TR2-1 white clover in response to changes in phosphate supply

The results presented in the previous section highlighted the specific localisation of *TR-ACO1* promoter-driven GFP expression as determined by fluorescence in the roots of transgenic white clover grown under Pi sufficient media. In this section, analysis of any changes in the expression pattern of the gene in response to changes in Pi supply is presented. Plants were grown with sufficient (1.0 mM) or depleted (10 μM) phosphate

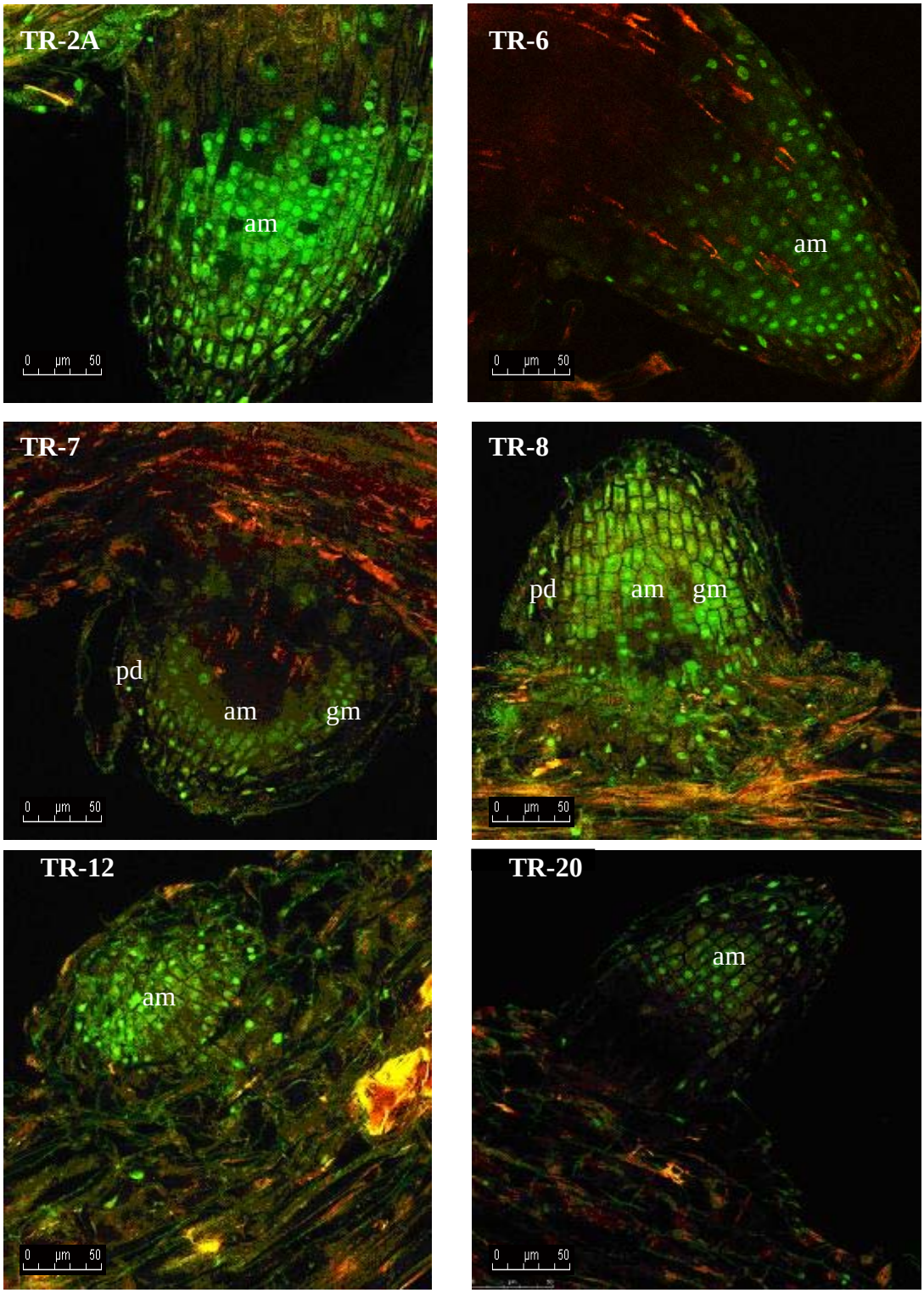

Figure 4.27 GFP expression, using confocal microscopy in the developing lateral roots of newly transformed white clover lines harbouring the *TR-ACO1p: :mGFP5-ER* gene. Root tissues were stained for 10 s with 10 ng.µL^{-1} propidium iodide prior to microscopy. Dual scanning was conducted with the filter for the excitation and emission of propidium iodide set at *ca.* 540 nm and *ca.* 610 nm, respectively. For GFP excitation and emission, the filter was set at *ca.* 480 nm and *ca.* 510 nm, respectively.
am – apical meristem, gm – ground meristem, pd - protoderm

(Section 2.1.2), and the roots were then examined by confocal microscopy. Observations were made at 1 d, 2 d, 4 d and 7 d after Pi depletion.

Confocal images of the tips of the main roots and lateral roots 1 d after Pi depletion are shown in Figure 4.28. In both the main roots and lateral roots of Pi sufficient plants, expression of GFP was generally lower when compared to those under Pi depletion. In the Pi sufficient main root (Figure 4.28A), GFP fluorescence was predominantly in the meristematic tissue, and extended towards the root cap. A weaker signal was detectable in the procambium, but was stronger in the outer layer of the ground meristem and in the protoderm. This signal however was relatively dull when compared to the fluorescence in the Pi deficient root (Figure 4.28B). In the root shown, the whole meristem showed intense GFP fluorescence. In the Pi sufficient lateral root (Figure 4.28C), fluorescence was mainly in the cells within the periphery of the meristem subtending into the tip of the root cap.

In the Pi depleted main roots (Figure 4.28B), the GFP signal was generally stronger when compared to those grown under Pi sufficiency. A strong GFP fluorescence was present in a range of cells within the meristematic tissue starting from the central core of the procambium up to the surrounding cells of the ground meristem tissue. This intensity of signal was observed in the whole region of meristematic tissue and then started to decline in the tissue just approaching the elongation zone. In the epidermis, the signal was lower but green fluorescence in a few cells was still detectable. Not much GFP fluorescence was observed in the root cap or in the whole tissue covering the apical meristem. In the Pi depleted lateral roots (Figure 4.28D), GFP fluorescence was also very strong. Intensive GFP fluorescence was detected in the whole apical

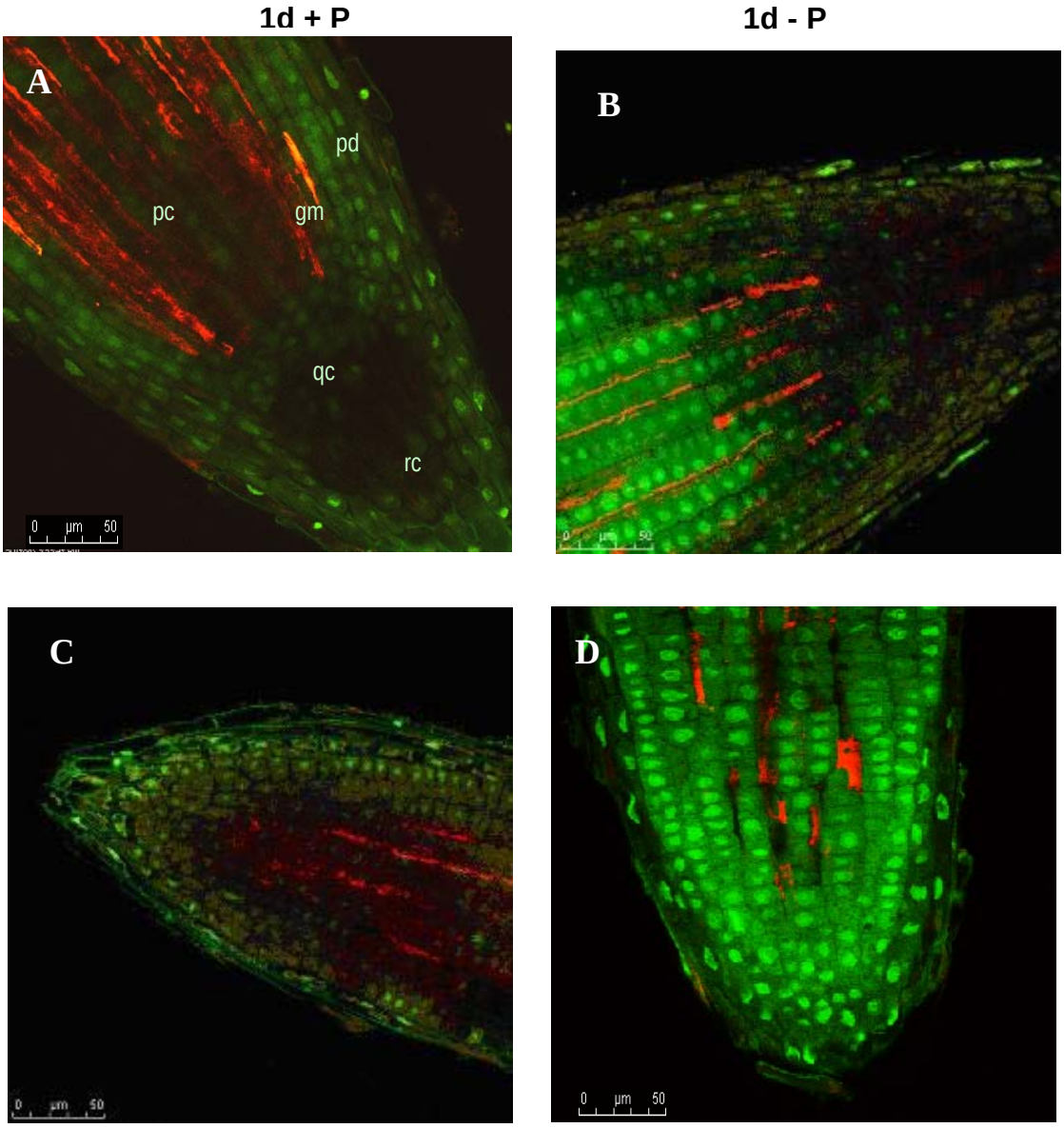

Figure 4.28 GFP expression, captured using confocal microscopy, in the main roots (A,B) and lateral roots (C,D) of Pi sufficient (A,C) and Pi depleted (B,D) white clover (TR2-1) harbouring the *TR-ACO1p: :mGFP5-ER* gene, 1 d after Pi depletion. Roots were stained with propidium iodide (10 ng.µL^{-1}) for *ca.*15 s followed by three times washing with distilled water and then mounted onto microscope slide. Dual scanning was conducted, with the microscope filter set at *ca.* 477 nm excitation and *ca.* 510 nm emission for GFP, and *ca.* 540nm and *ca.* 610nm, for the excitation and emission wavelength of the propidium iodide.

pc = procambium, gm = ground meristem, pd = protoderm,
qc = quiescent center, rc = root cap

meristem including the ground tissue, part of the procambium and, with a lesser signal, in the protoderm of the root.

The difference in the GFP expression in the lateral root primordium and in the developing lateral roots of Pi sufficient and Pi depleted plants a day after Pi depletion is shown in Figure 4.29. Examination of the lateral root primordium revealed that one day after Pi depletion GFP fluorescence was very marked in Pi depleted roots and again, the signal was more concentrated in the apical meristem (Figure 4.29B). In contrast, in the Pi sufficient roots, GFP expression was relatively dispersed within the peripheral region of the lateral root primordium, with signal originating from the pericycle of the main root (Figure 4.29A). Similarly, in the developing lateral root, GFP signal was stronger in Pi depleted roots (Figure 4.29D) and relatively weaker in roots under Pi sufficiency (Figure 4.29C).

By day 2 after Pi depletion, the *TR-ACO1p*-driven GFP expression appeared to be still upregulated as indicated by strong fluorescence in both the developing (Figure 4.30B) and developed lateral roots (Figure 4.30D) which were more intense and compact when compared to the developing lateral roots grown under Pi sufficiency (Figure 4.30A,C). Again, the whole central core of the procambium diffusing through to the layers of the ground tissue in Pi depleted roots was fully stained, with a marked reduction in GFP staining further up towards the base of the lateral root. There was relatively weak GFP signal in the protoderm, with only a few cells displaying GFP fluorescence. In contrast, there was moderate GFP fluorescence in the developing and developed lateral roots grown under Pi sufficiency. GFP fluorescence in these roots was mainly confined to the lower meristematic tissue of the procambium and the ground meristem (Figure 4.31A,C).

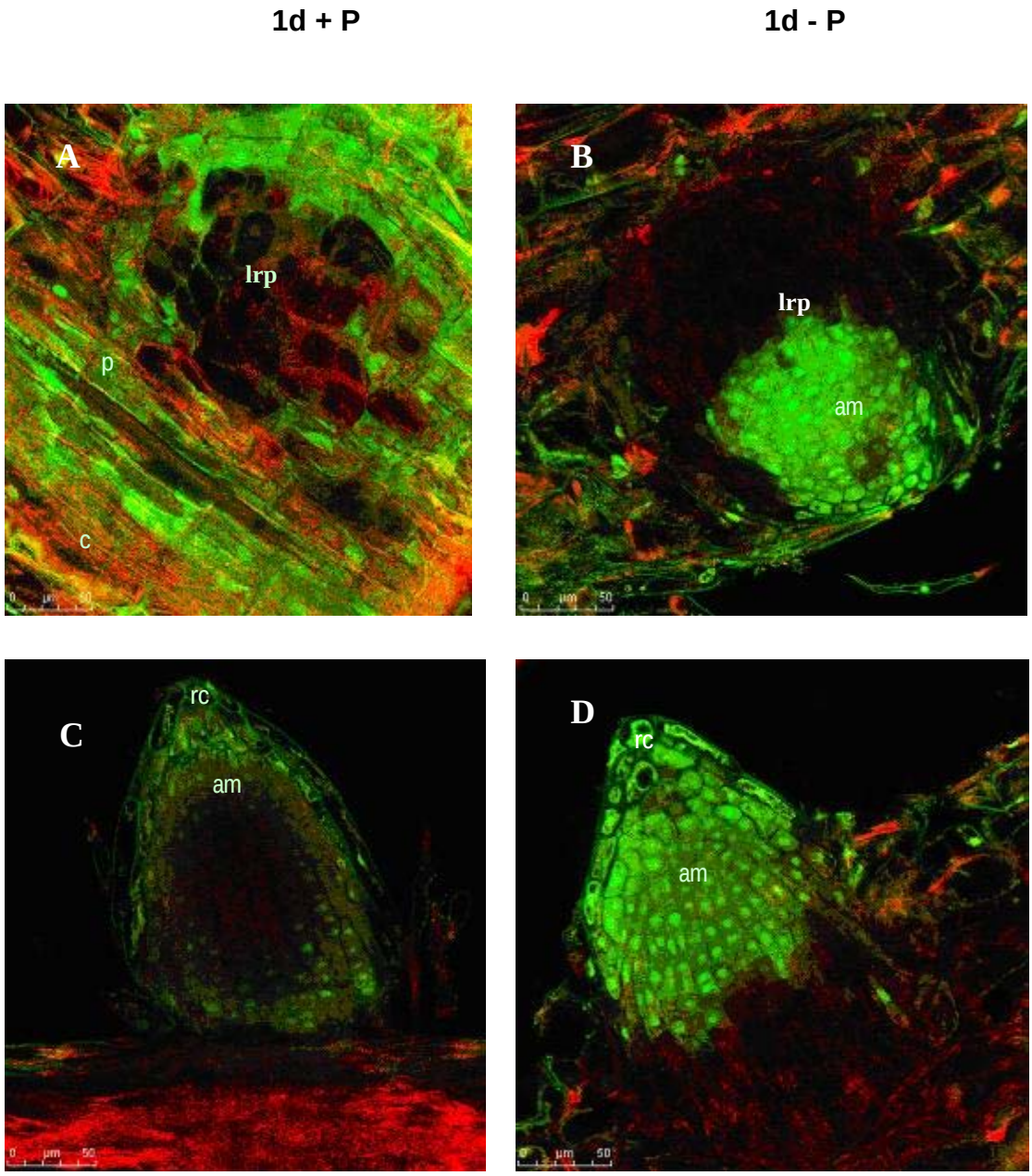

Figure 4.29 *TR-ACO1p*-driven GFP expression, captured using confocal microscopy, in the lateral root primodia (A,B) and newly developing lateral roots (C,D) of Pi sufficient (A,C) and Pi depleted (B,D) white clover (TR2-1) harbouring the *TR-ACO1p: :mGFP5-ER* gene, 1 d after Pi depletion. Roots were stained with propidium iodide (10 ng.μL^{-1}) for *ca.* 15 s followed by three times washing with distilled water and then mounted onto microscope slide with 50% glycerol. Dual scanning was done with microscope filter set at *ca.* 480 nm excitation and *ca.* 510 nm emission for GFP, and *ca.* 540nm and *ca.* 610nm, respectively for the excitation and emission wavelength of the propidium iodide.

am = apical meristem, lrp = lateral root primordium, p = pericycle,
rc = root cap, c = cortex

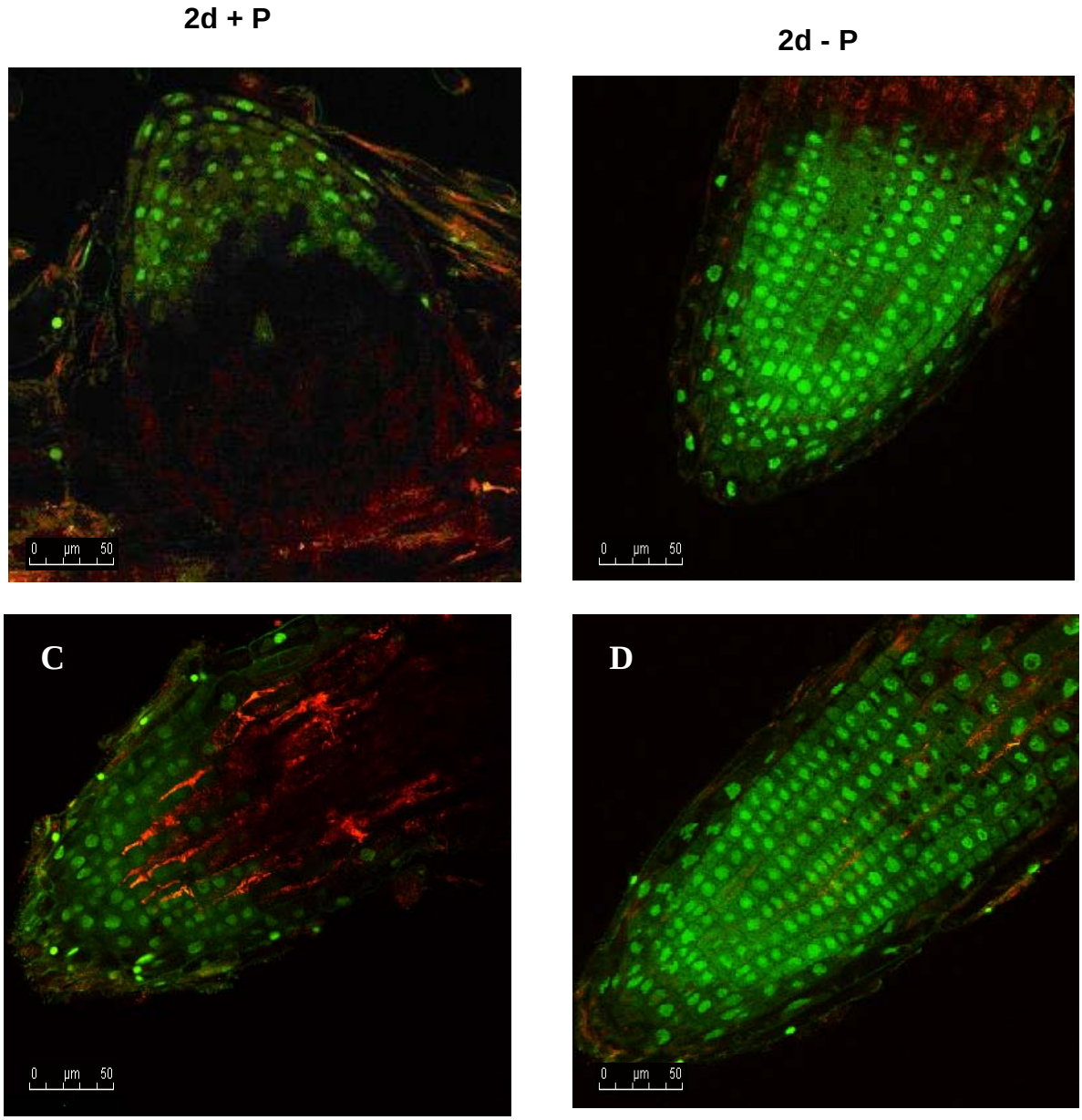

Figure 4.30 *TR-ACO1p*-driven GFP expression, captured using confocal microscopy, of developing and newly developed lateral roots of Pi sufficient (A,C) and Pi depleted (B,D) white clover (TR2-1) harbouring the *TR-ACO1p ::mGFP5-ER* gene, 2 d after Pi depletion. Roots were stained with propidium iodide (10 ng.µL^{-1}) for *ca.* 15 s followed by three times washing with distilled water and then mounted onto microscope slide. Dual scanning was done with microscope filter set at *ca.* 480 nm excitation and *ca.* 510 nm emission for GFP, and *ca.* 540 nm and *ca.* 610 nm, respectively for the excitation and emission wavelength of the propidium iodide.

After 4 d of Pi depletion, the GFP signal in Pi depleted roots was more reduced (Figure 4.31B, D) when compared to the signal during the first and second days after Pi starvation, although the GFP fluorescence in the tissue followed a similar pattern to that displayed at day 2. The GFP signal in Pi sufficient roots remain relatively weak but stable throughout all the observation points (Figure 4.31A,C).

At 7 d after Pi depletion, the GFP signal in Pi depleted roots was significantly reduced in both developing (Figure 4.32B) and developed lateral roots (Figure 4.32D) when compared to the signal during the second and fourth days after Pi depletion. The GFP signal in these roots, however, was still greater when compared to GFP fluorescence in Pi sufficient roots (Figure 4.32A, C). In the main roots of both Pi sufficient and Pi depleted plants (Figure 4.33), it was noted that the intensity of GFP accumulation was comparable. In both roots, there was quite weak GFP fluorescence and the signal was confined to some rows of cells in the meristematic tissue, in the epidermis and in the root cap.

GFP expression in the roots examined from the first day to the seventh day after Pi depletion was arbitrarily quantified in order to give an overall assessment on the trend of GFP fluorescence in these roots in response to changes in Pi availability. Due to the unavailability of appropriate image quantification software at the time this study was conducted, an arbitrary rating scale was devised to evaluate the GFP expression in each root. To do this, ten developing and developed lateral roots randomly selected from at least four stolon cuttings were evaluated. Root samples, *ca.* 2 cm from the tip were stained with propidium iodide and used for confocal microscopy.

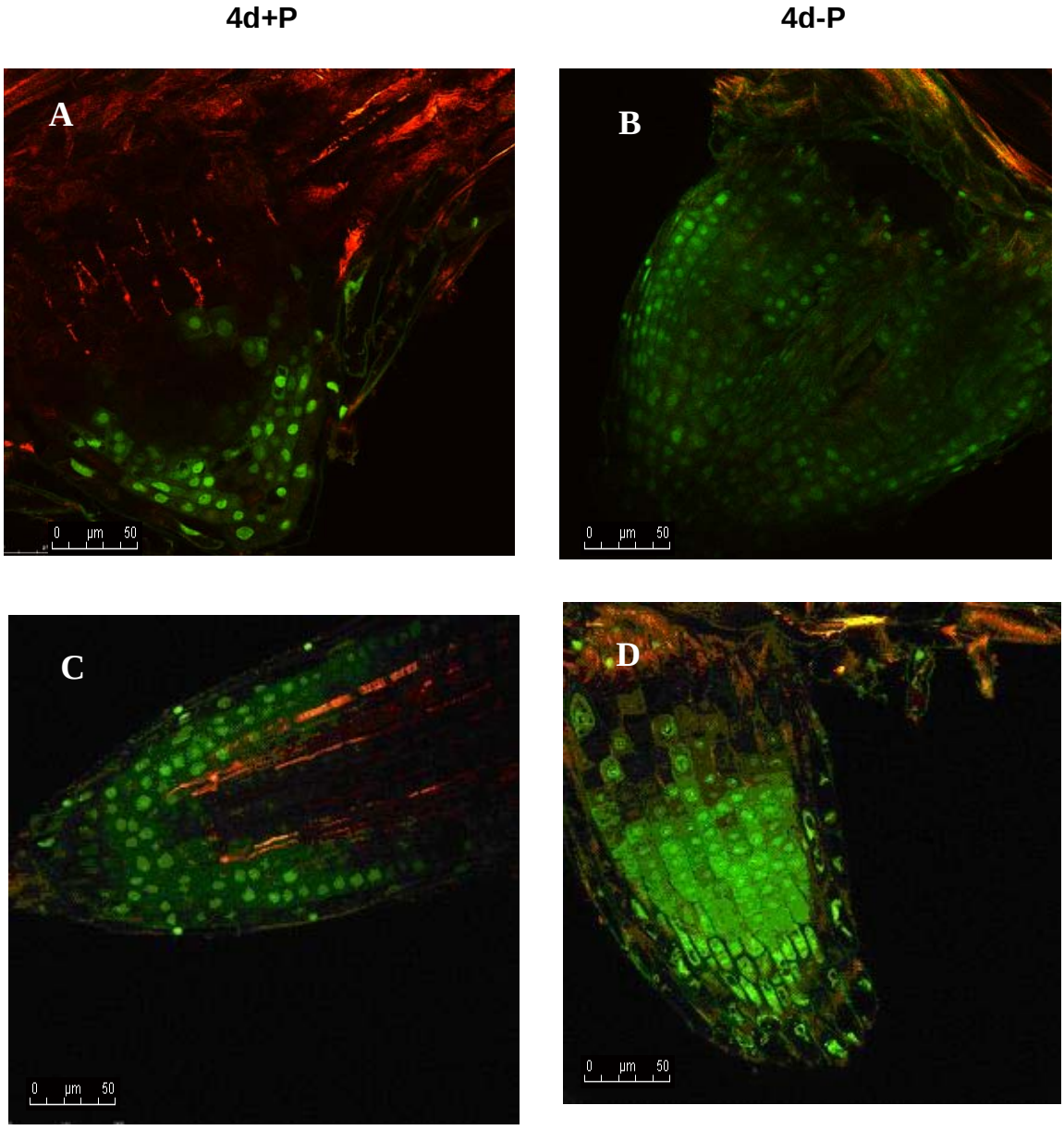

Figure 4.31 *TR-ACO1p*-driven GFP expression, captured using confocal microscopy, in the lateral root primordia (A,B) and lateral root tip (C,D) of Pi sufficient (A,C) and Pi depleted (B,D) white clover (TR2-1) harbouring the *TR-ACO1p::mGFP5-ER* gene, 4 d after Pi depletion. Roots were stained with propidium iodide (10 ng.µL^{-1}) for *ca.* 15 s followed by three times washing with distilled water and then mounted onto microscope slide. Dual scanning was done with microscope filter set at *ca.* 480 nm excitation and *ca.* 510 nm emission for GFP, and *ca.* 540 nm and *ca.* 610 nm, respectively for the excitation and emission wavelength of the propidium iodide.

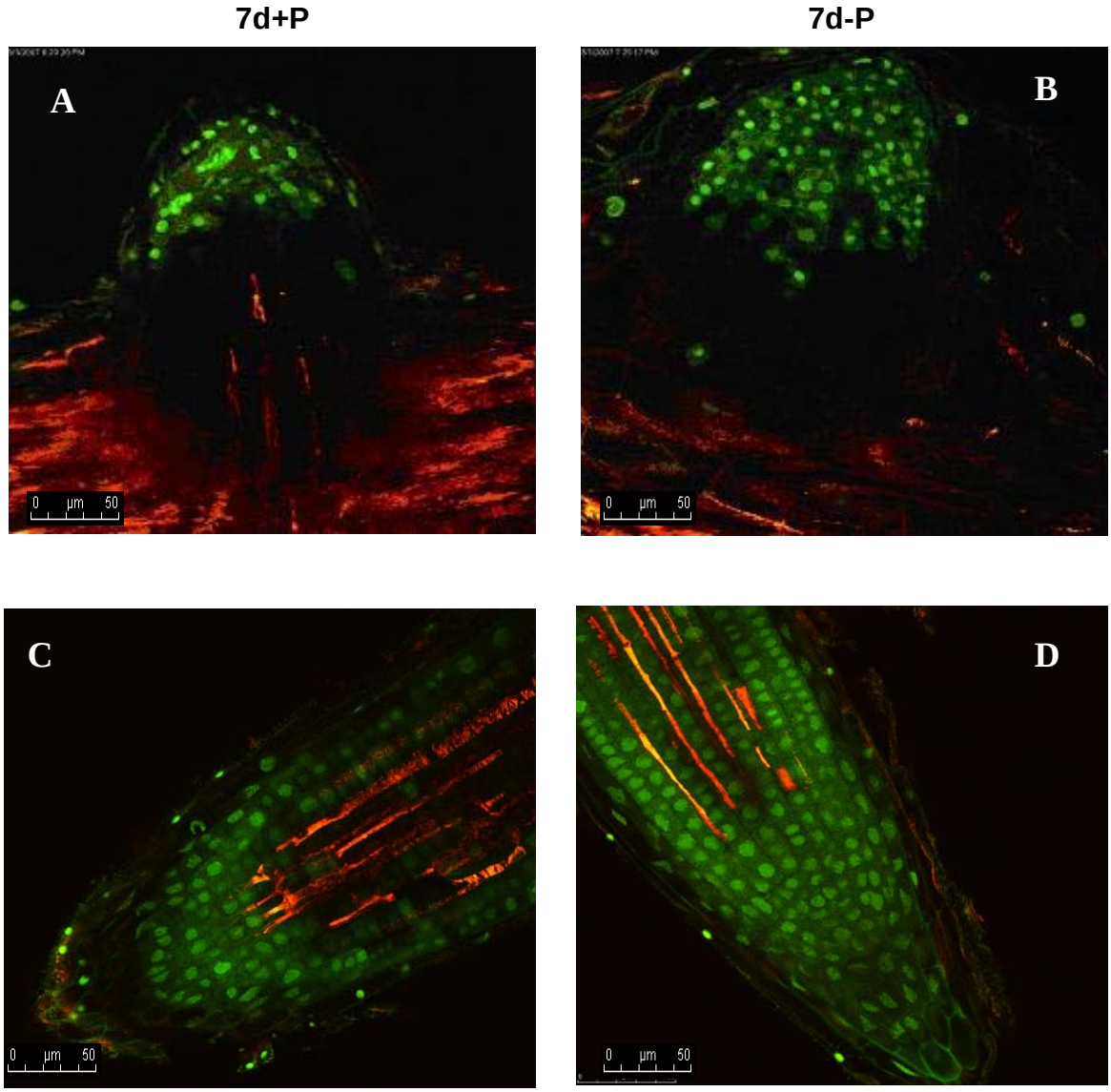

Figure 4.32 *TR-ACO1p*-driven GFP expression, captured using confocal microscopy, in the lateral root primordia (A,B) and lateral root tip (C,D) of Pi sufficient (A,C) and Pi depleted (B,D) white clover (TR2-1) harbouring the *TR-ACO1p::mGFP5-ER* gene, 7 d after Pi depletion. Roots were stained with propidium iodide (10 ng.µL^{-1}) for *ca.* 15 s followed by three times washing with distilled water and then mounted onto microscope slide. Tissues were layered with 50% glycerol before placing the glass cover slip. Dual scanning was done with microscope filter set at *ca.* 480 nm excitation and *ca.* 510 nm emission for GFP, and *ca.* 540 nm and *ca.* 610 nm, respectively for the excitation and emission wavelength of the propidium iodide.

Depending upon the intensity of the signal, a rating of 1 to 10 was assigned to each root being examined, with a score of 1 denoting least fluorescence and 10 the strongest GFP signal. The rating included the pooled observation on the lateral roots and lateral root primordia. At the end of each observation day, the scores per treatment were summarised and the mean value was recorded.

The summary of this evaluation is presented as Figure 4.34. As shown, the GFP signal in Pi sufficient roots was generally moderate, with a mean rating of 3.8 at day 0. From day 1 to day 7 after Pi depletion, the mean rating for the GFP signal in Pi sufficient roots ranged from 3.3 to 3.7, indicating a moderate and stable signal throughout the duration of the study. On the other hand, there was very strong fluorescence of GFP in Pi depleted roots at day 1, as indicated by a very high mean rating of 8.1. This rating gradually declined each day with a mean of 7.1 on the second day, reducing to 6.6 on the fourth day and finally to a mean of 4.2 on the seventh day. This trend of values in Pi depleted roots indicates that the *TR-ACO1* gene promoter activity was upregulated by phosphate stress within 24 h after Pi depletion, and then expression gradually subsided until day 7.

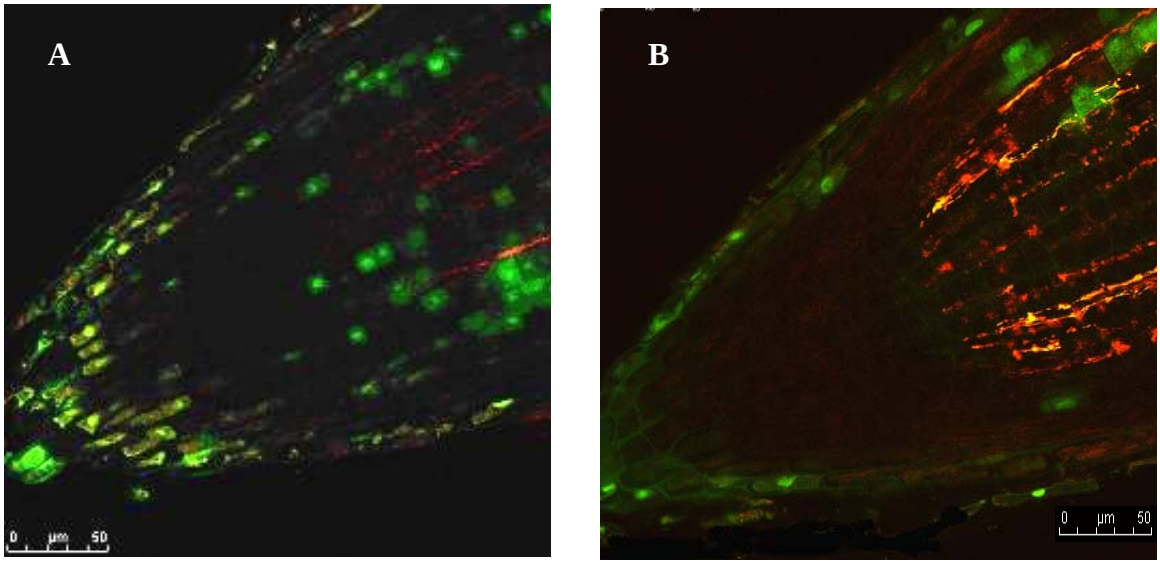

Figure 4.33 *TR-ACO1p*-driven GFP expression, captured using confocal microscopy, in the root tip of main roots of Pi sufficient (A) and Pi depleted (B) white clover (TR2-1) harbouring the *TR-ACO1p::mGFP5-ER* gene, 7 d after Pi depletion. Roots were stained with propidium iodide (10 ng.µL^{-1}) for *ca.* 15 s followed by three times washing with distilled water and then mounted onto microscope slide. Tissues were layered with 50% (v/v) glycerol before placing the glass cover slip. Dual scanning was done with microscope filter set at *ca.* 480 nm excitation and *ca.* 510 nm emission for GFP, and *ca.* 540 nm and *ca.* 610 nm, respectively for the excitation and emission wavelength of the propidium iodide.

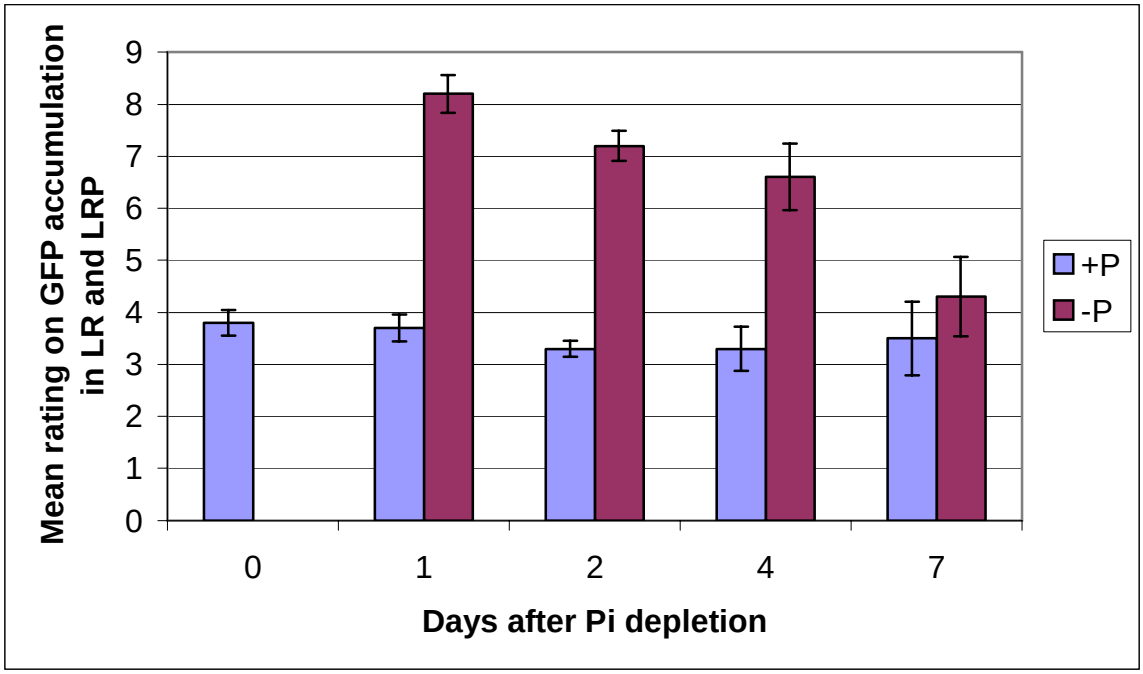

Figure 4.34 Arbitrary quantification of *TR-ACO1p*-driven GFP expression in the newly emerging lateral root (LR) and lateral root primordia (LRP) of the transgenic white clover line, TR2-1 subjected to Pi sufficiency (+P, 1.0 mM) or Pi depletion (–P, 10 μM). Ten developing and developed lateral roots randomly selected from at least four stolon cuttings were evaluated. Root samples, *ca.* 2 cm from the tip were stained with propidium iodide and used for confocal microscopy
An arbitrary rating scale of 1 – 10 was used, where 1 means least GFP accumulation and 10 the greatest GFP accumulation in the root**.** Error bars represent standard error of the mean; n = 10.

Chapter 5
Discussion

The first part of this thesis sought to determine the differential accumulation of TR–ACO proteins and expression of the *TR-ACO* gene family in white clover roots. The second part aimed to investigate the influence of Pi supply on TR-ACO protein accumulation and *TR-ACO* gene expression in the roots. Finally, the cellular localisation of gene expression driven by the promoter of the *TR-ACO1* gene was examined in response to Pi supply, using white clover plants transformed with a gene construct *TR-ACO1p::mGFP5-ER.*

5.1 Members of *TR-ACO* gene family are differentially expressed in white clover roots

5.1.1 Differential expression of *TR-ACO1* gene and accumulation of TR-ACO1 protein in the roots

This study has determined that members of *TR-ACO* gene family are spatially and developmentally regulated in white clover roots in a gene-specific manner. Using semi-quantitative Reverse Transcriptase-Polymerase chain reaction (sqRT-PCR), it was shown that the *TR-ACO1* gene was expressed in the roots and that the transcript was more abundant in the lateral roots relative to the main roots (Figure 3.2). This confirms, in part, the initial findings by Yoo (1999), where by northern analysis, he determined that the greatest amount of *TR-ACO1* transcript accumulated in the white clover roots, although the gene was also expressed in the leaf axillary buds and stolon apical bud (unpublished data). Yoo did not conduct an extensive study on the roots, and the current study provides significantly more detailed information on the expression of the *TR-ACO1* gene in the roots.

An immunodetection analysis using α-TR-ACO1 antibodies was performed, and the result showed a greater recognition of protein in the lateral roots (Figure 3.1), providing additional evidence that TR-ACO1 is spatially expressed in the roots, and further suggesting that the TR-ACO1-mediated ethylene synthesis is greater in the lateral roots when compared to the main roots. Further, the results of these analyses imply that the regulatory mechanism for the expression of the *TR-ACO1* gene occurred at the transcriptional level.

The tissue-specific localisation of the *TR-ACO1* promoter activity in the roots was also analysed using a single genetically-independent transgenic white clover line transformed with *TR-ACO1p::GUS* gene (generously provided by Chen and McManus, 2006). Results revealed predominant GUS staining in the lateral roots and less in the main roots (Figure 3.3A & B). Although there are some limitations to the use of a reporter gene in expression analysis, the GUS staining pattern broadly correlated with the result of sqRT-PCR and western analysis. Thus, it can be deduced that *TR-ACO1* is highly expressed in lateral roots when compared to the main roots.

To further analyse the localisation of the *TR-ACO1* promoter activity, sectioned GUS stained roots were examined by light microscopy and it was noted that predominant GUS staining was in the lateral root promordia (LRP) and in the stele (Figure 3.3C,D) suggesting that these regions of the root, where cells are actively dividing, are potential specific sites for the regulation of *TR-ACO1* gene expression in white clover roots. Apart from the strong blue staining in the lateral root primordia and stele, the blue stain was also detectable in the surrounding cells of the cortex out to the epidermis, although the stain was reasonably faint. It is difficult to assess this weak stain in the cortex. Was this due to real GUS activity, or only due to some diffusion from the cells? It was previously reported that as GUS activity is enzymatic, the product may diffuse out to the

surrounding cells where it was not originally produced (Mantis and Tague, 2000), and therefore may suggest an over expression of the gene. Since the staining in the cortex was very weak, there is a possibility that this could be due to the diffusion effect which may have contributed to the amplification of the signal in the root cortical tissue.

Tissue specific localisation of the promoter activity was further investigated using the GFP reporter gene which was fused to the same *TR-ACO1* promoter developed as part of this study. Prior to the development of these results, the validation of the transgenic plants was checked.

5.1.1.1 Confirmation of the presence of the T-DNA insert in the putative transgenic plants

The transgenic nature of the lines recovered after the transformation was confirmed by PCR using GFP gene-specific primers, and the gene copy number incorporated in the genome was determined by Southern hybridisation analysis. Ideally, transformants carrying a single T-DNA locus are preferred to examine gene expression since the position effect may influence the pattern of expression of the reporter gene (Peach and Velten, 1991; Ding *et al*., 2003). However, in the first transformation, the only putative transgenic line that survived (designated TR2-1) and was used for the majority of analysis, had four gene copy numbers in the genome. To address this problem, this transgenic line was used in the various biochemical and molecular analyses and results compared with that of the wild type. Analyses showed that the transgenic line behaved in the same way as that of the wild type indicating that the gene did not interfere with the normal function of the plant in terms of responses to Pi supply.

During genetic transformation, chances of random integration of the T-DNA into the plant chromosomes is possible and this may target areas which are transcriptionally active. This may sometimes result in huge variability in the transgenic expression (Nap

et al., 1996). In some instances, some *Agrobacterium*-mediated transformation event may result in gene silencing (Peach and Velten, 1991) or destruction of integrity of active genes especially for haploid species (Finnegan and McElroy, 1994). However, for diploid or polyploid species this rarely becomes a problem since the T-DNA is inserted into one allele and the other allele in the chromosome can still remain functional (Atwell and Eamus, 1999). Since white clover is a polyploid species, being an allotetraploid (2n = 32) (Voisey *et al.*, 1994; Ansari *et al.*, 1999; Majumdar, 2004) then the likelihood of the integrity of active genes being disrupted was expected to be minimal, and as observed in this study, the transgenic line behaved in the same way as the wild type.

The reproducibility of the observation was also given due consideration, and it was deemed necessary to obtain more genetically distinct lines for further observations. To do this, another batch of white clover transformations was conducted. During the second transformation, 11 putative genetically independent lines were produced and as shown in the Southern hybridisation analysis (Figure 4.5), the copy number of the integrated T-DNA varied from one to putatively eight copies, despite the fact that the restriction enzyme used did not cut the T-DNA insert. Examination of each transformant by confocal microscopy showed that apart from Line # 3 which had eight gene copy numbers, all other lines showed a similar pattern of expression to the TR2-1 line, indicating that the GFP expression observed in this line was real and not due to a position effect.

5.1.1.2 Localisation of the TR-ACO1 promoter activity as determined using transgenic white clover transformed with a TR-ACO1p::mGFP5-ER gene construct

Initial investigation was conducted using the one transgenic line, TR2-1. Using the GFP reporter gene construct, the promoter-driven GFP expression was noted in the lateral root primordia (Figure 4.27). In addition, GFP staining was also intense in the pericycle

and in the root apical meristem. (Figure 4.26), indicating the possible expression of the *TR-ACO1* gene in these tissues of the root.

The use of GFP in such analyses may also comprise some potential drawbacks such as the presence of auto fluorescence from certain fluorescing compounds in some plant tissues (Garabagi and Strommer, 2000), which may cause potential interference by masking the actual GFP signal, particularly in the leaves (Hraska *et al*., 2006). In the roots, the problem of visualisation of GFP by confocal microscopy can be minimal since the roots are virtually free from chlorophyll auto fluorescence. However, although auto fluorescence from chlorophyll-related substances may be nil, some endogenous biomolecules in the cell wall in various root sections may also autofluoresce and occasionally interfere in monitoring gene expression (van der Geest and Petolino, 1998). To address this problem, two measures were undertaken. Firstly, the root tissues were briefly stained with propidium iodide which stains the cell membrane and the nuclear chromatin (Krishan, 1975). In this way a relatively good contrast between red fluorescence from the propidium iodide and the green fluorescence from GFP was obtained. Secondly, confocal microscopy of the roots of wild type white clover was conducted to serve as a negative control. These roots of wild type white clover were also stained with propidium iodide and the microscope filter was set similar to that of the transgenic lines. Under these conditions, the background autofluorescence was minimal if not completely eliminated.

The GFP expression which suggests *TR-ACO1* promoter activity in the pericycle of the root is a significant finding in this study since the pericycle, which is an inner cell layer of the roots outside the vascular tissues, contains actively dividing cells that give rise to lateral root primordia (LRP) (Dubrovsky et al., 2000). The *TR-ACO1* promoter activity in the pericycle may suggest that the *TR-ACO1* gene participates in an important

developmental process in the zone of active cell division. This observation is in agreement with the observed induction of ACC oxidase in the layers of cells in the part of a stele in the pea root where nodule primordia are initiated (Heidstra *et al*., 1997) .

That *TR-ACO1* activity is induced in the LRP is also a novel finding in this study. Lateral roots (LR) are initiated from the pericycle, and LR formation is an important organogenetic process that contributes to the pattern of root system architecture in higher plants (Fukaki *et al.,* 2007). The first control point in LR formation is characterised by the specification of founder cells in the pericycle cells. This is then followed by the whole process of cell cycle progression and a subsequent stimulation of the molecular pathway towards LR initiation (De Smet et al., 2006). Previously, it has been reported that an increase in cell division in the pericycle region of the root leads to enhanced LR formation (Landsberg, 1996). In a very recently published report, which identified the major genes expressed in the pericycle of the maize primary root, SAM synthetase was among those encoded by the induced genes (Dembinsky et al., 2007). Interestingly, SAM synthetase is the enzyme that mediates the conversion of methionine to SAM which is further converted to the ethylene precursor ACC, and finally to ethylene. This suggests that the pericycle and meristem of the roots are putative sites for the synthesis of the hormone ethylene and may further indicate a role for ethylene in the development of the pericycle and meristem of white clover roots.

Ethylene is also produced in the root apex of wheat seedlings (Tari and Marton, 1999), and has been known to promote root tip growth and root hair formation in pea and in *Arabidopsis* (Tanimoto *et al.*, 1995; Heidstra *et al*., 1997). Further, ethylene is involved in the regulation of main root extension and lateral root spacing in *Phaseolus vulgaris* (Borch *et al.*, 1999), and in the development of the root meristem of *Medicago truncatula* (Rose *et al*., 2006). Interestingly, an alignment of the coding sequence of the

TR-ACO1 gene using the NCBI BLASTn, showed that the *TR-ACO1* gene had 95% and 90% identity with coding sequences from *Medicago truncatula* (AC121236.18) and from *Pisum sativum* (AB128037.1), respectively. However, in the study of Heidstra *et al.* (1997) or Rose *et. al* (2006) the specific root-associated *ACO* gene(s) was not identified. In this study, however, the *TR-ACO1* promoter activity was localised in the meristem, suggesting the possibility that *TR-ACO1* gene is the specific member of the *TR-ACO* gene family that plays this role in the proposed involvement of ethylene in development of root meristem in white clover.

In sunflower seedlings, a greater accumulation of *ACCO1* transcripts was occurred in roots particularly in the cell division zone (Liu *et al.*, 1997). Although sunflower is not a legume, the result of BLASTn analysis also showed that the coding sequence of *ACCO1* (U62553.1) shares 79% identity with that of the *TR-ACO1* gene. Having some degree of identity indicates the likelihood that these DNA sequences share some commonality in terms of the role played in the meristem region of the roots. Very recently, it has been proposed that ethylene is involved in the signalling pathway that promotes stem cell division in the quiescent centre of the *A. thaliana* root (Ortega-Martinez *et al.*, 2007). All these pieces of evidence show that the meristematic regions of the roots are potential sites for ethylene biosynthesis and that the involvement of the *TR-ACO1* gene, and other *ACO* genes from related species that share some degree of identity with *TR-ACO1* gene in their coding sequences, is significant. Although BLASTn analysis showed that *TR-ACO1* shared no significant similarity with the coding sequences of any *ACO* gene from *Arabidopsis*, it may be possible that there is some degree of commonality in the role played by ethylene in the meristematic region of the roots of some legumes and non-legume plants such as *Arabidopsis*. The indicative expression of *TR-ACO1* gene in the

meristem and actively dividing cells in white clover roots suggests a role for ethylene in promoting cell division and root growth.

The localisation of the *TR-ACO1* promoter-driven expression in the roots has a close resemblance with the pattern of *TR-ACO1* expression in the above ground portion of white clover, where the promoter-driven expression was directed to the young tissues such as the apical buds of the stolon, newly developed leaves, axillary buds, and in the petiolules of the younger leaves (Chen and McManus, 2006). This suggests that in both roots and shoots, the actively dividing cells and young tissues are potential sites of the ethylene biosynthesis and that the enzyme ACC oxidase, specifically that which is encoded by the *TR-ACO1* gene, plays a fundamental role in the biosynthetic pathway.

In the analysis of the transcription factor binding domains of the *TR-ACO1* promoter sequence, Chen and McManus (2006) determined that the 5′ flanking sequence of the gene contains a high number of development-related domains, specifically members of the MADS-box family. In this promoter, there are five MADS box domains, two of which are specified to be the *Agamous binding element* (AG) and the *Agamous-like3 binding element* (AGL3) (Chen and McManus, 2006). AGL3 has been suggested to be a DNA binding protein, and has been implicated in regulating a range of developmental signals in the younger tissues of the vegetative organs in *Arabidopsis* (Huang *et al.*, 1995). A number of MADS-box genes are also associated with the roots. An example is AGL21 which is highly expressed in the lateral root primordium and in the other root tissues where cell proliferation tends to occur. Another example is AGL12 which was also expressed in the primary root meristem (Burgeff *et al.*, 2002). Although these genes were detected in *Arabidopsis*, they may be involved in regulating gene expression in the meristematic region of white clover roots. However, AGL21 or AGL12 binding domains have not been identified in the *TR-ACO1* promoter.

5.1.2 Differential expression of *TR-ACO2* gene and accumulation of TR-ACO2 protein in the roots

In terms of *TR-ACO2*, results of sqRT-PCR analysis also showed greater accumulation of transcript in the lateral roots when compared to the main roots. However, when the transcript abundance of *TR-ACO1* and *TR-ACO2* in the main roots is compared, the accumulation of TR-ACO2 transcript was greater than that of the *TR-ACO1* (Figure 3.2). In addition, immunodetection analysis using an antibody raised against TR-ACO2 showed a greater accumulation of the TR-ACO2 protein in the lateral root when compared to the main roots (Figure 3.1), suggesting greater ethylene production in the lateral roots, and further indicating the role played by the enzyme TR-ACO2 in the biosynthetic pathway. This result also suggests that the ethylene produced has a role in regulating root growth and development. Although both TR-ACO1 and TR-ACO2 accumulate in the lateral roots in a greater amount than in the main root, these two enzymes may have different functions in different tissues.

Further analysis for TR-ACO2 was conducted using transgenic white clover harbouring the *TR-ACO2p::GUS* gene construct. Predominant GUS staining, which indicates *TR-ACO2* promoter activity, was detected in both the lateral roots and in the main roots (Figure 3.4A). Interestingly, towards the apical meristem of the main root, there was less staining when compared to *TR-ACO1*. In the sectioned tissue, GUS staining was noted all throughout the tissue from the main to the lateral roots and the expression was distributed throughout the tissue (Figure 3.4C). From the epidermis to the cortical cells and into the stele, GUS staining was intense. To some extent, this result was also comparable with the expression pattern in white clover leaves, in which predominant expression (as determined by northern analysis) was detected in the developed and mature green leaves and less so in the actively dividing tissues (Hunter *et al.*, 1999). In addition, the *TR-ACO2* promoter directed expression in the axillary buds and petiolules

in mature green tissues (Hunter *et al.*, 1999; Chen and McManus, 2006). In *Nicotiana glutinosa, pNG-ACO3* was found to be constitutively expressed in all tissues including the roots. In contrast, *pNG-ACO1* was predominantly expressed in the older tissues of the roots and not in the younger tissues (Kim *et al*., 1998) indicating that members of the *pNG-ACO* gene family are also spatially and temporally expressed in the roots.

Analysis, *in silico*, of the *TR-ACO2* promoter revealed that this promoter sequence contains sequences which are associated with environmental signals such as the sucrose response elements. Five boxes were identified as hormonal cues particularly IAA-Re, ABA-Re and SA-Re, and there were five development-related domains, mainly MADS-BOX domains and one *Agamous-like binding element* (AGL3) (Chen, 2005). This complexity of transcription factors that may bind to the specific DNA binding domains of *TR-ACO2* could possibly contribute to the constitutive gene expression in both the main and lateral roots. In comparison with the *TR-ACO1* promoter with at least three identified AGL domains, the *TR-ACO2* promoter sequence has only one (Chen and McManus, 2006) and this AGL domain is not identified to be involved in the development of the LRP or the meristem of the root. Since the *TR-ACO2* promoter sequence contains a high number of MADS box protein domains which are specific for floral meristem identity, this may suggest that the *TR-ACO2* gene may encode for the primary TR-ACO enzyme which mediates the synthesis of 'house-keeping' ethylene not only in the leaf tissues of white clover as observed by Hunter *et al.* (1999) and by Chen and McManus (2006), but also in the roots as observed in this study, and in other organs.

5.1.3 Differential expression of *TR-ACO3* gene in white clover roots

The result of sqRT-PCR showed a greater *TR-ACO3* transcript abundance in the main roots and less in the lateral roots, which is in contrast with what has been shown for the

TR-ACO1 and *TR-ACO2* genes, indicating a difference in the regulatory mechanism among the three members of the *TR-ACO* gene family.

This study also shows that the *TR-ACO3* promoter-driven GUS expression, that primarily occurred in the main roots, was absent from the lateral roots. Within the main root, the predominant GUS staining was in the maturation zone (Figure 3.5). Further analysis of the sectioned tissues revealed that, while there was GUS staining in different tissues within the longitudinal section from the epidermis to the cortical cells and stele, GUS expression was absent from the developing lateral roots as well as in the meristem, which was opposite to what had been detected for *TR-ACO1*. This suggests that the *TR-ACO3* gene is predominantly expressed in the relatively mature tissues of the white clover roots. This observation compliments the gene expression studies in the white clover leaves by Hunter *et al.* (1999) using northern analysis, and the results of *in situ* hybridisation (Chen and McManus, 2006) wherein *TR-ACO3* was found to be primarily expressed in the mature and senescent leaf tissues. Further, by GUS staining, Chen and McManus (2006) determined that the promoter sequence of the *TR-ACO3* gene directed greatest expression in the ontologically older tissues, indicating that the *TR-ACO3* gene is expressed preferentially in the mature tissues.

Analysis, *in silico*, has ascertained that the 5′ flanking sequences of *TR-ACO3* contain a high proportion of ethylene response elements (Chen and McManus, 2006) and since ethylene production is generally associated with maturation and senescence, this suggests that TR-ACO3 is the enzyme which mediates the ethylene biosynthesis in the mature and senescing tissues. The involvement of ACC oxidase in ethylene production which plays a role in the maturation and senescence of snow pea pods has also been reported (Pariasca *et al.*, 2001), confirming the complex involvement of ethylene in the maturation and senescence of various plant organs, not only in the leaves, but also in the

pods. In this study, a role for *TR-ACO3* generated ethylene in root maturation and senescence is also proposed.

In leaves, *TR-ACO3* gene expression is associated with ethylene production during maturation and senescence, and so its expression in the mature tissues in the root indicates the likelihood that *TR-ACO3* could also participate in some important development process associated with maturity. Various published reports have postulated the involvement of ethylene in root hair formation and in the legume-Rhizobium symbiosis in the roots. In fact, a marked reduction in root hair development was reported when the roots of *P. vulgaris* seedlings were treated with AVG, which is a potent inhibitor of ACC synthase activity. Upon addition of ACC, an immediate precursor of ethylene, root hair formation was enhanced (Srinivasan *et al.*, 1997) indicating a significant role played by ethylene in the process of root hair production. Even in non-legume plants such as in *Arabidopsis*, ethylene has been found to be an essential regulator of root hair development (Zhu *et al.*, 2006). Previously, ethylene participation in root hair development of *Arabidopsis* was viewed as a dual function. The first function is believed to be related to its role played in the initiation of root hairs from the epidermal cells, and secondly, for root hair elongation (Dolan, 2001). It is important to note that root hairs arise from the maturation zone as epidermal projections, and, since in legumes such as in *Medicago truncatula*, root hairs are known to be the primary site for the recognition and infection by the symbiotic nitrogen-fixing bacteria (Covitz *et al.*, 1998), it may then be possible that the expression of *TR-ACO3* in the mature root zone of white clover enhances ethylene production which may play a role in the root hair development and nodule formation in white clover roots. The findings that *TR-ACO3* is predominantly expressed in the maturation zone and the likelihood that ethylene participates in root hair development in white clover is significant since white clover is a

legume and nodule formation is considered an important developmental process. It should be noted that in this thesis, sufficient levels of nitrogen was included to inhibit nodule formation.

Evidence that members of the *TR-ACO* gene family are divergent and differentially expressed at distinct developmental stages in white clover roots has been provided in this thesis. Moreover, the pattern of expression in root tissues shows a close resemblance with the pattern of expression during leaf ontogeny in white clover. These findings suggest that each gene is developmentally regulated in a gene-specific manner not only in the leaves but also in the roots. Since the site of expression of *ACO* genes determines the site of release and action of ethylene (Grichko and Glick, 2001), it can then be postulated that in white clover roots, ethylene is synthesised from different tissues during root growth and development, and in the process, each of these three *TR-ACO* genes plays a distinct and diverse regulatory role that may be essential if the plant is to respond to the to a variety of physiological and environmental cues that are perceived by roots.

5.2 Adaptive responses of white clover roots to phosphate supply

5.2.1 Changes in root morphology in response to phosphate supply

Morphological studies show that the main roots of plants grown in Pi depleted media were significantly longer when compared to those under Pi sufficiency. The greatest growth rate occurred between the sixth and ninth day after Pi depletion (Figure 3.6B), and this was observed in at least two independent experiments. The current results strongly support the recent observations on some pasture species such as *Holcus lanatus* L. and *Lolium rigidum* Gaudin in which the specific root length increased in response to phosphate starvation. However, these Pi deficient roots had a smaller diameter relative to

the Pi sufficient roots (Hill *et al.*, 2006). In the current study, the diameter of the roots were not examined and, therefore' it was not possible to draw a correlation between root length and its diameter. However, since white clover *cv* HUIA is an elite genotype, it could be possible that the root response to low Pi may be species-specific, or may occur in a genotype-specific manner. For instance, in the *P. vulgaris* seedlings, 'DOR 364' which is known to be a Pi-inefficient genotype (low yield when grown in low Pi media), produced longer and deeper roots in response to a limiting amount of Pi whereas the Pi-efficient genotype 'G19833' (yield is almost two-fold when grown under low Pi) produced relatively shorter and shallower roots (Liao *et al.*, 2001), indicating that even in the same plant species, genotypes may exhibit different responses to Pi supply in terms of root morphology.

In this study, the increase in length of the primary roots in response to Pi depletion was observed in both the wild type (Figure 3.6B) and transgenic lines (data not shown), indicating that despite differences in their genetic constitution, the changes in the root morphology was the same, suggesting that the response is an essential coping mechanism of white clover to Pi limitation. Pi deficiency can trigger both biotic and abiotic stress in plants which in turn can stimulate cellular responses and signalling cascades essential for growth and development (Rohila and Yang, 2007). In *Arabidopsis*, the quiescent centre of the roots acts as the sensor for any environmental signal which, when perceived by the plants, can trigger mechanisms leading to changes in cell division and differentiation causing alterations in the architecture of the root system (Lopez-Bucio *et al.*, 2003; Sanchez-Calderon *et al.*, 2005). Possibly in white clover the response to Pi stress involves not only signals that induce cell division and differentiation but may also include signals for cell elongation which in turn results in the formation of longer roots.

A significant increase in the number of lateral roots was also noted in Pi depleted plants at day 6 (Figure 3.7A) and the greatest rate of root growth was noted between day 9 and day 12. This result indicates that it takes more than a week for the Pi depleted white clover to exhibit some morphological changes in response to Pi limitation under the plant growth conditions used in this study. Lateral roots arise from the anticlinal founder cells in the pericycle, and the succession of cell cycle leading to lateral root formation has been associated with the involvement of some plant hormones, particularly auxin (De Smet *et al.*, 2006). In this study, the *TR-ACO1* promoter-driven GFP fluorescence, reflecting the expression of the *TR-ACO1* gene, was intense in the pericycle of the root. Further, in Pi depleted roots, GFP fluorescence in the lateral root primordia was very intense a day after Pi depletion suggesting upregulation of the *TR-ACO1* gene, and therefore, indicating the possible involvement of this gene (and ethylene) in the phosphate-stressed induced lateral root formation in white clover.

While a significant increase in the number of lateral roots and length of main roots was observed in response to Pi depletion, the difference in the weight of root biomass, both on a fresh weight and on a dry weight basis, was insignificant when the Pi depleted and Pi sufficient roots were compared (Figure 3.9). This indicates that the increase in the length of roots and in the number of lateral roots is mainly due to some modification in the architecture of root system in response to Pi depletion and not due to an actual increase in root production in the plant. From previous studies, the root biomass accumulation in response to Pi supply appears to be species-specific or genotype-specific. In *P. vulgaris* for instance, the root biomass was not consistently affected by the availability of Pi as it was noted that the Pi-inefficient genotype (DOR 364) produced longer adventitious roots per unit weight of biomass relative to the Pi-efficient genotype (GI9833) (Miller *et al.*, 2003). Also, in maize seedlings supplied with either

high or low Pi, the difference in root biomass accumulation was determined to be independent of Pi treatment and instead attributed to genotypic differences (Zhu and Lynch, 2004). Similarly, in *Eichhornia crassipes,* an almost 2-fold increase in lateral root production and a more than 2-fold increase in lateral root length was observed in response to Pi limitation but the estimated reduction in root diameter was *ca.* 20%. Therefore, the difference in root biomass between the Pi treatments was insignificant (Xie and Yu, 2003). In the current study, the diameter of the roots was not measured and so it was not determined whether or not a difference in diameter exists which may have also contributed to the insignificant difference in the root biomass accumulation.

5.2.2 Anatomical changes in the roots in response to phosphate supply

Apart from some changes in the root morphology, one effect of the limiting amount of phosphate is the formation of intercellular spaces, which causes aerenchyma formation in the roots of plants. Formation of these intercellular spaces can be part of a normal developmental process or can be a form of response to some types of stress (Evans, 2004). In this study, intercellular spaces were observed in both longitudinal (Figure 3.10) and transverse sections (Figure 3.11) of Pi depleted roots, four days after Pi depletion. These were detected in the outer and middle sections of the cortex, and since these intercellular spaces were not noted in the sections of Pi sufficient roots, this may be indicative of a stress response to Pi limitation. Formation of intercellular spaces in the roots of *P. vulgaris* has also been associated with the reduction in the Pi concentration in the root zone, and the extent of the intercellular spaces observed in the root cortex corresponded to a decrease in the respiratory requirement as well as for the required phosphate in the roots of Pi starved plants (Fan *et al*., 2003). In the study with *P. vulgaris,* the reduction in root respiration in the Pi deficient roots was associated with the extent of aerenchyma formation in the root cross sectional area and this phenomenon

was attributed to the replacement of some living cortical cells with air spaces (Fan *et al.*, 2003). The requirement for Pi in aerenchymatous tissue was also found to be reduced since the Pi released from the cortical tissue to the intercellular gas space was instead diverted to other tissues, particularly to meet the Pi requirements for cell elongation which is crucial for the exploration of more nutrients within the root zone.

Two types of aerenchyma formation have been described (Evans, 2004). The first is schizogeny which is due to the differential growth of cells that result in separation of cells in affected tissues, and the second is lysigeny, in which actual cells die to create the gas spaces, sometimes in response to a range of abiotic stresses. Under lysigeny, some cells which were developed during the early stages of development, die and disappear when exposed to adverse environmental cues, leaving the intercellular spaces (Fan *et al.*, 2003). Having considered phosphate depletion as a form of an abiotic stress, it is possible that the intercellular spaces observed in the roots of white clover exposed to limiting amount of phosphate is an example of lysigeny, and the spaces are believed to be formed due to the collapse of some cells which may be essential in the reduction of the phosphate requirement in the roots.

Cell lysis and enhanced aerenchyma formation in the cortical cells in the roots of maize grown under limiting P was also associated with increased ethylene sensitivity (He *et al.*, 1992). This was confirmed when the ethylene action inhibitor, Ag^{+}, added at a low concentration (0.6 μM), was able to inhibit the formation of gas spaces in the root cortex of Pi-deficient plants (He *et al.*, 1992). In the current study, intercellular spaces were noted in roots grown in Pi depleted media. Since the *TR-ACO1* gene is upregulated in Pi depleted roots including the pericycle adjacent to the cortex, it is possible that an interaction exists between Pi and the ethylene produced *via* the induction of *TR-ACO1* gene expression in the formation of these intercellular gas spaces. The involvement of

ethylene in the formation of cortical aerenchyma in response to Pi deficiency has also been reported in peas (Lynch and Brown, 1997) wherein the plants exposed to low Pi showed an increased formation of intercellular spaces, indicating that this response to Pi depletion is not specific to white clover roots but also occurs in other legumes.

5.2.3 Leaf phosphate status and acid phosphatase activity in response to phosphate supply

Leaf Pi content has been previously used as an indicator to assess Pi deficiency symptoms in legume species such as white clover (Zhang and McManus, 2000) and in soybean (Li *et al.*, 2005). P is a macro nutrient, and is essential in various metabolic processes and in either the activation or inactivation of enzymes *via* phosphorylation. During conditions of limited availability of external Pi, the Pi from the older tissues is redistributed to the young leaves and other sink organs (Schachtman *et al.*, 1998). This remobilisation of Pi is essential for the sustained growth and development of the young tissues under Pi deficient conditions.

To analyse leaf Pi content in this study, leaf samples were collected from the first fully expanded leaf of white clover in two independent experiments.The first experiment was conducted for eight days. However, since the significant decline in the Pi level was detected on the eighth day, which was the last observation point, a longer time course of 21 d was then conducted. In Pi depleted plants, there was a relatively stable level of leaf Pi at *ca.* 0.05% per g FW up to day 6 after Pi depletion and then the level started to decline by day 7 (Fig 3.12). In the second experiment, the leaf Pi content in Pi depleted plants also started to significantly decline seven days after Pi depletion (Fig 4.8). To some extent this observation is comparable with that of Zhang and McManus (2000) where although a significant decline in leaf Pi was detected starting at two weeks after Pi starvation, the Pi level started to decline after a week. These results indicate that at least

up to a week after reduction in the external source of Pi, there is still a sufficient amount of internal Pi within the plant tissue which can be remobilised from the older to the younger tissues. The significant decline in the Pi level in the young leaf on day 7 further indicates that the metabolic pool of Pi within the plant tissue is beginning to become exhausted.

During conditions of Pi limitation, the cellular Pi level decreased significantly faster in the roots relative to the leaves. In *Arabidopsis*, for instance, after 24 h in Pi limiting conditions, the Pi content in roots was found to be more than 2-fold lower than the Pi content of the leaves. A significant decline in the Pi content in the leaves was detected only after three days in limiting Pi conditions (Wu *et al.*, 2003). In the study mentioned, however, the developmental stage of the leaf from which the Pi was extracted was not specified. In this thesis, the Pi content in the roots was not examined. Consequently, the temporal decline in the Pi content of the leaves in response to Pi depletion could not be compared relative to that of the roots. The steady level of leaf Pi within the first six days after Pi depletion in the current thesis, which corresponds to at least one week duration as observed by Zhang and McManus (2000), indicates that Pi homeostasis within the plant tissue can still be maintained within six days since the internal Pi is being mobilised from the older to the younger tissues and from other metabolic pools within the plant tissues. However, a decline in the roots can not be excluded.

Under conditions of sufficient supply of external Pi, the vacuole serves as the storage pool of Pi and an estimated 85-95% of the plant Pi is reserved as a ‘non-metabolic pool’. During situations when the Pi level is deficient, the Pi in the vacuole is also used to buffer the cytoplasmic Pi in the leaves of Pi deprived plants (Bieleski, 1973) . Thus, in conditions of severe deficiency nearly all of the Pi in the plant represents the ‘metabolic pool’ and an insignificant amount is left in the vacuole.

In conjunction with the leaf Pi assay, the activity of root acid phosphatase (APase) was also determined. Both water soluble and ionically-bound cell wall activity was examined. In terms of the water soluble proteins, the APase activity significantly increased by day 7 after Pi depletion (Figure 3.13A and Figure 4.9A), which was in concert with a significant decline in the leaf Pi level (Figure 3.12 and Figure 4.8), suggesting that by the time a significant reduction in the Pi level was detected, APase activity correspondingly increased. This form of APase is proposed to be important in the metabolic regulation of plants cells since APase is involved in the hydrolysis of organic compounds and remobilisation of Pi for plant nutrition (Theodorou and Plaxton, 1993; Duff *et al.,* 1994).

Using ionically-bound cell wall proteins, an increase in the APase activity was detected starting at day 2, but significant differences were noted after day 5. The Pi depleted roots had a two-fold and 2.6-fold increase in APase activity by day 7 and day 8, respectively (Figure 3.13 B). In the second experiment, a more than two-fold increase in APase activity occurred by day 14 (Figure 4.9B). This observation is in common with the findings of Wasaki *et al*. (1997), where by immunocytochemical analysis using antibodies raised against secretory acid phosphatase (S-APase), these authors determined that the S-APase protein in white lupin was located in the cell walls and intercellular spaces of the lateral roots. Further, the induction of activity was detectable as early as two days after Pi deprivation. This synchronised induction of APase activity with the decline in the leaf Pi content agreed with the enhanced APase activity from root and leaf tissue excised from Pi deprived white clover plants previously observed by Hunter and McManus (1999). The increase in cell wall APase activity is essential since these extracellular isoforms are proposed to participate in the acquisition and recycling of Pi during conditions of Pi limitation in some plant species such as white lupin (Abel *et al.*,

2002; Vance *et al.*, 2003; Wasaki *et al.*, 2003) and *Arabidopsis* (Abel *et al.*, 2002). Being involved in the recycling and acquisition and in the metabolic pathway of plants for effective Pi utilisation underlines the significance of the upregulation of these two forms of APase (soluble and ionically-bound) in white clover during conditions of limiting Pi.

5.3 TR-ACO protein accumulation and *TR-ACO* gene expression in response to phosphate supply

Members of the *TR-ACO* gene family varied in terms of their responses to Pi limitation. The results of the sq RT-PCR showed upregulation of the *TR-ACO1* gene in Pi depleted roots in a 24 h experiment (Figure 3.18). Accumulation of TR-ACO1 protein was also significantly increased by Pi depletion in a short-term experiment held over 7 days both in wild type (Figure 3.15) and in the transgenic line TR2-1 (Figures 4.11 and 4.12). Protein accumulation at 1 h and 6 h after Pi depletion did not show a consistent trend but a greater recognition by α-TR-ACO1 antibody was consistent starting at 12 h after Pi depletion over all three experiments, suggesting a rapid response to the limiting supply of Pi. This result correlates with the result of western analysis over a time course of seven days which consistently showed greater accumulation of protein in Pi depleted roots (Figures 3.15A and 4.11). Further, in a longer experiment, a similar increase in protein recognition by the α-TR-ACO1 antibody was also noted at 6 d and 9 d after Pi depletion (Figures 3.14A and 4.10A) showing an overlap with the shorter experiment of 7 d and a similar result. This suggests a post transcriptional increase in protein accumulation following the upregulation of the gene.

In the earlier sections (Figure 3.3 and Figure 4.25) it was shown that the *TR-ACO1* promoter directed predominant activity in the lateral root primordium, meristem, and in

the pericycle of the root, and that this gene is upregulated by Pi stress within 12 h after Pi depletion. This indicates that the changes at the molecular level probably occurred prior to some biochemical modifications as well as morphological and anatomical changes in the roots. Evidently *TR-ACO1* responded positively to Pi depletion which is a form of abiotic stress. One factor that may participate in the upregulation of this *TR-ACO1* gene is the presence of the motiff GAATATNC within the promoter sequence which shares 87.5% identity to the PHR1 binding site of a phosphate-starvation inducible gene. This is positioned at -761 upstream of the first ATG of the *TR-ACO1* coding sequence, suggesting that *TR-ACO1* may be a potential candidate gene which is important for the adaptation to Pi stress by white clover. By analysis *in silico*, it has recently been shown found that *ACO* genes are among the phosphate starvation inducible genes in two legume species *Cicer arietinum* and *P. vulgaris* (Graham *et al.*, 2006). However, the tissue analysed was not specified.

Another probable mechanism underlying the induction of the *TR-ACO1* gene can be the possible activation of certain protein kinases or phosphatases in response to Pi stress. During exposure to either biotic or abiotic stress, the mitogen-activated protein kinase (MAPK) cascade is activated which in turn transmits a signal to generate cellular responses in plants. Protein kinase cascades have been found to be activated in *Glycine max, P. vulgaris* and in *M. truncatula* in response to Pi starvation (Graham *et al.*, 2006). Since activation of protein kinases are usually associated with upregulation of genes or signal transduction pathways in some legumes in response to stress, it is possible that Pi depletion also activates some signals to induce ethylene biosynthesis in white clover.

Further, both protein phosphorylation and dephosphorylation have been shown to be necessary for the induction of *ACO* genes in *P. sativum* (Kwak and Lee, 1997) and *Vigna radiata* hypocotyls (Kim *et al.*, 1997). It is possible that in white clover then, once

Pi depletion is perceived by cells, a signal to stimulate certain protein kinases or phosphatases is transmitted which in turn may play a part in the upregulation of *TR-ACO1* gene. This concept, however, does not preclude the possible induction of the *TR-ACS* genes in response to Pi stress, since it is known that *ACS* is also induced by stress. In fact, in *Arabidopsis*, it has been determined that *ACS* genes such as *At-ACS2* and *At-ACS6* are induced, and enzyme activity increased, after the protein is phosphorylated by a MAPK which is activated by certain forms of stress (Liu and Zhang, 2004). Since ACO mediates the last committed step in ethylene biosynthesis, it is possible that the induction of ACS would consequently upregulate ACO. However, in tobacco infected with TMV, the temporal induction of these two enzymes occurs in a different way. Although accelerated ethylene production was associated with the increased accumulation of both ACS and ACO, the ACO induction was observed 2 h earlier than the induction of ACS (Kim *et al.*, 2003), indicating that the regulation of ACS does not always precede the regulation of ACO activity.

The upregulation of the *TR-ACO1* gene in response to Pi depletion can form part of the adaptive mechanism to stress. It was presented in the earlier sections that the greatest growth rate in lateral root production (Figure 3.7A) and main root length (Figure 3.6B) in Pi depleted plants occurred between day 6 and day 9 and this coincided with the period of time that the accumulation of TR-ACO1 protein was starting to level off making the amount of TR-ACO1 protein accumulation in both Pi depleted and Pi sufficient roots comparable. The increase in the intensity of the *TR-ACO1* promoter-driven GFP expression in the meristem of the Pi depleted roots suggests that an immediate cellular response leads to faster cell division and differentiation in preparation for rapid main root elongation. In this thesis, intense GFP accumulation has been observed in the LRP of Pi depleted roots, suggesting greater accumulation of TR-

ACO1 protein in this tissue in response to Pi depletion. Since the primordial root preconditions the formation of lateral roots and given that ACC oxidase is an essential enzyme in ethylene biosynthesis, it is thus proposed that ethylene is involved in the increase in lateral root production in Pi depleted white clover plants. This result also suggests that the roots developed some molecular and biochemical adaptations to the low Pi condition at least a week earlier than the observed changes in the root morphology. Having longer main roots and greater number of lateral roots provides the plant with a better foraging capacity and, hence, better sequestration of any available Pi within the root zone. Thus this study provides some evidence that ethylene is involved in the phosphate-stress induced lateral root production in white clover, and that the *TR-ACO1* gene which encodes for the enzyme TR-ACO1 is involved in the ethylene biosynthesis.

The TR-ACO2 protein accumulation was not significantly affected by short term Pi depletion. Differences in roots excised from plants grown in either Pi sufficient or Pi deficient media were detected only in a relatively long term experiment, with a greater accumulation of TR-ACO2 protein in Pi deficient roots starting at 15 d after Pi depletion (Figure 4.13). In a 12 h experiment, there was no significant difference in the transcript accumulation from extracts of roots obtained from either Pi sufficient or Pi deficient extracts both in wild type (Figure 3.17) and the TR2-1 line (Figure 4.14). Further, it has been suggested that *TR-ACO2* is constitutively expressed in mature green leaves and that TR-ACO2 is the predominant enzyme that mediates the TR-ACO activity in these tissues (Chen and McManus, 2006), indicating a role for TR-ACO2 as the major producer of the 'house-keeping' ethylene. However, further analysis revealed that the 5′ flanking sequence of the *TR-ACO2* gene contains a DNA-binding domain **CATTAATTCG** which has 90% homology with Box II of vegetative storage protein-β

(*Vsp*β) gene promoter. This Box II sequence is located within the phosphate response domain of the VSPβ promoter and has been proposed to mediate responses of some plants to phosphate availability (Tang *et al.*, 2001).

The *Vsp*β gene had also been been identified in a number of plants including alfalfa (Meuriot *et al.*, 2004), and white clover (Goulas *et al.*, 2001). Certain proteins related to the soybean VSPβ have also been detected in other legume species such as common bean and peas, although accumulation was relatively weak when compared to the soybean protein (Tang *et al.*, 2001).

The presence of the sequence motif in the *TR-ACO2* promoter with homology to the box II of the *Vsp*β promoter may suggest that *TR-ACO2* gene expression is regulated by Pi supply. In this thesis, no apparent induction by low P supply were observed over a 24-hour period using sqRT-PCR. However, the phosphate binding domain may play a role in mediating *TR-ACO2* upregulation within a longer period (several days) in low Pi.

The expression of the *TR-ACO3* gene in response to Pi availability did not follow the trends observed for *TR-ACO1* and *TR-ACO2.* At 1 h, 12 h and 24 h after Pi depletion there was a considerable decrease in the *TR-ACO3* transcript accumulation in Pi depleted extracts while at 6 h and 18 h, transcript accumulation was greater in the Pi depleted extracts. The difference was more noticeable in the Southern analysis of the cDNA blot (Figures 3.23 and 4.20). Other than the effect of Pi, there might be other factors which may have affected this seemingly erratic trend in gene expression. These include the time of the day of sample collection, or the length of time of exposure to the light at the sampling. In terms of the time, at times close to mid day (1 h, 12 h, and 24 h after Pi depletion), *TR-ACO3* gene was down regulated in Pi depleted roots while at times close to dawn (6 h) and sunset (18 h), there was a greater transcript abundance in Pi depleted

roots. This appears to indicate that during the time of the day when the plants are most active photosynthetically, the *TR-ACO3* gene was down regulated in response to Pi depletion. Then, in the early morning and late in the afternoon, the gene was upregulated. Analysis *in silico* revealed that the *TR-ACO3* promoter contains light responsive elements that include a small sub-unit of RUBISCO (Chen and McManus, 2006) and this may suggest that to some extent the expression of the *TR-ACO3* gene is influenced by the length of time of exposure to daylight. However, the pattern to associate this response to the light responsive elements is not yet well understood, given that expression was determined in the root tissues.

Overall, the results presented in this thesis provide further evidence that expression of members of the *TR-ACO* gene family is not only developmentally and spatially regulated in white clover roots but it is also divergent in terms of the temporal expression. Although the genes had been triggered by the same stimuli, in this case, Pi depletion, and despite the fact that the three genes share a high degree of homology in their coding sequences (Chen and McManus, 2006), each member of the gene family exhibited transient differential expression. This suggests that the greater divergence observed in their promoter sequences may contain regulatory elements that lead to the highly divergent regulatory pathways between the three genes in response to phosphate stress. The differential regulation of the three *TR-ACO* genes particularly in the roots underlines their significance in fine tuning the white clover response to a variety of stimuli not only during exposure to Pi stress, but probably also in response to other environmental cues.

5.4 Future work

This study has unravelled basic information on the differential expression of members of *TR-ACO* gene family in the roots of white clover, both spatially and temporally in response to Pi supply. However, within the project duration, there were interesting avenues of research which were not given due consideration and, therefore, provide potential study areas in the future.

- It would be interesting to investigate the possible involvement of the plant hormone auxin in the induction of ACC oxidase and in response to Pi depletion

In the previous discussion, evidence was shown that *TR-ACO1* is predominantly expressed in the lateral roots and ethylene has been implicated in the regulation of root extension and lateral root production. Although not explored in this study, it has been known for many years that root meristems are known sites of auxin synthesis (Ljung *et al.*, 2005) and that this hormone is also involved in lateral root formation. Therefore, the involvement of auxin in the cell division and elongation of roots should not be under estimated. An interaction between ethylene and auxin had been implicated in root and root hair elongation (Pitts *et al.*, 1998; Zhu *et al.*, 2006) and in the control of various root developmental processes (Yoon *et al.*, 1999; Rahman *et al.*, 2002; Takahashi *et al.*, 2003; Chilley *et al.*, 2006). Many years ago, it was proposed that auxin induces ethylene biosynthesis (Kang *et al*., 1971; Sakai and Imaseki, 1971; Aharoni and Yang, 1983; Castellano and Vioque, 2002) and that endogenous levels of auxin stimulate ethylene production from different parts of the plants such as roots and other vegetative tissues, stems, and leaves (Abeles and Rubinstein, 1964). Later, it was suggested that stimulation of ethylene production by auxin was due to enhanced synthesis of the ACC synthase which is an enzyme involved in the biosynthetic pathway (Abeles, 1966). Whether the

expression of *TR-ACO1* gene in the pericycle and in the meristem was due to auxin-induced ACC synthase upregulation or due to auxin-induced upregulation of the *TR-ACO1* gene is not yet known. While this association between auxin and ethylene signalling in white clover roots is still unclear, this offers an interesting research area in the future.

- An auxin inhibitor should be used to find out if the Pi stress-induced lateral root formation is a sole effect of the *TR-ACO* gene and ethylene biosynthesis, or whether it has to be induced by auxin.
- The direct effect of ethylene (added exogenously) on the Pi stress induced lateral root formation in white clover should also be investigated. While in this study, the association between ethylene and Pi supply has been implied after the upregulation of *TR-ACO1* gene in Pi depleted roots, a detailed study on the direct effect of added ethylene is necessary.
- The effects of using an anti-sense construct of *TR-ACO1* to transform white clover in terms of whether under Pi depletion, lateral root formation will not be induced also needs to be investigated. In addition, the effect of inhibitor of ACS activity (eg. AVG), or ACO activity can be assessed.
- An investigation on the tissue specific localisation of promoter activity of other members of the *TR-ACO* gene family needs to be investigated. *In situ* hybridisation would provide a detailed analysis of gene expression in the roots to further confirm the observed tissue specific localisation of the *TR-ACO1* promoter activity and to gain information on the tissue specific localisation of expression of the other members of the *TR-ACO* gene family.

References

Abel S, Ticconi CA, Delatorre CA (2002) Phosphate sensing in higher plants. *Physiologia Plantarum* **115:** 1-8

Abeles FB (1966) Auxin stimulation of ethylene evolution. *Plant Physiology* **41:** 585-588

Abeles FB, Morgan PW, Saltveit Jr. ME (1992) *Ethylene in plant biology*, Ed 2nd ed. Academic Press, New York

Abeles FB, Rubinstein B (1964) Regulation of ethylene evolution and leaf abscission by auxin. *Plant Physiology* **39:** 963-969

Adams DO, Yang SF (1979) Ethylene biosynthesis: Identification of 1-amino-cyclopropane-1-carboxylic acid as an intermediate in the conversion of methionine to ethylene. *Proceedings of the National Academy of Sciences of the United States of America* **76:** 170-174

Adams-Phillips L, Barry C, Giovannoni J (2004) Signal transduction systems regulating fruit ripening. *Trends in Plant Science* **9:** 331-338

Aharoni N, Yang SF (1983) Auxin-induced ethylene production as related to auxin metabolism in leaf-disks of tobacco and sugar-beet. *Plant Physiology* **73:** 598-604

Alexander L, Grierson D (2002) Ethylene biosynthesis and action in tomato: a model for climacteric fruit ripening. *Journal of Experimental Botany* **53:** 2039-2055

Almeida JPF, Luscher A, Frehner M, Oberson A, Nosberger J (1999) Partitioning of P and the activity of root acid phosphatase in white clover (*Trifolium repens* L.) are modified by increased atmospheric CO_2 and P fertilisation. *Plant and Soil* **210:** 159-166

Alonso JI, Stepanova AN (2004) The ethylene signaling pathway. *Science* **306:** 1513-1515

Ansari HA, Ellison NW, Reader SM, Badaeva ED, Friebe B, Miller TE, Williams WM (1999) Molecular cytogenetic organization of 5S and 18S-26S rDNA loci in white clover (*Trifolium repens* L.) and related species. *Annals of Botany* **83:** 199-206

Apelbaum A, Burgoon AC, Anderson JD, Solomos T, Lieberman M (1981) Some characteristics of the system converting 1-aminocyclopropane-1-carboxylic acid to ethylene *Plant Physiology* **67:** 80-84

Ashihara H, Li XN, Ukaji T (1988) Metabolic-regulation in plant-cell culture .25. Effect of inorganic-phosphate on the biosynthesis of purine and pyrimidine nucleotides in suspension-cultured cells of *Catharanthus roseus*. *Annals of Botany* **61:** 225-232

Atkinson RG, Bolitho KM, Wright MA, Iturriagagoitia-Bueno T, Reid SJ, Ross GS (1998) Apple ACC-oxidase and polygalacturonase: ripening-specific gene expression and promoter analysis in transgenic tomato. *Plant Molecular Biology* **38:** 449-460

Atwell BJ, Eamus D (1999) Differentiation and gene expression. In: *Plants in Action. Adaptation in Nature, Performance in Cultivation*. MacMillan Education Australia Pty Ltd., Australia

Bailly C, Bogatek R, Dumet D, Corbineau F, Come D (1995) Effects of 1-amino-cyclopropane-1-carboxylic acid and oxygen concentrations on *in-vivo* and *in-vitro* activity of ACC oxidase of sunflower hypocotyl segments. *Plant Growth Regulation* **17:** 133-139

Baker M, Williams W (1987) *White Clover*. CAB International Oxon, UK

Barry CS, Blume B, Bouzayen M, Cooper W, Hamilton AJ, Grierson D (1996) Differential expression of the 1-aminocyclopropane-1-carboxylate oxidase gene family of tomato. *Plant Journal* **9:** 525-535

Basu P, Zhang YJ, Lynch JP, Brown KM (2007) Ethylene modulates genetic, positional, and nutritional regulation of root plagiogravitropism. *Functional Plant Biology* **34:** 41-51

Bates TR, Lynch JP (2001) Root hairs confer a competitive advantage under low phosphorus availability. *Plant and Soil* **236:** 243-250

Bhadoria PS, El Dessougi H, Liebersbach H, Claassen N (2004) Phosphorus uptake kinetics, size of root system and growth of maize and groundnut in solution culture. *Plant and Soil* **262:** 327-336

Bhowmik PK, Matsui T (2004) Changes in the activity and expression of 1-aminocyclopropane-1-carboxylate (ACC) synthase, ACC oxidase, and phenylalanine ammonia-lyase in asparagus spears in response to wound-induced ethylene synthesis. *Hortscience* **39:** 1074-1078

Bhowmik PK, Matsui T (2005) Ethylene biosynthetic genes in 'Moso' bamboo shoot in response to wounding. *Postharvest Biology and Technology* **38:** 188-194

Bieleski RL (1973) Phosphate pools, phosphate transport, and phosphate availability. *Annual Review of Plant Physiology and Plant Molecular Biology* **24:** 225-252

Bio-Rad (n.d.) *Mini Trans-Blot Electrophoretic Transfer Cell Instruction Manual*

Bleecker AB, Kende H (2000) Ethylene: A gaseous signal molecule in plants. *Annual Review of Cell and Developmental Biology* **16:** 1-+

Blume B, Grierson D (1997) Expression of ACC oxidase promoter-GUS fusions in tomato and *Nicotiana plumbaginifolia* regulated by developmental and environmental stimuli. *Plant Journal* **12:** 731-746

Borch K, Bouma TJ, Lynch JP, Brown KM (1999) Ethylene: a regulator of root architectural responses to soil phosphorus availability. *Plant Cell and Environment* **22:** 425-431

Bouquin T, Lasserre E, Pradier Jrm, Pech J-C, BalaguÃ© C (1997) Wound and ethylene induction of the ACC oxidase melon gene *CM-ACO1* occurs *via* two direct and independent transduction pathways. *Plant Molecular Biology* **35:** 1029-1035

Bowling DJ, Dunlop J (1978) Uptake of phosphate by white clover. 1. Evidence for an electrogenic phosphate pump. *Journal of Experimental Botany* **29:** 1139-1146

Bradford K, Yang S (1980) Xylem transport of 1-aminocyclopropane-1-carboxylic acid, an ethylene precursor, in waterlogged tomato plants. *Plant Physiology* **65:** 322-326

Bragina TV, Martinovich LI, Rodionova NA, Bezborodov AM, Grineva GM (2001) Ethylene-induced activation of xylanase in adventitious roots of maize as a response to the stress effect of root submersion. *Applied Biochemistry and Microbiology* **37:** 618-621

Britsch L, Grisebach H (1986) Purification and characterization of flavonone 3-hydroxylase from *Petunia hybrida*. *European Journal of Biochemistry* **156:** 569-577

Buchanan B, Gruissem W, Jones R (2000) *Biochemistry and Molecular Biology of Plants*. American Society of Plant Physiologists, Rockville Maryland

Burgeff C, Liljegren SJ, Tapia-López R, Yanofsky MF, Alvarez-Buylla ER (2002) MADS-box gene expression in lateral primordia, meristems and differentiated tissues of Arabidopsis thaliana roots. *Planta* **214:** 365-372

Caradus JR, Snaydon RW (1987) Aspects of the phosphorus nutrition of white clover populations .1. Inorganic phosphorus content of leaf tissue. *Journal of Plant Nutrition* **10:** 273-285

Caradus JR, Snaydon RW (1987) Aspects of the phosphorus nutrition of white clover populations .2. Root exocellular acid phosphatase activity. *Journal of Plant Nutrition* **10:** 287-301

Castellano JM, Vioque B (2002) Characterisation of the ACC oxidase activity in transgenic auxin overproducing tomato during ripening. *Plant Growth Regulation* **38:** 203-208

Chae HS, Cho YG, Park MY, Lee MC, Eun MY, Kang BG, Kim WT (2000) Hormonal cross-talk between auxin and ethylene differentially regulates the expression of two members of the 1-aminocyclopropane-1-carboxylate oxidase gene family in rice (*Oryza sativa* L.). *Plant and Cell Physiology* **41:** 354-362

Chaudhry Z, Yoshioka T, Satoh S, Hase S, Ehara Y (1998) Stimulated ethylene production in tobacco (*Nicotiana tabacum* L. cv. Ky 57) leaves infected systemically with cucumber mosaic virus yellow strain. *Plant Science* **131:** 123-130

Chawla HS (2003) *Plant Biotechnology; A Practical Approach*. Science Publishers, Inc., Enfield, USA

Chen BCM, McManus MT (2006) Expression of 1-aminocyclopropane-1-carboxylate (ACC) oxidase genes during the development of vegetative tissues in white clover (*Trifolium repens* L.) is regulated by ontological cues. *Plant Molecular Biology* **60:** 451-467

Chen CM (2005) *Expression Studies of the ACC Oxidase Gene Family of White Clover (Trifolium repens L.)*. Ph.D. Thesis Massey University, Palmerston North

Chen YT, Lee YR, Yang CY, Wang YT, Yang SF, Shaw JF (2003) A novel papaya ACC oxidase gene (*CP-ACO2)* associated with late stage fruit ripening and leaf senescence. *Plant Science* **164:** 531-540

Chilley PM, Casson SA, Tarkowski P, Hawkins N, Wang KLC, Hussey PJ, Beale M, Ecker JR, Sandberg GK, Lindsey K (2006) The POLARIS peptide of Arabidopsis regulates auxin transport and root growth via effects on ethylene signaling. *Plant Cell* **18:** 3058-3072

Chomczynski P (1992) One-hour downward alkaline capillary transfer for blotting of DNA and RNA. *Analytical Biochemistry* **201:** 134-139

Chung MC, Chou SJ, Kuang LY, Charng YY, Yang SF (2002) Subcellular localization of 1-aminocyclopropane-1-carboxylic acid oxidase in apple fruit. *Plant and Cell Physiology* **43:** 549-554

Church G, Gilbert W (1984) Genomic sequencing. *Proceedings of the National Academy of Sciences of the United States of America* **81:** 1991-1995

Covitz PA, Smith LS, Long SR (1998) Expressed sequence tags from a root-hair-enriched *Medicago truncatula* cDNA library. *Plant Physiology* **117:** 1325-1332

Daram P, Brunner S, Rausch C, Steiner C, Amrhein N, Bucher M (1999) Pht2;1 encodes a low-affinity phosphate transporter from Arabidopsis. *Plant Cell* **11:** 2153-2166

Dembinsky D, Woll K, Saleem M, Liu Y, Fu Y, Borsuk LA, Lamkemeyer T, Fladerer C, Madlung J, Barbazuk B, Nordheim A, Nettleton D, Schnable PS, Hochholdinger F (2007) Transcriptomic and proteomic analyses of pericycle cells of the maize primary root. *Plant Physiology* **145:** 575-588

De Smet I, Vanneste S, Inze D, Beeckman T (2006) Lateral root initiation or the birth of a new meristem. *Plant Molecular Biology* **60:** 871-887

de Wild HPJ, Balk PA, Fernandes ECA, Peppelenbos HW (2005) The action site of carbon dioxide in relation to inhibition of ethylene production in tomato fruit. *Postharvest Biology and Technology* **36:** 273-280

Destefanobeltran LJC, Vancaeneghem W, Gielen J, Richard L, Vanmontagu M, Vanderstraeten D (1995) Characterization of three members of the ACC synthase gene family in *Solanum tuberosum* L. *Molecular & General Genetics* **246:** 496-508

Ding YL, Aldao-Humble G, Ludlow E, Drayton M, Lin YH, Nagel J, Dupal M, Zhao GQ, Pallaghy C, Kalla R, Emmerling M, Spangenberg G (2003) Efficient plant regeneration and *Agrobacterium*-mediated transformation in *Medicago* and *Trifolium* species. *Plant Science* **165:** 1419-1427

Dolan L (1997) The role of ethylene in the development of plant form. *Journal of Experimental Botany* **48:** 201-210

Dong JG, Fernandezmaculet JC, Yang SF (1992) Purification and characterization of 1-aminocyclopropane-1-carboxylate oxidase from apple fruit. *Proceedings of the National Academy of Sciences of the United States of America* **89:** 9789-9793

Drew MC, He CJ, Morgan PW (2000) Programmed cell death and aerenchyma formation in roots. *Trends in Plant Science* **5:** 123-127

Dubrovsky JG, Doerner PW, Colon-Carmona A, Rost TL (2000) Pericycle cell proliferation and lateral root initiation in Arabidopsis. *Plant Physiology* **124:** 1648-1657

Duff SMG, Sarath G, Plaxton WC (1994) The role of acid phosphatases in plant phosphorus metabolism. *Physiologia Plantarum* **90:** 791-800

Dunkley HM, Golden KD (1998) ACC oxidase from *Carica papaya:* Isolation and characterization. *Physiologia Plantarum* **103:** 225-232

English PJ, Lycett GW, Roberts JA, Jackson MB (1995) Increased 1-aminocyclopropane-1-carboxylic acid oxidase activity in shoots of flooded tomato plants raises ethylene production to physiologically active levels. *Plant Physiology* **109:** 1435-1440

Evans DE (2004) Aerenchyma formation. *New Phytologist* **161:** 35-49

Fan MS, Zhu JM, Richards C, Brown KM, Lynch JP (2003) Physiological roles for aerenchyma in phosphorus-stressed roots. *Functional Plant Biology* **30:** 493-506

Finlayson SA, Reid DM (1996) The effect of CO_2 on ethylene evolution and elongation rate in roots of sunflower (*Helianthus annuus*) seedlings. *Physiologia Plantarum* **98:** 875-881

Finlayson SA, Reid DM, Morgan PW (1997) Root and leaf specific ACC oxidase activity in corn and sunflower seedlings. *Phytochemistry* **45:** 869-877

Finnegan J, McElroy D (1994) Transgene inactivation - Plants fight back. *Bio-Technology* **12:** 883-888

Franco-Zorrilla JM, Gonzalez E, Bustos R, Linhares F, Leyva A, Paz-Ares J (2004) The transcriptional control of plant responses to phosphate limitation. *Journal of Experimental Botany* **55:** 285-293

Fukaki H, Okushima Y, Tasaka M (2007) Auxin-mediated lateral root formation in higher plants. *In* International Review of Cytology - a Survey of Cell Biology, Vol 256, Vol 256, pp 111-137

Gahoonia TS, Nielsen NE (1998) Direct evidence on participation of root hairs in phosphorus (^{32}P) uptake from soil. *Plant and Soil* **198:** 147-152

Gapper NE, Coupe SA, McKenzie MJ, Scott RW, Christey MC, Lill RE, McManus MT, Jameson PE (2005) Senescence-associated down-regulation of 1-aminocyclopropane-1-carboxylate (ACC) oxidase delays harvest-induced senescence in broccoli. *Functional Plant Biology* **32:** 891-901

Gapper NE, Coupe SA, McKenzie MJ, Sinclair BK, Lill RE, Jameson PE (2005) Regulation of harvest-induced senescence in broccoli (*Brassica oleracea* var. italica) by cytokinin, ethylene, and sucrose. *Journal of Plant Growth Regulation* **24:** 153-165

Gapper NE, McKenzie MJ, Christey MC, Braun RH, Coupe SA, Lill RE, Jameson PE (2002) *Agrobacterium tumefaciens*-mediated transformation to alter ethylene and cytokinin biosynthesis in broccoli. *Plant Cell Tissue and Organ Culture* **70:** 41-50

Garabagi F, Strommer J (2000) Green fluorescent protein as an all-purpose reporter in petunia. *Plant Molecular Biology Reporter* **18:** 219-226

Gibeaut DM, Hulett J, Cramer GR, Seemann JR (1997) Maximal biomass of *Arabidopsis thaliana* using a simple, low maintenance hydroponic method and favorable environmental conditions. *Plant Physiology* **115:** 317-319

Gilbert GA, Knight JD, Vance CP, Allan DL (2000) Proteoid root development of phosphorus deficient lupin is mimicked by auxin and phosphonate. *Annals of Botany* **85:** 921-928

Gomez-Jimenez MC, Matilla AJ, Garrido D (1998) Isolation and characterization of a cDNA encoding an ACC oxidase from *Cicer arietinum* and its expression during embryogenesis and seed germination. *Australian Journal of Plant Physiology* **25:** 765-773

Gomez-Jimenez MD, Garcia-Olivares E, Matilla AJ (2001) 1-aminocyclopropane-1-carboxylate oxidase from embryonic axes of germinating chick-pea (*Cicer arietinum* L.) seeds: Cellular immunolocalization and alterations in its expression by indole-3-acetic acid, abscisic acid and spermine. *Seed Science Research* **11:** 243-253

Gomez-Lim M, Valdes-Lopez V, Cruz-Hernandez A, Saucedo-Arias L (1993) Isolation and characterization of a gene involved in ethylene biosynthesis from *Arabidopsis thaliana*. *Gene* **134:** 217-221

Gong DM, McManus MT (2000) Purification and characterisation of two ACC oxidases expressed differentially during leaf ontogeny in white clover. *Physiologia Plantarum* **110:** 13-21

Goulas E, Le Dily F, Teissedre L, Corbel G, Robin C, Ourry A (2001) Vegetative storage proteins in white clover (*Trifolium repens* L.): Quantitative and qualitative features. *Annals of Botany* **88:** 789-795

Graham MA, Ramirez M, Valdes-Lopez O, Lara M, Tesfaye M, Vance CP, Hernandez G (2006) Identification of candidate phosphorus stress induced genes in *Phaseolus vulgaris* through clustering analysis across several plant species. *Functional Plant Biology* **33:** 789-797

Grichko VP, Glick BR (2001) Ethylene and flooding stress in plants. *Plant Physiology and Biochemistry* **39:** 1-9

Gunawardena A, Pearce DM, Jackson MB, Hawes CR, Evans DE (2001) Characterisation of programmed cell death during aerenchyma formation induced by ethylene or hypoxia in roots of maize (*Zea mays* L.). *Planta* **212:** 205-214

Guy M, Kende H (1984) Conversion of 1-aminocyclopropane-1-carboxylic acid to ethylene by isolated vacuoles of *Pisum-Sativum*-L. *Planta* **160:** 281-287

Hamilton A, Bouzayen M, Grierson D (1991) Identification of a tomato gene for the ethylene-forming enzyme by expression in yeast. *Proceedings of the National Academy of Sciences of the United States of America* **88:** 7434-7437

Hamilton AJ, Lycett GW, Grierson D (1990) Antisense gene that inhibits synthesis of the hormone ethylene in transgenic plants. *Nature* **346:** 284-286

Hammond JP, Bennett MJ, Bowen HC, Broadley MR, Eastwood DC, May ST, Rahn C, Swarup R, Woolaway KE, White PJ (2003) Changes in gene expression in Arabidopsis shoots during phosphate starvation and the potential for developing smart plants. *Plant Physiology* **132:** 578-596

Hase A, Nishikoori M, Okuyama H (2004) Induction of high affinity phosphate transporter in the duckweed *Spirodela oligorrhiza*. *Physiologia Plantarum* **120:** 271-279

Hay A, Watson L, Zhang C, McManus M (1998) Identification of cell wall proteins in roots of phosphate-deprived white clover plants. *Plant Physiology and Biochemistry* **36:** 305-311

Hayes JE, Richardson AE, Simpson RJ (1999) Phytase and acid phosphatase activities in extracts from roots of temperate pasture grass and legume seedlings. *Australian Journal of Plant Physiology* **26:** 801-809

He CJ, Morgan PW, Drew MC (1992) Enhanced sensitivity to ethylene in nitrogen-starved or phosphate-starved roots of *Zea mays* L. during aerenchyma formation. *Plant Physiology* **98:** 137-142

He Y, Liao H, Yan XL (2003) Localized supply of phosphorus induces root morphological and architectural changes of rice in split and stratified soil cultures. *Plant and Soil* **248:** 247-256

Heidstra R, Cai W, Yang WC, Yalcin Y, Peck S, AnneMie Emons AM, Kammen V, Bisseling T (1997) Ethylene provides positional information on cortical cell division but is not involved in Nod factor-induced root hair tip growth in Rhizobium-legume interaction. *Development* **124:** 1781-1787

Henzi MX, Christey MC, McNeil DL, Davies KM (1999) *Agrobacterium rhizogenes*-mediated transformation of broccoli (*Brassica oleracea L*-var. italica) with an antisense 1-aminocyclopropane-1-carboxylic acid oxidase gene. *Plant Science* **143:** 55-62

Hernandez G, Ramirez M, Valdes-Lopez O, Tesfaye M, Graham MA, Czechowski T, Schlereth A, Wandrey M, Erban A, Cheung F, Wu HC, Lara M, Town CD, Kopka J, Udvardi MK, Vance CP (2007) Phosphorus stress in common bean: root transcript and metabolic responses. *Plant Physiology* **144:** 752-767

Hewitt MM, Carr JM, Williamson CL, Slocum RD (2005) Effects of phosphate limitation on expression of genes involved in pyrimidine synthesis and salvaging in Arabidopsis. *Plant Physiology and Biochemistry* **43:** 91-99

Hill JO, Simpson RJ, Moore AD, Chapman DF (2006) Morphology and response of roots of pasture species to phosphorus and nitrogen nutrition. *Plant and Soil* **286:** 7-19

Hocking PJ, Jeffery S (2004) Cluster-root production and organic anion exudation in a group of old-world lupins and a new-world lupin. *Plant and Soil* **258:** 135-150

Hoffman N, Yang S, Ichihara A, Sakamura S (1982) Stereospecific conversion of 1 -aminocylclopropanecarboxylic acid to ethylene by plant tissues. Conversion of stereoisomers of 1-amino-2-ethylcyclopropanecarboxylic acid to 1-butene. *Plant Physiology* **70:** 195-199

Holdsworth M, Bird C, Ray J, Schuch W, Grierson D (1987) Structure and expression of an ethylene-related mRNA from tomato. *Nucleic Acids Res.* **15:** 731-739

Hraska M, Rakousky S, Curn V (2006) Green fluorescent protein as a vital marker for non-destructive detection of transformation events in transgenic plants. *Plant Cell Tissue and Organ Culture* **86:** 303-318

Huang H, Tudor M, Weiss CA, Hu Y, Ma H (1995) The Arabidopsis MADS-Box gene AGL3 is widely expressed and encodes a sequence-specific DNA-binding protein. *Plant Molecular Biology* **28:** 549-567

Hudgins JW, Ralph SG, Franceschi VR, Bohlmann J (2006) Ethylene in induced conifer defense: cDNA cloning, protein expression, and cellular and subcellular localization of 1-aminocyclopropane-1-carboxylate oxidase in resin duct and phenolic parenchyma cells. *Planta* **224:** 865-877

Hunter DA, McManus MT (1999) Comparison of acid phosphatases in two genotypes of white clover with different responses to applied phosphate. *Journal of Plant Nutrition* **22:** 679-692

Hunter DA, Reid MS (2001) A Simple and rapid method for isolating high quality RNA from flower petals, Vol 543. *International Society for Horticultural Science*, Leuven

Hunter DA, Yoo SD, Butcher SM, McManus MT (1999) Expression of 1-aminocyclopropane-1-carboxylate oxidase during leaf ontogeny in white clover. *Plant Physiology* **120:** 131-141

Itai A, Tanabe K, Tamura F, Tomomitsu M (2003) Cloning and characterization of a cDNA encoding 1-aminocyclopropane-1-carboxylate (ACC) synthase (PPACS3) from ripening fruit of Japanese pear (*Pyrus pyrifolia* Nakai). *Journal of the Japanese Society for Horticultural Science* **72:** 99-106

Jin ES, Lee JH, Kim WT (1998) Biochemical characterization of 1-aminocyclopropane-1-carboxylate oxidase in mung bean hypocotyls. *Journal of Biochemistry and Molecular Biology* **31:** 70-76

Jin YF, Zhu LC, Zhang YZ, Zhang SL (2002) Cloning and differential expression of a 1-aminocyclopropane-1-carboxylate synthase cDNA from peach. *Acta Botanica Sinica* **44:** 1182-1187

Johnson JF, Vance CP, Allan DL (1996) Phosphorus deficiency in *Lupinus albus* - Altered lateral root development and enhanced expression of phosphoenolpyruvate carboxylase. *Plant Physiology* **112:** 31-41

Johnson PR, Ecker JR (1998) The ethylene gas signal transduction pathway: A molecular perspective. *Annual Review of Genetics* **32:** 227-254

Jones ML, Woodson WR (1999) Differential expression of three members of the 1-aminocyclopropane-1-carboxylate synthase gene family in carnation. *Plant Physiology* **119:** 755-764

Jouany C, Cruz P, Petibon P, Duru M (2004) Diagnosing phosphorus status of natural grassland in the presence of white clover. *European Journal of Agronomy* **21:** 273-285

Jung T, Lee JH, Cho MH, Kim WT (2000) Induction of 1-aminocyclopropane-1-carboxylate oxidase mRNA by ethylene in mung bean roots: possible involvement of Ca^{2+} and phosphoinositides in ethylene signalling. *Plant Cell and Environment* **23:** 205-213

Kang BG, Newcomb W, Burg SP (1971) Mechanism of auxin-induced ethylene production. *Plant Physiology* **47:** 504-509

Karthikeyan AS, Varadarajan DK, Jain A, Held MA, Carpita NC, Raghothama KG (2007) Phosphate starvation responses are mediated by sugar signaling in Arabidopsis. *Planta* **225:** 907-918

Kato M, Hayakawa Y, Hyodo H, Ikoma Y, Yano M (2000) Wound-induced ethylene synthesis and expression and formation of 1-aminocyclopropane-1-carboxylate (ACC) synthase, ACC oxidase, phenylalanine ammonia-lyase, and peroxidase in wounded mesocarp tissue of *Cucurbita maxima. Plant and Cell Physiology* **41:** 440-447

Kato M, Hyodo H (1999) Purification and characterization of ACC oxidase and increase in its activity during ripening of pear fruit. *Journal of the Japanese Society for Horticultural Science* **68:** 551-557

Kato M, Kamo T, Wang R, Nishikawa F, Hyodo H, Ikoma Y, Sugiura M, Yano M (2002) Wound-induced ethylene synthesis in stem tissue of harvested broccoli and its effect on senescence and ethylene synthesis in broccoli florets. *Postharvest Biology and Technology* **24:** 69-78

Katz E, Riov J, Weiss D, Goldschmidt EE (2005) The climacteric-like behaviour of young, mature and wounded citrus leaves. *Journal of Experimental Botany* **56:** 1359-1367

Kende H (1989) Enzymes of ethylene biosynthesis. *Plant Physiology* **91:** 1-4

Kim JH, Kim WT, Kang BG (2001) IAA and N-6-benzyladenine inhibit ethylene-regulated expression of ACC oxidase and ACC synthase genes in mungbean hypocotyls. *Plant and Cell Physiology* **42:** 1056-1061

Kim YS, Choi D, Lee MM, Lee SH, Kim WT (1998) Biotic and abiotic stress-related expression of 1-aminocyclopropane-1-carboxylate oxidase gene family in *Nicotiana glutinosa* L. *Plant and Cell Physiology* **39:** 565-573

Kim CY, Liu Y, Thorne ET, Yang H, Fukushige H, Gassmann W, Hildebrand D, Sharp RE, Zhang S (2003) Activation of a stress-responsive mitogen-activated protein kinase cascade induces the biosynthesis of ethylene in plants. *Plant Cell* **15:** 2707-2718

Kim JH, Kim WT, Kang BG, Yang SF (1997) Induction of 1-aminocyclopropane-1-carboxylate oxidase mRNA by ethylene in mung bean hypocotyls: Involvement of both protein phosphorylation and dephosphorylation in ethylene signaling. *Plant Journal* **11:** 399-405

Klee HJ (2002) Control of ethylene-mediated processes in tomato at the level of receptors. *Journal of Experimental Botany* **53:** 2057-2063

Knoester M, Bol JF, Vanloon LC, Linthorst HJM (1995) Virus-induced gene-expression for enzymes of ethylene biosynthesis in hypersensitively reacting tobacco. *Molecular Plant-Microbe Interactions* **8:** 177-180

Koslanund R, Archbold DD, Pomper KW (2005) Pawpaw (*Asimina triloba* L.) Dunal fruit ripening. I. Ethylene biosynthesis and production. *Journal of the American Society for Horticultural Science* **130:** 638-642

Krishan A (1975) Rapid flow cytofluorometric analysis of mammalian cell cycle by propidium iodide staining. *The Journal of Cell Biology* **66:** 188-193

Kruzmane D, Ievinsh G (1999) Characterization of 1-aminocyclopropane-1-carboxylic acid oxidase from barley (*Hordeum vulgare* L.) seedlings and pine (*Pinus sylvestris* L.) needles. *Plant Science* **142:** 13-19

Kuai J, Dilley DR (1992) Extraction, partial purification and characterization of 1-aminocyclopropane-1-carboxylic acid oxidase from apple fruit. *Postharvest Biology and Technology* **1:** 203-211

Kwak SH, Lee SH (1997) The requirements for Ca^{2+}, protein phosphorylation, and dephosphorylation for ethylene signal transduction in *Pisum sativum* L. *Plant and Cell Physiology* **38:** 1142-1149

Laemmli UK (1970) Cleavage of structural proteins during the assembly of the head of bacteriophage T4. *Nature* **227:** 680-685

Lahey KA, Yuan RC, Burns JK, Ueng PP, Timmer LW, Chung KR (2004) Induction of phytohormones and differential gene expression in citrus flowers infected by the fungus *Colletotrichum acutatum*. *Molecular Plant-Microbe Interactions* **17:** 1394-1401

Landsberg EC (1996) Hormonal regulation of iron-stress response in sunflower roots: A morphological and cytological investigation. *Protoplasma* **194:** 69-80

Lasserre E, Bouquin T, Hernandez JA, Bull J, Pech JC, Balague C (1996) Structure and expression of three genes encoding ACC oxidase homologs from melon (*Cucumis melo* L). *Molecular and General Genetics* **251:** 81-90

Lasserre E, Godard F, Bouquin T, Hernandez JA, Pech JC, Roby D, Balague C (1997) Differential activation of two ACC oxidase gene promoters from melon during plant development and in response to pathogen attack. *Molecular & General Genetics* **256:** 211-222

Levy M, Rachmilevitch S, Abel S (2005) Transient *Agrobacterium*-mediated gene expression in the Arabidopsis hydroponics root system for subcellular localization studies. *Plant Molecular Biology Reporter* **23:** 179-184

Liang XW, Abel S, Keller JA, Shen NF, Theologis A (1992) The 1-amino-cyclopropane-1-carboxylate synthase gene family of *Arabidopsis thaliana*. *Proceedings of the National Academy of Sciences of the United States of America* **89:** 11046-11050

Liao H, Rubio G, Yan XL, Cao AQ, Brown KM, Lynch JP (2001) Effect of phosphorus availability on basal root shallowness in common bean. *Plant and Soil* **232:** 69-79

Li YD, Wang YJ, Tong YP, Gao JG, Zhang JS, Chen SY (2005) QTL mapping of phosphorus deficiency tolerance in soybean (*Glycine max* L. Merr.). *Euphytica* **142:** 137-142

Liu JH, LeeTamon SH, Reid DM (1997) Differential and wound-inducible expression of 1-aminocyclopropane-1-carboxylate oxidase genes in sunflower seedlings. *Plant Molecular Biology* **34:** 923-933

Liu Y, Zhang S (2004) Phosphorylation of 1-aminocyclopropane-1-carboxylic acid synthase by MPK6, a stress-responsive Mitogen-Activated Protein Kinase, induces ethylene biosynthesis in Arabidopsis. *Plant Cell* **16:** 3386-3399

Ljung K, Hull AK, Celenza J, Yamada M, Estelle M, Nonmanly J, Sandberg G (2005) Sites and regulation of auxin biosynthesis in *Arabidopsis* roots. *Plant Cell* **17:** 1090-1104

Lopez-Bucio J, Cruz-Ramirez A, Herrera-Estrella L (2003) The role of nutrient availability in regulating root architecture. *Current Opinion in Plant Biology* **6:** 280-287

Lopez-Bucio J, Hernandez-Abreu E, Sanchez-Calderon L, Nieto-Jacobo MF, Simpson J, Herrera-Estrella L (2002) Phosphate availability alters architecture and causes changes in hormone sensitivity in the *Arabidopsis* root system. *Plant Physiology* **129:** 244-256

Lotscher M, Hay MJM (1996) Distribution of phosphorus and calcium from nodal roots of *Trifolium repens*: The relative importance of transport via xylem or phloem. *New Phytologist* **133:** 445-452

Lotscher M, Hay MJM (1996) Distribution of mineral nutrient from nodal roots of *Trifolium repens*: Genotypic variation in intra-plant allocation of P32 and Ca45. *Physiologia Plantarum* **97:** 269-276

Lu Y, Wassmann R, Neue HU, Huang C (1999) Impact of phosphorus supply on root exudation, aerenchyma formation and methane emission of rice plants. *Biogeochemistry* **47:** 203-218

Lutts S, Kinet JM, Bouharmont J (1996) Ethylene production by leaves of rice (*Oryza sativa* L) in relation to salinity tolerance and exogenous putrescine application. *Plant Science* **116:** 15-25

Lynch J, Brown KM (1997) Ethylene and plant responses to nutritional stress. *Physiologia Plantarum* **100:** 613-619

Lynch JP, Brown KM (2001) Topsoil foraging - an architectural adaptation of plants to low phosphorus availability. *Plant and Soil* **237:** 225-237

Ma N, Cai L, Lu WJ, Tan H, Gao JP (2005) Exogenous ethylene influences flower opening of cut roses (*Rosa hybrida*) by regulating the genes encoding ethylene biosynthesis enzymes. *Science in China Series C-Life Sciences* **48:** 434-444

Ma Z, Baskin TI, Brown KM, Lynch JP (2003) Regulation of root elongation under phosphorus stress involves changes in ethylene responsiveness. *Plant Physiology* **131:** 1381-1390

Ma Z, Bielenberg DG, Brown KM, Lynch JP (2001) Regulation of root hair density by phosphorus availability in *Arabidopsis thaliana*. *Plant Cell and Environment* **24:** 459-467

Majumdar S, Banerjee, S. and Kumar De, K. (2004) Meiotic behaviour of chromosomes in PMCs and Karyotype of *Trifolium repens* L. from Darjeeling Himalaya. *ACTA Biologica Cracoviensia Series Botanica* **46:** 217-220

Malerba M, Crosti P, Bianchetti R (1995) Ferricyanide induced ethylene production is a plasma membrane proton pump dependent 1-aminocyclopropane-1-carboxylic acid (ACC) oxidase activation. *Journal of Plant Physiology* **147:** 182-190

Mantis J, Tague BW (2000) Comparing the utility of β-glucuronidase and green fluorescent protein for detection of weak promoter activity in *Arabidopsis thaliana*. *Plant Molecular Biology Reporter* **18:** 319-330

Mattoo AK, Lieberman M (1977) Localization of the ethylene-synthesizing system in apple tissue. *Plant Physiology* **60:** 794-799

Mayne R, Kende H (1986) Ethylene biosynthesis in isolated vacuoles of *Vicia faba*: Requirements for membrane integrity. *Planta* **167:** 159-165

Meuriot F, Noquet C, Avice J, Volenec J, Cunningham S, Sors T, Caillot S, Ourry A (2004) Methyl jasmonate alters N partitioning, N reserves accumulation and induces gene expression of a 32-kDa vegetative storage protein that possesses chitinase activity in *Medicago sativa* taproots. *Physiologia Plantarum* **120:** 113-123

Mbeguie-A-Mbeguie D, Chahine H, Gomez RM, Gouble B, Reich M, Audergon JM, Souty M, Albagnac G, Fils-Lycaon B (1999) Molecular cloning and expression of a cDNA encoding 1-aminocyclopropane-1-carboxylate (ACC) oxidase from apricot fruit (*Prunus armeniaca*). *Physiologia Plantarum* **105:** 294-303

McGarvey DJ, Christoffersen RE (1992) Characterization and kinetic parameters of ethylene-forming enzyme from avocado fruit. *Journal of Biological Chemistry* **267:** 5964-5967

McGarvey DJ, Sirevag R, Christoffersen RE (1992) Ripening-related gene from avocado fruit. Ethylene-inducible expression of the messenger RNA and polypeptide. *Plant Physiology* **98:** 554-559

Michael G (2001) The control of root hair formation: suggested mechanisms. *Journal of Plant Nutrition and Soil Science-Zeitschrift Fur Pflanzenernahrung Und Bodenkunde* **164:** 111-119

Miller CR, Ochoa I, Nielsen KL, Beck D, Lynch JP (2003) Genetic variation for adventitious rooting in response to low phosphorus availability: Potential utility for phosphorus acquisition from stratified soils. *Functional Plant Biology* **30:** 973-985

Mimura T (2001) Physiological control of phosphate uptake and phosphate homeostasis in plant cells. *Australian Journal of Plant Physiology* **28:** 653-658

Moeder W, Barry CS, Tauriainen AA, Betz C, Tuomainen J, Utriainen M, Grierson D, Sandermann H, Langebartels C, Kangasjarvi J (2002) Ethylene synthesis regulated by biphasic induction of 1-aminocyclopropane-1-carboxylic acid synthase and 1-aminocyclopropane-1-carboxylic acid oxidase genes is required for hydrogen peroxide accumulation and cell death in ozone-exposed tomato. *Plant Physiology* **130:** 1918-1926

Muller M, Schmidt W (2004) Environmentally induced plasticity of root hair development in arabidopsis. *Plant Physiology* **134:** 409-419

Muller R, Morant M, Jarmer H, Nilsson L, Nielsen TH (2007) Genome-wide analysis of the Arabidopsis leaf transcriptome reveals interaction of phosphate and sugar metabolism. *Plant Physiology* **143:** 156-171

Muller R, Nilsson L, Krintel C, Nielsen TH (2004) Gene expression during recovery from phosphate starvation in roots and shoots of *Arabidopsis thaliana*. *Physiologia Plantarum* **122:** 233-243

Muller R, Stummann BM, Sisler EC, Serek M (2001) Cultivar differences in regulation of ethylene production in miniature rose flowers (*Rosa hybrida* L.). *Gartenbauwissenschaft* **66:** 34-38

Murray TA, McManus MT (2005) Developmental regulation of 1-aminocyclopropane-1-carboxylate synthase gene expression during leaf ontogeny in white clover. *Physiologia Plantarum* **124:** 107-120

Nakagawa N, Mori H, Yamazaki K, Imaseki H (1991) Cloning of a complementary-DNA for uxin-induced 1-aminocyclopropane-1-carboxylate synthase and differential expression of the gene by auxin and wounding. *Plant and Cell Physiology* **32:** 1153-1163

Nap JP, Mlynarova L, Stiekema WJ (1996) From transgene expression to public acceptance of transgenic plants: A matter of predictability. *Field Crops Research* **45:** 5-10

Ohnishi M, Mimura T, Tsujimura T, Mitsuhashi N, Washitani-Nemoto S, Maeshima M, Martinoia E (2007) Inorganic phosphate uptake in intact vacuoles isolated from suspension-cultured cells of *Catharanthus roseus* (L.) G. Don under varying Pi status. *Planta* **225:** 711-718

Olson DC, White JA, Edelman L, Harkins RN, Kende H (1991) Differential expression of 2 genes for 1-aminocyclopropane-1-carboxylate synthase in tomato fruits. *Proceedings of the National Academy of Sciences of the United States of America* **88:** 5340-5344

Ortega-Martinez O, Pernas M, Carol RJ, Dolan L (2007) Ethylene modulates stem cell division in the *Arabidopsis thaliana* root. *Science* **317:** 507-510

Pariasca JAT, Sunaga A, Miyazaki T, Hisaka H, Sonoda M, Nakagawa H, Sato T (2001) Cloning of cDNAs encoding senescence-associated genes, ACC synthase and ACC oxidase from stored snow pea pods (*Pisum sativum* L. var saccharatum) and their expression during pod storage. *Postharvest Biology and Technology* **22:** 239-247

Pathak N, Asif MH, Dhawan P, Srivastava MK, Nath P (2003) Expression and activities of ethylene biosynthesis enzymes during ripening of banana fruits and effect of 1-MCP treatment. *Plant Growth Regulation* **40:** 11-19

Peach C, Velten J (1991) Transgene expression variability (Position Effect) of CAT and GUS eporter genes driven by linked divergent T-DNA promoters. *Plant Molecular Biology* **17:** 49-60

Peck SC, Reinhardt D, Olson DC, Boller T, Kende H (1992) Localization of the ethylene-forming enzyme from tomatoes, 1-aminocyclopropane-1-carboxylate oxidase, in transgenic yeast. *Journal of Plant Physiology* **140:** 681-686

Peek CS, Robson AD, Kuo J (2003) The formation, morphology and anatomy of cluster root of *Lupinus albus* L. as dependent on soil type and phosphorus supply. *Plant and Soil* **248:** 237-246

Peng HP, Lin TY, Wang NN, Shih MC (2005) Differential expression of genes encoding 1-aminocyclopropane-1-carboxylate synthase in Arabidopsis during hypoxia. *Plant Molecular Biology* **58:** 15-25

Pitts RJ, Cernac A, Estelle M (1998) Auxin and ethylene promote root hair elongation in Arabidopsis. *Plant Journal* **16:** 553-560

Plaxton WC (2004) Plant response to stress: Biochemical adaptations to phosphate deficiency. *In* RM Goodman, ed, *Encyclopedia of Plant and Crop Science.* Marcel Dekker, New York, pp 976-980

Porter AJR, Borlakoglu JT, John P (1986) Activity of the ethylene-forming enzyme in relation to plant-cell structure and organization. *Journal of Plant Physiology* **125:** 207-216

Raghothama KG (2000) Phosphate transport and signaling. *Current Opinion in Plant Biology* **3:** 182-187

Raghothama KG (2000) Phosphorus acquisition; plant in the driver's seat! *Trends in Plant Science* **5:** 412-413

Raghothama KG, Karthikeyan AS (2005) Phosphate acquisition. *Plant and Soil* **274:** 37-49

Rahman A, Hosokawa S, Oono Y, Amakawa T, Goto N, Tsurumi S (2002) Auxin and ethylene response interactions during Arabidopsis root hair development dissected by auxin influx modulators. *Plant Physiology* **130:** 1908-1917

Ramassamy S, Olmos E, Bouzayen M, Pech JC, Latche A (1998) 1-aminocyclopropane-1-carboxylate oxidase of apple fruit is periplasmic. *Journal of Experimental Botany* **49:** 1909-1915

Rasori A, Bertolasi B, Furini A, Bonghi C, Tonutti P, Ramina A (2003) Functional analysis of peach ACC oxidase promoters in transgenic tomato and in ripening peach fruit. *Plant Science* **165:** 523-530

Rausch C, Bucher M (2002) Molecular mechanisms of phosphate transport in plants. *Planta* **216:** 23-37

Reinhardt D, Kende H, Boller T (1994) Subcellular-localization of 1-aminocyclopropane-1-carboxylate oxidase in tomato cells. *Planta* **195:** 142-146

Reymond M, Svistoonoff S, Loudet O, Nussaume L, Desnos T (2006) Identification of QTL controlling root growth response to phosphate starvation in *Arabidopsis thaliana*. *Plant Cell and Environment* **29:** 115-125

Rodriguez-Gacio MD, Nicolas C, Matilla AJ (2004) The final step of the ethylene biosynthesis pathway in turnip tops (*Brassica rapa*): molecular characterization of the 1-aminocyclopropane-1-carboxylate oxidase *BR-ACO1* throughout zygotic embryogenesis and germination of heterogeneous seeds. *Physiologia Plantarum* **121:** 132-140

Rohila JS, Yang YN (2007) Rice mitogen-activated protein kinase gene family and its role in biotic and abiotic stress response. *Journal of Integrative Plant Biology* **49:** 751-759

Rombaldi C, Lelievre JM, Latche A, Petitprez M, Bouzayen M, Pech JC (1994) Immunocytolocalization of 1-aminocyclopropane-1-carboxylic acid oxidase in tomato and apple fruit. *Planta* **192:** 453-460

Romera FJ, Welch RM, Norvell WA, Schaefer SC (1996) Iron requirement for and effects of promoters and inhibitors of ethylene action on stimulation of Fe(III)-chelate reductase in roots of strategy I species. *Biometals* **9:** 45-50

Rose RJ, Wang XD, Nolan KE, Rolfe BG (2006) Root meristems in *Medicago truncatula* tissue culture arise from vascular-derived procambial-like cells in a process regulated by ethylene. *Journal of Experimental Botany* **57:** 2227-2235

Ross GS, Knighton ML, Layyee M (1992) An ethylene-related cDNA from ripening apples. *Plant Molecular Biology* **19:** 231-238

Rubio V, Linhares F, Solano R, Martin AC, Iglesias J, Leyva A, Paz-Ares J (2001) A conserved MYB transcription factor involved in phosphate starvation signaling both in vascular plants and in unicellular algae. *Genes and Development* **15:** 2122-2133

Ruperti B, Bonghi C, Rasori A, Ramina A, Tonutti P (2001) Characterization and expression of two members of the peach 1-aminocyclopropane-1-carboxylate oxidase gene family. *Physiologia Plantarum* **111:** 336-344

Sakai S, Imaseki H (1971) Auxin-induced ethylene production by mungbean hypocotyl segments. *Plant and Cell Physiology* **12:** 349-359

Sambrook J, Fritsch EFa, Maniatis T (1989) *Molecular Cloning: A Laboratory Manual*, Vol 1. Spring Harbor Laboratory Press, New York

Sanchez AM, Mariani C (2002) Expression of the ACC synthase and ACC oxidase coding genes after self-pollination and incongruous pollination of tobacco pistils. *Plant Molecular Biology* **48:** 351-359

Sanchez-Calderon L, Lopez-Bucio J, Chacon-Lopez A, Cruz-Ramirez A, Nieto-Jacobo F, Dubrovsky JG, Herrera-Estrella L (2005) Phosphate starvation induces a determinate developmental program in the roots of *Arabidopsis thaliana*. *Plant and Cell Physiology* **46:** 174-184

Sato T, Theologis A (1989) Cloning the mRNA encoding 1-aminocyclopropane-1-carboxylate synthase, the key enzyme for ethylene biosynthesis in plants. *PNAS* **86:** 6621-6625

Sato T, Oeller PW, Theologis A (1991) The 1- aminocyclopropane- 1-carboxylate synthase of *Cucurbita*. *Journal of Biological Chemistry* **266**: 3752-3759

Schachtman DP, Reid RJ, Ayling SM (1998) Phosphorus uptake by plants: From soil to cell. *Plant Physiology* **116:** 447-453

Schikora A, Schmidt W (2001) Acclimative changes in root epidermal cell fate in response to Fe and P deficiency: a specific role for auxin? *Protoplasma* **218:** 67-75

Schmidt W (2001) From faith to fate: Ethylene signaling in morphogenic responses to P and Fe deficiency. *Journal of Plant Nutrition and Soil Science-Zeitschrift Fur Pflanzenernahrung Und Bodenkunde* **164:** 147-154

Shane MW, Cramer MD, Funayama-Noguchi S, Cawthray GR, Millar AH, Day DA, Lambers H (2004) Development physiology of cluster-root carboxylate synthesis and exudation in harsh hakea. Expression of phosphoenolpyruvate carboxylase and the alternative oxidase. *Plant Physiology* **135:** 549-560

Shimano F, Ashihara H (2006) Effect of long-term phosphate starvation on the levels and metabolism of purine nucleotides in suspension-cultured *Catharanthus roseus* cells. *Phytochemistry* **67:** 132-141

Shin H, Shin HS, Dewbre GR, Harrison MJ (2004) Phosphate transport in Arabidopsis: Pht1;1 and Pht1;4 play a major role in phosphate acquisition from both low- and high-phosphate environments. *Plant Journal* **39:** 629-642

Shiomi S, Yamamoto M, Ono T, Kakiuchi K, Nakamoto J, Nakatsuka A, Kubo Y, Nakamura R, Inaba A, Imaseki H (1998) cDNA cloning of ACC synthase and ACC oxidase genes in cucumber fruit and their differential expression by wounding and auxin. *Journal of the Japanese Society for Horticultural Science* **67:** 685-692

Smith FW, Mudge SR, Rae AL, Glassop D (2003) Phosphate transport in plants. *Plant and Soil* **248:** 71-83

Smith FW, Rae AL, Hawkesford MJ (2000) Molecular mechanisms of phosphate and sulphate transport in plants. *Biochimica Et Biophysica Acta-Biomembranes* **1465:** 236-245

Smith JJ, Ververidis P, John P (1992) Characterization of the ethylene-forming enzyme partially purified from melon. *Phytochemistry* **31:** 1485-1494

Song JD, Kim JH, Lee DH, Rhew TH, Cho SH, Lee CH (2005) Developmental regulation of the expression of 1-aminocyclopropane-1-carboxylic acid (ACC) synthase and ACC oxidase genes in hypocotyls of etiolated mung bean seedlings. *Plant Science* **168:** 1149-1155

Song JD, Lee DH, Rhew TH, Lee CH (2003) Wound-induced expression of ACC synthase genes in etiolated mung bean hypocotyls. *Journal of Plant Biology* **46:** 199-203

Spanu P, Reinhardt D, Boller T (1991) Analysis and cloning of the ethylene-forming enzyme from tomato by functional expression of its mRNA in *Xenopus laevis* oocytes. *EMBO J.* **10:** 2007-2013

Srinivasan M, Petersen DJ, Holl FB (1997) Altered root hair morphogenesis in *Phaseolus vulgaris* in response to bacterial coinoculation and the presence of aminoethoxy vinyl glycine (AVG). *Microbiological Research* **152:** 151-156

Steffens B, Sauter M (2005) Epidermal cell death in rice is regulated by ethylene, gibberellin, and abscisic acid. *Plant Physiology* **139:** 713-721

Suzuki Y, Asoda T, Matsumoto Y, Terai H, Kato M (2005) Suppression of the expression of genes encoding ethylene biosynthetic enzymes in harvested broccoli with high temperature treatment. *Postharvest Biology and Technology* **36:** 265-271

Takahashi H, Kawahara A, Inoue Y (2003) Ethylene promotes the induction by auxin of the cortical microtubule randomization required for low-pH-induced root hair initiation in lettuce (*Lactuca sativa* L.) seedlings. *Plant and Cell Physiology* **44:** 932-940

Tang X, Gomes A, Bhatia A, Woodson WR (1994) Pistil-specific and ethylene-regulated expression of 1-aminocyclopropane-1-carboxylate oxidase genes in petunia flowers. *Plant Cell* **6:** 1227-1239

Tang Z, Sadka A, Morishige DT, Mullet JE (2001) Homeodomain leucine zipper proteins bind to the phosphate response domain of the soybean VSPβ tripartite promoter. *Plant Physiology* **125:** 797-809

Tanimoto M, Roberts K, Dolan L (1995) Ethylene is a positive regulator of root hair development in *Arabidopsis thaliana*. *Plant Journal* **8:** 943-948

Tari I, Marton Z (1999) Ethylene production by the roots of wheat seedlings (*Triticum aestivum L*-cv. GK Othalom) grown in 1 mM nitrate or in an N-free nutrient solution: a possible role for ethylene in root elongation. *Novenytermeles* **48:** 269-278

Theodorou ME, Plaxton WC (1993) Metabolic adaptations of plant respiration to nutritional phosphate deprivation. *Plant Physiology* **101:** 339-344

Torrey J (1976) Root hormones and plant growth. *Annual Review of Plant Physiology* **27:** 435-459

Uhde-Stone C, Liu JQ, Zinn KE, Allan DL, Vance CP (2005) Transgenic proteoid roots of white lupin: a vehicle for characterizing and silencing root genes involved in adaptation to P stress. *Plant Journal* **44:** 840-853

Uhde-Stone C, Zinn KE, Ramirez-Yanez M, Li AG, Vance CP, Allan DL (2003) Nylon filter arrays reveal differential gene expression in proteoid roots of white lupin in response to phosphorus deficiency. *Plant Physiology* **131:** 1064-1079

Ukaji T, Ashihara H (1987) Metabolic regulation in plant-cell culture .20. Effect of inorganic phosphate on the levels of amino-acids in suspension-cultured cells of *Catharanthus roseus*. *Annals of Botany* **60:** 109-114

Van der Geest AHM, Petolino JF (1998) Expression of a modified green fluorescent protein gene in transgenic maize plants and progeny. *Plant Cell Reports* **17:** 760-764

Van der Straeten D, Van Wiemeersch L, Goodman HMa, Van Montagu M (1990) Cloning and sequence of two different cDNAs encoding 1-aminocyclopropane-1-carboxylate synthase in tomato. *Proceedings of the National Academy of Sciences of the United States of America* **87:** 4859–4863

Vance CP, Uhde-Stone C, Allan DL (2003) Phosphorus acquisition and use: critical adaptations by plants for securing a nonrenewable resource. *New Phytologist* **157:** 423-447

Ververidis P, John P (1991) Complete recovery in vitro of ethylene-forming enzyme activity. *Phytochemistry* **30:** 725-727

Visser EJW, Pierik R (2007) Inhibition of root elongation by ethylene in wetland and non-wetland plant species and the impact of longitudinal ventilation. *Plant Cell and Environment* **30:** 31-38

Voisey CR, White DWR, Wigley PJ, Chilcott CN, McGregor PG, Woodfield DR (1994) Release of transgenic white clover plants expressing *Bacillus thuringiensis* genes - An ecological perspective. *Biocontrol Science and Technology* **4:** 475-481

Wagner KG, Backer AI (1992) Dynamics of nucleotides in plants studied on a cellular basis. *International Review of Cytology-a Survey of Cell Biology* **134:** 1-84

Wang KLC, Li H, Ecker JR (2002) Ethylene biosynthesis and signaling networks. *Plant Cell* **14:** S131-S151

Wang NN, Shih MC, Li N (2005) The GUS reporter-aided analysis of the promoter activities of Arabidopsis ACC synthase genes *AtACS4, AtACS5,* and *AtACS7* induced by hormones and stresses. *Journal of Experimental Botany* **56:** 909-920

Wasaki J, Ando M, Ozawa K, Omura M, Osaki M, Ito H, Matsui H, Tadano T (1997) Properties of secretory acid phosphatase from lupin roots under phosphorus-deficient conditions.*Soil Science and Plant Nutrition* **43:** 981-986

Wasaki J, Yonetani R, Kuroda S, Shinano T, Yazaki J, Fujii F, Shimbo K, Yamamoto K, Sakata K, Sasaki T, Kishimoto N, Kikuchi S, Yamagishi M, Osaki M (2003) Transcriptomic analysis of metabolic changes by phosphorus stress in rice plant roots. *Plant Cell and Environment* **26:** 1515-1523

Watt M, Evans JR (1999) Proteoid roots. Physiology and development. *Plant Physiology* **121:** 317-323

Weterings K, Pezzotti M, Cornelissen M, Mariani C (2002) Dynamic 1-aminocyclopropane-1-carboxylate-synthase and -oxidase transcript accumulation patterns during pollen tube growth in tobacco styles. *Plant Physiology* **130:** 1190-1200

Williams OJ, Golden KD (2002) Purification and characterization of ACC oxidase from *Artocarpus altilis. Plant Physiology and Biochemistry* **40:** 273-279

Williamson LC, Ribrioux S, Fitter AH, Leyser HMO (2001) Phosphate availability regulates root system architecture in Arabidopsis. *Plant Physiology* **126:** 875-882

Wu P, Ma LG, Hou XL, Wang MY, Wu YR, Liu FY, Deng XW (2003) Phosphate starvation triggers distinct alterations of genome expression in Arabidopsis roots and leaves. *Plant Physiology* **132:** 1260-1271

Wylegalla C, Meyer R, Wagner KG (1985) Nucleotide pools in suspension-cultured cells of *Datura innoxia* .2. Correlation with nutrient-uptake and macromolecular-synthesis. *Planta* **166:** 446-451

Xie YJ, Yu D (2003) The significance of lateral roots in phosphorus (P) acquisition of water hyacinth *(Eichhornia crassipes*). *Aquatic Botany* **75:** 311-321

Yamagami T, Tsuchisaka A, Yamada K, Haddon WF, Harden LA, Theologis A (2003) Biochemical diversity among the 1-amino-cyclopropane-1-carboxylate synthase isozymes encoded by the Arabidopsis gene family. *Journal of Biological Chemistry* **278:** 49102-49112

Yang S, Hoffman N (1984) Ethylene biosynthesis and its regulation in higher plants. *Annual Review in Plant Physiology* **35:** 155-189

Yoo SD (1999) *Molecular Characterisation of Ethylene Biosynthesis during Leaf Ontogeny in White Clover (Trifolium repens* L.). Ph.D. Thesis Massey University, Palmerston North

Yoon IS, Park DH, Mori H, Imaseki H, Kang BG (1999) Characterization of an auxin-inducible 1-aminocyclopropane-1-carboxylate synthase gene, VR-ACS6, of mungbean (*Vigna radiata* (L.) Wilczek) and hormonal interactions on the promoter activity in transgenic tobacco. *Plant and Cell Physiology* **40:** 431-438

Zanetti ME, Terrile MC, Arce D, Godoy AV, San Segundo B, Casalongue C (2002) Isolation and characterization of a potato cDNA corresponding to a 1-aminocyclopropane-1-carboxylate (ACC) oxidase gene differentially activated by stress. *Journal of Experimental Botany* **53:** 2455-2457

Zhang C, McManus MT (2000) Identification and characterisation of two distinct acid phosphatases in cell walls of roots of white clover. *Plant Physiology and Biochemistry* **38:** 259-270

Zhang YJ, Lynch JP, Brown KM (2003) Ethylene and phosphorus availability have interacting yet distinct effects on root hair development. *Journal of Experimental Botany* **54:** 2351-2361

Zheng QL, Nakatsuka A, Itamura H (2006) Involvement of negative feedback regulation in wound-induced ethylene synthesis in 'Saijo' persimmon. *Journal of Agricultural and Food Chemistry* **54:** 5875-5879

Zheng QL, Nakatsuka A, Taira S, Itamura H (2005) Enzymatic activities and gene expression of 1-aminocyclopropane-1-carboxylic acid (ACC) synthase and ACC oxidase in persimmon fruit. *Postharvest Biology and Technology* **37:** 286-290

Zhu CH, Gan LJ, Shen ZG, Xia K (2006) Interactions between jasmonates and ethylene in the regulation of root hair development in Arabidopsis. *Journal of Experimental Botany* **57:** 1299-1308

Zhu JM, Lynch JP (2004) The contribution of lateral rooting to phosphorus acquisition efficiency in maize (*Zea mays*) seedlings. *Functional Plant Biology* **31:** 949-958

Appendix I

Table A.1 Composition of the Hoagland solution with one-third strength macro and full strength micronutrients (Gibeaut *et al.*, 1997)

A. Macronutrients	**Working concentration (mM)**	**Weight (g) per litre of 10x stock solution**
KNO_3	1.25	1.264
$Ca(NO_3)_2$	1.50	3.543
$MgSO_4$	0.75	1.849
KH_2PO_4	1.00	1.360

B. Micronutrients	**Working concentration (μM)**	**Weight (mg) per litre of 100x stock solution**
KCl	50.0	372.8
H_3BO_3	50.0	309.2
$MnSO_4$	10.0	151.0
$ZnSO_4$	2.0	57.5
$CuSO_4$	1.5	37.5
$(NH_4)_6Mo_7O_{24}$	0.075	9.30
Na_2O_3Si	0.10	2.10
Fe Na EDTA	72.0	2642.8

Appendix II

Table A.2 Composition of Murashigi and Skoog (MS) basal salt mixture (Murashige and Skoog, 1962)

Macro stock	Final conc ($mg.L^{-1}$)	20 x Stock ($g.L^{-1}$)
NH_4NO_3	1650	33
KNO_3	1900	33
$CaCl_2.2H_2O$	440	8.8
KH_2PO_4	170	3.4
$MgSO_4.7H_2O$	370	7.4

Micro stock	Final conc ($mg.L^{-1}$)	200 x Stock ($g.L^{-1}$)
H_3BO_3	6.2	1.24
$MnSO_4.4H_2O$	22.2	4.46
$ZnSO_4.7H_2O$	8.6	1.72
KI	0.83	0.166
$Na_2MoO_4.2H_2O$	0.25	0.05
$CuSO_4.5H_2O$	0.025	0.005
$CoCl_2.6H_2O$	0.025	0.005

Vitamins	Final conc ($mg.L^{-1}$)	100 x Stock ($mg.mL^{-1}$)
Nicotinic Acid	10	1.0
Thiamine.HCl	100	10.0
Pyridoxine.HCl	10	1.0

FeNaEDTA	Final conc ($mg.L^{-1}$)	100 x Stock (mg per 100mL)
NaEDTA.2H2O	3.73	37.3
FeSO4.7H2O	2.78	27.8

MS media composition, pH 5.7	Amount per litre
Macro stock	50 mL
Micro stock	5 mL
Vitamins	10 mL
FeNaEDTA	10 mL
Myo-Inositol	100 mg
Sucrose	30 g

Appendix III

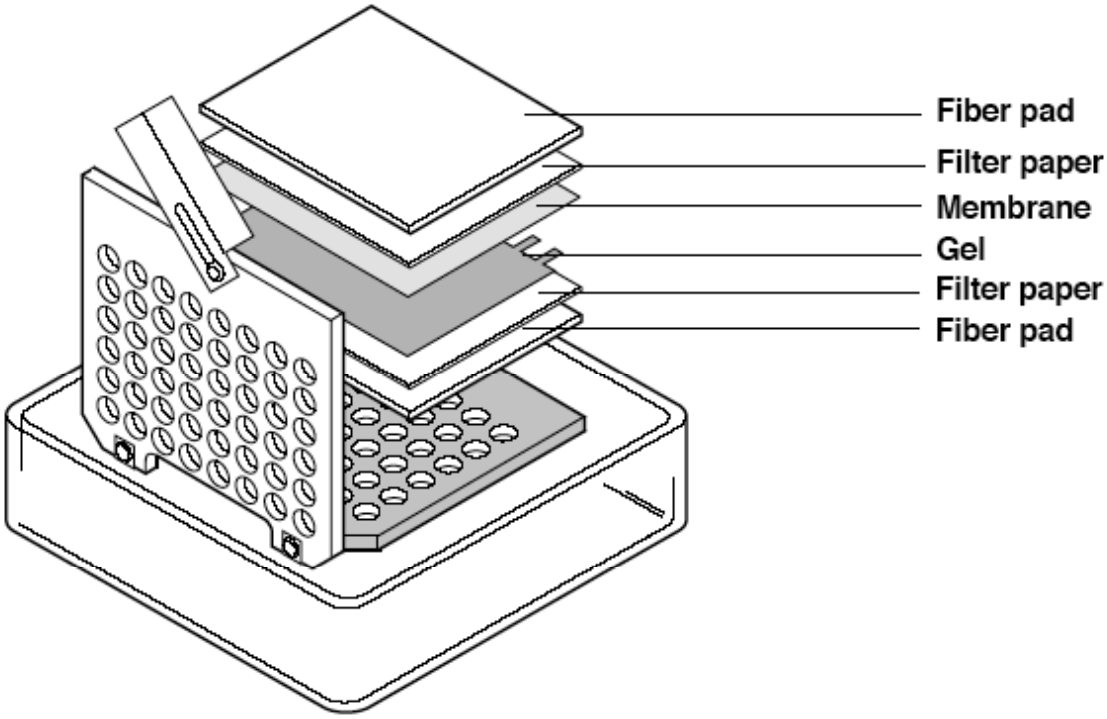

Figure A.1 Set up of the cassette for the transfer of protein from gel to membrane (Adapted from Bio-Rad Mini Trans-Blot Instruction manual (Bio-Rad, n.d.)